# Force potentiation as a modulator of contractile performance: Implications for control of skeletal muscle force and energetics of work

William Gittings, MSc

Submitted in partial fulfillment of the requirements
for the degree of Doctorate of Philosophy
(Health Biosciences)

Faculty of Applied Health Sciences
Brock University
500 Glenridge Ave.
St. Catharines, Ontario
L2S 3A1

# Abstract

This thesis investigated the modulation of dynamic contractile function and energetics of work by posttetanic potentiation (PTP). Mechanical experiments were conducted *in vitro* using software-controlled protocols to stimulate/determine contractile function during ramp shortening, and muscles were frozen during parallel incubations for biochemical analysis.

The central feature of this research was the comparison of fast hindlimb muscles from wildtype and skeletal myosin light chain kinase knockout (skMLCK$^{-/-}$) mice that does not express the primary mechanism for PTP: myosin regulatory light chain (RLC) phosphorylation. In contrast to smooth/cardiac muscles where RLC phosphorylation is indispensable, its precise physiological role in skeletal muscle is unclear.

It was initially determined that tetanic potentiation was shortening speed dependent, and this sensitivity of the PTP mechanism to muscle shortening extended the stimulation frequency domain over which PTP was manifest. Thus, the physiological utility of RLC phosphorylation to augment contractile function *in vivo* may be more extensive than previously considered. Subsequent experiments studied the contraction-type dependence for PTP and demonstrated that the enhancement of contractile function was dependent on force level. Surprisingly, in the absence of RLC phosphorylation, skMLCK$^{-/-}$ muscles exhibited significant concentric PTP; consequently, up to ~50% of the dynamic PTP response in wildtype muscle may be attributed to an alternate mechanism.

When the interaction of PTP and the catchlike property (CLP) was examined, we determined that unlike the acute augmentation of peak force by the CLP, RLC phosphorylation produced a longer-lasting enhancement of force and work in the potentiated state. Nevertheless, despite the apparent interference between these mechanisms, both offer physiological utility and may be complementary in achieving optimal contractile function *in vivo*.

Finally, when the energetic implications of PTP were explored, we determined that during a brief period of repetitive concentric activation, total work performed was ~60% greater in wildtype vs. skMLCK$^{-/-}$ muscles but there was no genotype difference in High-Energy Phosphate Consumption or Economy (i.e. HEPC: work).

In summary, this thesis provides novel insight into the modulatory effects of PTP and RLC phosphorylation, and through the observation of alternative mechanisms for PTP we further develop our understanding of the history-dependence of fast skeletal muscle function.

# Acknowledgements

I would like to acknowledge the many advisors, colleagues, friends, and supporters that helped me complete my graduate work at Brock, and to express my sincere appreciation for their contributions.

Since beginning my graduate work with Rene I have had the opportunity to research and work independently in the lab and this required a lot of trust from my supervisor. In fact, I think that Rene's approach to supervision without micromanagement allowed me the opportunity to learn through experience and become responsible for solving the inevitable setbacks that occurred; all of which was central to my development as a researcher and student. Over time, I have adopted the best aspects of Rene's approach to research, and these positive influences can be seen throughout the writing and content of this thesis. I would like to thank Rene for several years of great experience and training, during which I received significant mentorship and encouragement.

I received much support and advice from a group of dedicated faculty members and collaborators during my time at Brock, including my supervisory committee (Drs. Peters, Gabriel, and Tupling), faculty members in the Centre for Bone and Muscle Health (Drs. Ward and Leblanc), leading experts in the field (Drs. R.W. Grange and J.T. Stull), and the Brock Animal Care staff, led by Dayle Carlson and Shawn Bukovac.

Over the years I have had been fortunate to work and collaborate with a great group of student researchers. The work was never as satisfying as when the experience was shared with others, both in failure and success. I will remember the great conference experiences (Barrie, Toronto, Quebec City, Seattle, Boston) and the people with whom I shared these great times. Dr. Ian Smith made important contributions to my work and has been a regular and enthusiastic resource for my learning and development. I would like to thank Dan Caterini for his Briscola tutelage in 'the dungeon'. Jordan Bunda has recently made significant contributions to our lab in terms of developing methods and setting a new standard of professionalism, both of which benefited me greatly in the final year of my work.

Most importantly, I would like to acknowledge my wife Carrie and members of both families for their great support during several years as a graduate student. Their encouragement gave me the stamina and patience to complete this work, and I am thankful for the sacrifices made so that I could pursue my academic development.

# Dedication

This dissertation is dedicated to my daughter Addison Claire, who was a constant source of motivation at my side during the final months of writing, and whose arrival into our lives this summer was such a joy and inspiration.

# Table of Contents

# List of Abbreviations

| | |
|---|---|
| *PTP* | Posttetanic potentiation |
| *PAP* | Postactivation potentiation |
| *EDL* | Extensor digitorum longus |
| *skMLCK* | Skeletal muscle myosin light chain kinase |
| *skMLCK$^{-/-}$* | Skeletal muscle myosin light chain kinase knockout |
| *$Ca^{2+}$* | Calcium |
| *CaM* | Calcium-calmodulin complex |
| *RLC* | Regulatory light chain |
| *ELC* | Essential Light Chain |
| *Tm* | Tropomyosin |
| *Tn* | Troponin |
| *ECC* | Excitation-contraction coupling |
| *SR* | Sarcoplasmic reticulum |
| *SERCA* | Sarco/endoplasmic reticulum calcium ATPase |
| *$F_{max}$* | Maximal force |
| *$P_o$* | Peak tetanic force |
| *$P_t$* | Peak twitch force |
| *$V_{max}$* | Maximal shortening velocity (Load-Clamp) |
| *$V_o$* | Maximal unloaded shortening Velocity (Slack Test) |
| *$L_o$* | Optimal length (for peak force) |
| *+dP/dt* | Rate of force development |
| *-dP/dt* | Rate of force relaxation |
| *$f_{app}$* | Rate constant: crossbridge transition to force-generating state |
| *$g_{app}$* | Rate constant: crossbridge transition to non force-generating state |
| *αFS* | Fraction of force-generating crossbridges ($f_{app}/f_{app}+g_{app}$) |
| *CLP* | Catchlike Property |
| *CFT* | Constant Frequency Train |
| *CLT* | Catchlike Train |
| *MU* | Motor unit |
| *ATP* | Adenosine Triphosphate |
| *ADP* | Adenosine Diphosphate |
| *AMP* | Adenosine Monophosphate |
| *AK* | Adenylate Kinase |
| *ATPase* | Adenosine Triphosphatase |
| *CK* | Creatine Kinase |
| *DHPR, RyR* | Dihydropyridine Receptor, Ryanodine Receptor |
| *HEPC* | High-Energy Phosphate Consumption |
| *ICT* | Intracellular Calcium Transient |
| *kDa* | kiloDalton |
| *MLCP* | Myosin Light Chain Phosphatase (PP1c) |
| *$Na^+/K^+$-ATPase* | Sodium-Potassium ATPase Pump |
| *PCr* | Phosphocreatine |
| *$P_i$* | Inorganic Phosphate |
| *FuI* | Fusion Index |

# List of Figures

# List of Tables

**Chapter 5: Study #2**



**Chapter 6: Study #3**



**Chapter 7: Study #4**

# List of Equations

# Chapter 1: Introduction

In fast skeletal muscle, the net outcome of previous activity is often detrimental to performance and contributes to the state of reduced force and work capacity known as fatigue. However, prior events may also function to increase or potentiate the contractile response of skeletal muscles in meaningful ways. Indeed, this aspect of the history-dependence of muscle contractile activity may oppose muscle fatigue (Bernard et al., 1941; Brown & Tuttle, 1926; Gruber, 1922). Although now established as a fundamental property of the fast twitch skeletal muscle phenotype, the precise influence of potentiation on unfatigued or fatigued performance remains unclear. This uncertainty relates to the physiological utility of force potentiation and whether it exists to: *i)* augment maximal force generation and power during brief supramaximal effort (i.e. flight or fight response), or *ii)* act as a molecular gearshift to improve contractile function during sustained submaximal use to help mitigate the effects of fatigue (i.e. increase $Ca^{2+}$ sensitivity and sparing of central motor drive).

It is now understood that posttranslational modification of the myosin molecule (i.e. myosin RLC phosphorylation) and transitory fluctuations in $Ca^{2+}$ homeostasis, to a lesser extent, are the important mechanisms responsible for the potentiation of contractile function in fast skeletal muscle (Stull et al., 2011). Of these mechanisms, myosin RLC phosphorylation has been more rigorously characterized, and its effect on muscle function has been described at the level of the myosin crossbridge, the single fibre, the intact muscle as well as *in vivo*. The important observation that myosin RLC phosphorylation is simultaneously triggered by the same signal that regulates muscular contraction (i.e. $Ca^{2+}$) (Pires, 1974) suggests that it plays an essential role in the function of fast skeletal muscle. However, recent technological advances such as the development of myosin light chain kinase ($skMLCK^{-/-}$) deficient mice have demonstrated that fast skeletal muscles work quite well in the absence of myosin RLC phosphorylation (Zhi et al., 2005). Whether force potentiation by myosin RLC phosphorylation is an evolutionary remnant of smooth or cardiac muscle phenotypes has been considered (Duggal et al., 2014); however, it may be conserved in fast skeletal muscles because it offers some adaptive benefit.

The purpose of this thesis is to investigate the modulation of skeletal muscle contractile function and energetics by posttetanic potentiation (PTP). More specifically,

the use of skMLCK$^{-/-}$ mice as an experimental control for myosin RLC phosphorylation allows us to parse out some of the finer details related to the presence of alternative mechanisms for force potentiation. The intact mouse extensor digitorum longus (EDL) muscle studied *in vitro* is the experimental model of choice for this work because: *i)* we have the unique and exclusive opportunity to breed and house skMLCK$^{-/-}$ mice at Brock, *ii)* it permits significant control of environmental factors such as temperature, *iii)* EDL muscles are large enough to use for most biochemical analysis techniques, and *iv)* studying whole muscle function retains considerable physiological relevance with respect to $Ca^{2+}$ signaling and maintaining intact fibre/sarcomere structure.

The studies that follow explore the modulation of contractile function by PTP and examine the way these events interact with important functional relationships and processes such as: *i)* the force frequency and force velocity relationships, *ii)* thin filament activation and cooperativity, *iii)* motoneuronal doublets and the catchlike property, and *iv)* the energetic cost of muscular work.

# Chapter 2: Review of Literature

The force production that results from skeletal muscle activation involves a complex set of mechanochemical processes that may be classified as regulatory or modulatory; the former describes those mechanisms that must be intact for the physiological event to occur, and the latter any adjustment or variation that modifies the event in some way. To gain a better understanding of how muscles work *in vivo*, investigation of the various processes that simultaneously fine-tune function should be studied and understood within the greater regulatory scheme itself. To this end, the proceeding review will examine what we know about muscle force potentiation and its function within the fast skeletal muscle phenotype.

In the first section the physiology of fast skeletal muscles will be explored with specific reference to microanatomy of the contractile apparatus, the mechanism of muscle contraction via excitation-contraction coupling, and functional relationships. The second section of this review will provide a general introduction of activity dependent potentiation and provide useful definitions as an introduction to the research that follows. In particular, this section will detail the mechanism of myosin RLC phosphorylation and the structure/function implications with respect to the mechanics of muscle contraction. In section three, current research regarding the neuromuscular control of force production will be discussed with respect to activity dependent potentiation and emphasis on motor unit firing patterns. Finally, in section four, the bioenergetics of fast skeletal muscle contraction will be investigated with the metabolic cost of myosin RLC phosphorylation and economy of muscular work as important points of emphasis.

## *Structure and function of fast skeletal muscle*

The microanatomy and function of the contractile apparatus is an important starting point as the modulatory effects of various mechanisms are often explained by myosin motor protein function and crossbridge kinetics (i.e. binding, detachment, and cycling rate). Indeed, this type of reductionist approach is used regularly in the study of potentiation to help compare findings from *in vitro* muscle models with those from permeabilized fibre preparations or motility assays.

### *Skeletal muscle contractile apparatus*

The production of force in an intact muscle is the net outcome of countless cyclic motor protein interactions that operate within each discrete contractile unit (sarcomere). Although anchored by a complex array of structural proteins, force production occurs primarily through the interaction of actin and myosin. Skeletal muscle force production is thick filament based but thin filament regulated. This means that the structures responsible for the activation of the force production mechanism are contained in the actin protein complex, and conversely, that myosin contains the assembly which converts chemical energy into mechanical force. These myofilaments are arranged in a hexagonal array where each myosin is surrounded by six actin filaments, an arrangement that maximizes the opportunities for direct physical interactions. Because the myosin backbone is anchored only to the midline of the sarcomere while the actin filaments are secured to the opposing z-disks, the result of force-producing interactions between the filaments is a longitudinal contraction of the system (in the absence of an external load). Therefore, the net effect of simultaneous sarcomeric shortening is the production of muscle force. In this system, the degree of filament overlap and the interfilament distance between the actin and myosin proteins are important factors that affect the likelihood of crossbridge binding and subsequent force production, and will be discussed in the sections that follow.

### *Myosin structure and the crossbridge cycle*

Myosin is a large protein and consists of two heavy chains (~200kDa) and two light chains (~20kDa), referred to as the essential (ELC) and regulatory light chains (RLC). Skeletal muscles are most often categorized by the relative expression of the heavy chains contained within them (i.e. type I, IIA, IIX, and IIB). Barany (1967) was the

first to describe a strong positive relationship between myosin ATPase rates and shortening speeds of skeletal muscles and did so across an impressive range of species and muscles. Moreover, through the work of Hill (1949) and others (Seow & Ford, 1991), we also know that speed of shortening and muscular power in mammalian muscles is inversely related to body mass in a predictable manner. Understood in the context of this thesis, we can therefore appreciate that the fast skeletal muscle phenotype expressed in mice hindlimb muscles is highly specialized to produce powerful, high-speed contractions. Indeed, we have previously determined that mouse extensor digitorum longus (EDL) muscles contain ≥99% fast skeletal muscle isoforms (IIA/IIX/IIB) and >60% type IIB fibres (Gittings et al., 2011). Thus, although some heterogeneity of structure and function exist within the mouse EDL, we believe the intact EDL model to be a good representation of fast skeletal muscle physiology.

While the rate of ATP hydrolysis and crossbridge cycling is specific to the heavy chain isoform expressed, the mechanism and process of force production is similar between fibre types (Rayment, 1996). The conformational changes in the myosin molecule that ultimately produce force are dependent on the contents of the nucleotide-binding pocket, which changes during recurrent hydrolysis of ATP (Gordon et al., 2000). In an activated muscle, the myosin crossbridge binds to actin following hydrolysis of ATP in the catalytic domain of the myosin head (Gordon et al., 2000). The energy liberated during hydrolysis is used to prime the crossbridge in a specialized high-energy configuration for attachment (Gordon et al., 2000). With the release of an inorganic phosphate moiety, the crossbridge initiates a powerstroke that pulls the actin filament toward the M-Line of the sarcomere. The powerstroke itself is understood to involve conformational changes between protein subunits in the region between the head and neck of the molecule (also known as the lever arm)(McKillop & Geeves, 1993; Rayment et al., 1993). Following the powerstroke the residual ADP is released from the myosin head, freeing the nucleotide-binding pocket to attract a new ATP molecule. Upon binding ATP the crossbridge detaches from the thin filament-binding site and will continue the cycle recurrently while the system is activated.

The role of the regulatory and essential light chains in the crossbridge cycle is primarily structural as they support the position of the myosin head with respect to the myosin backbone (Craig and Woodhead, 2006). These structures help to amplify the rotational movements of the lever arm during ATP hydrolysis (Geeves & Holmes, 1999).

However, despite the role of the light chains in the energy transduction process, *in vitro* myosin preparations in which light chains have been removed still maintain their catalytic function with respect to ATP hydrolysis (Rayment, 1996). A more detailed discussion of the modulatory role of the RLC will be included in the review with respect to activity dependent potentiation and myosin RLC phosphorylation.

*Figure 2.1. Myosin structure and crossbridge kinetics*

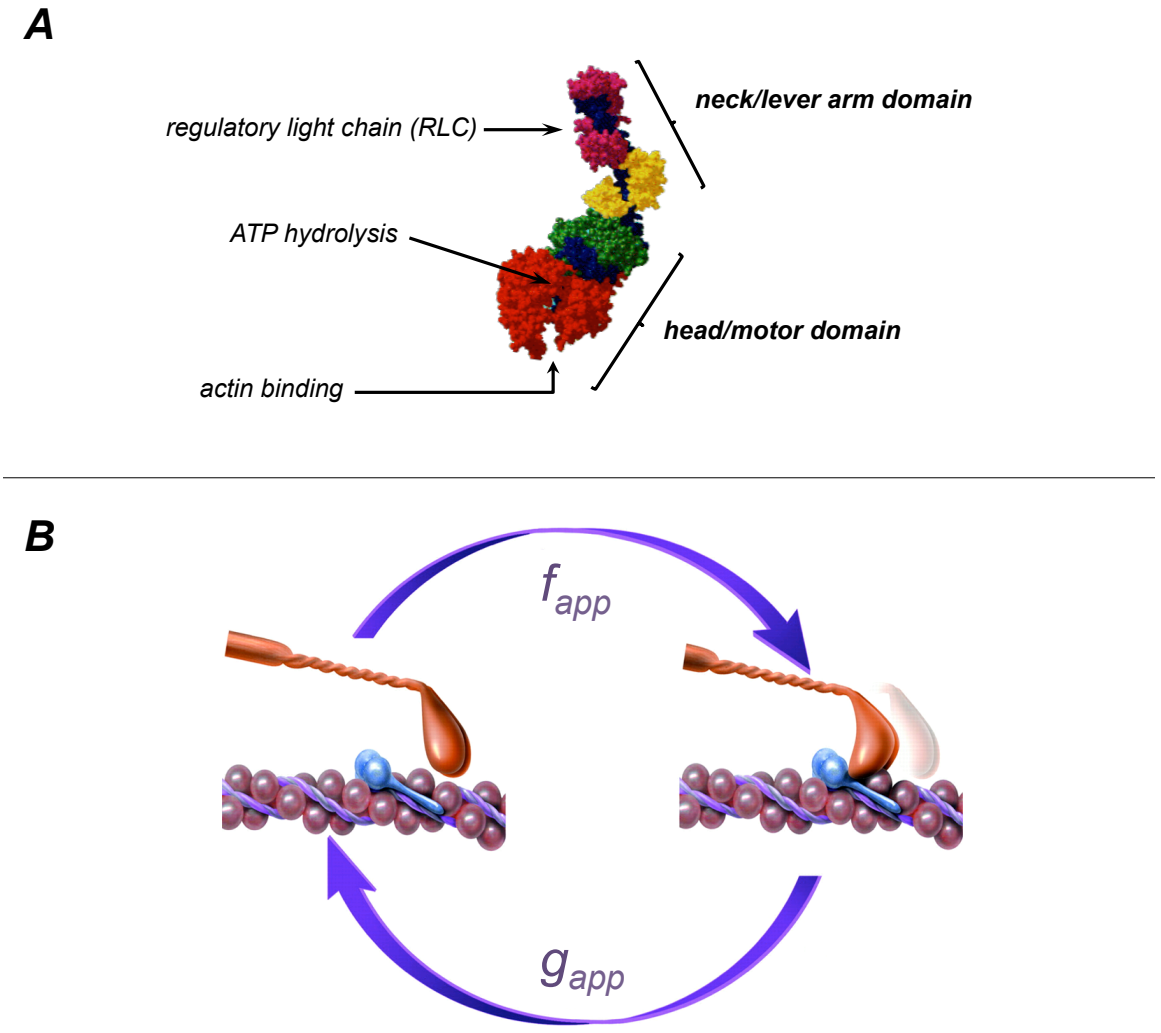


**A**. Important functional domains of the myosin head and neck regions.
**B**. The simplified two state model of crossbridge kinetics (Sieck and Regnier, 2001)

*Thin filament regulation of force and cooperative activation*

The thin filament (actin) contains the regulatory subunits troponin (Tn) and tropomyosin (Tm) that bind $Ca^{2+}$ and help to expose the myosin binding sites for the formation of force-producing crossbridge interactions. Each regulatory unit in the helical chain contains a Tn and Tm molecule that spans seven actin molecules ($A_7$TnTm)(Gordon et al., 2000). In addition to housing the regulatory structures that permit the binding of myosin and ultimately force transduction, the thin filament complex also serves an important function by propagating the activation signals within the sarcomere (adjacent Tm molecules overlap each other)(Moraczewska, 2002).

The three-state model described by McKillop & Geeves (1993) describes the thin filament as *blocked*, *closed,* or *open* with respect to activation. In the *blocked* state, the binding of myosin to actin is prevented by the troponin-tropomyosin complex (i.e. the normal state of relaxed, inactivated muscle). When $Ca^{2+}$ is released from the SR it may bind with various ligands in the cell but a significant portion binds to troponin subunit C (TnC) due to its high $Ca^{2+}$ affinity; this signal weakens the actin-troponin association and partially exposes myosin binding sites within the regulatory unit (*closed state*)(McKillop and Geeves, 1993). In this state, myosin crossbridges may initially form weak interactions with the thin filament (McKillop and Geeves, 1993). The combined effect of $Ca^{2+}$ activation and weak crossbridge binding produces a conformational change in the Tn-Tm complex that fully exposes actin-binding sites, a signal which is propagated within and between regulatory units (*open state*)(Moraczewska, 2002). Myosin crossbridges that have hydrolyzed ATP ($ADP{\bullet}P_i$) may then bind to actin binding sites as long as the thin filament remains in the *open state*. In this scheme, the activation of the thin filament fluctuates dynamically and is influenced by both the presence of myoplasmic $Ca^{2+}$ and physical interactions with myosin crossbridges themselves (Gordon et al., 2000). However, the specific mechanisms that together influence the affinity for $Ca^{2+}$ binding to TnC and myosin crossbridge attachment are not completely understood. This concept of cooperativity between the myofilaments and their respective subunits is relevant to the current work, though studying these mechanisms is difficult and often limited to the study of single and skinned-fibres as well as isolated myofilament preparations. To this end, while muscle is generally understood to be activated and

controlled by $Ca^{2+}$ binding to TnC, the actual mechanism of muscle contraction at the protein level is likely more complex and nuanced than initially conceived.

A cooperative mechanism could be defined as an event where the outcome is dependent on contributions from multiple structures or components. In the context of muscle contraction, cooperativity most often describes the theory that both $Ca^{2+}$ signaling and myosin crossbridge strong-binding function together to regulate thin filament activation and force production. In addition, because the mechanism of force production by crossbridge cycling is order-dependent, the cooperative relationships that exist may be related temporally as well (Tanner et al., 2012). However, as we cannot directly assay thin filament activation in an intact muscle the following description of will briefly introduce cooperativity only in the context of the present experiments and as background to the discussion that follows. For a more comprehensive explanation please see Gordon et al. (2000) or Moraczewska (2002). Important cooperative relationships in skeletal muscle contraction with respect to the current work include the following:

- Myosin crossbridges that strongly attach to actin binding sites enhance Tm movement and structurally maintain the *open* status of the thin filament, cooperatively promoting activation within and possibly between neighboring regulatory units ($Actin_7TnTm$)(Gordon et al., 2000).

- Strongly bound myosin crossbridges may enhance the $Ca^{2+}$ binding affinity of TnC to propagate the activation process (Gordon et al., 2000).

- Myosin crossbridges that remain strongly bound and cycling can delay force relaxation in the time that follows the $Ca^{2+}$ transient (i.e. when myoplasmic $[Ca^{2+}]$ has diminished (Patel et al., 1998).

- During rapid shortening of activated skeletal muscle, myosin crossbridges rapidly detach to permit myofilament sliding (Edman, 1975). The detachment of these cycling crossbridges may contribute to the reduced activation state of the muscle observed during subsequent force redevelopment even in the presence of elevated myoplasmic $[Ca^{2+}]$ (Vandenboom et al., 2002).

The examples of cooperativity listed above share a common theme: myosin crossbridge binding, cycling, and detachment may be important contributors to the regulation of force production in skeletal muscle. Importantly, a central underlying mechanism responsible for force potentiation (myosin RLC phosphorylation) is understood to increase the rate of myosin crossbridge formation (detailed discussion

below). It is essential therefore to recognize that although force potentiation is a modulation of the normal force response in fast skeletal muscles, the mechanism(s) responsible for the effect may also contribute to the greater regulatory scheme especially during periods of force development, active shortening, and relaxation.

*The two-state model of myosin crossbridge kinetics*

The fine details that illustrate how force production occurs at the protein level may be too complex and nuanced to include when describing contractile function in an intact muscle. This thesis will therefore use the two-state model as conceived by Huxley (1957) and formalized by Brenner & Eisenberg (1986) and Brenner (1988)(see Figure 1), which compartmentalizes the various stages of the crossbridge cycle into two states; either *1)* strongly bound and producing force, or *2)* detached and not producing force. Specifically, the model introduces the rate constants $f_{app}$ and $g_{app}$ to describe the reciprocal processes of crossbridge attachment and detachment, respectively, and depicts the cyclic transitions between force-generating and non force-generating states that occur in the total pool of crossbridges during activation (see Equation 1 below).

$$\alpha FS = \frac{(f_{app})}{(f_{app} + g_{app})} \qquad (1)$$

In this model, the term $\alpha FS$ describes the proportion of myosin crossbridges that are transitioning to a force-producing state (i.e. attaching, $f_{app}$) as a fraction of the total crossbridges in the system ($f_{app}+g_{app}$). Assuming that the force produced by each cycling crossbridge is equal (Huxley, 1957), the force produced by the muscle should be proportional to the fraction of crossbridges that are bound and producing force. Using this approach, any theoretical modulation to $f_{app}$ or $g_{app}$ should affect the fraction of crossbridges that are actively cycling in the muscle and ultimately should be observable in the net force response of the muscle. The rate constant $f_{app}$ is controlled by the regulatory signal of $Ca^{2+}$ binding to TnC, which permits rigor binding and cycling of crossbridges (Brenner, 1988). In the context of the present experiments, the magnitude of $f_{app}$ is manifest in the rate of force development and is required for development of maximal force (i.e. $\alpha FS \rightarrow 1$ when $f_{app}$ is maximal). Conversely, the rate constant $g_{app}$ is not regulated by a singular factor or easily measureable, as a small population of crossbridges must detach to continue cyclic force production. When $g_{app}$ progressively

increases and $f_{app}$ decreases (i.e. $\alpha FS \rightarrow 0$), relaxation from force eventually occurs, but involves a more complex process that includes reduced myoplasmic [$Ca^{2+}$] and progressive thin-filament deactivation.

*Force-pCa relationship & $Ca^{2+}$ sensitivity*

The force-pCa relationship typically describes the resultant steady-state force produced in a skinned fibre preparation when exposed to a range of $Ca^{2+}$ concentrations (see Figure 3)(Konishi, 1998; Persechini et al., 1985). The classic sigmoidal shape is commonly used as an index to describe the $Ca^{2+}$ sensitivity of the muscle preparation and can be transformed by various factors, including changes to muscle length, pH, temperature, and importantly, myosin RLC phosphorylation (Sweeney and Stull, 1990). With respect to the current research the force-pCa relationship and concept of $Ca^{2+}$ sensitivity are important when linking the findings of mechanistic studies (i.e. skinned fibre) with observed changes in the force response of intact muscles (*in vitro* or *in situ*). Specifically, in intact muscle preparations, myoplasmic $Ca^{2+}$ concentrations can be controlled only indirectly via the intensity and/or rate of external stimulation: the force-frequency relationship is therefore used as a surrogate for the force-pCa relationship for understanding $Ca^{2+}$ sensitivity.

When evaluating changes in the force response of intact muscle preparations we make the assumption that force may be modulated by; *i)* changes in the amplitude of the $Ca^{2+}$ signal (i.e. $Ca^{2+}$ release transient), or *ii)* a variation in the force response to the signal itself (i.e. $Ca^{2+}$ sensitivity). To this end, the sections that follow will explore the regulation of $Ca^{2+}$ and modulations to $Ca^{2+}$ sensitivity that occur during and following sustained activation.

*Regulation of $Ca^{2+}$ signaling and homeostasis*

Activation of skeletal muscle begins with depolarization of the sarcolemmal membrane and results in the release of $Ca^{2+}$ into the myoplasm: a mechanism known as excitation-contraction coupling (ECC). The transmission of the activation signal involves electrical, mechanical, and chemical transduction, and can elicit a force response in only a few milliseconds. Although the ECC mechanism can be heavily modulated during repetitive use, many of these changes ultimately influence the dynamics of $Ca^{2+}$ release from and sequestration by the SR. This section will focus primarily on explaining how myoplasmic $Ca^{2+}$ levels are regulated during fast skeletal muscle contractions, and the

possible modulations that occur during and persist following activation which are relevant to force potentiation.

Fast skeletal muscles express structures and functional characteristics that allow rapid force development and relaxation, which are essential for cyclic movements like locomotion, jumping, and bounding (Schiaffino and Reggiani, 2011). In particular, for muscle fibres to work effectively they must be able to globally activate all myofibrils simultaneously; a requirement which is made possible via the t-tubule system that delivers the surface membrane depolarization signal to the interior of the fibre and the individual calcium release units. Calcium release units are macromolecular protein complexes that transduce the membrane voltage signal in the t-tubule system to the terminal cisternae of the SR, which wrap around each myofibril at each end of the sarcomere adjacent to the A-band region (i.e. the Triad)(Favero, 1999). The calcium release unit is comprised of a tetrad of dihydropyridine receptors that are bound to respective subunits of the ryanodine receptor (RyR) that together span the t-tubule/SR membranes (Beard et al., 2008). Upon sensing a voltage change, the DHPR receptors trigger an allosteric conformational change in the RyR that permits $Ca^{2+}$ release from the SR (Beard et al., 2009). The magnitude and rate of $Ca^{2+}$ release can be amplified by the $Ca^{2+}$ signal itself as increasing intracellular [$Ca^{2+}$] may activate the RyR, also known as calcium-induced calcium release (CICR)(Endo, 2009). The $Ca^{2+}$ release event is also coordinated by the involvement of calsequestrin (CSQ), which is located in the SR lumen, as well as transmembrane proteins triadin and junctin, which together may modulate RyR function (Beard et al., 2008; Favero, 1999, Beard et al., 2009). For example, in addition to storing large concentrations of $Ca^{2+}$ in close proximity to the RyR and release channels, CSQ is also understood to regulate the RyR via triadin and junctin (Beard et al., 2009; Murphy et al., 2009).

As the $Ca^{2+}$ signal is so important to myriad cell functions and has an energetic cost associated with maintaining homeostasis (i.e. sarco-endoplasmic reticulum $Ca^{2+}$ ATPase), it is not surprising that the release mechanism itself has redundant mechanisms and an intricate design of modulatory effectors. For example, a host of other controls have been implicated in the $Ca^{2+}$ release process, including regional nucleotide concentrations, $Mg^{2+}$, muscle glycogen content, and various other pharmacological or chemical molecules (i.e. caffeine)(Konishi, 1998; Steele and Duke, 2003; Favero, 1999).

As $Ca^{2+}$ diffuses into the myoplasm from each end of the sarcomere it rapidly binds to a variety of proteins with high $Ca^{2+}$ affinity, including troponin subunit C (TnC), secondary messengers such as calmodulin (CaM), and $Ca^{2+}$ buffers such as parvalbumin. However, almost as quickly as intracellular [$Ca^{2+}$] increases, it is actively recovered into the SR by the sarco/endoplasmic reticulum calcium ATPase (SERCA). It is the brevity of the signal (i.e. $Ca^{2+}$ transient) that allows fast skeletal muscles to cycle between force and relaxation so rapidly, and incredibly, the $Ca^{2+}$ transient in fast skeletal muscles is dissipated by the time the myofilament force response is fully activated (Konishi, 1998).

The role of SERCA in controlling intracellular [$Ca^{2+}$] is critical both at rest and during activation. The majority of SERCA proteins (~90%) are found in the longitudinal portions of the SR that span the sarcomere and are located in parallel to the myofilaments (Tupling, 2004). SERCA function is also highly regulated by the expression and abundance of SR proteins sarcolipin (SLN) and phospholamban (PLN), as well as direct effects of intracellular [$Ca^{2+}$] and other molecules (i.e. nucleotides, metabolic byproducts). At rest, SERCA maintains free myoplasmic [$Ca^{2+}$] at 50-100nM and total SR [$Ca^{2+}$] may exceed 20mM)(Beard et al., 2009). Although the energetic requirements for SERCA function will be discussed below, it is important to note that maintaining this $Ca^{2+}$ homeostasis and concentration gradient in skeletal muscle is an active process (~2 mol $Ca^{2+}$ per mol ATP are transported) and may represent a substantial component of ATP use in the cell (Smith et al., 2010). With respect to the task of $Ca^{2+}$ sequestration, CSQ plays an additional role in maintaining a very low concentration of free $Ca^{2+}$ in the SR lumen (≤1mM) by binding up to 50 $Ca^{2+}$ per molecule (Murphy et al., 2009), which greatly assists SERCA as it transports $Ca^{2+}$ across the SR membrane against such a substantial concentration gradient. Finally, much like the $Ca^{2+}$ release mechanism, SERCA function itself can be modulated by a host of other local factors that can influence the rate and amount of $Ca^{2+}$ sequestration. In the next section, these factors will be discussed as they relate to maintaining $Ca^{2+}$ homeostasis during sustained or repetitive activation.

*$Ca^{2+}$ handling and sensitivity during sustained activation*

The discovery that $Ca^{2+}$ release is attenuated during sustained activation and is at least partially responsible for the decrease in force observed during fatigue has been well documented but is not completely understood (as reviewed by Allen et al., 2008). This

hypothesis has been tested in numerous studies that have been able to restore force levels in fatigued muscles using pharmacological $Ca^{2+}$ release agonists such as caffeine (Westerblad and Allen, 1991). The reduction in $Ca^{2+}$ release during or following heavy use may be attributed to a variety (or combination) of mechanisms, including; *1)* ECC failure occurring between the neuromuscular junction and the calcium release unit, *2)* direct inhibition of the RyR release channel, *3)* a reduced SR $Ca^{2+}$ load, or *4)* structural/functional modification of the calcium release unit (Favero, 1999; Allen et al., 2008). Of these factors, acute decreases in $Ca^{2+}$ release are most likely due to local changes in the intracellular milieu in the triad region and are metabolic in nature (i.e. ↑ ADP/AMP/IMP/$P_i$/$Mg^{2+}$/ROS, ↓ ATP, PCr, glycogen)(Steele and Duke, 2003). During severe fatigue and following extended use the magnitude of $Ca^{2+}$ release may be further inhibited by a reduced SR $Ca^{2+}$ load or gradient, which may arise from insufficient SERCA activity, buffering of free calcium by inorganic phosphate in the SR, or progressive intracellular $Ca^{2+}$ leak (Allen et al., 2008). Finally, the reduction in muscle force capacity that persists long after activity has terminated, especially at low frequencies, may also be related to $Ca^{2+}$ release dysfunction (Tupling, 2004; Westerblad et al., 2000). A variety of factors have been shown to depress SERCA-mediated $Ca^{2+}$ transport during sustained use and augmented intracellular free [$Ca^{2+}$] levels have been observed during prolonged activation (Westerblad et al., 2000); evidence that $Ca^{2+}$ homeostasis cannot be maintained indefinitely. It has further been demonstrated that persistently elevated free [$Ca^{2+}$] levels can modify the structure and function of the calcium release unit by physically uncoupling the DHPR and RyR (Tupling, 2004), and the deficit is dependent on the intensity and duration of the exposure.

Considered together, the modulations to normal $Ca^{2+}$ signaling described above are just part of the significant challenge that working muscles face in maintaining the optimal compartmentalization and homeostasis of $Ca^{2+}$ in the muscle fibre. The ultimate outcome of these mechanisms is the reduced $Ca^{2+}$-activated contractile function that is characteristic of working fast skeletal muscles. This suboptimal function is further exacerbated by decreases in the $Ca^{2+}$ sensitivity of the contractile apparatus that occur in response to metabolic disturbances to homeostasis, especially in tissues that rely on glycolytic and high-energy phosphate-based energy provision (Cooke, 2007). In particular, the accumulation of metabolic byproducts, progressive acidification of the muscle fibre, and disrupted redox status of the fibre may directly inhibit various stages of

the crossbridge cycle itself and the efficacy of force production (Cooke, 2007). For example, the rapid accumulation of inorganic phosphate ($P_i$) that occurs in fast skeletal muscles has frequently been linked to fatigue, and skinned-fibre models have demonstrated a strong depressive effect of 20-30mM [$P_i$] on maximal force production ($F_{max}$) and $Ca^{2+}$ sensitivity (Allen and Westerblad, 2001). Moreover, similar experiments with elevated [ADP] (~200μM) have demonstrated a substantial inhibition of maximal shortening velocity ($V_{max}$) and myofibrillar ATPase rates in skinned rabbit psoas fibres (Cooke, 2007).

*Activation history-dependence of contractile function*

Early characterization of motor unit and fibre types often differentiated muscle tissue by its predisposition to be fatigued, and it has become clear that the reduced contractile function in fast skeletal muscles during sustained activation is the inevitable tradeoff for the capacity to produce maximal force, shortening velocity, and power. As discussed above, skeletal muscles likely display reduced activation signaling and an inhibited response to the signal itself with prolonged use. This temporal association is the rationale for studying how certain features of fast skeletal muscles that increase $Ca^{2+}$ sensitivity (i.e. force potentiation) contribute to contractile performance (Grange et al., 1993). Fatigue is a classic example of history dependence; the concept that contractile performance of skeletal muscle is often influenced by its activation history. Importantly, contractile performance can also be augmented by previous activity, and this specific feature of fast skeletal muscle forms the basis of the current work.

### *Activity-dependent potentiation*

Skeletal muscle contractile performance can be augmented by recent activation, an observation that has been frequently documented throughout the 20th century. However, while the potentiation of muscle force has been well characterized in a variety of experimental models and paradigms, a unifying term has only recently been suggested: activity dependent potentiation therefore describes the enhanced amplitude of a submaximal contraction by prior activation (MacIntosh, 2010). This term is meant to encompass the names commonly used to describe this type of effect, including Posttetanic Potentiation (PTP), Staircase Potentiation or Treppe, and Postactivation Potentiation (PAP).

*Posttetanic Potentiation (PTP)*

The acute but transient increase in isometric twitch force that follows a period of electrical stimulation is known as Posttetanic Potentiation (PTP). Although the activation that serves to potentiate the muscle preparation is generally elicited at high frequencies (i.e. tetanic stimulation), extended low frequency stimulation has also been employed with comparable outcomes (refer to Vandenboom et al., 2013 for a recent review). PTP is most commonly expressed as a percentage change in force (or some other contractile measure) between identical events that occur before and soon after a potentiating or 'conditioning' stimulus (see Figure 2 for schematic). This paradigm has also been extended to include more complex contractile events such as incompletely fused tetani (Gittings et al., 2012) and concentric contractions (Grange et al., 1998), though the isometric twitch has long been the standard indicator for PTP. One of the challenges in precisely quantifying PTP has been the counteracting influence of fatigue on force production that may obscure the anticipated effect; in fact, the coexistence of these conflicting mechanisms has been studied but is still not completely understood (MacIntosh and Rassier, 2000). The magnitude of the PTP effect on the isometric twitch is generally modest (~20-30%) and transitory; the augmented force response of the muscle preparation remains near maximal following the termination of the potentiating stimulus (~10-20s) and progressively dissipates over a period of seconds to minutes (Close and Hoh, 1968; Krarup, 1981).

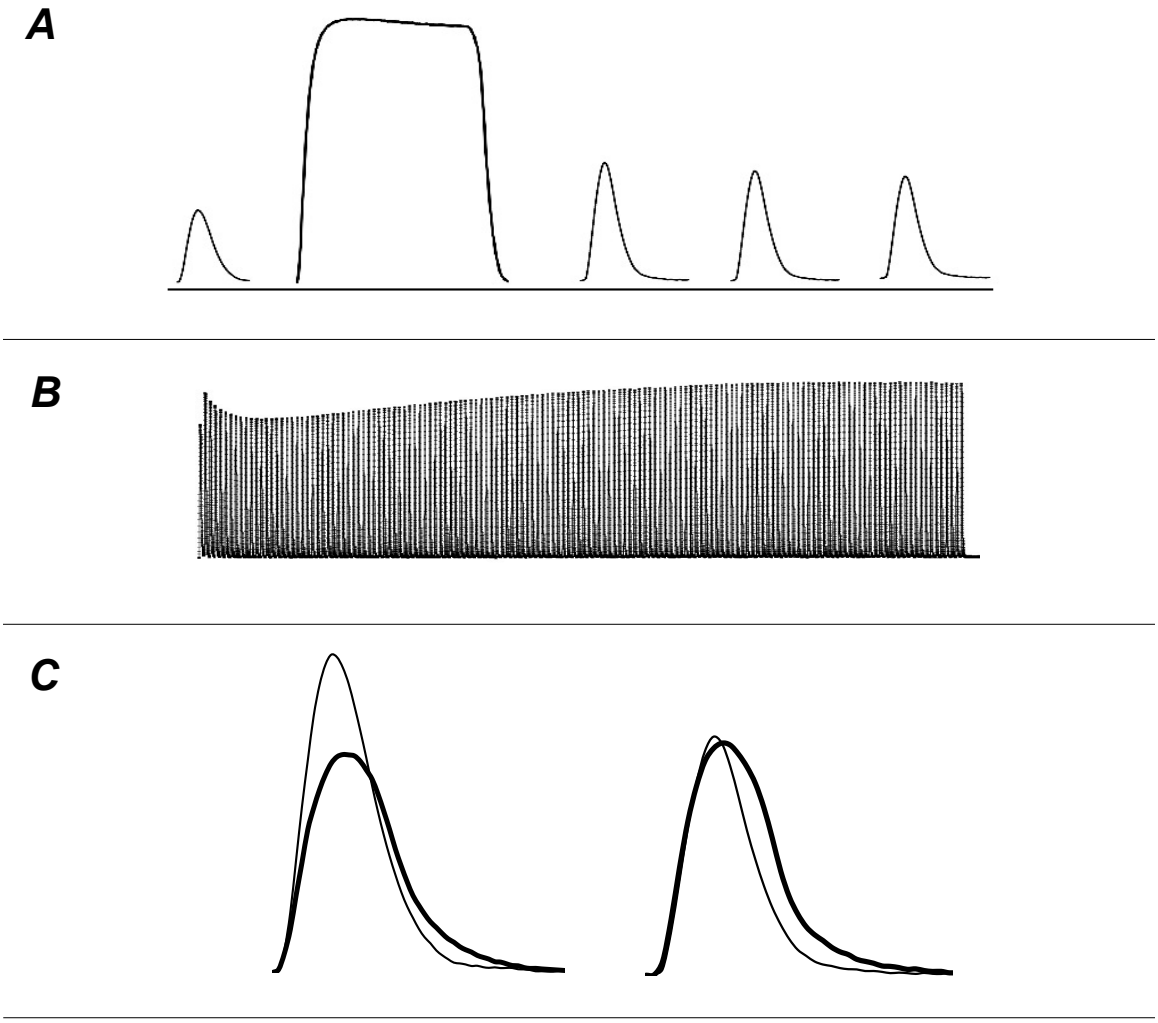


*Figure 2.2. Activity Dependent Potentiation in skeletal muscle*

**A**. Posttetanic Potentiation (PTP) of wildtype mouse EDL muscle (*in vitro*, 25° C) following a single high frequency stimulus (100 Hz for 1 sec)

**B**. Staircase Potentiation in wildtype mouse EDL muscle (*in vitro*, 25° C) during 15 sec of 10 Hz stimulation

**C**. Posttetanic twitch responses of EDL muscles (*in vitro*, 25° C) from wildtype (left) and skMLCK$^{-/-}$ (right). Thick line is control or pre-tetanic twitch while thin line is post-tetanic twitch in both genotypes.

*Staircase Potentiation*

One of the earliest observations of history dependence in skeletal muscle was the progressive increase in the amplitude of repeated low frequency stimulation, a phenomenon that was termed Treppe or the 'Bowditch Effect' (Bernard et al., 1941; Brown & Tuttle, 1926; Gruber, 1922). Staircase potentiation has since been characterized in a variety of experimental models, although its appearance is largely dependent on factors specific to each muscle preparation and environmental conditions such as length and temperature. Similar to PTP, the phenomenon of staircase potentiation has most often been studied at low frequencies (~5-10Hz), but evidence suggests that even brief incompletely-fused tetani up to ~70Hz may increase in amplitude when elicited in close succession (MacIntosh and Willis, 2000). The characteristic timeline for staircase potentiation differs somewhat from PTP, as the force level of individual pulses often initially decline (5-10%) before increasing progressively in a stimulus train that may persist for an extended period of time. A graphic representation of staircase potentiation is shown in Figure 2, Panel B.

*Postactivation Potentiation (PAP)*

In human muscle, the acute increase in magnitude of an evoked contraction that results from previous voluntary activation is referred to as Postactivation Potentiation (PAP). Generally PAP is studied using a bracketed approach, like PTP, where a given event is compared before and after a brief period of high-intensity voluntary activation (usually in the form of an MVC). However, staircase potentiation has also been successfully studied in human muscle using electrical stimulation (Desmedt and Hainaut, 1968). To identify PAP *in vivo* researchers must associate the observed change in force production with a measurement of the activation level of the muscle (i.e. M-wave amplitude) to determine whether the operative muscle displayed an improved contractile response without a concomitant change in the degree of activation (i.e. evidence that motor unit recruitment is not responsible for the increase in force observed). This model is limited from a mechanistic standpoint but has been important in supporting the theory that force potentiation may significantly improve human muscular performance (Tillin and Bishop, 2009). In fact, interest in this topic has been significant in recent years with many review papers (Bishop, 2003; Hodgson et al., 2005; MacIntosh et al., 2012; Sale, 2002; Tillin and Bishop, 2009) and several studies that have explored the possible acute

effect of potentiating activity on performance (Gossen and Sale, 2000; Hamada et al., 2000; Mitchell and Sale, 2011). Conclusive evidence that PAP is effective as a mechanism to increase functional performance has been elusive, although some indication exists that powerful movements like jumping can be improved following potentiating activity (Tillin and Bishop, 2009). It is tempting to attribute increases in functional performance that result from a specific warm-up to PAP; however, without demonstrating an increased response to an evoked stimulation or controlling for muscle activation the use of the term PAP or potentiation may in some cases be misleading or inappropriate. If the ultimate goal of the research itself is to detail the specific effect of previous activation on muscle performance, other *in vitro* and *in situ* mammalian models may be preferable. *In vivo* models of PAP study may also be subject to confounding factors that contribute to the effect of warm-up activity on muscle function, including enhanced muscle temperature, neuromuscular conduction rates, blood flow, and/or psychological readiness (as reviewed by Bishop, 2003).

*Mechanistic basis for activity dependent potentiation*

An increased force response of a muscle (i.e. distal to the depolarization of the surface membrane) could theoretically be caused by an increase in the $Ca^{2+}$ sensitivity of the myofilaments or an increase in $Ca^{2+}$-activated force (i.e. amplified $Ca^{2+}$ signal). There is evidence to suggest that both mechanisms contribute to activity dependent potentiation (Vandenboom et al., 2013); however, the relative contribution of each is likely dependent on the stimulation pattern and/or experimental paradigm employed. In this regard, PTP is most often associated with an increase in $Ca^{2+}$ sensitivity while staircase potentiation is associated with altered $Ca^{2+}$ homeostasis (Vandenboom et al., 2013).

The most extensive mechanistic work related to activity dependent potentiation, spanning multiple decades, has been the study of augmented $Ca^{2+}$ sensitivity by posttranslational modification to the myosin molecule via phosphorylation of the regulatory light chains (RLC). The following section will therefore highlight the regulation and functional significance of myosin RLC phosphorylation in fast skeletal muscle.

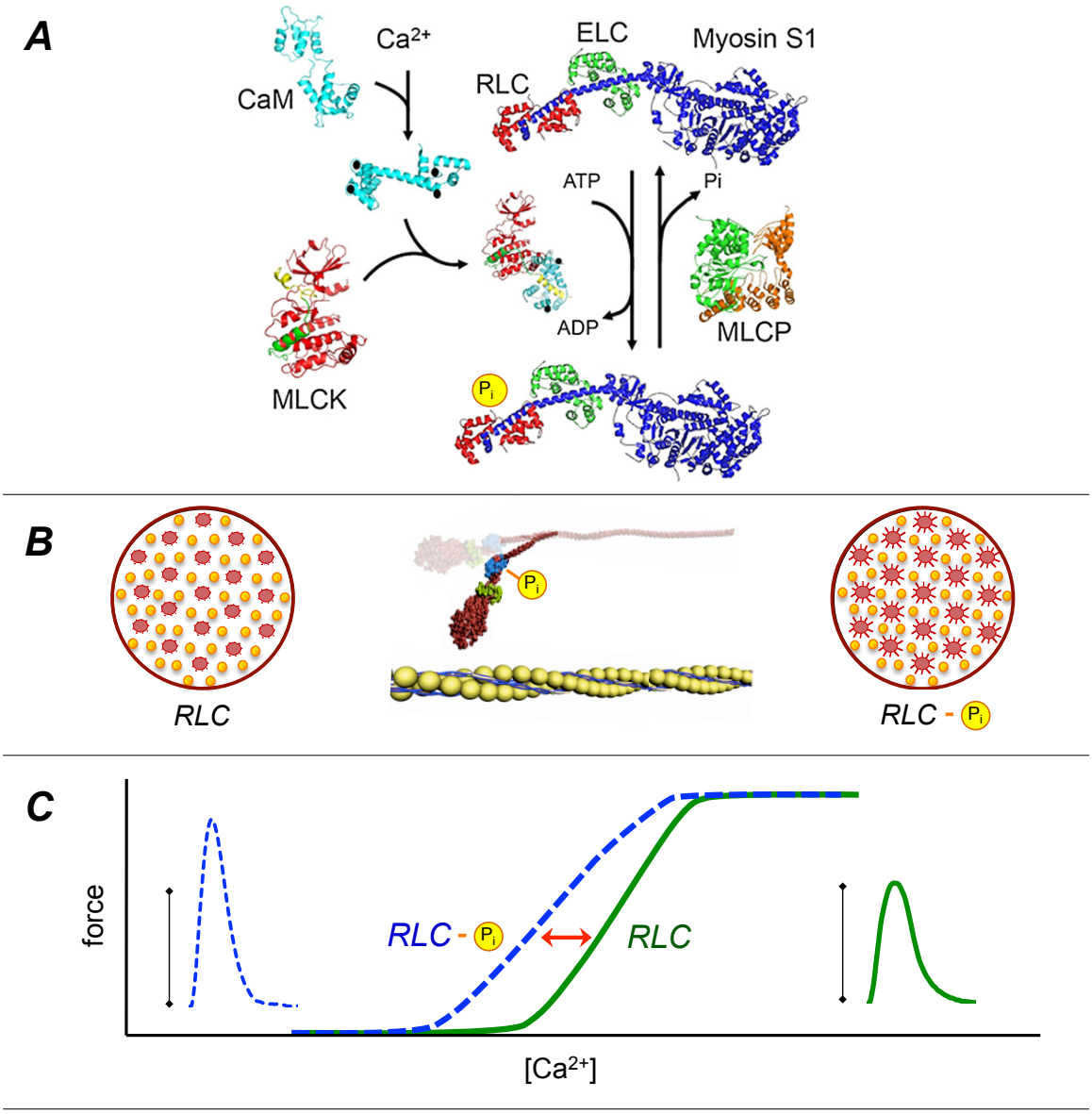


*Figure 2.3. Myosin RLC phosphorylation: Regulation, Structure, and Function*

**A**. Regulation of myosin RLC phosphorylation by skMLCK & MLCP (Stull et al., 2011)
**B**. Structural consequence of myosin RLC phosphorylation at the crossbridge level and reduced interfilament spacing schematic (myofibril cross-section view)
**C**. Myosin RLC phosphorylation causes a leftward shift in the force-$Ca^{2+}$ relationship at submaximal [$Ca^{2+}$] and represents a change in $Ca^{2+}$ sensitivity

*Myosin RLC phosphorylation: Regulation*

The observation that the regulatory light chain (RLC) of myosin is phosphorylatable initially suggested that myofilament function itself might be modulated at the protein level in addition to the primary excitation-contraction coupling mechanism that regulates force (Perrie et al., 1973; Pires et al., 1974). Moreover, the study of contraction-relaxation cycles in frog muscle demonstrated that RLC phosphate content was similarly elevated for muscles stimulated at resting length and muscle stretched beyond the point of myofilament overlap, suggesting that phosphorylation was likely stimulation-based rather than mechanical (Barany et al., 1979). The regulatory scheme for myosin RLC phosphorylation, as well as the primary structural and functional properties associated with it, are shown in Figure 3.

It is well established that intracellular [$Ca^{2+}$] is the signal that initiates phosphorylation of the myosin RLC via calmodulin (CaM) and a dedicated enzyme, skeletal myosin light chain kinase (skMLCK)(reviewed by Stull et al., 2011). The opposing dephosphorylation of myosin RLC in skeletal muscle occurs through the action of a ubiquitous type-1 protein phosphatase (MLCP), encoded by myosin phosphatase targeting subunit 2 (MYPT2)(Manning and Stull, 1982). Importantly, the maximal rate of RLC phosphorylation may be up to 50-fold greater than the rate of RLC dephosphorylation in intact skeletal muscles (Stull et al., 2011). This imbalance in the maximal activity of skMLCK versus MLCP is central to the concept of history-dependence as it permits the rapid application and slow removal of the phosphorylation mechanism. Moreover, although the influx of intracellular [$Ca^{2+}$] independently and simultaneously activates both myosin RLC phosphorylation and force production, the formation of the $Ca^{2+}{}_4$•CaM•skMLCK complex occurs at a much slower rate than $Ca^{2+}$•TnC binding (Stull et al., 2011). Consequently, RLC phosphorylation may continue to occur during and following the force response of the muscle, or until intracellular [$Ca^{2+}$] has decreased and $Ca^{2+}{}_4$•CaM has dissociated from skMLCK (Stull et al., 2011). Recent evidence has shown that the duration and intensity of the muscle stimulation (i.e. [$Ca^{2+}$] not [CaM]) determines the fraction of skMLCK that is activated (Ryder et al., 2007), while the relative abundance of skMLCK is the primary limiting factor that determines the capacity for increasing fractional myosin RLC phosphate content (i.e. mol P-skRLC/mol skRLC)(Ryder et al., 2007).

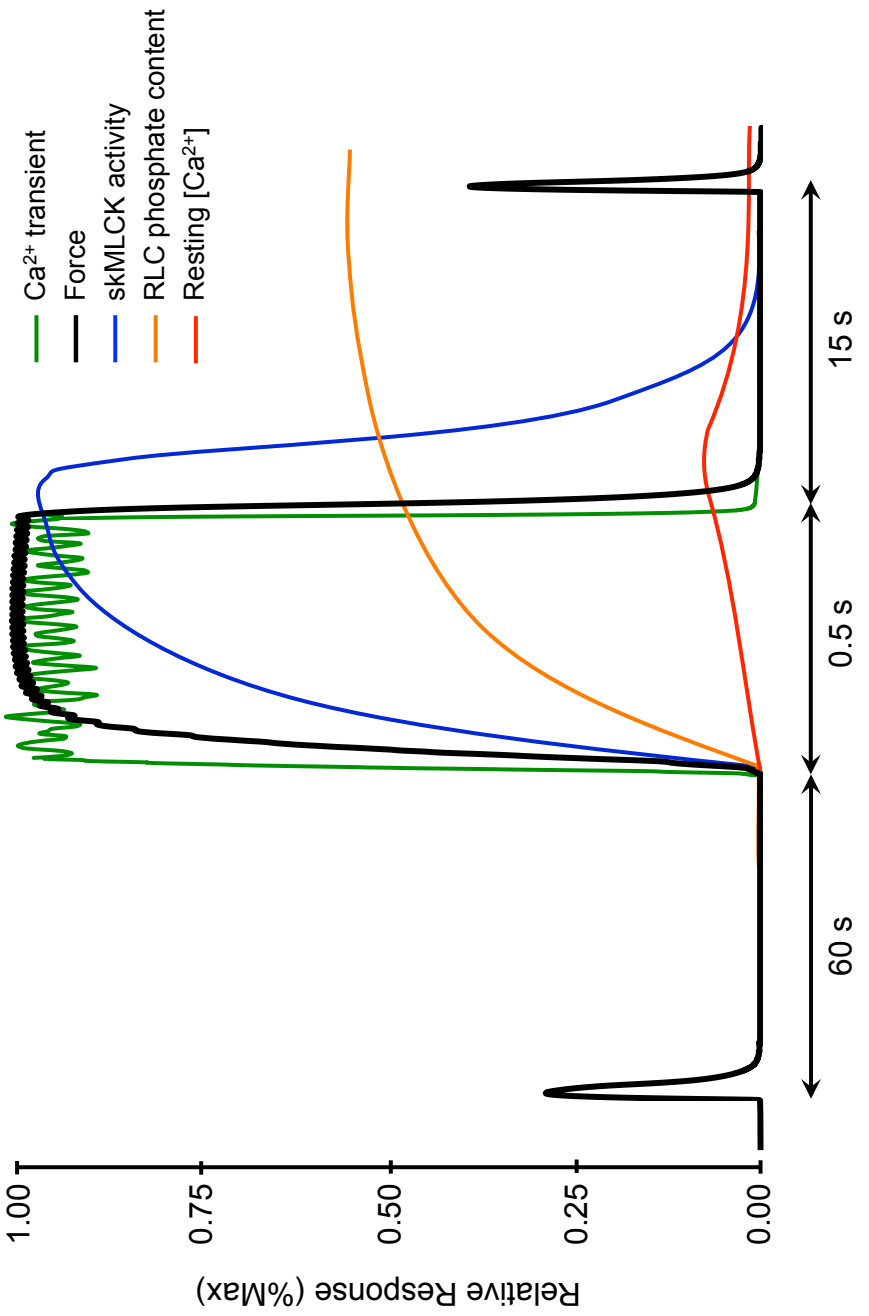


Figure 2.4. $Ca^{2+}$-activated myosin RLC phosphorylation cascade
Summary of the regulatory pathway that leads to elevated myosin RLC phosphate content and posttetanic potentiation (PTP) following a brief high frequency tetanic stimulation. Traces based on data from Stull et al., 2011 and Smith et al., 2013.

Secondary regulation of myosin RLC phosphorylation is present in the relative expressions of skMLCK versus MLCP, representing an important point of distinction between skeletal muscle fibre types (as reviewed by Stull et al., 2011). For example, in the continuum of myosin heavy chain fibre types, the ratio of skMLCK to MLCP is highest for primarily glycolytic fibre types and markedly decreased in slower more oxidative fibres. To this end, recent evidence has shown that mouse lumbrical muscles with a predominantly type II fibre type profile fail to display any stimulation-induced myosin RLC phosphorylation due to skMLCK and MLCP levels that more closely resemble soleus than EDL muscles (Smith et al., 2011). This report is consistent with other work that has correlated the potentiation of twitch force to the ratio of skMLCK and MLCP expression, as well as myosin RLC phosphate content, in mouse EDL, soleus, and lumbrical muscles (Ryder et al., 2007). Despite this evidence, it is presently unclear whether the limited capacity to phosphorylate the RLC in type IIA and IIX fibres may contribute to force potentiation in mixed muscles, or whether this phenomenon is uniquely limited to type IIB fibres. The observation that force potentiation is present and robust in human skeletal muscles (i.e. in the absence of type IIB fibres) may suggest that varying expression of proteins other than the myosin heavy chain may contribute to the link between myosin RLC phosphorylation and force potentiation.

In addition to the enzyme expression differences (i.e. skMLCK vs. MLCP) that may exist between fibre types, there may be other reasons that explain why myosin RLC phosphorylation and potentiation are conserved in only the fastest fibre types. For example, although moderate levels of RLC phosphorylation can be attained in soleus muscles with sustained stimulation (Moore and Stull, 1984) or transgenic up-regulation of skMLCK (Ryder et al., 2007), no concomitant force potentiation is observed. One possible explanation for this apparent inconsistency may be the heterogeneity of myosin RLC isoform expression, which may influence the mechanistic link between RLC phosphorylation and force potentiation. It has been shown that up to five distinct isoforms of the RLC exist in skeletal muscle (MLC1s, MLC2s, MLC1f, MLC2f, MLC3f)(Bicer and Reiser, 2004; Gonsalez et al., 2002) and meaningful shifts in expression occur during slow to fast fibre transitions with hindlimb suspension and/or Clenbuterol treatment (Bozzo et al., 2003; Stevens et al., 2000). A progressive shift to faster RLC isoforms was accompanied by greater RLC phosphorylation capacity in the murine hindlimb muscles, although it is unclear whether this observation occurred independent to relative changes

in myosin heavy chain expression. Interestingly, similar shifts in RLC and myosin heavy chain expression have been demonstrated in fast to slow transitions in fibre type as well (Bozzo et al., 2005). While the precise links between isoform expression and RLC phosphorylation are not well defined, it is plausible that differential RLC isoform expression could represent a manner of phenotypic control that determines whether or not a skeletal muscle potentiates. Although speculative, fast isoforms of the myosin RLC may be more amenable to phosphorylation during stimulation, or the structural changes that result from phosphorylation may be myosin RLC isoform-dependent.

*Myosin RLC phosphorylation and myofilament structure*

Phosphorylation of the RLC results in a structural alteration to the myosin molecule that ultimately affects the crossbridge cycle in steps that precede the powerstroke (i.e. crossbridge attachment, or $f_{app}$)(Sweeney and Stull, 1990). This structural alteration forms the basis for the increase in $Ca^{2+}$ sensitivity that is manifest as force potentiation (Levine et al., 1998). At rest or when non-phosphorylated, the head domain of each myosin exists in a tightly ordered configuration along the thick filament backbone (Levine et al., 1996). When phosphorylated, this configuration becomes highly disordered as myosin heads translate away from the thick filament backbone (Levine et al., 1996). The basis of this effect may be electrostatic charge repulsion between the negatively charged thick filament backbone and the negatively charged phosphate moiety that is bound to the head domain (Alamo et al., 2008). Disordering of the myosin heads with RLC phosphorylation effectively decreases the interfilament spacing between myosin and actin (Yang et al., 1998) and increases the efficacy of crossbridge binding to TnC during activation (Metzger et al., 1989). Specifically, is has been proposed that the structural changes produced by RLC phosphorylation may allow the formation of the actomyosin complex via $Ca^{2+}$-activation alone and without additional cooperative activation (as discussed by Vandenboom et al., 2013). While the structural outcome associated with myosin RLC phosphorylation is understood to occur within the myosin level arm domain, there is also evidence to suggest that an intact myofilament lattice is required to see functional changes in motor function. For example, Greenberg et al. (2009) did not observe a phosphorylation-dependent shift in $Ca^{2+}$-sensitivity during *in vitro* motility assays where myosin molecules were isolated from the thick filament backbone. Moreover, Metzger et al. (1989) were able to disrupt the potentiation of

isometric force at low [$Ca^{2+}$] by removing the crossbridge-binding subunit of troponin (TnC) in skinned skeletal muscle fibres. Together these studies support the idea that interfilament interactions (i.e. within and between myosin and actin proteins) are important for the myosin RLC phosphorylation-mediated changes in crossbridge structure and function that modulate muscle force.

Unlike smooth muscle function, myosin RLC phosphorylation via skMLCK is not usually considered part of the regulatory scheme for force production in skeletal muscle (i.e. $Ca^{2+}$-activated force is possible without it). However, there is some evidence that skMLCK itself may exert an inhibitory effect on crossbridge formation (i.e. myosin-actin binding) in the non-activated state, as was shown during *in vitro* motility assays (Fujita et al., 1999). This inhibition was removed in the presence of $Ca^{2+}$ and CaM and was observed to be independent of the phosphorylation status of the preparation (Fujita et al., 1999). Therefore, although RLC phosphorylation is not required for force production to occur, skMLCK may modulate the efficacy of crossbridge formation at the level of the myosin crossbridge (Fujita et al., 1999). To our knowledge, this example of crossbridge-binding inhibition has not been studied in intact muscles; however, it could be a mechanism that contributes to the increase in rate of force development that is characteristic of potentiated muscles.

*Functional consequences of myosin RLC phosphorylation and crossbridge kinetics*

The disordering of myosin crossbridges that occurs with myosin RLC phosphorylation increases the $Ca^{2+}$ sensitivity of the myofilaments, which means that for a given myoplasmic [$Ca^{2+}$] or activation signal there are more rapid and numerous force-producing interactions between myosin and actin. To this end, Sweeney & Stull (1990) conceptualized a model that explains how the unitary effect of myosin RLC phosphorylation on crossbridge function translates into altered whole muscle function: the foundation of this phenomenon is an increase in the rate of crossbridge attachment ($f_{app}$) during activation without a change to crossbridge detachment rate ($g_{app}$)(see also Brenner, 1988; Metzger et al., 1989). The increase in $f_{app}$ (and rate of force development in intact muscles) by myosin RLC phosphorylation is proportional to the fractional phosphate content incorporated onto the thick filament by skMLCK (Vandenboom et al., 1997). However, although the effect of myosin RLC phosphorylation on crossbridge kinetics should be ubiquitous, Sweeney and Stull (1990) found that steady state force

production of skinned fibres was potentiated only at submaximal intracellular [$Ca^{2+}$] but not at saturating levels. It was concluded that myosin RLC phosphorylation influences force in an analogous manner to $Ca^{2+}$ binding to troponin (i.e. by increasing $f_{app}$); however, the causal link between myosin RLC phosphorylation and force potentiation was dependent on the activation level of the thin filament regulatory system. Consequently, the beneficial effect of myosin RLC phosphorylation on force production via crossbridge attachment rate diminishes as intracellular [$Ca^{2+}$] and force levels rise (Sweeney and Stull, 1990).

This relationship has important physiological significance with respect to muscle function as it implies that the greatest effect of myosin RLC phosphorylation on contractile function should be at low levels of activation and/or the left side of the force-frequency relationship. Research studying potentiation across the isometric force-frequency relationship supports this explanation, as the potentiation of forces by myosin RLC phosphorylation in intact muscles is limited to low frequencies at or below levels required for fusion (≤15Hz)(Vandenboom et a., 1993). As a result of this work and others, the isometric twitch has and continues to be the standard indicator of force potentiation in skeletal muscle due to its propensity to be augmented. Conversely, isometric stimulation that produces summated tetani (i.e. 100-200 Hz) is generally considered to be insensitive to potentiation by myosin RLC phosphorylation (Gittings et al., 2011; Vandenboom et al., 1993) as this situation represents a fully activated contractile system. However, it has been shown that brief isometric stimulation (2-5 pulses) at moderate frequencies (up to 70Hz) display force potentiation in rat gastrocnemius muscle in situ at 35°C (MacIntosh and Willis, 2000). Other work using similar methods has shown that contractile function during very brief isotonic contractions up to 400Hz may be potentiated (MacIntosh et al., 2008). This research and others (Vandenboom et al., 1995) highlight the primary outcome of elevated myosin RLC phosphorylation on muscle contractile function: an enhanced rate of force development that exists at all levels of activation. Therefore, it is apparent that frequency of stimulation on its own cannot predict the magnitude of force potentiation. Hence, potentiation of skeletal muscle force at any frequency should be theoretically possible during the rising phase of the response provided stimulation duration is brief and peak force is not reached.

In addition to stimulus duration, other evidence complicates the relationship between force potentiation and stimulation frequency. For example, the magnitude of twitch force potentiation at the same level of myosin RLC phosphorylation is significantly greater during muscle shortening (vs. isometric)(Grange et al. 1995) and is positively associated with increasing shortening speeds (Caterini et al., 2011). Therefore, the efficacy of myosin RLC phosphorylation to potentiate force appears to be dependent on various other factors including muscle length, contraction type, and the dynamic contractile conditions that exist in working muscles. Further work is required to better understand the relationship between force potentiation and frequency of stimulation under dynamic conditions if the effect of myosin RLC phosphorylation on physiological function *in vivo* is to be better understood.

*Posttetanic Potentiation (PTP) and dynamic muscle function*

Considering muscle function only in the context of isometric and/or isotonic conditions may not be particularly useful when attempting to understand *in vivo* muscle function. While some muscles are devoted to maintaining stability during movement and operate near isometric, movement and locomotion are produced by working muscles that produce force against varying loads during shortening. Josephson (1993) notes that the rate at which muscles perform work depends on force production, the velocity at which it shortens, and the kinetics of force development and relaxation. Force potentiation via myosin RLC phosphorylation has the potential to affect all aspects of dynamic muscle function and is particularly relevant to the work in this thesis. There is general consensus that dynamic muscle function is more sensitive to the effect(s) of potentiation as compared to isometric (Vandenboom et al., 2013); however, the complex interplay between potentiation and active muscle shortening is not well understood.

Grange et al. (1995) were among the first to investigate how the augmented force response associated with myosin RLC phosphorylation influences dynamic function. Their work with mouse EDL muscles showed that both the rate and extent of displacement (i.e. muscle shortening) were potentiated during zero-load clamp and afterloaded twitches following a high frequency potentiating stimulus- an effect that enhanced both work and power during the brief activation period. Similar results have been observed during repetitive stimulation of the medial gastrocnemius muscle *in situ* (i.e. staircase potentiation), displaying that the extent and velocity of isotonic shortening

can be potentiated during brief activation even at moderate and high frequencies (70-400Hz)(Macintosh and Bryan, 2002; Macintosh et al. 2008a). These studies imply that a simple increase in force development by potentiation might allow work to be performed at a greater velocity (i.e. shorter time), or alternatively, permit a set amount of work or power to be performed at a lower activation level (i.e. frequency or duration of stimulation).

The relationship between myosin RLC phosphorylation and dynamic muscle function has been further investigated in mouse EDL muscle using the work loop technique (Caterini et al., 2011; Grange et al., 1998), where single pulses (i.e. twitches) are applied during repetitive sinusoidal length changes. This approach may be physiologically relevant as it quantifies the total work produced during a twitch while both force and shortening velocity are variable (not 'clamped'). Work and power produced during these rhythmic stimulation patterns are readily potentiated following high frequency stimulation (Grange et al., 1998), and importantly, the relative increase in contractile function is graded to myosin RLC phosphate content (Xeni et al., 2011). Further evidence from this line of work has indicated that concentric twitches display greater potentiation than isometric (at the same level of myosin RLC phosphorylation)(Xeni et al., 2011) and that potentiation of concentric force is positively associated with increasing shortening velocities (Caterini et al., 2011).

The research mentioned above provides a strong foundation for additional study of myosin RLC phosphorylation and for developing a model that describes the role that potentiation plays in modulating dynamic contractile function. Of particular interest would be the systematic investigation of contractile potentiation across the activation frequency and shortening velocity spectrums, as well as detailing what it is about actively shortening muscle that makes it particularly amenable to the effects of potentiation.

*Transgenic mouse models: Effect of skMLCK knockout and upregulation*

Important progress in the study of myosin RLC phosphorylation and activity-dependent potentiation has been the development of transgenic mice that do not express skMLCK (i.e. knockout, $^{-/-}$), or alternatively, overexpress skMLCK (Ryder et al., 2007; Zhi et al., 2005). In skMLCK$^{-/-}$ animals, myosin RLC phosphorylation is interrupted selectively in skeletal muscles but remains intact in cardiac and smooth muscles where it is crucial for viability and survival. Zhi et al. (2005) were the first to demonstrate the

attenuation of PTP and staircase in skMLCK$^{-/-}$ muscles that do not exhibit an increase in myosin RLC phosphorylation following stimulation. The causative link between myosin RLC phosphorylation and twitch potentiation became more compelling when Ryder et al. (2007) reported that a ~22-fold increase in skMLCK expression contributes to greater myosin RLC phosphorylation and potentiation in EDL muscles. However, in addition to satisfying many of the uncertainties regarding myosin RLC phosphorylation in skeletal muscle, these studies produced additional mechanistic questions. For example, although PTP was completely attenuated in skMLCK$^{-/-}$ muscles, significant staircase potentiation remained present in the absence of myosin RLC phosphorylation (twitch forces increased to 30% in skMLCK$^{-/-}$ vs. 55% in wildtype)(Zhi et al., 2005). A more recent study has corroborated these findings by demonstrating that despite no increase in isometric twitch and myosin RLC phosphorylation 15s following high-frequency stimulation, isometric twitches elicited during intermittent tetani were potentiated up to 14% in skMLCK$^{-/-}$ muscles (Gittings et al., 2011). In conclusion, as a result of this work with transgenic mice there is convincing evidence that mechanisms other than myosin RLC phosphorylation contribute to force potentiation especially during repetitive or sustained activation.

*Potentiation without myosin RLC phosphorylation: alternate mechanism for PTP?*

There is growing evidence that elevated myosin RLC phosphorylation may not be necessary for twitch potentiation to occur, and altered $Ca^{2+}$ homeostasis is the most commonly implicated mechanism (see Vandenboom et al., 2013 for a recent review). Smith et al. (2013) recently reported a moderate degree of PTP (~17%) following a brief potentiating stimulus (20Hz for 2s) in mouse lumbrical muscles, without an increase in myosin RLC phosphate content. The authors concluded that a short-lived elevation in resting [$Ca^{2+}$] that followed the potentiating stimulus likely mediated this brief (lasting 20-30s) potentiation of isometric twitch force. Staircase and PTP have also been reported following various interventions (i.e. spinal hemisection and pharmacologically induced atrophy) that disrupt the RLC phosphorylation mechanism in rat gastrocnemius muscles (Tubman et al., 1996; Tubman et al., 1997; Rassier et al., 1999; Macintosh et al., 2008b). However, without $Ca^{2+}$ signaling data in these studies, the results are largely inferred from the concomitant changes in RLC phosphate content and twitch force that were observed following the interventions.

Interestingly, a recent set of experiments from our lab using skMLCK$^{-/-}$ EDL muscles has shown that PTP may in fact be present in the absence of the myosin RLC phosphorylation mechanism; a finding which conflicts with previous reports that isometric twitch potentiation is absent in skMLCK$^{-/-}$ animals (Zhi et al. 2005; Gittings 2011). An important feature of these experiments was the use of a less intense potentiating stimulus to potentiate the muscles (i.e. 160 stimuli elicited over 20s versus 240 pulses/10s [Gittings et al., 2011] and 300 pulses/2s [Zhi et al. 2005]). Although a more concentrated or prolonged potentiating stimulus may induce greater PTP via myosin RLC phosphorylation there is a simultaneous probability of inducing significant fatigue. The coexistence and opposing effects of potentiation and fatigue have been well documented (Gittings et al., 2011; Rassier and MacIntosh, 2000) but are not completely understood. In fact, the temporary effect of fatigue itself may obscure the myosin RLC phosphorylation-independent potentiation that exists immediately following stimulation, and might explain why PTP was initially reported as absent in skMLCK$^{-/-}$ muscles (Zhi et al., 2005).

Identifying and characterizing a myosin RLC phosphorylation-independent mechanism for PTP is complicated by the use of various potentiating stimulus regimes that are unique to the muscle preparation in use, as well as other factors specific to the experimental models utilized (i.e. temperature and/or fibre type differences). Furthermore and most importantly, it remains unclear how myosin RLC phosphorylation and alternate mechanisms may interact to potentiate contractile function across various frequencies of stimulation and shortening speeds, as well as more generally during dynamic muscle activity. Thus, if a comprehensive model explaining how force potentiation modulates muscle function *in vivo* is to be constructed, it should account for myosin RLC phosphorylation-independent mechanisms of force potentiation under a variety of physiologically relevant conditions.

In addition to the putative $Ca^{2+}$-based mechanism discussed above, there may be alternate mechanisms for potentiation in skeletal muscle that result from previous activation. However, as these effects generally occur as a byproduct of prolonged activation and metabolic turnover, and are generally manifest during muscle fatigue, categorizing them as 'potentiating' mechanisms may be inappropriate. Nevertheless, they should be considered.

First, an emerging area of study is the production and effects of reactive oxygen and nitrogen species (i.e. ROS and RNS, respectively) on muscle physiology. These metabolic byproducts that are free radicals and can induce long-term effects such as altered gene/protein expression or produce acute effects which may be reversible (Lamb and Westerblad, 2011), and generally affect $Ca^{2+}$ sensitivity and/or $Ca^{2+}$ release (Allen et al., 2008). For example, of such as mechanism is S-glutathionylation of troponin subunit I ($TnI_f$), which has been shown to increase the $Ca^{2+}$ sensitivity of the contractile apparatus in fast-twitch muscle fibres from rats and humans, and may help to counter the effects of fatigue and influence muscle performance (Mollica et al, 2012). However, although this mechanism increases $Ca^{2+}$ sensitivity to a similar extent as myosin RLC phosphorylation, it may occur concomitantly with other factors that nullify or offset its effects (Mollica et al, 2012).

Second, there is evidence that byproducts of rapid high-energy phosphate turnover, as is characteristic of fast skeletal muscles, may influence $Ca^{2+}$ sensitivity and force. For example, Fryer et al. (1995) have shown that depletion of PCr concentrations in the physiological range can augment $Ca^{2+}$ sensitivity in skinned fast twitch fibres. However, large elevations of inorganic phosphate, which are directly and temporally linked to the depletion of [PCr], have an opposite effect on $Ca^{2+}$ sensitivity and can depress $F_{max}$. Otherwise, Godt and Nosek (1989) have shown that elevated [ADP] can augment force and $Ca^{2+}$ sensitivity by direct effects on the myosin crossbridge itself. The net outcome of these individual effects of metabolic byproducts on crossbridge function remains unclear, and in particular the interaction of these various components of the 'intracellular milieu' during prolonged activation are not well understood.

Finally, a consequence of activation *in vivo* or resulting from evoked stimulation may be the net efflux of $K^+$ ions that leads to elevated extracellular and reduced intracellular $[K^+]$ in exercising muscles, respectively. It has been reported that elevated extracellular $[K^+]$ can initially augment submaximal forces by 60-100% in mammalian muscle without affecting maximal tetanic force (Renaud and Light, 1992; Cairns et al., 1997). It is proposed that this effect initially helps to augment contractile function but may actually contribute to fatigue during prolonged use when elevated extracellular $[K^+]$ contributes to significant membrane depolarization and reduced excitability (McKenna et al., 2008). The mechanism for this effect is not completely understood but is not associated with a prolongation of the action potential (Yenson et al., 2002). These authors

speculated that the $K^+$-induced depolarization of the cell membrane might influence the DHPR receptor or voltage sensor in the t-tubule system that augments the rate and extent of $Ca^{2+}$ release by the SR.

In summary, although myosin RLC phosphorylation and alterations to $Ca^{2+}$ homeostasis following evoked stimulation are most commonly cited as the primary and secondary mechanisms for force potentiation, tertiary mechanisms such as those introduced above may prove to be significant contributors.

### *Skeletal muscle force control by rate coding: Interactions with PTP*

Gradation and control of skeletal muscle force is coordinated by organized recruitment of motor units (MU) and by regulated frequency of MU firing (i.e. rate coding)(De Luca and Contessa, 2012). Although this mechanism of force control operates independent of myosin RLC phosphorylation and potentiation *per se*, it is unclear whether they interact during sustained or repeated activation. MU recruitment patterns cannot be assessed *in vitro* because nerve supply and cortical control of the MU pool is absent. Furthermore, field stimulation of intact muscles *in vitro* is supramaximal to ensure that all fibres are activated with each contractile event. Due to the relative homogeneity of the mouse EDL fibre type profile (i.e. >90% IIX/B [Gittings et al., 2011]), the overall performance of this muscle *in vitro* may better resemble the behavior of a single fast motor unit as it functions *in vivo*. Consequently, and despite its limitations, the mouse EDL model remains an effective tool for studying the interaction between potentiation and rate coding (i.e. stimulation frequency) as it relates to both force development and maintenance of submaximal forces.

*Force potentiation and motor unit firing rates in vivo*

Perhaps the best support that potentiation influences force control via rate coding is the observation that the neural input (i.e. MU firing rate) required for submaximal torque production (i.e. 10-50% MVC) is reduced in potentiated muscles. This phenomenon has been shown to occur initially during sustained voluntary force maintenance (Person and Kudina, 1972; Adam & De Luca, 2005; Erim et al., 1996; and Dorfman et al., 1990) and transiently following maximal voluntary potentiating activity (Klein, 2001; Inglis et al., 2011). While it is tempting to assume a causal relationship between the concomitant changes in force production and MU firing rates that initially occur during activity *in vivo*, there is no conclusive mechanistic link to verify it. The primary challenge in this regard is to identify and characterize an afferent pathway that transmits real-time mechanical information to integrate with the descending motor control command, a neuromuscular feedback system that can only be studied *in vivo*. Second, there is no control condition for studying potentiated muscle in the absence of potentiation (for example, to determine if the decrease in MU firing rate that occurs following an MVC exists independent of force potentiation). Finally, animal evidence suggests that potentiation is limited to only the fastest muscle phenotypes (i.e. type IIB

and possibly IIX), which would presumably be recruited at moderate to high force levels. The obvious fibre type differences between humans and animals notwithstanding (i.e. type IIB fibre expression), it is remarkable that a significant pool of 'potentiatable' motor units would be recruited at low submaximal force levels (i.e. 10-30% MVC) and potentiated to the extent that would cause a decrease in MU firing rates. The mouse *in vitro* model does not offer the means to solve this research problem, however, the relationship between potentiation and MU firing rates is important and this review would be remiss not to include it.

*The Catchlike Property (CLP)*

The catchlike property (CLP) of skeletal muscle refers to the increase in force summation that results from unusually brief inter-pulse intervals (IPI) at the onset of a stimulus train (Binder-McCleod and Kesar, 2005) (see Figure 4 for schematic). Similar to activity dependent potentiation, the CLP may be characteristic of fast twitch skeletal muscle (or MU) function *in vivo* (Binder-McCleod and Kesar, 2005). These effects can be generated when closely spaced 'doublet' (or 'triplet') pulses are elicited at the onset of an otherwise constant frequency train of stimuli and, like PTP, are most pronounced at low stimulus frequencies (i.e. submaximal force levels). For example, Hennig and Lomo (1987) recorded MU discharge patterns in rat EDL and soleus muscles during normal motor behavior *in vivo* and demonstrated that initial doublets at the onset of activation are characteristic of fast MUs of the EDL. In addition, there is ample evidence that doublet discharges occur during human muscle function (as reviewed by Garland and Griffin 1999; Binder-McCleod and Kesar 2005) and may be more prevalent following training and during ballistic voluntary movements (Van Cutsem et al., 1998).

It is currently unclear why doublet discharges occur transiently across muscle and/or MU types, and additionally, whether the closely spaced pulses represent a motor pattern of functional significance or are a random/spontaneous neuromuscular event (Garland and Griffin, 1999). However, there is general consensus that the catchlike effect is a property of the muscle cell itself and occurs distal to the motor neuron/neuromuscular junction (as reviewed by Binder-McCleod and Kesar, 2005), and is not associated with modifications to the propagation of the muscle surface action potential (Duchateau and Hainaut, 1968a).

There are two mechanisms commonly associated with the CLP in skeletal muscle and both are likely contributors to the augmentation in contractile function that results from doublet pulses at the onset of stimulus. The first is an increase in muscle stiffness where the high force level produced by the initial pulses help to remove compliance by stretching the series elastic elements in the system (Parmiggiani and Stein, 1981). This mechanism is supported by the observation that the CLP is muscle length and contraction type dependent; typically the effect is reduced at long vs. short lengths (Abbate et al., 2000; Lee et al., 1999; Fortuna et al., 2012) and during eccentric vs. concentric contractions (BinderMcCleod & Lee 1996; Sandercock & Heckman, 1997; Callister et al., 2003). The second mechanism is a relative increase in $Ca^{2+}$ release that results from the initial double stimulation, which has been measured in single barnacle muscle fibres (Duchateau & Hainaut 1986b) and single fibres from mouse flexor brevis muscles (Abbate 2002a). Support for this mechanism is evidence that the CLP is enhanced when excitation-contraction coupling is compromised or during low frequency fatigue (Bentley & Lehman, 2005; as discussed by Binder McCleod 2005). However, Abbate et al., (2002a) observed that the brief increase in intracellular [$Ca^{2+}$] that followed triplet stimulation did not persist over the same period as force enhancement. Thus, although an additional pulse or pulses may transiently increase the intracellular [$Ca^{2+}$] it seems to be buffered almost immediately by $Ca^{2+}$ binding proteins (i.e. TnC, CaM, and parvalbumin). The more prolonged mechanistic effect of additional $Ca^{2+}$ release with doublet stimulation is likely mediated by a cooperative increase in $Ca^{2+}$ sensitivity (Abbate et al., 2002a).

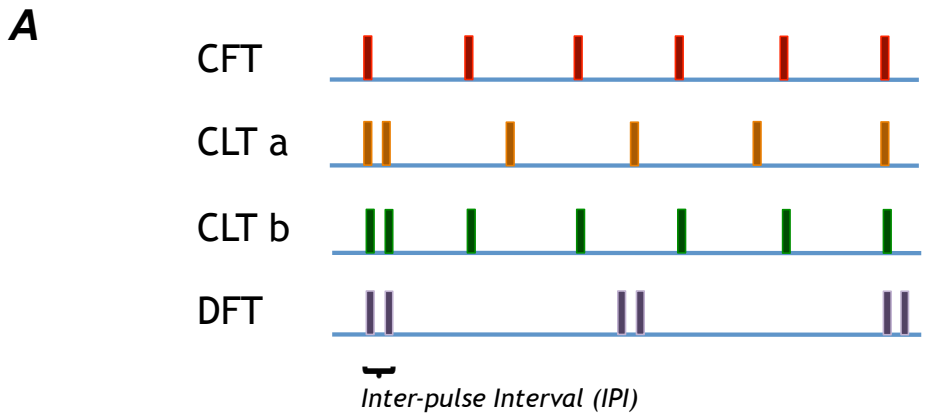


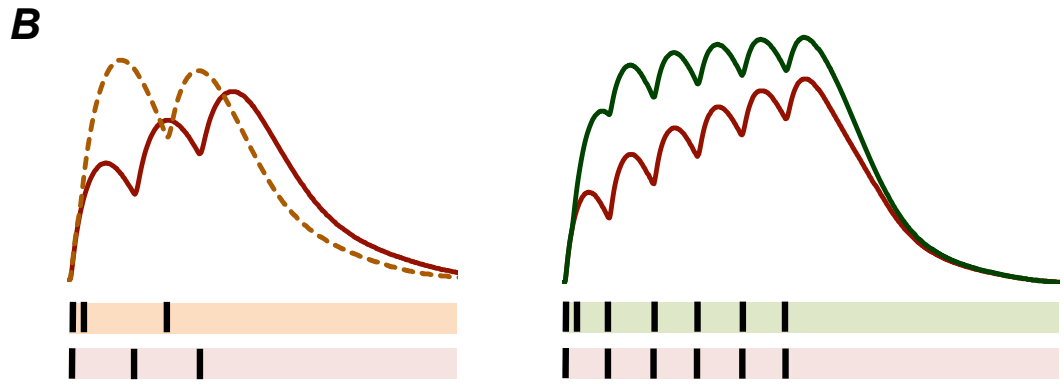


*Figure 2.5. The Catchlike Property (CLP) in skeletal muscle*

**A**. Common stimulation profiles used in the study of the CLP
- *CFT* – Constant frequency train
- *CLTa* – Catchlike train (same average frequency as the CFT)
- *CLTb* – Catchlike train (addition of a single pulse to the CFT)
- *DFT* – Double frequency train (same average frequency as the CFT)

**B**. Example traces demonstrating the catchlike effect on force production
- Left – Comparison of CFT (red) and CLTa (orange) stimulus trains
- Right – Comparison of CFT (red) and CLTb (green) stimulus trains

*Interaction of the CLP and PTP*

Burke et al. (1976) have been credited with describing the 'catchlike' effect and popularizing the term itself. More important to the current work, however, is that they identified and discussed the possible interaction between the CLP and PTP in skeletal muscle. Other researchers have further developed this topic but the true relationship between these mechanisms of force enhancement are not well understood. Comparing single and double pulse stimulation before and after high frequency potentiating stimulation in fast muscle units of cat gastrocnemius, Burke et al. (1976) demonstrated that the catchlike effect was blunted in the potentiated state. This finding has recently been supported by Ding et al. (2003), who showed a negative linear relationship between the magnitude of the CLP and PTP in human quadriceps muscle. Abbate et al. (2000) explored these mechanisms by studying power output in rat gastrocnemius muscles in situ at various stimulation frequencies (80, 120, and 200 Hz) and shortening speeds. Their work showed that both the high frequency initial pulses (HFIP) and PTP were capable of augmenting mechanical power, an effect that was shortening speed dependent. Using similar experiments, Abbate et al., (2001b) measured mechanical efficiency (i.e. total work/high energy phosphate turnover) with and without HFIP at the onset of stimulus trains at 60 and 90Hz. They concluded that the effect of one or two additional pulses at the onset of a stimulus train does not influence energy turnover enough to affect whole muscle efficiency (Abbate et al., 2001b).

Despite the research presented above, the interaction between the CLP and PTP in skeletal muscle requires further work. A complicating factor is that both means of force enhancement are associated with mixed mechanisms that may involve changes in $[Ca^{2+}]$ and/or $Ca^{2+}$ sensitivity, and additionally, both similarly dependent on a variety of factors (i.e. length, contraction type, stimulation frequency). An important and physiologically relevant question is whether one or both mechanisms are required to reach the optimal contractile output of skeletal muscle: Are the mechanisms simply redundant or additive? Additionally, it is unclear exactly what component of the PTP response (i.e. myosin RLC phosphorylation vs. elevated resting $[Ca^{2+}]$) inhibits or blunts the CLP response. Otazu et al. (2001) tested the interaction between the CLP and PTP using a sophisticated computer model that tracks the activation ($Ca^{2+}$ release, buffering, and SR sequestration) and contraction dynamics (isometric force production) of a myofibril. Interestingly, this

model did not include myosin RLC phosphorylation and thus may be thought of as a 'knockout' system for this feature. Their model was able to demonstrate myosin RLC phosphorylation-independent PTP mediated by an increase in resting [$Ca^{2+}$] following high frequency stimulation, and additionally, reproduced the catchlike effect during a low frequency stimulus train. Perhaps most interesting is that, like previous work with real muscle tissue, this model also demonstrated a robust CLP response only in the non-potentiated state. Therefore, it is tempting to predict that previous activation alone, and not myosin RLC phosphorylation-dependent potentiation, may contribute to the negative interaction between the CLP and PTP. Further work would be required to make more conclusive statements, however.

### *The metabolic profile of fast skeletal muscle*

Skeletal muscles demonstrate a close relationship between form and function that is mediated by neural and hormonal factors (Schiaffino and Reggiani, 2011). Accordingly, the metabolic profile of a muscle reflects the habitual demands placed on it (i.e. activation patterns, duty cycle) as well as the associated chronic energetic requirements. In fast skeletal muscles, the trade-off for allowing rapid shortening, relaxation, and ion-handling processes is a demand for ATP that cannot be satisfied indefinitely (Schiaffino and Reggiani, 2011). In fact, the characteristic depression in contractile function that accompanies prolonged use (i.e. fatigue) may demonstrate adaptive value: an example of how fast skeletal muscles must modulate their function with the ultimate goal of maintaining [ATP] from depleting to lethal levels (MacIntosh and Shahi, 2011; MacIntosh, 2012, Myburgh, 2004). Cooke (2007) likened this modulation of function to driving down the highway at full speed in a Porsche (i.e. excessive fuel consumption) until the tank depletes, at which time the car turns into a Volkswagen with a slower top speed but with enhanced fuel economy. As an ATP consuming process that alters contractile function during use, myosin RLC phosphorylation is a good example of history-dependent modulation that may significantly influence the energetics of repeated muscular work. However, the true contribution of myosin RLC phosphorylation (and force potentiation, by extension) to the metabolic profile of fast skeletal muscle remains unclear.

*Predominant energy systems and the cellular Adenylate Energy Charge*

The maintenance of [ATP] levels during muscular work in fast skeletal muscles such as the mouse EDL is accomplished predominantly by substrate level phosphorylation, a fact that is not surprising given the predominant myosin fibre types expressed (see Figure 2.6 for an example cross section). The small concentration of stored ATP that is available at rest is sufficient to power only seconds of work and must be resynthesized to buffer rates of ATP turnover that can exceed resting rates by two orders of magnitude during maximal effort (Tiidus et al., 2012). In primarily anaerobic muscles, the rapid synthesis of ATP required to fuel muscular work is accomplished largely by the breakdown of glycogen, pyruvate, and phosphocreatine stores as shown below in Equations 2, 3, and 4.

$$Glycogen_n + 3\ ADP + 3\ P_i + 2\ NAD^+ \rightarrow Glycogen_{n-1} + 2\ Pyruvate + 3\ ATP + 2\ NADH + 2\ H^+ \quad (2)$$

$$Pyruvate + NADH + H^+ \xleftrightarrow{Lactate\ Dehydrogenase} Lactate + NAD^+ \quad (3)$$

$$PCr + ADP + H^+ \xleftrightarrow{CK} ATP + Cr \quad (4)$$

During normal activity, the total pool of adenylate molecules that represent the energy currency of the cell remains constant; however, the relative concentration of the various molecules at any time represents the energetic state of the system. The Energy Charge describes the phosphorylating power of the total adenylate pool and is shown in Equation 5 below.

$$Energy\ Charge = \frac{([ATP]+0.5[ADP])}{([ATP]+[ADP]+[AMP])} \quad (5)$$

Of primary importance to harnessing the energy liberated by ATP hydrolysis and driving the principal ATPase reactions is rapidly buffering increases in [ADP], and by extension, maintaining a high [ATP]/[ADP] ratio (Tiidus et al., 2012). This task is accomplished primarily by Creatine Kinase (CK)(shown above), Adenylate Kinase (AK), and AMP Deaminase reactions (shown below).

$$2\ ADP \xleftrightarrow{AK} ATP + AMP \quad (6)$$

$$AMP \xleftrightarrow{AMP\ Deaminase} IMP + NH_3 \quad (7)$$

Although the AK reaction produces ATP its most important function is transferring a phosphate from one ADP molecule to another, and in so doing reduces the [ADP] considerably (Tiidus et al., 2012). During intense activity that may produce elevated levels of AMP, the AMP Deaminase reaction is required to continue flux through the AK reaction and involves the irreversible removal of the base adenine from AMP to produce inosine monophosphate (IMP) and an ammonium ion ($NH_3$). Although the ultimate cost of the AMP Deaminase reaction is a shrinking of the active pool of adenylate molecules, the IMP can be converted back to AMP as part of the purine nucleotide cycle (Tiidus et al., 2012).

*High-energy phosphate consumption (HEPC) as an indicator of total ATP turnover*

Total chemical energy usage in fast murine skeletal muscles is often calculated by comparing specific nucleotide and metabolite concentrations in muscles before and after performing a given amount of contractile activity (Crow and Kushmerick, 1982a; Kushmerick et al., 1992). An important calculation for this purpose is High-energy phosphate consumption (HEPC), which estimates the total ATP yield from substrate-level phosphorylation (see Equation 8 below).

$$HEPC = 1.5\Delta[Lactate] - \Delta[PCr] - 2\,\Delta[ATP] \quad (8)$$

This method makes the following assumptions; *i)* glycogen is the only source of lactate production, *ii)* the term -2Δ[ATP] actually accounts for both the decrease in [ATP] and increase in [IMP], which are assumed to be equivalent as they are associated stoichiometrically, and *iii)* there is no ATP contribution from oxidative phosphorylation (Barsotti and Butler, 1984; Zhang et al., 2006). It is possible that the potentiating stimulus itself provides the necessary inertia to partially activate oxidative phosphorylation; however, even at full capacity it is unlikely that this source of ATP contributes more than 5-10% of the energy required (please refer to Westra et al. 1988 for further information).

### *The economy of muscular work and force potentiation*

Muscular economy is the ratio of work produced to energy consumed (Goldspink, 1978), and is commonly used as a surrogate for mechanical efficiency (Equation 10) when studying intact muscles, in part because it is technically challenging and requires specialized equipment to measure heat production attributable to myosin ATPase activity (De Haan et al., 1986; Smith et al., 2005). Furthermore, only a fraction of the total energy produced in an intact muscle is available to generate muscular work, which reflects the fact that a significant portion of ATP is consumed for ion trafficking (i.e. $Na^+$-$K^+$ ATPase and SERCA).

$$Economy = Work / HEPC \tag{9}$$

$$Mechanical\ Efficiency = Work / (Work + Heat\ produced) \tag{10}$$

When applicable, this thesis will use Equation 9 to calculate the economy of working EDL muscles. Comparisons between wildtype and skMLCK$^{-/-}$ muscles will operate under the assumption that any observed differences in work or energy turnover (HEPC) between genotypes is attributable to differences in myosin RLC phosphorylation.

*Myosin RLC phosphorylation and muscular economy*

Myosin RLC phosphorylation influences contractile function and is an ATP consuming process; consequently, it seems fitting to study the economy of potentiated muscle. In fact, gaining a better understanding of the energetic requirement for myosin RLC phosphorylation has important ramifications for how we view its physiological role in skeletal muscle. The few studies that have investigated the energetic consequence(s) of myosin RLC phosphorylation have yielded conflicting results.

Initially, Crow and Kushmerick (1982b) correlated the progressive decrease in energy cost during an isometric tetanus with a concomitant increase in myosin RLC phosphorylation (mouse EDL at 20° C). Further work suggested that the reduction in energy cost for contraction by myosin RLC phosphorylation was due to a decrease in the actomyosin turnover rate (Crow and Kushmerick, 1982c). In direct opposition to these studies, subsequent work in rat EDL muscles revealed that there was no consistent relationship between phosphorylation of the myosin RLC and average rate of chemical usage (Barsotti and Butler, 1984). Furthermore, it was revealed that myosin RLC

phosphorylation does not influence crossbridge turnover rate in mouse EDL muscles (Butler et al. 1983). It has since been conceded that the progressive decrease in energy cost for contraction during prolonged or repetitive tetani occurs independent of myosin RLC phosphorylation (Kushmerick, 1985); however, the exact mechanisms are not clear. To date, only one study has attempted to quantify the energetic cost of force potentiation during dynamic contractions (Abbate et al. 2001a). In this study, the energy cost for contraction was increased more than muscular work when potentiated, suggesting that economy was reduced. However, the authors concluded that the increased energetic cost was a direct result of the increase in muscle performance rather than a property of potentiation (Abbate et al., 2001a).

When the aforementioned studies are considered together, it is clear that a major limitation is the lack of a control condition that would allow for the study of metabolism without myosin RLC phosphorylation. Specifically, the effect of myosin RLC phosphorylation on muscle energetics cannot be determined unless a given amount of work is produced with and without the mechanism intact and directly compared (i.e. using skMLCK$^{-/-}$ mice).

An additional challenge is the measurement of metabolic and contractile function during the initial seconds of stimulation, where myosin RLC phosphorylation and energy turnover are the most variable. If the potentiated state is truly the normal operating state of fast skeletal muscles (Brown and Loeb, 1998), evaluating the true effect of myosin RLC phosphorylation on the economy of skeletal muscle would be best accomplished during a period of sustained muscular work with stable levels myosin RLC phosphate content.

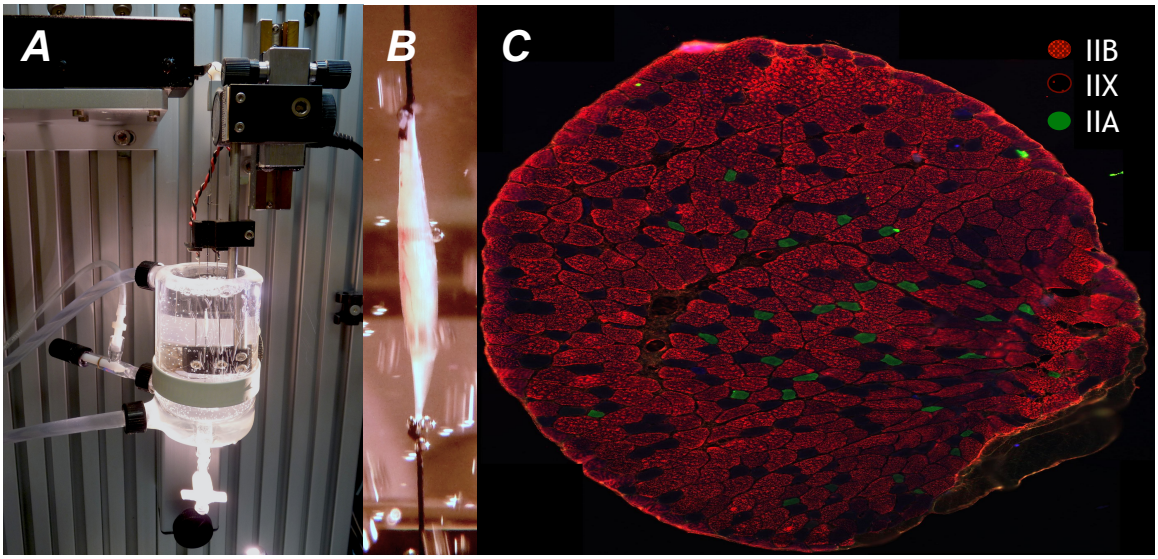


*Figure 2.6. Intact mouse EDL model in vitro*

**A**. 1200A intact muscle system from Aurora Scientific, Inc. (300C-LR servomotor, jacketed organ bath, length micrometer, vertical electrode and clamp assembly)
**B**. Intact EDL muscle suspended in Tyrode's solution using silk suture
**C**. EDL Cross section with histochemical staining for myosin heavy chain expression

# Chapter 3:

## *Statement of the Problem*

Interest in force potentiation as a modulator of skeletal muscle function *in vivo* continues to grow; however, proper translation of knowledge between mechanistic and applied research is often inadequate (Macintosh, 2012b). Our incomplete understanding of this feature of skeletal muscle may contribute to this problem. The primary objective of this thesis was to explore the role of force potentiation in fast skeletal muscles of the mouse and investigate how it modulates dynamic force production and the economy of muscular work. The intact mouse EDL *in vitro* is an ideal model to study force potentiation under controlled environmental conditions and permits the application of carefully designed stimulation paradigms and muscle length manipulations.

A central feature of this thesis was the study of muscle function in skMLCK-deficient mice as an experimental control for myosin RLC phosphorylation, the primary mechanism for posttetanic potentiation. Myosin RLC phosphorylation is activated by the same signal that regulates muscle force (i.e. $Ca^{2+}$), which makes the study of muscle function in the absence of force potentiation very difficult. The inclusion of these transgenic animals into our experiments has allowed us to explore how fast muscles function in the absence of force modulation by RLC phosphorylation, and importantly, to observe and characterize the presence and relative contribution of myosin RLC phosphorylation-independent mechanisms to the observed force potentiation.

***Purpose & Hypothesis: Study 1 – Chapter 4***

**Tetanic force potentiation of mouse fast muscle is shortening speed dependent**

*Purpose*

The purpose of this study was to determine how the frequency-dependence for tetanic force potentiation would be influenced by manipulating the velocity of muscle shortening in EDL muscles from adult wildtype mice.

*Hypothesis*

We hypothesized that muscle force potentiation would be positively associated with increasing shortening velocity and would thus facilitate the potentiation of moderate to high stimulation frequency tetani (≥ 60-100 Hz). The rationale for this prediction was founded in the force-velocity relationship: we expected that the relative enhancement of contractile function by force potentiation would be greatest during conditions in which force production was reduced or suboptimal (i.e. at moderate to high shortening velocities for all frequencies of stimulation). The rapidly shortening intact muscle was considered an incompletely activated system where the affinity for myosin crossbridge binding would be suboptimal (αFS is reduced), and importantly, the relative effect of RLC-dependent force potentiation would be more pronounced (vs. isometric).

***Purpose & Hypothesis: Study 2 – Chapter 5***

## The Force Dependence of Isometric and Concentric Potentiation in Mouse Muscle With and Without Skeletal Myosin Light Chain Kinase

*Purpose*

This study was designed to investigate the force-dependence of potentiation in EDL muscles from wildtype and skMLCK$^{-/-}$ mice and to explore the interactions between force potentiation and the activation state of the muscle at the time of stimulation. We tested whether a brief period of isometric activation prior to shortening would influence the subsequent concentric potentiation response.

Supplementary to this primary aim, the study was also designed to test the effect of stimulation timing on the magnitude of concentric force potentiation (i.e. comparing concentric potentiation when stimulation was elicited coincident with shortening or during passive shortening).

*Hypothesis*

Our hypothesis was that crossbridge-induced cooperative activation by the preceding isometric activation would decrease the concentric potentiation response that followed.

In regard to the secondary objective, we hypothesized that the concentric force response would be smaller if the activation of the muscle occurred while the muscles was shortening and consequently that the relative effect of concentric force potentiation would be greater.

***Purpose & Hypothesis: Study 3 – Chapter 6***

**Genotype specific interaction of posttetanic potentiation and the catchlike property in mouse skeletal muscle with and without RLC phosphorylation**

*Purpose*

Contractile function may be modulated by multiple mechanisms *in vivo* that may operate simultaneously to enhance contractile function. The purpose of this study was to investigate the interaction between force potentiation and the catchlike property (CLP) on concentric force and power enhancement in EDL muscles from wildtype and skMLCK$^{-/-}$ mice. Both mechanisms have been observed to augment the rate and extent of force development in fast skeletal muscles; however, their coexistence during activation and the relative effect of each on the augmentation of contractile function is not well understood.

*Hypothesis*

We hypothesized that these mechanisms operate redundantly in skeletal muscle and that the catchlike effect would be muted in potentiated muscle from wildtype mice but not in skMLCK$^{-/-}$ muscles, where myosin RLC phosphorylation-mediated potentiation is absent.

***Purpose & Hypothesis: Study 4 – Chapter 7***

## The economy of working fast skeletal muscles in the presence and absence of myosin phosphorylation

*Purpose*

Myosin RLC phosphorylation is an ATP consuming mechanism that augments contractile performance; however, it is unclear whether this mechanism operates at a net metabolic cost to the muscle to preserve contractile function during fatigue, or whether the event itself can improve the economy of muscular work during sustained use. Consequently, the purpose of this study was to investigate how myosin RLC phosphorylation affects the economy and energetic cost of dynamic contractions in potentiated EDL muscles from wildtype and skMLCK$^{-/-}$ mice. We conducted this work with an improved study design to directly assess the finding of Abbate et al. (2001b) who associated posttetanic potentiation with an increase in the energy cost for work.

*Hypothesis*

We conducted this work under the hypothesis that the greater amount of work performed by wildtype muscles would be associated with a greater total energy turnover, consistent with the findings of Abbate et al. (2001b). With respect to contractile economy, we hypothesized that muscles from wildtype mice would have reduced contractile economy vs. skMLCK$^{-/-}$ counterparts, which might account for the increased energetic cost of maintaining myosin RLC phosphorylation during repetitive use.

# References


Abbate, F., Sargeant, A. J., Verdijk, P. W. L., & de Haan, A. (2000). Effects of high-frequency initial pulses and posttetanic potentiation on power output of skeletal muscle. Journal of Applied Physiology, 88(1), 35–40.

Abbate, F., de Ruiter, C. J., & de Haan, A. (2001a). High-frequency initial pulses do not affect efficiency in rat fast skeletal muscle. The Journal of Experimental Biology, 204, 1503–1508.

Abbate, F., Van Der Velden, J., Stienen, G. J., & de Haan, A. (2001b). Post-tetanic potentiation increases energy cost to a higher extent than work in rat fast skeletal muscle. Journal of Muscle Research and Cell Motility, 22(8), 703–710.

Abbate, F., Bruton, J. D., de Haan, A., & Westerblad, H. (2002a). Prolonged force increase following a high-frequency burst is not due to a sustained elevation of [Ca2+]i. American Journal of Physiology. Cell Physiology, 283(1), C42–C47.

Abbate, F., de Ruiter, C. J., Offringa, C., Sargeant, A. J., & de Haan, A. (2002b). In situ rat fast skeletal muscle is more efficient at submaximal than at maximal activation levels. Journal of Applied Physiology, 92(5), 2089–2096.

Adam, A., & De Luca, C. J. (2005). Firing rates of motor units in human vastus lateralis muscle during fatiguing isometric contractions. Journal of Applied Physiology, 99(1), 268–280.

Adler, M., Lebeda, F. J., Kauffman, F. C., & Deshpande, S. S. (1999). Mechanism of action of sodium cyanide on rat diaphragm muscle. Journal of Applied Toxicology : JAT, 19(6), 411–419.

Alamo, L., Wriggers, W., Pinto, A., Bártoli, F., Salazar, L., Zhao, F.-Q., et al. (2008). Three-Dimensional Reconstruction of Tarantula Myosin Filaments Suggests How Phosphorylation May Regulate Myosin Activity. Journal of Molecular Biology, 384(4), 780–797.

Albaum, H. G., Tepperman, J., & Bodansky O. (1946). The in vivo inactivation by cyanide of brain cytochrome oxidase and its effect on glycolysis and on the high energy phosphorus compounds in brain. Journal of Biological Chemistry, 164, 45–51.

Allen, D. G., & Westerblad, H. (2001). Role of phosphate and calcium stores in muscle fatigue. Journal of Physiology, 536(Pt 3), 657–665.

Allen, D. G., Lamb, G. D., & Westerblad, H. (2008). Skeletal Muscle Fatigue: Cellular Mechanisms. Physiological Reviews, 88(1), 287–332.

Allen, D. G., Lee, J. A., & Westerblad, H. (1989). Intracellular calcium and tension during fatigue in isolated single muscle fibres from Xenopus laevis. The Journal of Physiology, 415(1), 433–458.

Ariano, M. A., Edgerton, V. R., & Armstrong, R. B. (1973). Hindlimb muscle fiber populations of five mammals. Journal of Histochemistry & Cytochemistry, 21(1), 51–55.

Askew, G. N., & Marsh, R. L. (1997). The effects of length trajectory on the mechanical power output of mouse skeletal muscles. The Journal of Experimental Biology, 200(Pt 24), 3119–3131.

Atkinson, D. E. (2012). Cellular Energy Metabolism and its Regulation. Elsevier.

Baker, A. J., Brandes, R., Schendel, T. M., Trocha, S. D., Miller, R. G., & Weiner, M. W. (1994). Energy use by contractile and noncontractile processes in skeletal muscle estimated by 31P-NMR. American Journal of Physiology -- Legacy Content, 266(3 Pt 1), C825–C831.

Barclay, C. J. (1994). Efficiency of fast- and slow-twitch muscles of the mouse performing cyclic contractions. The Journal of Experimental Biology, 193(1), 65–78.

Barclay, C. J. (1996). Mechanical efficiency and fatigue of fast and slow muscles of the mouse. The Journal of Physiology, 497 ( Pt 3), 781–794.

Barclay, C. J. (2005). Modelling diffusive O2 supply to isolated preparations of mammalian skeletal and cardiac muscle. Journal of Muscle Research and Cell Motility, 26(4-5), 225–235. doi:10.1007/s10974-005-9013-x

Barclay, C. J. (2012). Quantifying Ca2+ release and inactivation of Ca2+ release in fast- and slow-twitch muscles. The Journal of Physiology, 590, 6199–6212.

Barclay, C. J., & Lichtwark, G. A. (2007). The mechanics of mouse skeletal muscle when shortening during relaxation. Journal of Biomechanics, 40(14), 3121–3129.

Barclay, C. J., & Loiselle, D. S. (2007). Can activation account for 80% of skeletal muscle energy use during isometric contraction? American Journal of Physiology. Cell Physiology, 292(1), C612–author reply C613–4.

Barclay, C. J., Arnold, P. D., & Gibbs, C. L. (1995). Fatigue and heat production in repeated contractions of mouse skeletal muscle. The Journal of Physiology, 488(3), 741–752.

Barclay, C. J., Curtin, N. A., & Woledge, R. C. (1993). Changes in crossbridge and non-crossbridge energetics during moderate fatigue of frog muscle fibres. The Journal of Physiology, 468(1), 543–556.

Barclay, C. J., Lichtwark, G. A., & Curtin, N. A. (2008). The energetic cost of activation in mouse fast-twitch muscle is the same whether measured using reduced filament overlap or N-benzyl-p-toluenesulphonamide. Acta Physiologica (Oxford, England), 193(4), 381–391.

Barclay, C. J., Woledge, R. C., & Curtin, N. A. (2007). Energy turnover for Ca2+ cycling in skeletal muscle. Journal of Muscle Research and Cell Motility, 28(4-5), 259–274.

Barclay, C. J., Woledge, R. C., & Curtin, N. A. (2010a). Inferring crossbridge properties from skeletal muscle energetics. Progress in Biophysics and Molecular Biology, 102(1), 53–71.

Barclay, C. J., Woledge, R. C., & Curtin, N. A. (2010b). Is the efficiency of mammalian (mouse) skeletal muscle temperature dependent? The Journal of Physiology, 588(Pt 19), 3819–3831.

Barsotti, R. J., & Butler, T. M. (1984). Chemical energy usage and myosin light chain phosphorylation in mammalian skeletal muscle. Journal of Muscle Research and Cell Motility, 5(1), 45–64.

Baylor, S. M., & Hollingworth, S. (2003). Sarcoplasmic reticulum calcium release compared in slow-twitch and fast-twitch fibres of mouse muscle. Journal of Physiology, 551(Pt 1), 125–138.

Baylor, S. M., & Hollingworth, S. (2011). Calcium indicators and calcium signalling in skeletal muscle fibres during excitation-contraction coupling. Progress in Biophysics and Molecular Biology, 105(3), 162–179.

Bárány, K., & Bárány, M. (1977). Phosphorylation of the 18,000-dalton light chain of myosin during a single tetanus of frog muscle. Journal of Biological Chemistry, 252(14), 4752–4754.

Bárány, K., Bárány, M., Gillis, J. M., & Kushmerick, M. J. (1979). Phosphorylation-dephosphorylation of the 18,000-dalton light chain of myosin during the contraction-relaxation cycle of frog muscle. Journal of Biological Chemistry, 254(9), 3617–3623.

Bárány, K., Bárány, M., Gillis, J. M., & Kushmerick, M. J. (1980). Myosin light chain phosphorylation during the contraction cycle of frog muscle. Federation Proceedings, 39(5), 1547–1551.

Bárány, M. (1967). ATPase Activity of Myosin Correlated with Speed of Muscle Shortening. The Journal of General Physiology, 50(6), 197–218.

Beard, N. A., Wei, L., & Dulhunty, A. F. (2009a). Ca(2+) signaling in striated muscle: the elusive roles of triadin, junctin, and calsequestrin. European Biophysics Journal, 39(1), 27–36.

Beard, N. A., Wei, L., & Dulhunty, A. F. (2009b). Control of muscle ryanodine receptor calcium release channels by proteins in the sarcoplasmic reticulum lumen. Clinical and Experimental Pharmacology and Physiology, 36(3), 340–345.

Behrmann, E., Müller, M., Penczek, P. A., Mannherz, H. G., Manstein, D. J., & Raunser, S. (2012). Structure of the rigor actin-tropomyosin-myosin complex. Cell, 150(2), 327–338.

Bellinger, A. M., Reiken, S., Dura, M., Murphy, P. W., Deng, S.-X., Landry, D. W., et al. (2008). Remodeling of ryanodine receptor complex causes “leaky” channels: a molecular mechanism for decreased exercise capacity. Proceedings of the National Academy of Sciences of the United States of America, 105(6), 2198–2202.

Bentley, L. F., & Lehman, S. L. (2005). Doublets and low-frequency fatigue in potentiated human muscle. Acta Physiologica Scandinavica, 185(1), 51–60.

Bergmeyer, H. U., GraBl, M., & Walter, H. E. (1983). Methods in enzymatic analysis.

Bergström, M., & Hultman, E. (1988). Energy cost and fatigue during intermittent electrical stimulation of human skeletal muscle. Journal of Applied Physiology, 65(4), 1500–1505.

Bernhard, C. G., Euler, U. S. V., & Skoglund, C. R. (1941). Post-tetanic Action Potentials in Mammalian Muscle. Acta Physiologica Scandinavica, 2(3-4), 284–288.

Bicer, S., & Reiser, P. J. (2004). Myosin light chain isoform expression among single mammalian skeletal muscle fibers: species variations. Journal of Muscle Research and Cell Motility, 25(8), 623–633.

Binder-Macleod, S. A., & Barrish, W. J. (1992). Force response of rat soleus muscle to variable-frequency train stimulation. Journal of neurophysiology,68(4), 1068-1078.

Binder Macleod, S., & Kesar, T. (2005). Catchlike property of skeletal muscle: Recent findings and clinical implications. Muscle & Nerve, 31(6), 681–693.

Binder-Macleod, S. A., & Barker, C. B. (1991). Use of a catchlike property of human skeletal muscle to reduce fatigue. Muscle & Nerve, 14(9), 850–857.

Binder-Macleod, S. A., & Lee, S. C. (1996). Catchlike property of human muscle during isovelocity movements. Journal of Applied Physiology, 80(6), 2051–2059.

Binder-Macleod, S. A., Lee, S. C. K., & Baadte, S. A. (1997). Reduction of the fatigue-induced

force decline in human skeletal muscle by optimized stimulation trains. Archives of Physical Medicine and Rehabilitation, 78(10), 1129–1137.
Bishop, D. (2003). Warm Up I: potential mechanisms and the effects of passive warm up on exercise performance. Sports Medicine, 33(6), 439–454.
Blumenthal, D. K., & Stull, J. T. (1980). Activation of skeletal muscle myosin light chain kinase by calcium(2+) and calmodulin. Biochemistry (Washington), 19(24), 5608–5614.
Boschek, C. B., Sun, H., Bigelow, D. J., & Squier, T. C. (2008). Different Conformational Switches Underlie the Calmodulin-Dependent Modulation of Calcium Pumps and Channels †. Biochemistry (Washington), 47(6), 1640–1651.
Bozzo, C., Spolaore, B., Toniolo, L., Stevens, L., Bastide, B., Cieniewski-Bernard, C., et al. (2005). Nerve influence on myosin light chain phosphorylation in slow and fast skeletal muscles. FEBS Journal, 272(22), 5771–5785.
Bozzo, C., Stevens, L., Toniolo, L., Mounier, Y., & Reggiani, C. (2003). Increased phosphorylation of myosin light chain associated with slow-to-fast transition in rat soleus. American Journal of Physiology. Cell Physiology, 285(3), C575–C583.
Brenner, B. (1988). Effect of Ca2+ on cross-bridge turnover kinetics in skinned single rabbit psoas fibers: implications for regulation of muscle contraction. Proceedings of the National Academy of Sciences, 85(9), 3265–3269.
Brenner, B., & Eisenberg, E. (1986). Rate of force generation in muscle: correlation with actomyosin ATPase activity in solution. Proceedings of the National Academy of Sciences, 83(10), 3542–3546.
Brito, R., Alamo, L., Lundberg, U., Guerrero, J. R., Pinto, A., Sulbarán, G., et al. (2011). A Molecular Model of Phosphorylation-Based Activation and Potentiation of Tarantula Muscle Thick Filaments. Journal of Molecular Biology, 414(1), 44–61.
Brooks, S. V., & Faulkner, J. A. (1988). Contractile properties of skeletal muscles from young, adult and aged mice. The Journal of Physiology, 404(1), 71–82.
Brooks, S.V., Faulkner, J.A. and McCubbrey, D.A.. "Power outputs of slow and fast skeletal muscles of mice." Journal of Applied Physiology 68.3 (1990): 1282-1285.
Brooks, S. V., & Faulkner, J. A. (1991). Forces and powers of slow and fast skeletal muscles in mice during repeated contractions. The Journal of Physiology, 436(1), 701–710.
Brooks, S. V., Zerba, E., & Faulkner, J. A. (1995). Injury to muscle fibres after single stretches of passive and maximally stimulated muscles in mice. Journal of Physiology, 488 (Pt 2), 459–469.
Brown, I. E., & LOEB, G. E. (1998). Post-Activation Potentiation—A Clue for Simplifying Models of Muscle Dynamics. American Zoologist, 38(4), 743–754.
Brown, I. E., & Loeb, G. E. (1999). Measured and modeled properties of mammalian skeletal muscle. I. The effects of post-activation potentiation on the time course and velocity dependencies of force production. Journal of Muscle Research and Cell Motility, 20(5-6), 443–456.
Brown, I. E., Cheng, E. J., & Loeb, G. E. (1999b). Measured and modeled properties of mammalian skeletal muscle. II. The effects of stimulus frequency on force-length and force-velocity relationships. Journal of Muscle Research and Cell Motility, 20(7), 627–643.
Brown, I. E., & Loeb, G. E. (2000a). Measured and modeled properties of mammalian skeletal muscle: III. the effects of stimulus frequency on stretch-induced force enhancement and shortening-induced force depression. Journal of Muscle Research and Cell Motility, 21(1), 21–31.
Brown, I. E., & Loeb, G. E. (2000b). Measured and modeled properties of mammalian skeletal muscle: IV. dynamics of activation and deactivation. Journal of Muscle Research and Cell Motility, 21(1), 33–47.
Brown, L. T., & Tuttle, W. W. (1926). The phenomenon of treppe in intact human skeletal muscle. Am Physiol Soc., 77, 483-490.
Buller, A. J., Kean, C. J., Ranatunga, K. W., & Smith, J. M. (1981). Post-tetanic depression of twitch tension in the cat soleus muscle. Experimental Neurology, 73(1), 78–89.
Burke, R. E., Rudomin, P., & Zajac, F. E. (1970). Catch property in single mammalian motor units. Science, 168(3927), 122-124.
Burke, R. E., Rudomin, P., & Zajac, F. E., III. (1976). The effect of activation history on tension production by individual muscle units. Brain Research, 109(3), 515–529.
Butler, T. M., Siegman, M. J., Mooers, S. U., & Barsotti, R. J. (1983). Myosin light chain phosphorylation does not modulate cross-bridge cycling rate in mouse skeletal muscle. Science, 220(4602), 1167–1169.

Cairns SP, Hing WA, Slack JR, Mills RG, Loiselle DS. (1997). Different effects of raised [$K^+$]o on membrane potential and contraction in mouse fast- and slow-twitch muscle. Am J Physiol Cell Physiol 273: C598–C611.

Calderón, J. C., Bolaños, P., & Caputo, C. (2014). The excitation–contraction coupling mechanism in skeletal muscle. Biophysical Reviews.

Callister, R. J., Reinking, R. M., & Stuart, D. G. (2003). Effects of fatigue on the catchlike property in a turtle hindlimb muscle. Journal of Comparative Physiology A, 189(12), 857–866.

Caterini, D., Gittings, W., Huang, J., & Vandenboom, R. (2011). The effect of work cycle frequency on the potentiation of dynamic force in mouse fast twitch skeletal muscle. The Journal of Experimental Biology, 214(Pt 23), 3915–3923.

Celichowski, J., & Grottel, K. (1995). The relationship between fusion index and stimulation frequency in tetani of motor units in rat medial gastrocnemius. Archives Italiennes De Biologie, 133(2), 81–87.

Celichowski, J., Pogrzebna, M., & Krutki, P. (2006). Monophasic and biphasic relaxation during motor unit tetanic contractions of variable fusion degree. Archives Italiennes De Biologie, 144(2), 89–98.

Chin, E. R. (2010). Intracellular Ca2+ signaling in skeletal muscle: decoding a complex message. Exercise and Sport Sciences Reviews, 38(2), 76–85.

Claflin, D. R., & Faulkner, J. A. (1985). Shortening velocity extrapolated to zero load and unloaded shortening velocity of whole rat skeletal muscle. The Journal of Physiology, 359(1), 357–363.

Close, R., & Hoh, J. F. (1968). The after-effects of repetitive stimulation on the isometric twitch contraction of rat fast skeletal muscle. Journal of Physiology, 197(2), 461–477.

Cooke, R. (2007). Modulation of the actomyosin interaction during fatigue of skeletal muscle. Muscle & Nerve, 36(6), 756–777.

Cooke, R. (2011). The role of the myosin ATPase activity in adaptive thermogenesis by skeletal muscle. Biophysical reviews, 3(1), 33-45.

Craig, R., & Woodhead, J. L. (2006). Structure and function of myosin filaments. Current Opinion in Structural Biology, 16(2), 204–212.

Crow, M. T., & Kushmerick, M. J. (1982a). Chemical energetics of slow- and fast-twitch muscles of the mouse. The Journal of General Physiology, 79(1), 147–166.

Crow, M. T., & Kushmerick, M. J. (1982b). Myosin light chain phosphorylation is associated with a decrease in the energy cost for contraction in fast twitch mouse muscle. Journal of Biological Chemistry, 257(5), 2121–2124.

Crow, M. T., & Kushmerick, M. J. (1982c). Phosphorylation of myosin light chains in mouse fast-twitch muscle associated with reduced actomyosin turnover rate. Science, 217(4562), 835–837.

Crow, M. T., & Kushmerick, M. J. (1983). Correlated reduction of velocity of shortening and the rate of energy utilization in mouse fast-twitch muscle during a continuous tetanus. The Journal of General Physiology, 82(5), 703–720.

De Haan, A., de Jong, J., van Doorn, J. E., Huijing, P. A., Woittiez, R. D., & Westra, H. G. (1986). Muscle economy of isometric contractions as a function of stimulation time and relative muscle length. Pflügers Archiv : European Journal of Physiology, 407(4), 445–450.

De Luca, C. J., & Contessa, P. (2012). Hierarchical control of motor units in voluntary contractions. Journal of Neurophysiology.

De Luca, C. J., & Hostage, E. C. (2010). Relationship Between Firing Rate and Recruitment Threshold of Motoneurons in Voluntary Isometric Contractions. Journal of Neurophysiology, 104(2), 1034–1046.

De Luca, C. J., Foley, P. J., & Erim, Z. (1996). Motor unit control properties in constant-force isometric contractions. Journal of Neurophysiology, 76(3), 1503–1516.

Decostre, V., Gillis, J. M., & Gailly, P. (2000). Effect of adrenaline on the post-tetanic potentiation in mouse skeletal muscle. Journal of Muscle Research and Cell Motility, 21(3), 247–254.

Delp, M. D., & Duan, C. (1996). Composition and size of type I, IIA, IID/X, and IIB fibers and citrate synthase activity of rat muscle. Journal of Applied Physiology, 80(1), 261–270.

Desmedt, J. J. E., & Hainaut, K. (1968). Kinetics of myofilament activation in potentiated contraction: Staircase phenomenon in human skeletal muscle. Nature, 217(5128), 529–532.

Ding, J., Storaska, J. A., & Binder-Macleod, S. A. (2003). Effect of potentiation on the catchlike property of human skeletal muscles. Muscle & Nerve, 27(3), 312–319.

Dorfman, L. J., Howard, J. E., & McGill, K. C. (1990). Triphasic behavioral response of motor units to submaximal fatiguing exercise. Muscle & Nerve, 13(7), 621–628.

Duchateau, J., & Hainaut, K. (1986a). Nonlinear summation of contractions in striated muscle. I. Twitch potentiation in human muscle. Journal of Muscle Research and Cell Motility, 7(1), 11–17.

Duchateau, J., & Hainaut, K. (1986b). Nonlinear summation of contractions in striated muscle. II. Potentiation of intracellular Ca2+ movements in single barnacle muscle fibres. Journal of Muscle Research and Cell Motility, 7(1), 18–24.

Duggal, D., Nagwekar, J., Rich, R., Midde, K., Fudala, R., Gryczynski, I., & Borejdo, J. (2014). Phosphorylation of myosin regulatory light chain has minimal effect on kinetics and distribution of orientations of cross bridges of rabbit skeletal muscle. American Journal of Physiology. Regulatory, Integrative and Comparative Physiology, 306(4), R222–33.

Dulhunty, A. F. (2006). Excitation-contraction coupling from the 1950s into the new millennium. Clinical and Experimental Pharmacology and Physiology, 33(9), 763–772.

Dunford, E. C., Herbst, E. A., Jeoung, N. H., Gittings, W., Inglis, J. G., Vandenboom, R., et al. (2011). PDH activation during in vitro muscle contractions in PDH kinase 2 knockout mice: effect of PDH kinase 1 compensation. American Journal of Physiology. Regulatory, Integrative and Comparative Physiology, 300(6), R1487–93.

Ebashi, S. (1991). Excitation-contraction coupling and the mechanism of muscle contraction. Physiology, 53(1), 1–16.

Edelman, G. M., & Gally, J. A. (2001). Degeneracy and complexity in biological systems. Proceedings of the National Academy of Sciences, 98(24), 13763–13768.

Edman, K. A. (1975). Mechanical deactivation induced by active shortening in isolated muscle fibres of the frog. Journal of Physiology, 246(1), 255–275.

Edman, K. A. P., & Flitney, F. W. (1982). Laser diffraction studies of sarcomere dynamics during "isometric" relaxation in isolated muscle fibres of the frog. The Journal of Physiology, 329(1), 1–20.

Endo, M. (2009). Calcium-induced calcium release in skeletal muscle. Physiological Reviews, 89(4), 1153–1176.

Enoka, R. M., & Stuart, D. G. (1992). Neurobiology of muscle fatigue. Journal of Applied Physiology, 72(5), 1631–1648.

Erim, Z., De Luca, C. J., Mineo, K., & Aoki, T. (1996). Rank-ordered regulation of motor units. Muscle & Nerve, 19(5), 563–573.

Faulkner, J. A., Zerba, E., & Brooks, S. V. (1990). Muscle temperature of mammals: cooling impairs most functional properties. American Journal of Physiology -- Legacy Content, 259(2 Pt 2), R259–65.

Favero, T. G. (1999). Sarcoplasmic reticulum Ca2+ release and muscle fatigue. Journal of Applied Physiology.

Fenn, W. O. (1923). A quantitative comparison between the energy liberated and the work performed by the isolated sartorius muscle of the frog. Journal of Physiology, 58(2-3), 175–203.

Fenn, W. O. (1924). The relation between the work performed and the energy liberated in muscular contraction. Journal of Physiology, 58(6), 373–395.

Fortuna, R., Vaz, M. A., & Herzog, W. (2012). Catchlike property in human adductor pollicis muscle. Journal of Electromyography and Kinesiology, 22(2), 228–233.

Fowles, J. R., & Green, H. J. (2011). Coexistence of potentiation and low-frequency fatigue during voluntary exercise in human skeletal muscle. Canadian Journal of Physiology and Pharmacology, 81(12), 1092–1100.

Franks-Skiba, K., Lardelli, R., Goh, G., & Cooke, R. (2007). Myosin light chain phosphorylation inhibits muscle fiber shortening velocity in the presence of vanadate. American Journal of Physiology. Regulatory, Integrative and Comparative Physiology, 292(4), R1603–R1612.

Fryer, M. W., Owen, V. J., Lamb, G. D., & Stephenson, D. G. (1995). Effects of creatine phosphate and P (i) on Ca2+ movements and tension development in rat skinned skeletal muscle fibres. The Journal of physiology, 482(1), 123-140.

Fujita, K., Ye, L. H., Sato, M., Okagaki, T., Nagamachi, Y., & Kohama, K. (1999). Myosin light chain kinase from skeletal muscle regulates an ATP-dependent interaction between actin and myosin by binding to actin. Molecular and Cellular Biochemistry, 190(1-2), 85–90.

Gandevia, S. C. (2001). Spinal and supraspinal factors in human muscle fatigue. Physiological Reviews. 81.4 (2001): 1725-1789.

Garland, S. J., Griffin, L., & Ivanova, T. (1997). Motor unit discharge rate is not associated with muscle relaxation time in sustained submaximal contractions in humans. Neuroscience Letters, 239(1), 25–28.

Garland, S. J., & Gossen, E. R. (2002). The Muscular Wisdom Hypothesis in Human Muscle Fatigue. Exercise and Sport Sciences Reviews, 30(1), 45.

Garland, S. J., & Griffin, L. (2011). Motor Unit Double Discharges: Statistical Anomaly or Functional Entity? Canadian Journal of Applied Physiology, 24(2), 113–130.

Geeves, M. A., & Holmes, K. C. (1999). Structural mechanism of muscle contraction. Annual Review of Biochemistry, 68(1), 687–728.
Geeves, M., Griffiths, H., Mijailovich, S., & Smith, D. (2011). Cooperative [Ca2+]-Dependent Regulation of the Rate of Myosin Binding to Actin: Solution Data and the Tropomyosin Chain Model. Biophysical Journal, 100(11), 2679–2687.
Gittings, W., Huang, J., Smith, I. C., Quadrilatero, J., & Vandenboom, R. (2011). The effect of skeletal myosin light chain kinase gene ablation on the fatigability of mouse fast muscle. Journal of Muscle Research and Cell Motility, 31(5-6), 337–348.
Gittings, W., Huang, J., & Vandenboom, R. (2012). Tetanic force potentiation of mouse fast muscle is shortening speed dependent. Journal of Muscle Research and Cell Motility, 33(5), 359–368.
Gittings, W., Aggarwal, H., Stull, J. T., & Vandenboom, R. (2015). The force dependence of isometric and concentric potentiation in mouse muscle with and without skeletal myosin light chain kinase. Canadian Journal of Physiology and Pharmacology, 93(1), 23–32.
Godt, R. E., & Nosek, T. M. (1989). Changes of intracellular milieu with fatigue or hypoxia depress contraction of skinned rabbit skeletal and cardiac muscle. The Journal of Physiology, 412(1), 155-180.
Goldspink, G. (1978). Energy turnover during contraction of different types of muscle. Biomechanics VI-A.
Gonzalez, B., Negredo, P., Hernando, R., & Manso, R. (2002). Protein variants of skeletal muscle regulatory myosin light chain isoforms: prevalence in mammals, generation and transitions during muscle remodelling. Pflügers Archive: European Journal of Physiology, 443(3), 377–386.
Gordon, A. M., Homsher, E., & Regnier, M. (2000). Regulation of contraction in striated muscle. Physiological Reviews, 80(2), 853–924.
Gossen, E. R., & Sale, D. G. (2000). Effect of postactivation potentiation on dynamic knee extension performance. European Journal of Applied Physiology, 83(6), 524–530.
Grange, R. W., Cory, C. R., Vandenboom, R., & Houston, M. E. (1995). Myosin phosphorylation augments force-displacement and force-velocity relationships of mouse fast muscle. American Journal of Physiology -- Legacy Content, 269(3 Pt 1), C713–24.
Grange, R. W., Vandenboom, R., & Houston, M. E. (1993). Physiological significance of myosin phosphorylation in skeletal muscle. Canadian Journal of Applied Physiology = Revue Canadienne De Physiologie Appliquée, 18(3), 229–242.
Grange, R. W., Vandenboom, R., Xeni, J., & Houston, M. E. (1998). Potentiation of in vitro concentric work in mouse fast muscle. Journal of Applied Physiology, 84(1), 236–243.
Greenberg, M. J., Mealy, T. R., Jones, M., Szczesna-Cordary, D., & Moore, J. R. (2010). The direct molecular effects of fatigue and myosin regulatory light chain phosphorylation on the actomyosin contractile apparatus. American Journal of Physiology. Regulatory, Integrative and Comparative Physiology, 298(4), R989–96.
Greenberg, M. J., Mealy, T. R., Watt, J. D., Jones, M., Szczesna-Cordary, D., & Moore, J. R. (2009). The molecular effects of skeletal muscle myosin regulatory light chain phosphorylation. American Journal of Physiology. Regulatory, Integrative and Comparative Physiology, 297(2), R265–74.
Gruber, C. M. (1922). The staircase phenomenon in mammalian skeletal muscle. Am J Physiol. 63: 338-48.
Hamada, T., Sale, D. G., MacDougall, J. D., & Tarnopolsky, M. A. (2000). Postactivation potentiation, fiber type, and twitch contraction time in human knee extensor muscles. Journal of Applied Physiology, 88(6), 2131–2137.
Hardie, D. G., & Hawley, S. A. (2001). AMP-activated protein kinase: the energy charge hypothesis revisited. Bioessays, 23(12), 1112–1119.
Harris, R. C., Hultman, E., & Nordesjö, L. O. (1974). Glycogen, glycolytic intermediates and high-energy phosphates determined in biopsy samples of musculus quadriceps femoris of man at rest. Methods and variance of values. Scandinavian Journal of Clinical and Laboratory Investigation, 33(2), 109–120.
Hennig, R., & Lømo, T. (1985). Firing patterns of motor units in normal rats. 314(6007), 164–166.
Hennig, R., & Lømo, T. (1987). Gradation of force output in normal fast and slow muscles of the rat. Acta Physiologica Scandinavica, 130(1), 133–142.
Hill, A. V. (1949). The dimensions of animals and their muscular dynamics.
Hill, A. V. (1951). The Effect of Series Compliance on the Tension Developed in a Muscle Twitch. Proceedings of the Royal Society of London B: Biological Sciences, 138(892), 325–329.
Hodgson, M., Docherty, D., & Robbins, D. (2005). Post-activation potentiation: underlying physiology and implications for motor performance. Sports Medicine, 35(7), 585–595.

Hogan, M. C., Ingham, E., & Kurdak, S. S. (1998). Contraction duration affects metabolic energy cost and fatigue in skeletal muscle. American Journal of Physiology -- Legacy Content, 274(3 Pt 1), E397–E402.

Hollingworth, S., Kim, M. M., & Baylor, S. M. (2012). Measurement and simulation of myoplasmic calcium transients in mouse slow-twitch muscle fibres. The Journal of Physiology, 590(3), 575–594.

Holmberg E and Waldeck B. On the possible role of potassium ions in the action of terbutaline on skeletal muscle contractions. Acta Pharmacol Toxicol 46: 141–149, 1980.

Homsher, E. (1987). Muscle enthalpy production and its relationship to actomyosin ATPase. Physiology, 49(1), 673–690.

Homsher, E., Mommaerts, W. F., Ricchiuti, N. V., & Wallner, A. (1972). Activation heat, activation metabolism and tension-related heat in frog semitendinosus muscles. Journal of Physiology, 220(3), 601–625.

Houston, M. E., & Grange, R. W. (1990). Myosin phosphorylation, twitch potentiation, and fatigue in human skeletal muscle. Canadian Journal of Physiology ….

Huxley, A. F. (1957). Muscle structure and theories of contraction. Progress in Biophysics and Biophysical Chemistry, 7, 255–318.

Inglis, J. G., Howard, J., McIntosh, K., Gabriel, D. A., & Vandenboom, R. (2011). Decreased motor unit discharge rate in the potentiated human tibialis anterior muscle. Acta Physiologica (Oxford, England), 201(4), 483–492.

James, R. S., Altringham, J. D., & Goldspink, D. F. (1995). The mechanical properties of fast and slow skeletal muscles of the mouse in relation to their locomotory function. The Journal of Experimental Biology, 198(Pt 2), 491–502.

Josephson, R. K. (1993). Contraction Dynamics and Power Output of Skeletal Muscle. Physiology, 55(1), 527–546.

Josephson, R. K. (1999). Dissecting muscle power output. The Journal of Experimental Biology, 202(Pt 23), 3369–3375.

Judge, L. W. (2009). The Application of Postactivation Potentiation to the Track and Field Thrower. Strength & Conditioning Journal, 31(3), 34–36.

Julian, F. J., & Morgan, D. L. (1979). The effect on tension of non-uniform distribution of length changes applied to frog muscle fibres. The Journal of Physiology, 293(1), 379–392.

Kamm, K. E., & Stull, J. T. (2001). Dedicated myosin light chain kinases with diverse cellular functions. Journal of Biological Chemistry, 276(7), 4527–4530.

Karatzaferi, C., Franks-Skiba, K., & Cooke, R. (2008). Inhibition of shortening velocity of skinned skeletal muscle fibers in conditions that mimic fatigue. American Journal of Physiology. Regulatory, Integrative and Comparative Physiology, 294(3), R948–R955.

Kawai, M., Brandt, P. W., & Cox, R. N. (1984). The Role of Ca2+ in Cross-Bridge Kinetics in Chemically Skinned Rabbit Psoas Fibers. In Contractile Mechanisms in Muscle (Vol. 37, pp. 657–672). Boston, MA: Springer US.

Kamm, K. E., & Stull, J. T. (2001). Dedicated myosin light chain kinases with diverse cellular functions. Journal of Biological Chemistry, 276(7), 4527-4530.

Klein, C. S., Ivanova, T. D., Rice, C. L., & Garland, S. J. (2001). Motor unit discharge rate following twitch potentiation in human triceps brachii muscle. Neuroscience Letters, 316(3), 153–156.

Klug, G. A., Botterman, B. R., & Stull, J. T. (1982). The effect of low frequency stimulation on myosin light chain phosphorylation in skeletal muscle. Journal of Biological Chemistry, 257(9), 4688–4690.

Konishi, M. (1998). Cytoplasmic Free Concentrations of Ca2+ and Mg2+ in Skeletal Muscle Fibers at Rest and during Contraction. The Japanese Journal of Physiology, 48(6), 421–438.

Krarup, C. (1981a). Enhancement and diminution of mechanical tension evoked by staircase and by tetanus in rat muscle. Journal of Physiology, 311, 355–372.

Krarup, C. (1981b). Temperature dependence of enhancement and diminution of tension evoked by staircase and by tetanus in rat muscle. Journal of Physiology, 311, 373–387.

Krarup, C. (1981c). The effect of dantrolene on the enhancement and diminution of tension evoked by staircase and by tetanus in rat muscle. Journal of Physiology, 311, 389–400.

Krutki, P., Mrówczyński, W., Raikova, R., & Celichowski, J. (2014). Concomitant changes in afterhyperpolarization and twitch following repetitive stimulation of fast motoneurones and motor units. Experimental Brain Research, 232(2), 443–452.

Krutki, P., Pogrzebna, M., Drzymała, H., Raikova, R., & Celichowski, J. (2008). Force generated by fast motor units of the rat medial gastrocnemius muscle during stimulation with pulses at variable intervals. Journal of Physiology and Pharmacology : an Official Journal of the Polish Physiological Society, 59(1), 85–100.

Kushmerick, M. J. (1985). Patterns in mammalian muscle energetics. The Journal of Experimental Biology, 115(1), 165–177.
Kushmerick, M. J., & Crow, M. (1982). Chemical energy balance in amphibian and mammalian muscles. Federation Proceedings, 41(2), 163–168.
Kushmerick, M. J., & Crow, M. T. (1981). Chemical energetics, mechanics, and phosphorylation of regulatory light chains in mammalian fast-and slow-twitch muscles. Society of General Physiologists series 37 (1981): 159-172.
Kushmerick, M. J., Moerland, T. S., & Wiseman, R. W. (1992). Mammalian skeletal muscle fibers distinguished by contents of phosphocreatine, ATP, and Pi. Proceedings of the National Academy of Sciences of the United States of America, 89(16), 7521–7525.
Lännergren, J., Bruton, J. D., & Westerblad, H. (2000). Vacuole formation in fatigued skeletal muscle fibres from frog and mouse: effects of extracellular lactate. The Journal of Physiology, 526(3), 597–611.
Leblond, H., L'Espérance, M., Orsal, D., & Rossignol, S. (2003). Treadmill locomotion in the intact and spinal mouse. The Journal of Neuroscience : the Official Journal of the Society for Neuroscience, 23(36), 11411–11419.
Lee, S. C., Gerdom, M. L., & Binder-Macleod, S. A. (1999). Effects of length on the catchlike property of human quadriceps femoris muscle. Physical Therapy, 79(8), 738–748.
Leong, P., & MacLennan, D. H. (1998). Complex interactions between skeletal muscle ryanodine receptor and dihydropyridine receptor proteins. Biochemistry and Cell Biology, 76(5), 681–694.
Levine, R. J., Kensler, R. W., Yang, Z., Stull, J. T., & Sweeney, H. L. (1996). Myosin light chain phosphorylation affects the structure of rabbit skeletal muscle thick filaments. Biophysical Journal, 71(2), 898–907.
Levine, R. J., Yang, Z., Epstein, N. D., Fananapazir, L., Stull, J. T., & Sweeney, H. (1998). Structural and Functional Responses of Mammalian Thick Filaments to Alterations in Myosin Regulatory Light Chains. Journal of Structural Biology, 122(1-2), 149–161.
Lewis, D. B., & Barclay, C. J. (2014). Efficiency and cross-bridge work output of skeletal muscle is decreased at low levels of activation. Pflügers Archiv : European Journal of Physiology, 466(3), 599–609
Lichtwark, G. A., & Barclay, C. J. (2010). The influence of tendon compliance on muscle power output and efficiency during cyclic contractions. The Journal of Experimental Biology, 213(5), 707–714.
Macintosh, B. R. (2003). Role of Calcium Sensitivity Modulation in Skeletal Muscle Performance. Physiology, 18(6), 222–225.
Macintosh, B. R. (2010a). Cellular and Whole Muscle Studies of Activity Dependent Potentiation. In D. E. Rassier, Muscle Biophysics (Vol. 682, pp. 315–342). New York, NY: Springer New York.
Macintosh, B. R., & Bryan, S. N. (2002). Potentiation of shortening and velocity of shortening during repeated isotonic tetanic contractions in mammalian skeletal muscle. Pflügers Archiv : European Journal of Physiology, 443(5-6), 804–812.
Macintosh, B. R., & MacNaughton, M. B. (2005). The length dependence of muscle active force: considerations for parallel elastic properties. Journal of Applied Physiology, 98(5), 1666–1673
Macintosh, B. R., & Shahi, M. R. S. (2011). A peripheral governor regulates muscle contraction. Applied Physiology, Nutrition, and Metabolism = Physiologie Appliquée, Nutrition Et Métabolisme, 36(1), 1–11.
Macintosh, B. R., & Willis, J. C. (2000). Force-frequency relationship and potentiation in mammalian skeletal muscle. Journal of Applied Physiology, 88(6), 2088–2096.
Macintosh, B. R., Holash, R. J., & Renaud, J.-M. (2012a). Skeletal muscle fatigue--regulation of excitation-contraction coupling to avoid metabolic catastrophe. Journal of Cell Science, 125(Pt 9), 2105–2114.
Macintosh, B. R., MacNaughton, M. B., & MacDougall, J. D. (2006). Skeletal Muscle.
Macintosh, B. R., Robillard, M.-E., & Tomaras, E. K. (2012b). Should postactivation potentiation be the goal of your warm-up? Applied Physiology, Nutrition, and Metabolism = Physiologie Appliquée, Nutrition Et Métabolisme, 37(3), 546–550.
Macintosh, B. R., Smith, M. J., & Rassier, D. E. (2008a). Staircase but not posttetanic potentiation in rat muscle after spinal cord hemisection. Muscle & Nerve, 38(5), 1455–1465
Macintosh, B. R., Taub, E. C., Dormer, G. N., & Tomaras, E. K. (2008b). Potentiation of isometric and isotonic contractions during high-frequency stimulation. Pflügers Archiv : European Journal of Physiology, 456(2), 449–458.
Manning, D. R., & Stull, J. T. (1982). Myosin light chain phosphorylation-dephosphorylation in mammalian skeletal muscle. American Journal of Physiology -- Legacy Content, 242(3), C234–41.

Manuel, M., & Heckman, C. J. (2011). Adult mouse motor units develop almost all of their force in the subprimary range: a new all-or-none strategy for force recruitment? The Journal of Neuroscience : the Official Journal of the Society for Neuroscience, 31(42), 15188–15194

Marsden, C. D., Meadows, J. C., & Merton, P. A. (1983). "Muscular wisdom" that minimizes fatigue during prolonged effort in man: peak rates of motoneuron discharge and slowing of discharge during fatigue. Advances in Neurology, 39, 169–211.

Marsh, R. L. (1999). How muscles deal with real-world loads: the influence of length trajectory on muscle performance. The Journal of Experimental Biology, 202(Pt 23), 3377–3385.

Matsumura, F., & Hartshorne, D. J. (2008). Myosin phosphatase target subunit: Many roles in cell function. Biochemical and Biophysical Research Communications, 369(1), 149–156.

McKenna, M. J., Bangsbo, J., & Renaud, J. M. (2008). Muscle K+, Na+, and Cl− disturbances and Na+-K+ pump inactivation: implications for fatigue. Journal of Applied Physiology, 104(1), 288-295.

McKillop, D.F., Geeves, M. A. (1993). Regulation of the interaction between actin and myosin subfragment 1: evidence for three states of the thin filament. Biophysical Journal, 65(2), 693–701.

Metzger, J. M., Greaser, M. L., & Moss, R. L. (1989). Variations in cross-bridge attachment rate and tension with phosphorylation of myosin in mammalian skinned skeletal muscle fibers. Implications for twitch potentiation in intact muscle. The Journal of General Physiology, 93(5), 855–883.

Mijailovich, S. M., Kayser-Herold, O., Li, X., Griffiths, H., & Geeves, M. A. (2012). Cooperative regulation of myosin-S1 binding to actin filaments by a continuous flexible Tm–Tn chain. European Biophysics Journal, 41(12), 1015–1032.

Mitchell, C. J., & Sale, D. G. (2011). Enhancement of jump performance after a 5-RM squat is associated with postactivation potentiation. European Journal of Applied Physiology, 111(8), 1957–1963.

Mollica, J. P., Dutka, T. L., Merry, T. L., Lamboley, C. R., McConell, G. K., McKenna, M. J., ... & Lamb, G. D. (2012). S-Glutathionylation of troponin I (fast) increases contractile apparatus Ca2+ sensitivity in fast-twitch muscle fibres of rats and humans. The Journal of physiology, 590(6), 1443-1463.

Moore, R. L., Palmer, B. M., Williams, S. L., Tanabe, H. I. R. O. Y. U. K. I., Grange, R. W., & Houston, M. E. (1990). Effect of temperature on myosin phosphorylation in mouse skeletal muscle. American Journal of Physiology-Cell Physiology, 259(3), C432-C438

Moore, R. L., & Stull, J. T. (1984). Myosin light chain phosphorylation in fast and slow skeletal muscles in situ. American Journal of Physiology-Cell Physiology,247(5), C462-C471.

Moraczewska, J. (2002). Structural determinants of cooperativity in acto-myosin interactions. Acta Biochimica Polonica, 49(4), 805–812.

Morgan, M., Perry, S. V., & Ottaway, J. (1976). Myosin light-chain phosphatase. The Biochemical Journal, 157(3), 687–697.

Morris, C. A., Tobacman, L. S., & Homsher, E. (2001). Modulation of contractile activation in skeletal muscle by a calcium-insensitive troponin C mutant. Journal of Biological Chemistry.

Mrowczynski, W., Krutki, P., Chakarov, V., & Celichowski, J. (2011). Modulation of afterhyperpolarization evoked by doublets and increasing number of stimuli in rat motoneurons. Journal of Motor Behavior, 43(1), 63–71.

Murphy, R. M., Larkins, N. T., Mollica, J. P., Beard, N. A., & Lamb, G. D. (2009). Calsequestrin content and SERCA determine normal and maximal Ca2+ storage levels in sarcoplasmic reticulum of fast- and slow-twitch fibres of rat. The Journal of Physiology, 587(2), 443–460.

Myburgh, K.H. (2004a). Can any metabolites partially alleviate fatigue manifestations at the cross-bridge? Medicine and Science in Sports and Exercise, 36(1), 20–27.

Myburgh, K.H. (2004b). Protecting muscle ATP: positive roles for peripheral defense mechanisms-introduction. Medicine and Science in Sports and Exercise, 36(1), 16–19.

Nelson-Wong, E., Howarth, S., Winter, D. A., & Callaghan, J. P. (2009). Application of Autocorrelation and Cross-correlation Analyses in Human Movement and Rehabilitation Research. Journal of Orthopaedic & Sports Physical Therapy, 39(4), 287–295.

Norris, S. M., Bombardier, E., Smith, I. C., Vigna, C., & Tupling, A. R. (2010). ATP consumption by sarcoplasmic reticulum Ca2+ pumps accounts for 50% of resting metabolic rate in mouse fast and slow twitch skeletal muscle. American Journal of Physiology. Cell Physiology, 298(3), C521–C529.

Otazu, G. H., Futami, R., & Hoshimiya, N. (2001). A muscle activation model of variable stimulation frequency response and stimulation history, based on positive feedback in calcium dynamics. Biological Cybernetics, 84(3), 193–206.

Parmiggiani, F., & Stein, R. B. (1981). Nonlinear summation of contractions in cat muscles. II. Later facilitation and stiffness changes. The Journal of General Physiology, 78(3), 295–311.

Patel, J. R., Diffee, G. M., Huang, X. P., & Moss, R. L. (1998). Phosphorylation of myosin regulatory light chain eliminates force-dependent changes in relaxation rates in skeletal muscle. Biophysical Journal, 74(1), 360–368.
Perrie, W. T., Smillie, L. B., & Perry, S. V. (1973). A phosphorylated light-chain component of myosin from skeletal muscle. Biochem. J, 135, 151-164.
Persechini, A., Stull, J. T., & Cooke, R. (1985). The effect of myosin phosphorylation on the contractile properties of skinned rabbit skeletal muscle fibers. Journal of Biological Chemistry, 260(13), 7951–7954.
Person, R. S., & Kudina, L. P. (1972). Discharge frequency and discharge pattern of human motor units during voluntary contraction of muscle. Electroencephalography and Clinical Neurophysiology, 32(5), 471–483.
Pires, E., Perry, S. V., & Thomas, M. (1974). Myosin light-chain kinase, a new enzyme from striated muscle. FEBS Letters, 41(2), 292–296.
Rall, J. A. (1984). Energetic aspects of skeletal muscle contraction: implications of fiber types. Exercise and Sport Sciences Reviews, 13, 33–74.
Rankin, L. L., Enoka, R. M., Volz, K. A., & Stuart, D. G. (1988). Coexistence of twitch potentiation and tetanic force decline in rat hindlimb muscle. Journal of Applied Physiology, 65(6), 2687-2695.
Rassier, D. E. (2010). Muscle Biophysics. (D. E. Rassier) (Vol. 682). New York, NY: Springer New York.
Rassier, D. E., & MacIntosh, B. R. (1999). Length dependence of active force production in skeletal muscle. Journal of Applied ….
Rassier, D. E., & MacIntosh, B. R. (2000). Coexistence of potentiation and fatigue in skeletal muscle. Brazilian Journal of Medical and Biological Research, 33(5), 499–508.
Rassier, D. E., Tubman, L. A., & MacIntosh, B. R. (1999). Staircase in mammalian muscle without light chain phosphorylation. Brazilian Journal of Medical and Biological Research, 32(1), 121–130.
Rayment, I. (1996). The structural basis of the myosin ATPase activity. Journal of Biological Chemistry, 271(27), 15850–15853.
Rayment, I., & Holden, H. M. (1994). The three-dimensional structure of a molecular motor. Trends in Biochemical Sciences, 19(3), 129–134.
Rayment, I., Holden, H. M., Whittaker, M., Yohn, C. B., Lorenz, M., Holmes, K. C., & Milligan, R. A. (1993). Structure of the actin-myosin complex and its implications for muscle contraction. Science, 261(5117), 58–65.
Reggiani, C., Potma, E. J., Bottinelli, R., Canepari, M., Pellegrino, M. A., & Stienen, G. J. (1997). Chemo-mechanical energy transduction in relation to myosin isoform composition in skeletal muscle fibres of the rat. Journal of Physiology, 502 ( Pt 2), 449–460.
Renaud, J. M., & Light, P. (1992). Effects of K+ on the twitch and tetanic contraction in the sartorius muscle of the frog, Rana pipiens. Implication for fatigue in vivo. Canadian journal of physiology and pharmacology, 70(9), 1236-1246.
Ritz-Gold, C. J., Cooke, R., Blumenthal, D. K., & Stull, J. T. (1980). Light chain phosphorylation alters the conformation of skeletal muscle myosin. Biochemical and Biophysical Research Communications, 93(1), 209–214.
Rolfe, D. F., & Brown, G. C. (1997). Cellular energy utilization and molecular origin of standard metabolic rate in mammals. Physiological Reviews, 77(3), 731–758.
Russ, D. W., Elliott, M. A., Vandenborne, K., Walter, G. A., & Binder-Macleod, S. A. (2002). Metabolic costs of isometric force generation and maintenance of human skeletal muscle. American Journal of Physiology - Endocrinology and Metabolism, 282(2), E448–E457.
Ryder, J. W., Lau, K. S., Kamm, K. E., & Stull, J. T. (2007). Enhanced skeletal muscle contraction with myosin light chain phosphorylation by a calmodulin-sensing kinase. Journal of Biological Chemistry.
Sahlin, K., & Harris, R. C. (2011). The creatine kinase reaction: a simple reaction with functional complexity. Amino Acids, 40(5), 1363–1367.
Sahlin, K., Harris, R. C., Nylind, B., & Hultman, E. (1976). Lactate content and pH in muscle samples obtained after dynamic exercise. Pflügers Archiv : European Journal of Physiology, 367(2), 143–149.
Sale, D. G. (2002). Postactivation Potentiation: Role in Human Performance. Exercise and Sport Sciences Reviews, 30(3), 138.
Sandercock, T. G., & Heckman, C. J. (1997). Doublet potentiation during eccentric and concentric contractions of cat soleus muscle. Journal of Applied Physiology, 82(4), 1219–1228.
Schiaffino, S., & Reggiani, C. (2011). Fiber types in mammalian skeletal muscles. Physiological Reviews.

Seow, C. Y., & Ford, L. E. (1991). Shortening velocity and power output of skinned muscle fibers from mammals having a 25,000-fold range of body mass. The Journal of General Physiology, 97(3), 541–560.

Sieck, G. C., & Regnier, M. (2001). Invited review: plasticity and energetic demands of contraction in skeletal and cardiac muscle. Journal of Applied Physiology. 90(3), 1158-1164.

Siegman, M. J., Mooers, S. U., Warren, T. B., Warshaw, D. M., Ikebe, M., & Butler, T. M. (1994). Comparison of the effects of 2,3-butanedione monoxime on force production, myosin light chain phosphorylation and chemical energy usage in intact and permeabilized smooth and skeletal muscles. Journal of Muscle Research and Cell Motility, 15(4), 457–472.

Smith, C. B., Cheng, A. J., & Rice, C. L. (2011). Potentiation of the triceps brachii during voluntary submaximal contractions. Muscle & Nerve, 43(6), 859–865.

Smith, I. C., Gittings, W., Huang, J., McMillan, E. M., Quadrilatero, J., Tupling, A. R., & Vandenboom, R. (2013). Potentiation in mouse lumbrical muscle without myosin light chain phosphorylation: is resting calcium responsible? The Journal of General Physiology, 141(3), 297–308.

Smith, I. C., Huang, J., Quadrilatero, J., Tupling, A. R., & Vandenboom, R. (2010). Posttetanic potentiation in mdx muscle. Journal of Muscle Research and Cell Motility, 31(4), 267–277.

Smith, N. P., Barclay, C. J., & Loiselle, D. S. (2005). The efficiency of muscle contraction. Progress in Biophysics and Molecular Biology, 88(1), 1–58.

Spriet, L. L. (1989). ATP utilization and provision in fast-twitch skeletal muscle during tetanic contractions. American Journal of Physiology -- Legacy Content, 257(4 Pt 1), E595–E605.

Steele, D. S., & Duke, A. M. (2003). Metabolic factors contributing to altered Ca2+ regulation in skeletal muscle fatigue. Acta Physiologica Scandinavica, 179(1), 39–48.

Stevens, L., Firinga, C., Gohlsch, B., Bastide, B., Mounier, Y., & Pette, D. (2000). Effects of unweighting and clenbuterol on myosin light and heavy chains in fast and slow muscles of rat. American Journal of Physiology. Cell Physiology, 279(5), C1558–C1563.

Stuart, D. S., Lingley, M. D., Grange, R. W., & Houston, M. E. (2011). Myosin light chain phosphorylation and contractile performance of human skeletal muscle. Canadian Journal of Physiology and Pharmacology, 66(1), 49–54.

Stull, J. T., Kamm, K. E., & Vandenboom, R. (2011). Myosin light chain kinase and the role of myosin light chain phosphorylation in skeletal muscle. Archives of Biochemistry and Biophysics, 510(2), 120–128.

Stull, J. T., Nunnally, M. H., Moore, R. L., & Blumenthal, D. K. (1985). Myosin light chain kinases and myosin phosphorylation in skeletal muscle. Advances in Enzyme Regulation, 23, 123–140.

Sweeney, H. L. (1994). The importance of the creatine kinase reaction: the concept of metabolic capacitance. Medicine and Science in Sports and Exercise, 26(1), 30–36.

Sweeney, H. L., & Houdusse, A. (2010). Structural and functional insights into the Myosin motor mechanism. Biophysics, 39, 539–557.

Sweeney, H. L., & Stull, J. T. (1986). Phosphorylation of myosin in permeabilized mammalian cardiac and skeletal muscle cells. American Journal of Physiology -- Legacy Content, 250(4 Pt 1), C657–C660.

Sweeney, H. L., & Stull, J. T. (1990). Alteration of cross-bridge kinetics by myosin light chain phosphorylation in rabbit skeletal muscle: implications for regulation of actin-myosin interaction. Proceedings of the National Academy of Sciences of the United States of America, 87(1), 414–418

Sweeney, H. L., Bowman, B. F., & Stull, J. T. (1993). Myosin light chain phosphorylation in vertebrate striated muscle: regulation and function. American Journal of Physiology -- Legacy Content, 264(5 Pt 1), C1085–C1095.

Sweeney, H. L., Yang, Z., Zhi, G., Stull, J. T., & Trybus, K. M. (1994). Charge replacement near the phosphorylatable serine of the myosin regulatory light chain mimics aspects of phosphorylation. Proceedings of the National Academy of Sciences of the United States of America, 91(4), 1490–1494. doi:10.2307/2364127

Tallis, J., James, R. S., Cox, V. M., & Duncan, M. J. (2012). The effect of physiological concentrations of caffeine on the power output of maximally and submaximally stimulated mouse EDL (fast) and soleus (slow) muscle. Journal of Applied Physiology, 112(1), 64–71.

Tanner, B. C. W., Daniel, T. L., & Regnier, M. (2012). Filament Compliance Influences Cooperative Activation of Thin Filaments and the Dynamics of Force Production in Skeletal Muscle. PLoS Computational Biology, 8(5), e1002506.

Tansey, K. E., & Botterman, B. R. (1996a). Activation of type-identified motor units during centrally evoked contractions in the cat medial gastrocnemius muscle. I. Motor-unit recruitment. Journal of Neurophysiology.

Tansey, K. E., & Botterman, B. R. (1996b). Activation of type-identified motor units during centrally evoked contractions in the cat medial gastrocnemius muscle. II. Motoneuron firing-rate modulation. Journal of Neurophysiology.

Tiidus, P., Tupling, A. R., & Houston, M. (2012). Biochemistry primer for exercise science.

Tillin, M. N. A., & Bishop, D. (2009). Factors Modulating Post-Activation Potentiation and its Effect on Performance of Subsequent Explosive Activities. Sports Medicine, 39(2), 147–166.

Tomaras, E. K., & Macintosh, B. R. (2011). Less is more: standard warm-up causes fatigue and less warm-up permits greater cycling power output. Journal of Applied Physiology (Bethesda, Md. : 1985), 111(1), 228–235.

Tononi, G., Sporns, O., & Edelman, G. M. (1999). Measures of degeneracy and redundancy in biological networks. Proceedings of the National Academy of Sciences, 96(6), 3257–3262.

Tubman, L. A., MacIntosh, B. R., & Maki, W. A. (1996). Myosin light chain phosphorylation and posttetanic potentiation in fatigued skeletal muscle. Pflügers Archiv.

Tubman, L. A., Rassier, D. E., & MacIntosh, B. R. (1996). Absence of myosin light chain phosphorylation and twitch potentiation in atrophied skeletal muscle. Canadian journal of physiology and pharmacology, 74(6), 723-728.

Tubman, L. A., Rassier, D. E., & Macintosh, B. R. (1997). Attenuation of myosin light chain phosphorylation and posttetanic potentiation in atrophied skeletal muscle. Pflügers Archiv : European Journal of Physiology, 434(6), 848–851.

Tupling, A.R. (2009). Excitation-Contraction Coupling. In Encyclopedia of Neuroscience (pp. 1479–1483). Springer Berlin Heidelberg.

Tupling, A. R. (2011). The Sarcoplasmic Reticulum in Muscle Fatigue and Disease: Role of the Sarco(endo)plasmic Reticulum Ca2+-ATPase. Canadian Journal of Applied Physiology, 29(3), 308–329.

Vandenboom, R. (2004). The myofibrillar complex and fatigue: a review. Canadian Journal of Applied Physiology = Revue Canadienne De Physiologie Appliquée, 29(3), 330–356.

Vandenboom, R., & Houston, M. E. (1996). Phosphorylation of myosin and twitch potentiation in fatigued skeletal muscle. Canadian Journal of Physiology and Pharmacology, 74(12), 1315–1321.

Vandenboom, R., Claflin, D. R., & Julian, F. J. (1998). Effects of rapid shortening on rate of force regeneration and myoplasmic [Ca2+] in intact frog skeletal muscle fibres. The Journal of Physiology, 511(1), 171–180. doi:10.1111/j.1469-7793.1998.171bi.x

Vandenboom, R., Gittings, W., Smith, I. C., Grange, R. W., & Stull, J. T. (2013). Myosin phosphorylation and force potentiation in skeletal muscle: evidence from animal models. Journal of Muscle Research and Cell Motility, 34(5-6), 317–332.

Vandenboom, R., Grange, R. W., & Houston, M. E. (1993). Threshold for force potentiation associated with skeletal myosin phosphorylation. American Journal of Physiology -- Legacy Content, 265(6 Pt 1), C1456–62.

Vandenboom, R., Grange, R. W., & Houston, M. E. (1995). Myosin phosphorylation enhances rate of force development in fast-twitch skeletal muscle. American Journal of Physiology -- Legacy Content, 268(3 Pt 1), C596–603.

Vandenboom, R., Hannon, J. D., & Sieck, G. C. (2002). Isotonic force modulates force redevelopment rate of intact frog muscle fibres: evidence for cross-bridge induced thin filament activation. Journal of Physiology, 543(Pt 2), 555–566.

Vandenboom, R., Xeni, J., Bestic, N. M., & Houston, M. E. (1997). Increased force development rates of fatigued mouse skeletal muscle are graded to myosin light chain phosphate content. American Journal of Physiology -- Legacy Content, 272(6 Pt 2), R1980–4.

Van Cutsem, M., Duchateau, J., & Hainaut, K. (1998). Changes in single motor unit behaviour contribute to the increase in contraction speed after dynamic training in humans. The Journal of Physiology, 513(1), 295–305.

Walker SM. Action potentials in rat muscle with twitch tension potentiated by KCl treatment, adrenalectomy, tetanus, and treppe. Am J Physiol 154: 63–72, 1948.

Westerblad, H., & Allen, D. G. (1991). Changes of myoplasmic calcium concentration during fatigue in single mouse muscle fibers. The Journal of General Physiology, 98(3), 615–635.

Westerblad, H., Bruton, J. D., & Katz, A. (2010). Skeletal muscle: Energy metabolism, fiber types, fatigue and adaptability. Experimental Cell Research, 316(18), 3093–3099.

Westerblad, H., Bruton, J. D., Allen, D. G., & Lännergren, J. (2000). Functional significance of Ca2+ in long-lasting fatigue of skeletal muscle. European Journal of Applied Physiology, 83(2-3), 166–174,

Westra, H. G., de Haan, A., van Doorn, J. E., & de Haan, E. J. (1985). The effect of intensive interval training on the anaerobic power of the rat quadriceps muscle. Journal of Sports Sciences, 3(2), 139–150. doi:10.1080/02640418508729743

Westra, H. G., de Haan, A., van Doorn, J. E., & de Haan, E. J. (1988). Anaerobic chemical changes and mechanical output during isometric tetani of rat skeletal muscle in situ. Pflügers Archiv : European Journal of Physiology, 412(1-2), 121–127.

Woledge, R. C., Curtin, N. A., & Homsher, E. (1985). Energetic aspects of muscle contraction. Monographs of the Physiological Society, 41, 1–357.

Xeni, J., Gittings, W. B., Caterini, D., Huang, J., Houston, M. E., Grange, R. W., & Vandenboom, R. (2011). Myosin light-chain phosphorylation and potentiation of dynamic function in mouse fast muscle. Pflügers Archiv : European Journal of Physiology, 462(2), 349–358.

Yang, Z., Stull, J. T., Levine, R. J., & Sweeney, H. (1998). Changes in Interfilament Spacing Mimic the Effects of Myosin Regulatory Light Chain Phosphorylation in Rabbit Psoas Fibers. Journal of Structural Biology, 122(1-2), 139–148.

Yensen, C., Matar, W., & Renaud, J. M. (2002). K+-induced twitch potentiation is not due to longer action potential. American Journal of Physiology-Cell Physiology, 283(1), C169-C177.

Zhang, S.-J., Andersson, D. C., Sandström, M. E., Westerblad, H., & Katz, A. (2006). Cross bridges account for only 20% of total ATP consumption during submaximal isometric contraction in mouse fast-twitch skeletal muscle. American Journal of Physiology. Cell Physiology, 291(1), C147–C154.

Zhi, G., Ryder, J. W., Huang, J., Ding, P., Chen, Y., Zhao, Y., et al. (2005). Myosin light chain kinase and myosin phosphorylation effect frequency-dependent potentiation of skeletal muscle contraction. Proceedings of the National Academy of Sciences of the United States of America, 102(48), 17519–17524.

Zot, A. S., & Potter, J. D. (1989). Reciprocal coupling between troponin C and myosin crossbridge attachment. Biochemistry (Washington), 28(16), 6751–6756.

# Chapter 4

## Study #1

**Tetanic force potentiation of mouse fast muscle is shortening speed dependent**

William Gittings, Jian Huang, and Rene Vandenboom

As published in: Journal of Muscle Research and Cell Motility, 33(5), 359–368, 2012

**Author contributions:**

*William Gittings*: study design, data collection and experimentation, manuscript writing

*Jian Huang*: myosin RLC phosphorylation analysis

*Dr. Rene Vandenboom*: study design input, funding (NSERC), manuscript writing

Running head: Concentric force potentiation


## *Abstract*

The activity dependent potentiation of peak isometric force associated with phosphorylation of the myosin regulatory light chain (RLC) is generally restricted to low activation frequencies. The purpose of this study was to determine if muscle shortening speed influenced the stimulus frequency domain over which concentric force potentiation was observed. To this end, mouse extensor digitorum longus (EDL) muscles (*in vitro*, 25 °C) were activated at a range of test frequencies (10, 25, 45, 70 or 100 Hz) during shortening ramps at 0.10, 0.30 or 0.50 of the maximal velocity of shortening ($V_{max}$). This procedure was performed before and after a standard potentiating stimulus (PS) that elevated RLC phosphorylation from 0.08±0.01 (rest) to 0.55±0.01 (stimulated) moles phosphate per mol RLC, respectively (n = 9–11) ($P < 0.01$). When data from all test frequencies were collapsed, the PS potentiated mean concentric force at 0.10, 0.30 and 0.50 $V_{max}$ to 1.02±0.03, 1.37±0.03 and 1.59±0.05 of unpotentiated, pre-PS values, respectively (n = 8, $P < 0.05$). In addition, increasing shortening speed also increased the activation frequency at which concentric force potentiation was maximal, i.e. from 10 Hz at 0.10 $V_{max}$ to 10–25 and 25–45 Hz at 0.30 and 0.50 $V_{max}$, respectively. These results indicate that both the magnitude of and activation frequency dependence for concentric force potentiation of mouse EDL muscle is shortening speed dependent. Thus, muscle-shortening speed may be a critical factor determining the functional utility of the myosin RLC phosphorylation mechanism.



Keywords: relaxation rate, myosin phosphorylation, regulatory light chains, shortening ramps, mouse muscle in vitro

## *Introduction*

An important, defining characteristic property of mammalian fast twitch skeletal muscle is force potentiation, defined as the transient increase in twitch force observed during or after contractile activity (e.g., Close and Hoh 1968). Myriad studies provide evidence that the primary intracellular mechanism responsible for potentiation is myosin light chain kinase (MLCK) mediated phosphorylation of the myosin regulatory light chain (RLC). For example, fast twitch skeletal muscles containing MLCK have been used to demonstrate strong temporal correlations between isometric and dynamic twitch force potentiation and RLC phosphorylation (Grange et al. 1995; Klug et al. 1982; Manning and Stull 1982; Moore and Stull 1984; Xeni et al. 2011). In contrast, tetanic stimulation of slow twitch muscle, which contains much-reduced MLCK and a concomitant reduced ability to phosphorylate the RLC, produces post-contractile depressions in force (e.g., Buller et al. 1981). Indeed, recent studies using muscles from $MLCK^{-/-}$ knockout mice show that, in the absence of RLC phosphorylation, isometric twitch potentiation is either attenuated or eliminated (Gittings et al. 2011; Zhi et al. 2005). As a result, MLCK mediated phosphorylation of the RLC may represent a molecular memory that enhances mechanical performance of fast muscle fibre types (MacIntosh 2010).

Studies performed on permeabilized skeletal fibres show how the MLCK catalyzed phosphorylation of the RLC may influence muscle contraction (Stull et al. 2011). Structural studies performed on a variety of permeabilized fibre models shows that the addition of a negatively charged moiety to a serine residue alters myosin structure and/or position on the thick filament surface (Alamo et al. 2008; Brito et al. 2011). This action, in turn, appears to facilitate the ability of phosphorylated cross-bridges to interact with the thin filament. As described using Brenner's (1988) model for cross-bridge cycling, phosphorylation of the RLC increases the transition from non-force to force-generating states ($f_{app}$) during $Ca^{2+}$ activation; the reverse transition ($g_{app}$) is not, however, altered (Sweeney and Stull 1990). This effect on cross-bridge cycling may increase the $Ca^{2+}$ sensitivity of steady-state force development, as displayed by permeabilized skeletal fibres in the phosphorylated state (Metzger et al. 1989; Persechini et al. 1985; Sweeney and Stull 1986), and in turn, accounts mechanistically for the twitch force potentiation observed in various fast twitch skeletal muscle models (Sweeney et al. 1993).

An important gap in our knowledge regarding the functional role of myosin phosphorylation is how this mechanism modulates skeletal muscle force during tetanic contractions (isometric or isotonic) typical of *in vivo* activity. For example, although highly dependent upon absolute force requirements (De Luca and Hostage 2010; Erim et al. 1996) the discharge rate of fast twitch motor units in the cat and rat hindlimb may approach or exceed 50 Hz (Hennig and Lømo 1985; Tansey and Botterman 1996a, b). Interestingly, when high frequency contractions have been studied in the rat hindlimb, potentiation induced increases in isometric and isotonic force have been reported (e.g. Abbate et al. 2000; MacIntosh and Bryan 2002; MacIntosh and Willis 2000; MacIntosh et al. 2008). Thus, these studies suggest that potentiation may enhance acute mechanical performance across the entire activation frequency range for fast twitch skeletal muscle. Despite this, little is known regarding how muscle shortening speed, a critical factor determining muscle force and power (Josephson 1999), influences the frequency dependence of potentiation in fast twitch skeletal muscle.

The purpose of this study was to determine the influence of muscle shortening speed on the activation frequency dependence of concentric force potentiation for mouse extensor digitorum longus (EDL) muscle *in vitro* (25 °C). To do this, muscles were activated at 10–100 Hz during constant amplitude, but different speed, shortening ramps equivalent to 0.10, 0.30 or 0.50 $V_{max}$ before and after a potentiating stimulus (PS) that elevated myosin RLC phosphorylation. We hypothesized that increasing speeds of shortening would modify the ability of the myosin RLC phosphorylation mechanism to enhance concentric force.

## *Methods*

All procedures utilized have received full ethical approval from the Brock University Animal Care and Use Committee. Adult C57BL/6 mice (17–22g) were anaesthetized with a peritoneal injection of sodium pentobarbital (60 mg/kg body weight), diluted with 0.9% saline in a 1 ml syringe. The EDL was surgically excised and suspended using non-absorbent silk suture tied directly to both proximal and distal tendons (distal suture was clamped securely in the bath apparatus while the proximal suture was tied directly to a stainless steel wire attached to the servomotor/transducer). Each experiment commenced with a brief (100 ms), high frequency (100 Hz) tetanus to remove any sources of compliance in the system before the experiment began; after this point, changes in passive tension were negligible. The jacketed vertical organ bath was continuously oxygenated (95% $O_2$, 5% $CO_2$) with Tyrode's (Lannergren et al., 2000) solution maintained at 25 ± 0.1° C. Muscle stimulation was applied using flanking platinum electrodes, provided by a Model 701B biphasic stimulator (Aurora Scientific Incorporated, Aurora ON) with voltage set to 1.25 times the threshold required to elicit maximal twitch force. Following muscle suspension a 40 min equilibration period took place during which optimal length for isometric twitch force ($L_o$) was determined. Muscle length at each stage of each experiment was controlled via LINUX software and force data obtained from a dual-mode servomotor (Model 305B, Aurora Scientific Inc., Aurora ON). All data was collected at 2,000 Hz and saved to disk for future analysis (ASI 600a software).

### *Experimental protocol*

The main purpose of these experiments was to test the influence of muscle shortening speed during shortening ramps on the activation frequency dependence of potentiation. Accordingly, we assessed concentric force in the unpotentiated and potentiated states in response to stimulation at 10, 25, 45, 70 and 100 Hz while the muscle was shortening at one of three pre-selected speeds (0.10, 0.30, or 0.50 of $V_{max}$). For each muscle, concentric force potentiation was measured at each of the test frequencies at one speed of shortening. The order of test frequencies and the condition (shortening speed) was randomized between muscles; however, the same test frequency was always elicited before and after a PS. The bracketing protocol used to induce potentiation is illustrated in Figure 4.1. The determination of unpotentiated and

potentiated concentric forces at each frequency required a pair of closely spaced but identical shortening ramps performed 10 s before and 10 s after a tetanic PS known to cause potentiation with little fatigue (Vandenboom et al. 1997). In all cases, the first shortening ramp was performed without the muscle being activated (i.e. passive) and the second was performed with the muscle being stimulated at one of the test frequencies. The magnitude of change to each of the different contractile parameters we examined was assessed by dividing post-responses by pre-responses at each stimulation frequency. This basic procedure was repeated five times per muscle (i.e. once per test frequency) with muscles remaining quiescent for at least 20 min between consecutive procedures to allow potentiation to dissipate.

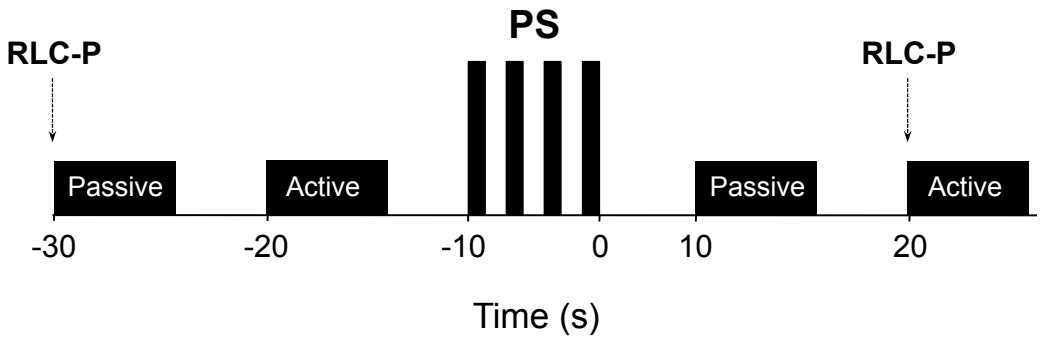


*Figure 4.1. Experimental timeline.*

Experimental timeline for determining influence of potentiation on concentric force responses of mouse EDL muscle in vitro (25°C). Unpotentiated and potentiated data were collected via a pair of shortening ramps, one passive and one stimulated, applied just prior to and after the application of a potentiating stimulus (PS). The PS consisted of four brief (400 ms) but high frequency (100 Hz) volleys occurring within a 10 s time window. RLC-P: In parallel experiments muscles were frozen for myosin RLC phosphate content to coincide with control and potentiated responses.

*Shortening Ramps*

Each shortening ramp was of a fixed amplitude and decreased muscle length from ~1.10 to 0.90 $L_o$. The three different speeds of ramp corresponded to 0.10, 0.30 and 0.50 $V_{max}$ of mouse EDL muscle (25° C). These three shortening ramp rates were scaled to a $V_{max}$ value of 9.8 muscle lengths per second as determined previously in our laboratory (Gittings et al. 2011). Muscles were activated at slightly different times after shortening commenced in the active ramps, by necessity, to ensure that force development occurred at the same relative length (~1.08 $L_o$) between conditions (delay of 25 ms for 0.1 $V_{max}$, 10 ms for 0.3 $V_{max}$, and 5 ms for 0.5 $V_{max}$). Stimulus volley duration was varied to ensure that contractions were always completed before the end of the ramp, allowing for complete concentric force relaxation during the ramp itself. Peak concentric force was consistently reached between 1.01 and 1.03 $L_o$ for all conditions. For each condition, instantaneous values of concentric force and kinetics were measured at the same relative muscle length prior to (and following) the PS to prevent any force–length effect as a confounding variable in the results. The ramp and activation durations used in this study accord with those reported for mouse hindlimb muscle in vivo during treadmill locomotion of 58–150 ms (Leblond et al. 2003).

*Analysis of force and work during shortening ramps*

Total, passive and active concentric forces were recorded during each shortening ramp and stimulus period. Active forces were obtained by subtracting the passive force response from the matching total force response; the mean concentric force was determined as the arithmetic average of the force produced from the initiation to the cessation of the active tension record. Mechanical work was determined by calculating the integral of the active force–displacement function for each individual contraction; power was calculated by dividing work by the time period over which active work was produced. When normalized to wet weight, unpotentiated values for force and/or power accorded well with previous values reported for mouse EDL muscle during shortening ramps (Askew and Marsh 1997; Brooks and Faulkner, 1991; Tallis et al. 2012). The first derivative for concentric force increase (+d$P$/d$t$) and decrease (-d$P$/d$t$) was determined at the start and end of each stimulation period, respectively, and expressed as mN per sec.

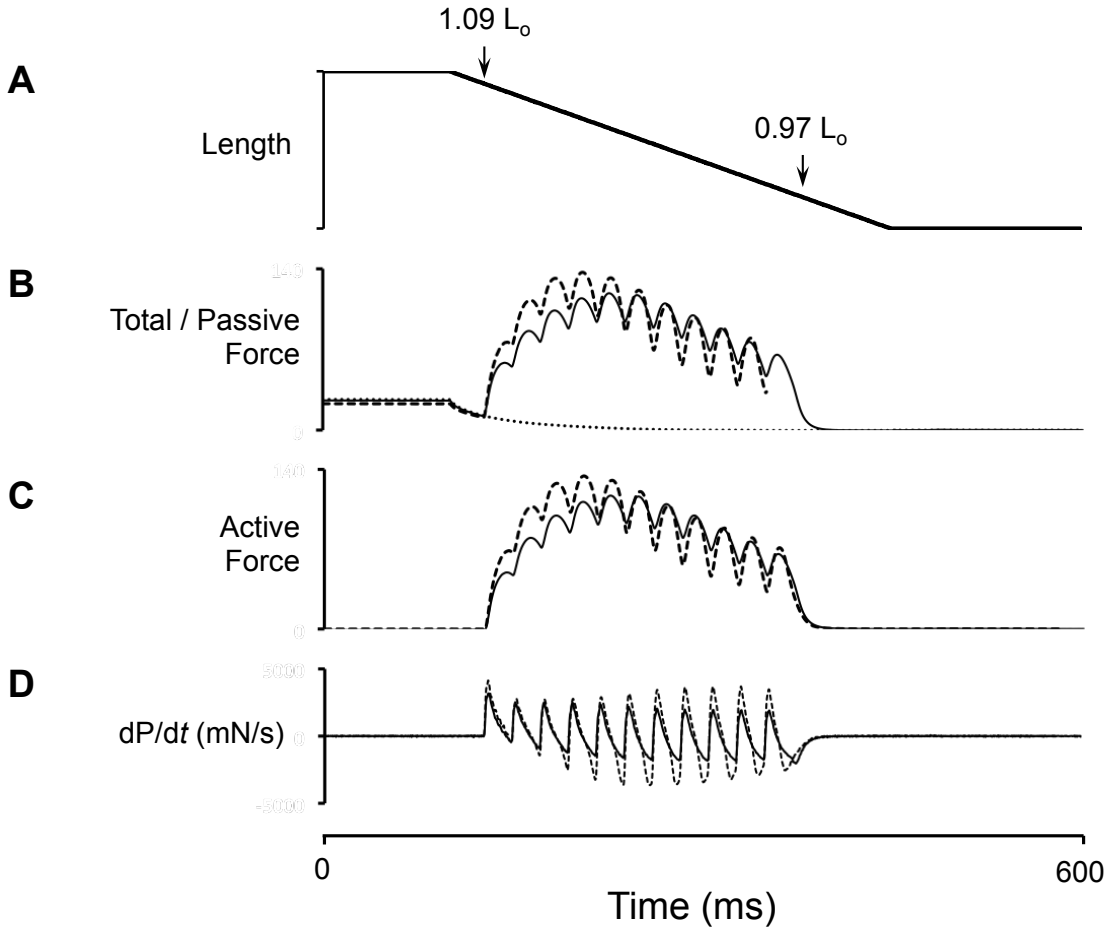


*Figure 4.2. Representative records illustrating method for determining concentric force and force kinetics during ramp shortening.*

(**A**) During each shortening ramp the muscle was allowed to shorten from 1.10 to 0.90 of optimal length (Lo) with fixed amplitude (20% $L_o$). (**B**) Total and passive force responses at 45 Hz. (**C**) Active force determined by subtracting the passive from the total force trace. (D) The differentiated record of active force used to determine force kinetics.

*Myosin phosphorylation*

Parallel experiments were conducted in separate muscles to determine the RLC phosphate content in muscles quick frozen in liquid nitrogen-cooled tongs 1 min before and 10 s after a single PS, time points that aligned with pre and post-contractile measures. All muscles were stored at -80° C until packed on dry ice and shipped to the laboratory of Dr. James Stull (University of Texas, Southwestern Medical Center, Dallas, TX) for quantification of RLC phosphorylation. Details regarding these methods and procedures have been presented (Ryder et al. 2007).

*Control experiments*

These experiments were conducted to account for the possible differential influence of stimulation frequency as a contributor to the magnitude of potentiation between conditions (i.e. 10 vs. 100 Hz). To this end we repeated our experimental procedure on a subset of EDL muscles (n = 4) with the exception that a PS was not applied between the pre- and post-contractile responses. For simplicity, although all test frequencies were tested only the 0.30 $V_{max}$ shortening ramp speed was used.

*Statistical analysis*

The effect of the PS on concentric force and relaxation kinetics was tested with a Two-way Repeated Measures ANOVA to evaluate the main effect(s) of stimulation frequency and shortening speed on concentric potentiation, force kinetics, and normalized forces before and after the PS. Post hoc analysis using the Šidák correction was used to identify significant differences between speeds and within each speed for repeated contractile measures at each frequency. A two-way ANOVA was used to test for differences in myosin RLC phosphorylation levels between unstimulated and stimulated muscles frozen after the first and fifth PS of the experiments. Differences between time points and between unstimulated and stimulated muscles was conducted with Tukey's HSD test. In all cases, the critical p-value to consider means significantly different was set at $p < 0.05$. All data are reported as Mean ± SEM.

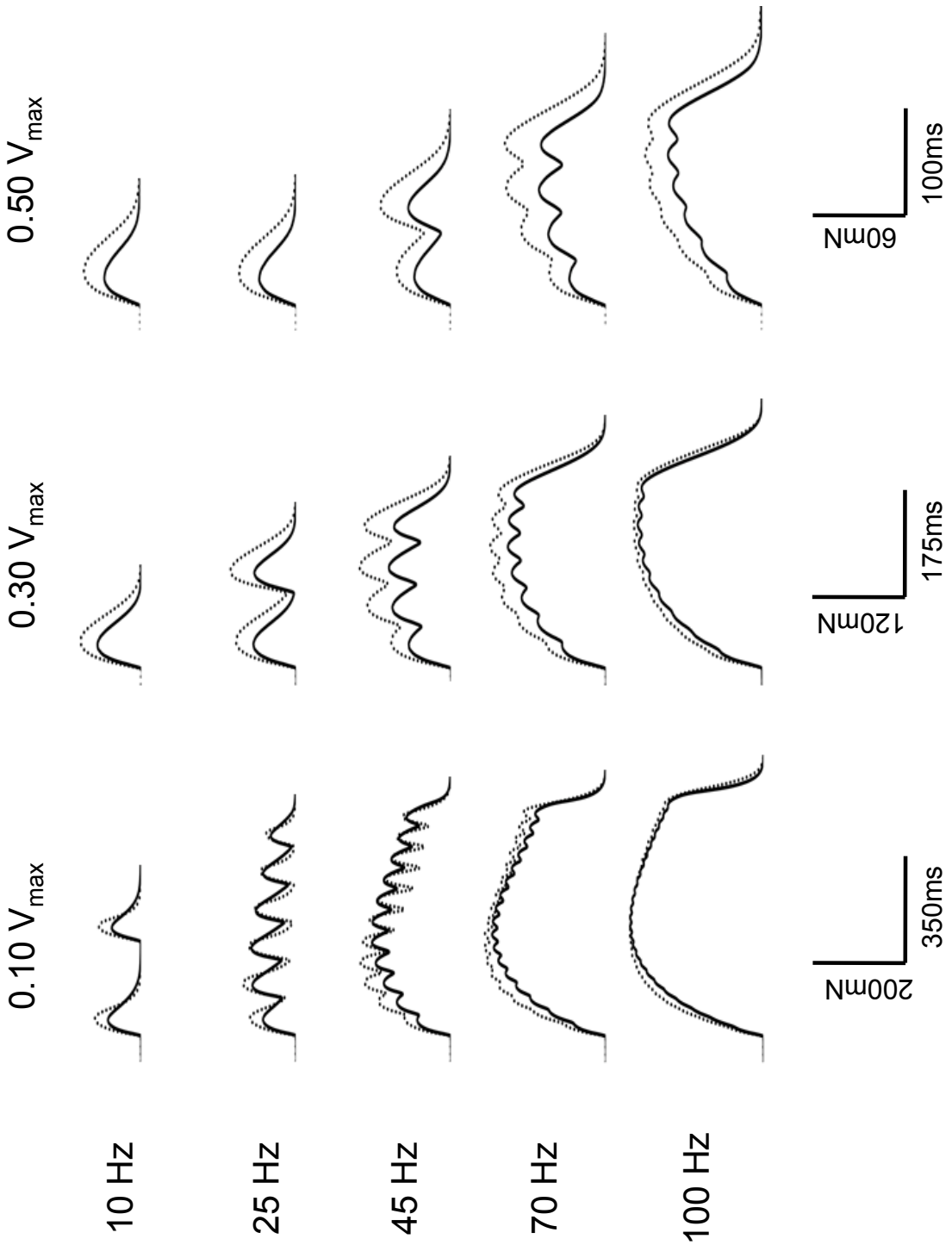


*Figure 4.3. Representative force traces at each frequency and shortening speed.*

In all panels the unpotentiated and potentiated records are the thick solid and the thin broken traces, respectively.

## *Results*

The influence of muscle shortening speed on potentiation of concentric forces was studied using a protocol wherein we applied shortening ramps before and after a PS that elevated myosin RLC phosphorylation. Representative force records from experiments testing the influence of a PS on concentric forces at all frequencies are shown in Figure. 4.3. The influence of the PS on relative concentric force at each speed is summarized in Figure. 4.4. These data clearly illustrate the speed-dependent increase in concentric force; when collapsed across frequencies, concentric force at 0.10, 0.30 and 0.05 $V_{max}$ was increased to 1.02 ± 0.03, 1.37 ± 0.03 and 1.59 ± 0.05 of unpotentiated controls, respectively. Moreover, although potentiation tended to be greatest at low versus high frequencies within each condition of speed, these curves highlight how the activation frequency dependence for potentiation was altered by shortening speed. For example, at 0.10 $V_{max}$ potentiation was greatest at 10 Hz but diminished or absent at all other frequencies (average: 1.00 ± 0.03 at 25–100 Hz). By contrast, potentiation at 0.30 and 0.50 $V_{max}$ was greatest at 10–25 and 25–45 Hz, respectively, and although present, diminished steadily with higher frequency stimulation. Figure 4.6 depicts the strong linear relationship we found between relative concentric force and relative work and/or power at each speed and activation frequency. This relationship describes how changes in concentric force associated with potentiation might be expected to enhance the ability of fast twitch muscle to perform mechanical work and produce power. Interestingly, even when normalized to maximal responses, potentiation increased low frequency relative to high-frequency force within each condition of speed, an effect that increased with shortening speed (Figure. 4.5).

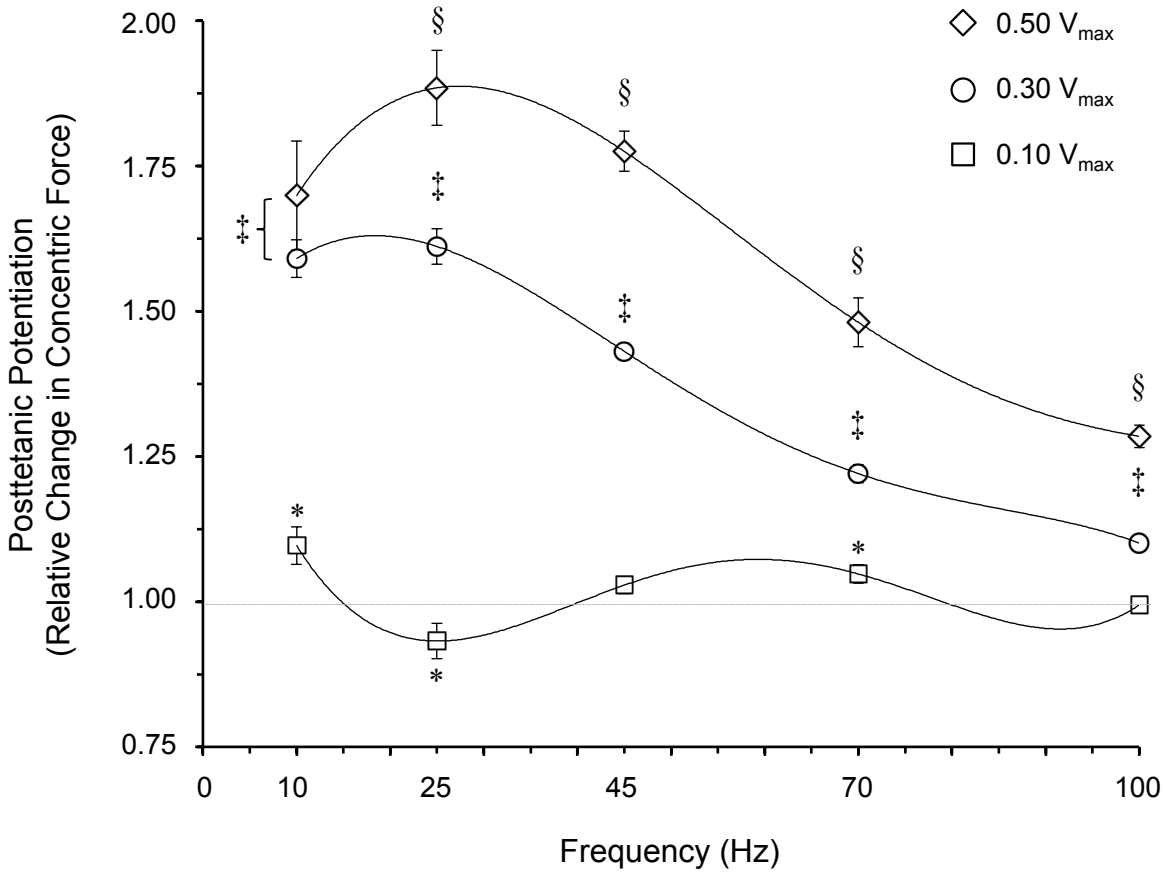


*Figure 4.4. Concentric force potentiation at each shortening speed.*

Relative concentric force of mouse EDL at different shortening speeds and activation frequencies. Data set at each speed is fit by a 4th order polynomial for illustration purposes ($r > 0.95$).
*value at 0.10 $V_{max}$ different than 1.00 (unpotentiated value) ($P < 0.05$)
‡value at 0.30 $V_{max}$ greater than respective value at 0.10 $V_{max}$ ($P < 0.05$)
§value at 0.50 $V_{max}$ greater than respective values at 0.10 and 0.30 $V_{max}$ ($P < 0.05$)

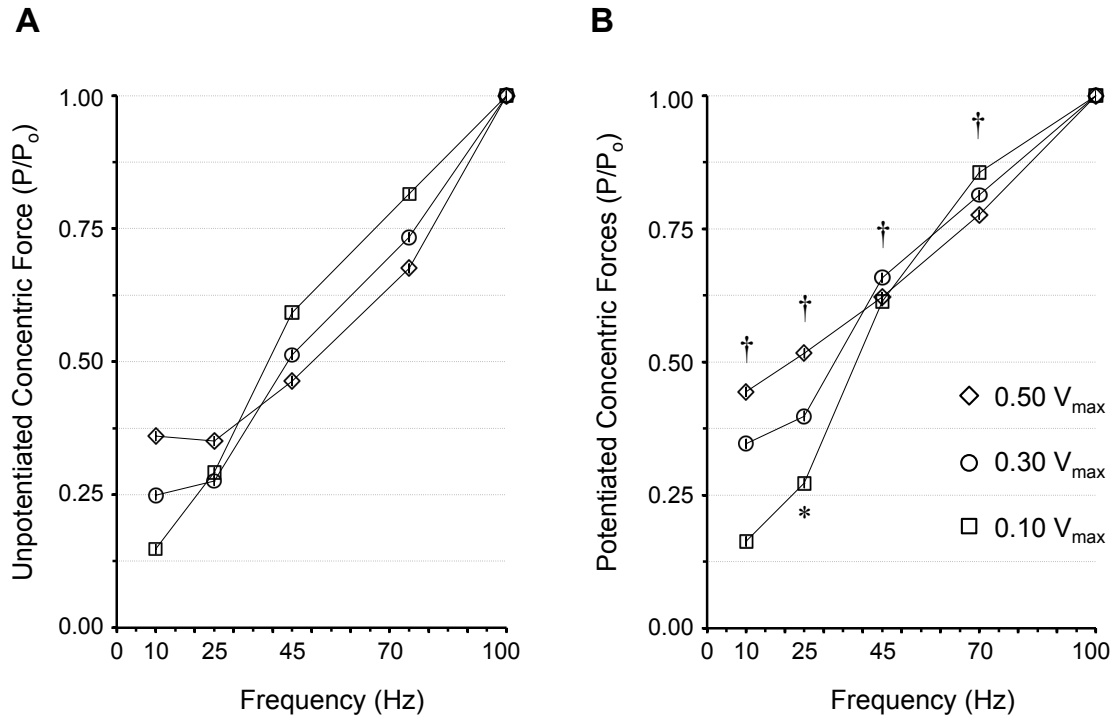


*Figure 4.5. Normalized unpotentiated and potentiated concentric forces*

Normalized concentric force-frequency responses at 0.10, 0.30 and 0.50 $V_{max}$ for unpotentiated (**A**) and potentiated (**B**) conditions. In both panels, forces at 10, 25, 45 and 70 Hz were scaled to corresponding force at 100 Hz.
†potentiated force at 0.30 and 0.50 $V_{max}$ greater than unpotentiated force ($P < 0.05$)
*potentiated force at 0.10 $V_{max}$ less than unpotentiated force ($P < 0.05$)

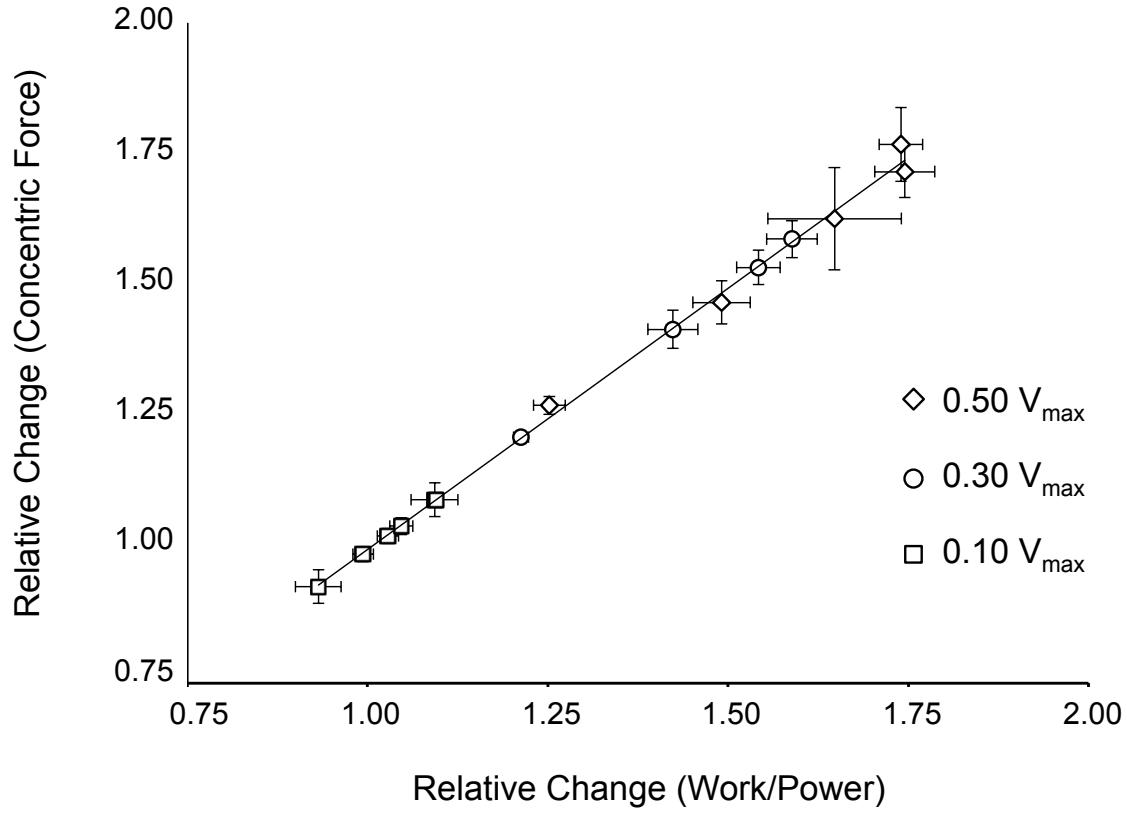


*Figure 4.6. Relative potentiation of force versus work/power*

Relative work/power plotted versus relative concentric force at each shortening speed and activation frequency. Line is best fit to the data using linear regression where y = 0.99 + 0.01x (r = 0.99).

*Rate of force development and relaxation*

A general observation from our experiments was that the fusion of tetanic forces was reduced compared to before the PS, an effect that was generally independent of potentiation per se. Relative changes to +dP/dt and -dP/dt are shown in Figure 4.7, respectively. The PS increased the +dP/dt at all activation frequencies and all speeds (by up to 2-fold). Although there was a speed dependent component to this increase, there was no activation frequency dependence apparent in these data. With respect to the -dP/d*t* it was apparent that the influence of the PS was more complex on this parameter than on +dP/d*t*. For example, despite considerable within speed variability at 0.10 $V_{max}$, when

averaged across all activation rates there was a general trend for -dP/dt to increase (i.e. relaxation slowed) with decreasing speed. For example, during shortening at either 0.50 or 0.30 $V_{max}$, the -dP/d*t* was either unchanged or moderately increased across the activation frequency range studied, with little or no activation frequency dependence detected for these changes at either speed. On the other hand, during shortening at 0.10 $V_{max}$ there was a strong activation frequency dependence for these responses as relative -dP/dt was increased at 10–45 Hz and decreased at 70–100 Hz after compared to before the PS. In addition, the relative -dP/dt measured at this speed was increased more than the other speeds at low and increased less than the other speeds at high activation rates, respectively.

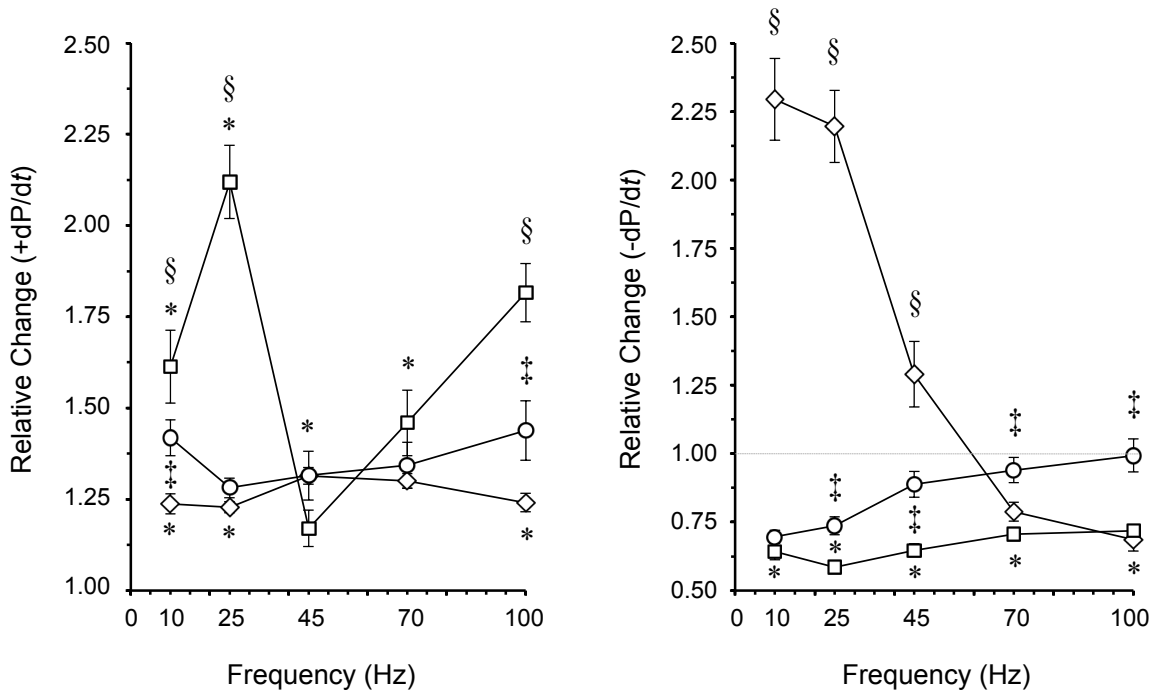


*Figure 4.7. Relative change in force kinetics*

(**A**) Change in force development rate (+dP/dt) and (**B**) force relaxation rate (-dP/dt) at different shortening speeds and activation rates.
*value different than unpotentiated value (1.00) at that frequency and speed ($P < 0.05$)
‡value at 0.30 $V_{max}$ greater than respective values at 0.10 $V_{max}$ ($P < 0.05$)
§value at 0.50 $V_{max}$ different from respective values at 0.10 and 0.30 $V_{max}$ ($P < 0.05$).

*Control experiments*

The bracketing procedure used in the main set of experiments was replicated using a single speed (0.30 $V_{max}$) without an intervening PS (n = 4). In these experiments, neither concentric force nor -dP/dt was changed by more than 2% at any activation frequency (data not shown). However, the +dP/dt did show an activation frequency dependence during these experiments as, for example, this parameter was increased by 6.0±0.2, 11.0±0.4 and 13.0±0.2% during stimulation at 45, 70 and 100 Hz, respectively. These changes were, however, minor compared to the change observed in the presence of the PS at these frequencies.

*Myosin RLC phosphorylation*

Consistent with previous data from this laboratory (Caterini et al. 2011; Xeni et al. 2011) the PS elevated RLC phosphate content of EDL muscles several fold from rest in a highly repeatable manner (Figure 4.8).

*Model viability and stability*

We monitored tetanic forces during repeated PS to assess muscle viability over the course of the main set of experiments. Peak isometric force ($P_o$) measured during the first tetanus of each PS varied by only 7 % from the first to the last protocol (210 ± 11.1 to 222 ± 11.0 mN, respectively) (n = 24). Based on these data, there was no evidence of muscle deterioration over the course of these experiments, as predicted by the parameters for small muscle work established by Barclay (2005).

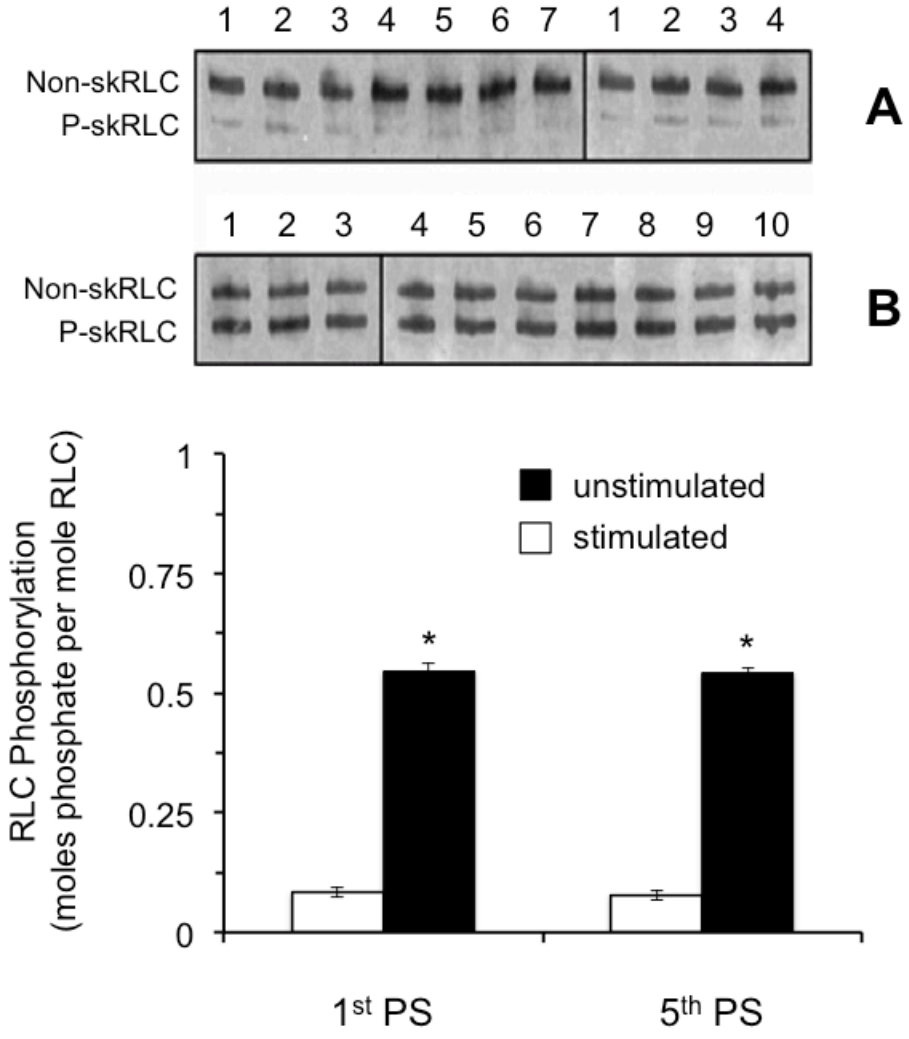


*Figure 4.8. Myosin RLC phosphorylation analysis in mouse EDL muscles*

Representative blots showing unphosphorylated (skRLC) and phosphorylated (P-skRLC) bands in resting and stimulated muscles, respectively. (**A**) Shows unstimulated muscles frozen before potentiating stimulus 1 or 5 (lanes 1–6 and 7–11, respectively). (**B**) Shows stimulated muscles frozen after potentiating stimulus 1 or 5 (lanes 1–5 and 6–10, respectively). Different blots used to construct both A and B (i.e. boxes). (*Bottom*) Summary of all blots showing RLC phosphorylation (expressed as mol phos per mol RLC as quantified by optical density). Values are Mean ± SEM (n = 5–6 per group).
*stimulated value greater than corresponding resting value ($P < 0.001$).

## *Discussion*

The purpose of this study was to systematically assess the influence of muscle shortening speed on the activation frequency dependence for the potentiation of concentric force and work in a mouse fast muscle model. Our results extend previous studies (MacIntosh and Willis 2000; Abbate et al. 2000) associating myosin RLC phosphorylation with enhanced mechanical function by detailing how muscle shortening speed increases the activation frequency domain over which potentiation is manifest.

*Effect of shortening speed*

Recent work from our lab using the work cycle technique has shown that concentric twitch force potentiation is proportional to myosin phosphorylation (Xeni et al. 2011) and is shortening speed dependent (Caterini et al. 2011). The present work using shortening ramps to vary muscle shortening speed confirm the speed dependence for concentric force potentiation and extend previous data by showing that this effect is present across the activation frequency domain for rodent skeletal muscle. In terms of activation-frequency dependence, concentric force potentiation at 0.10 $V_{max}$ was greatest at 10 Hz and generally unaltered at higher frequencies with no easily identifiable upper limit for potentiation. On the other hand, at 0.30–0.50 $V_{max}$ concentric force potentiation was observed across the entire stimulus frequency range, although there was a clear reduction in potentiation at 45–100 compared to 10–25 Hz at each speed. Thus, a novel aspect of our data is the influence of shortening speed to increase the frequency domain over which concentric force is potentiated. Indeed, a theoretical model presented in Figure 4.9 predicts an upper limit for concentric force potentiation that is perhaps relevant for closely spaced doublet or triplet pulses reported at the onset of contraction in freely moving rats (Hennig and Lømo 1987).

*Relation to previous studies*

Previous studies examining the activation frequency dependence of potentiation have produced conflicting results. On the one hand, despite differences in fatigue level caused by a more severe PS regime, the isometric potentiation vs. activation frequency response reported for mouse EDL muscle *in vitro* (25 °C) by Vandenboom et al. (1993) resembles the present data for shortening at 0.10 $V_{max}$. Taken together these and the present results suggest that isometric or slow shortening minimizes the potentiation

influence at all but the lowest frequencies. In contrast to these results, however, are reports from rat hindlimb muscle that show little or no activation-frequency dependence for isometric potentiation. For example, MacIntosh and Willis (2000) used rat medial gastrocnemius muscle *in situ* to show uniform potentiation of peak isometric force during very brief stimulation at 20–80 Hz. Additionally, MacIntosh et al. (2008) used high frequency doublet contractions to show the presence of potentiation at even 200 Hz in rat hindlimb muscle. On the surface these results would seem to indicate that the activation frequency dependence was similar for both isometric and concentric contractions. Because only very brief contractions were used, this conclusion may only apply to the rising phase, and not to peak tetanic force levels, however.

Our results are in general agreement with Abbate et al. (2000) who used rat medial gastrocnemius muscle *in situ* to show that the potentiation of power during high frequency tetani (80–120 Hz) was restricted to fast speeds of shortening. Indeed, a speed dependent increase in concentric force potentiation is consistent with results from permeabilized skeletal fibres showing that myosin RLC phosphorylation increases $f_{app}$ to augment the fraction of strongly-bound, force generating cross-bridges ($\alpha FS$) (Brenner 1988; Sweeney and Stull 1990). Notably, this effect has been shown to be strongest when αFS is lowest, thus explaining why myosin phosphorylation enhances isometric twitch but not isometric tetanic force (Sweeney et al. 1993). If the effect of ramp shortening and ramp-shortening speed on concentric forces may be understood in terms of crossbridge cycling kinetics, i.e. the reduction in force with increasing speed is due to a decrease in $f_{app}$ and/or increase in $g_{app}$, thus amplifying the influence of myosin phosphorylation mediated increases in $f_{app}$ on force. In addition to accounting for why potentiation increased with shortening speed this explanation accounts for why shortening at 0.10 $V_{max}$ produced potentiation similar to isometric, i.e. at this slow speed the decrease in $f_{app}$ and/or increase in $g_{app}$ is not dissimilar enough from the isometric $g_{app}$ to alter force, especially at higher frequencies. Our data thus reveal the presence of a shortening speed threshold between 0.10 and 0.30 $V_{max}$, above which the potentiation influence is amplified relative to isometric. Finally, the general decrease in concentric force potentiation observed with increasing activation frequency at each shortening speed is consistent with a $Ca^{2+}$ induced increase in αFS with increasing force.

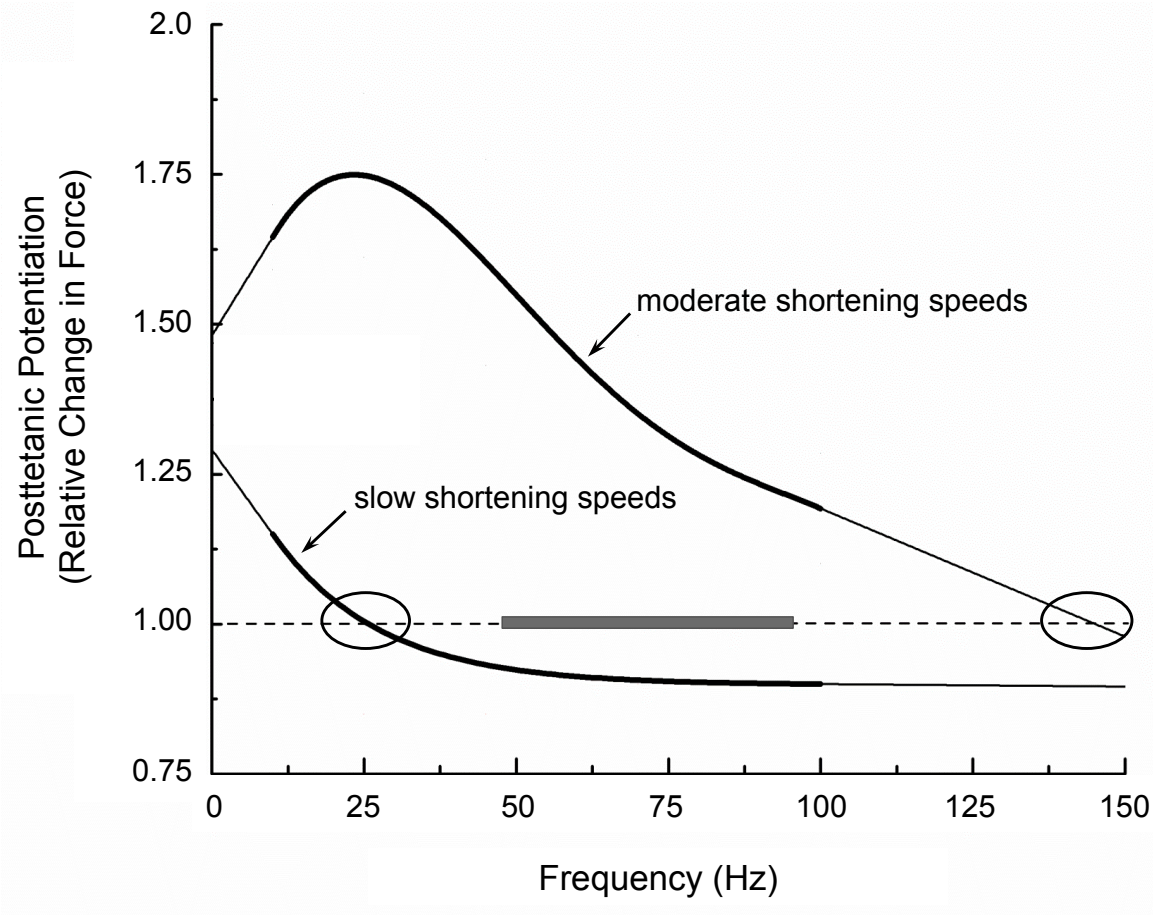


*Figure 4.9. Model for the influence of shortening speed on the activation frequency dependence for concentric force potentiation.*

For illustration purposes, the curves shown were created by combining two concentric PTP responses as follows: *i*) the intermediate response of the 0.30 and 0.50 $V_{max}$ data, and *ii*) the intermediate response of 0.10 $V_{max}$ and isometric data from Vandenboom et al. (1993) (top and bottom, respectively). Thick segment corresponds to actual data set while thinned segments depict extrapolations to y-axis and to the zero-crossing potentiation (i.e. 1.00). The y-intercept predicts 28 and 47% potentiation of 1 Hz force at slow and moderate speeds of shortening, respectively. The ellipsoids identify an upper limit for potentiation of ~25 and 145 Hz for slow and moderate shortening, respectively. The shaded box depicts median activation rates for rodent EDL muscle (c.f. Schiaffino and Reggiani 2011).

*Concentric force kinetics*

A complicating factor using high frequency stimulation is the influence of altered force development or relaxation kinetics on tetanic force summation, independent of potentiation per se. This effect may be particularly relevant for mid-frequency, unfused contractions. Indeed, a general observation was that the fusion of forces was decreased by the PS, an effect present at all frequencies. Although the mechanism is unknown, the effect of the PS on overall force in the face of these increased relaxation rates is all the more impressive. In contrast to these relaxation data is the pattern of change to -dF/dt observed during shortening at 0.10 $V_{max}$. The large increase observed in this parameter at low-activation rates may have helped mitigate the level of potentiation attained at these frequencies at 0.30 or 0.50 $V_{max}$. In contrast, however, the slowed relaxation rates observed at high activation rates may have augmented force somewhat at this slow speed relative to either 0.30 or 0.50 $V_{max}$. A slowed relaxation rate from isometric tetani has been demonstrated previously in potentiated cat and mouse muscle *in situ* and *in vitro*, respectively (Brown and Loeb 1999; Gittings et al. 2011). Further, phosphorylation of the RLC has been shown to slow relaxation and eliminate force-dependent relaxation from high levels of $Ca^{2+}$ activated steady-state force development in permeabilized rabbit psoas skeletal fibres (Patel et al. 1998). In principal, this effect is consistent with a persistent increase in $f_{app}$ that enhances $Ca^{2+}$ sensitivity, but not maximal force following stimulation. If so, this effect appears to be present during relaxation from high force produced by slow shortening.

## *Limitations*

We did not actively monitor sarcomere lengths during shortening and thus cannot detail if ramp speed dependent variations in sarcomere length were present. In the intact skeletal frog fibre, it has been shown that slower speed, high force shortening may produce sarcomere non-uniformities compared to faster speed, low force shortening (Julian and Morgan 1979). Thus, although our within-speed condition results were unlikely to be affected, we cannot exclude the possibility that differences in sarcomere dynamics influencing viscoelastic properties contributed to the observed speed dependence in our results, particularly for force relaxation at 0.10 $V_{max}$.

### *Summary*

The magnitude and extent of concentric force potentiation of mouse EDL muscle is highly sensitive to muscle shortening speed. Increasing the rate of ramp length change from near isometric to moderate speeds of shortening greatly increases the activation frequency domain over which concentric force is potentiated. This effect of shortening may increase the functional utility of the myosin phosphorylation mechanism on muscle work and power during locomotion at a wide range of activation levels.

### *Acknowledgments*

This study was supported by funds provided by the Natural Sciences and Engineering. Research Council of Canada (RV). Additional data analysis performed by Adam Murphy.

### *Conflict of interests*

The authors do not have any conflicting interests regarding the findings or interpretations of this manuscript.

## *References*


Abbate F, Sargeant AJ, Verdijk PW, de Haan A (2000). Effects of high-frequency initial pulses and posttetanic potentiation on power output of skeletal muscle. J Appl Physiol. 88: 35 – 40.

Alamo L, Wriggers W, Pinto A, Bártoli F, Salazar L, Zhao FQ, Craig R, Padrón R. (2008). Three-dimensional reconstruction of tarantula myosin filaments suggests how phosphorylation may regulate myosin activity. J Mol Biol. 384(4): 780-797.

Barclay CJ (2005). Modelling diffusive $O_2$ supply to isolated preparations of mammalian skeletal and cardiac muscle. *J Muscle Res Cell Motil*. 26: 225-235.

Brenner B (1988) Effect of $Ca^{2+}$ on cross-bridge turnover kinetics in skinned single rabbit psoas fibers: implications for regulation of muscle contraction. Proc Natl Acad Sci US A. 85: 3265-3269.

Brito R, Alamo L, Lundberg U, Guerrero JR, Pinto A, Sulbarán G, Gawinowicz MA, Craig R, Padrón R (2011). A molecular model of phosphorylation-based activation and potentiation of tarantula muscle thick filaments. J Mol Biol. 414(1):44-61.

Broman H, De Luca CJ, Mambrito B (1985) Motor unit recruitment and firing rates interaction in the control of human muscles. Brain Res. 337(2): 311-319.

Brown IE, Loeb GE (1999) Measured and modeled properties of mammalian skeletal muscle. I. The effects of post-activation potentiation on the time course and velocity dependencies of force production. J Muscle Res Cell Motil 20: 443-456.

Caterini D, Gittings W, Huang J, Vandenboom R (2011) The effect of work cycle frequency on the potentiation of dynamic function in fast mouse muscle. J Exp Biol 214: 3915 – 3923.

Close R, Hoh JF (1968) The after-effects of repetitive stimulation on the isometric twitch contraction of rat fast skeletal muscle. J Physiol. 197: 461 - 477.

De Luca CJ (1985) Control properties of motor units. J Exp Biol. 115: 125 - 136.

De Luca CJ, Hostage EC (2010) Relationship between firing rate and recruitment threshold of motoneurons in voluntary isometric contractions. J Neurophysiol 104(2): 1034 – 1046.

Erim Y, De Luca C, Mineo K, Aoki, T (1996) Rank-ordered regulation of motor units. Muscle & Nerve, 19: 563-573.

Franks-Skiba K, Lardelli R, Goh G, Cooke R (2007) Myosin light chain phosphorylation inhibits muscle fiber shortening velocity in the presence of vanadate. *Am J Physiol Regul Integr Comp Physiol*. **292**, R1603-1612.

Gittings W, Huang J, Smith I, Quadrilatero J, Vandenboom R (2011) The influence of myosin light chain kinase (MLCK) gene ablation on the contractile performance of skeletal muscles during fatigue. J Muscle Res Cell Motil 31: 337-348.

Grange RW, Cory CR, Vandenboom R, Houston ME (1995) Myosin phosphorylation augments the force-displacement and force-velocity relationships of mouse fast muscle. Am J Physiol 269: C713-C724.

Grange RW, Vandenboom R, Xeni J, Houston ME (1998) Potentiation of in vitro concentric work in mouse fast muscle. J Appl Physiol 84: 236-243.

Hennig R, Lømo T. (1985) Firing patterns of motor units in normal rats. Nature. 314(6007): 164-166.

Hennig R, Lømo T. (1987) Gradation of force output in normal fast and slow muscles of the rat. Acta Physiol Scand. 130(1): 133-142.

Josephson RK. (1999) Dissecting muscle power output. J Exp Biol 202: 3369-3375.

Julian FJ, Morgan DL (1979). The effect on tension of non-uniform distribution of length changes applied to frog muscle fibers. J. Physiol. 293: 379-392.

Karatzaferi C, Franks-Skiba K, Cooke R. (2008) Inhibition of shortening velocity of skinned skeletal muscle fibers in conditions that mimic fatigue. *Am J Physiol Regul Integr Comp Physiol.* **294,** R948-955.

Klug GA, Botterman BR, Stull JT (1982) The effect of low frequency stimulation on myosin light chain phosphorylation in skeletal muscle. J Biol Chem 257: 4688-4670.

Leblond H, L'Esperance M, Orsal D, Rossignol S (2003) Treadmill locomotion in the intact and spinal mouse. J Neurosci 23: 11411-11419.

MacIntosh BR, Bryan SN (2002) Potentiation of shortening and velocity of shortening during repeated isotonic tetanic contractions in mammalian skeletal muscle. Pflugers Arch 443: 804-812.

MacIntosh BR, Taub EC, Dormer GN, Tomaras EK (2008) Potentiation of isometric and isotonic contractions during high-frequency stimulation. Pflugers Arch. 456: 449-458.

MacIntosh BR, Willis JC (2000) Force-frequency relationship and potentiation in mammalian skeletal muscle. J Appl Physiol. 88(6): 2088 – 2096.

Manning DR, Stull JT (1982) Myosin light chain phosphorylation-dephosphorylation in mammalian skeletal muscle. Am J Physiol 242: C234-C241.

Moore RL, Stull JT (1984) Myosin light chain phosphorylation in fast and slow skeletal muscles in situ. Am J Physiol Cell Physiol. 247(5): C462-C471.

Patel JR, Diffee GM, Huang XP, Moss RL (1998) Phosphorylation of myosin regulatory light chain eliminates force-dependent changes in relaxation rates in skeletal muscle. Biophys J. 74: 360–368.

Persechini A, Stull JT, Cooke R (1985) The effect of myosin phosphorylation on the contractile properties of skinned rabbit skeletal muscle fibers. J Biol Chem 260: 7951-7954.

Ryder JW, Lau KS, Kamm KE, Stull JT (2007) Enhanced skeletal muscle contraction with myosin light chain phosphorylation by a calmodulin-sensing kinase. J Biol Chem 282: 20447-20454.

Schiaffino S, Reggiani C (2011) Fiber types in mammalian skeletal muscles. Physiol Rev. 91(4): 1447-531.

Stewart M, Franks-Skiba K, Cooke R. (2009) Myosin regulatory light chain phosphorylation inhibits shortening velocities of skeletal muscle fibers in the presence of the myosin inhibitor blebbistatin. *J Muscle Res Cell Motil*. **30**, 17-27.

Stull JT, Kamm C, Vandenboom R (2011) Myosin Light Chain Kinase and the Role of Myosin Light Chain Phosphorylation in Skeletal Muscle. Arch Biochem Biophys 510: 120-128.

Sweeney HL, Stull JT (1990) Alteration of cross-bridge kinetics by myosin light chain phosphorylation in rabbit skeletal muscle: Implications for regulation of actin-myosin interaction. Proc Natl Acad Sci USA 87: 414-418.

Sweeney HL, Bowman BF, Stull JT (1993) Myosin light chain phosphorylation in vertebrate striated muscle: regulation and function. Am J Physiol. 264: C1085-1095.

Tansey KE, Botterman BR (1996a) Activation of type-identified motor units during centrally evoked contractions in the cat medial gastrocnemius muscle. I. Motor-unit recruitment. J Neurophysiol. 75(1): 26-37.

Tansey KE and Botterman BR (1996b) Activation of type-identified motor units during centrally evoked contractions in the cat medial gastrocnemius muscle. II. Motoneuron firing-rate modulation. J Neurophysiol. 75(1): 38-50.

Vandenboom R, Grange RW, Houston ME (1993) Threshold for force potentiation associated with skeletal myosin phosphorylation. Am J Physiol 265: C1456-1462.

Vandenboom R, Grange RW, Houston ME (1995) Myosin phosphorylation enhances rate of force development in fast-twitch skeletal muscle. Am J Physiol 268: C596-C603.

Vandenboom R, Xeni J, Bestic M, Houston ME. (1997) Increased force development rates of fatigued skeletal muscle are graded to myosin light chain phosphate content. *Am J Physiol* 272, R1980-R1984.

Xeni J, Gittings W, Caterini D, Huang J, Houston ME, Grange RW, Vandenboom R (2011). Myosin light chain phosphorylation and potentiation of dynamic function in mouse fast muscle. Pflugers Archiv. 362: 349-358.

Zhi G, Ryder JW, Huang J, Ding P, Chen Y, Zhao Y, Kamm KE, Stull JT (2005) Myosin light chain kinase and myosin phosphorylation effect frequency-dependent potentiation of skeletal muscle contraction. Proc Natl Acad Sc USA 102: 17519-17524.

# Supplement to Study #1

**Shortening Speed Dependence of Concentric Force Potentiation in the Absence of Myosin Phosphorylation**

William Gittings, Jordan Bunda, James T. Stull, and Rene Vandenboom

As published in: To be submitted 08/15 to Journal of Experimental Biology

**Author contributions:**

*William Gittings*: study design, data collection, analysis, manuscript writing

*Jordan Bunda*: data collection and analysis, manuscript writing

*Dr. JT. Stull*: skMLCK$^{-/-}$ mice breeding pairs, technical assistance, manuscript revisions

*Dr. Rene Vandenboom*: study design input, funding (NSERC), manuscript writing

NOTE: This study is a replication of Study #1 using skMLCK knockout (skMLCK$^{-/-}$) muscles, as our breeding colony was not available for use when the first project was conducted (Gittings et al. 2012). The manuscript is written and formatted for The Journal of Experimental Biology as a Short Communication.

## *Abstract*

We investigated the influence of shortening speed and activation frequency on concentric force potentiation of mouse fast muscle devoid of skeletal myosin light chain kinase (skMLCK$^{-/-}$). EDL muscles were activated *in vitro* (25°C) across a range of stimulation frequencies (10-100 Hz) during shortening ramps at 0.10, 0.30 or 0.50 of $V_{max}$ before and after a potentiating stimulus (PS). At 0.30 and 0.50 $V_{max}$, mean concentric force (collapsed across all frequencies) was increased to 1.17±0.02 and 1.27±0.02 of unpotentiated (pre-PS) values; the frequency at which potentiation was maximal was also increased with shortening speed (25 and 45 Hz, respectively) ($n$ =4, $P$ < 0.01 for all speeds). In contrast, mean concentric force at 0.10 $V_{max}$ was depressed (to 0.85±0.02 of pre-PS values). Thus, although attenuated by ~ 45% relative to wildtype muscles with skMLCK, our data confirms that concentric force potentiation of muscles without skMLCK remains speed dependent (Gittings et al. 2012).


Keywords: myosin, phosphorylation, concentric, force, potentiation, regulatory light chain, RLC, skeletal muscle, myosin light chain kinase, skMLCK.

## *Introduction*

Contractile function of fast twitch skeletal muscles from a variety of species is continually modulated in a history dependent manner. One example of this modulation is posttetanic potentiation (PTP), the transient increase in muscle force, work or power that follows high-frequency stimulation (Vandenboom et al., 2013). Although highly muscle and paradigm dependent, the PTP of rodent wildtype muscle is strongly correlated with stimulation-induced elevations in skeletal myosin light chain kinase (skMLCK) catalyzed phosphorylation of the myosin regulatory light chain (RLC) (e.g., Grange et al. 1998; Klug et al. 1982; Manning and Stull, 1982; Moore and Stull, 1984; Moore et al. 1990; Palmer and Moore, 1989; Vandenboom et al. 1995; 1997; Xeni et al. 2011). Work on a variety of striated muscle systems indicates that the mechanism for this increase is a structure-function alteration to the myosin heavy chain that increases the calcium ($Ca^{2+}$) sensitivity of force development (e.g., Alamo et al. 2015). Work on muscles from skMLCK deficient mice has, however, shown that divergent mechanisms for PTP may also exist, however. For example, although Zhi et al. (2005) showed that isometric twitch potentiation was eliminated in skMLCK$^{-/-}$ muscles without RLC phosphorylation, other forms of potentiation remained (see also Gittings et al. 2011). Moreover, Gittings et al. (2015) recently showed that, although isometric twitch forces were not potentiated, skMLCK$^{-/-}$ muscles displayed considerable potentiation of concentric forces at tetanic frequencies of stimulation. Thus, although these studies confirm the importance of skMLCK-catalyzed phosphorylation of the RLC, they also indicate the presence of an alternative or complementary mechanism for PTP of "physiological" type contractions. Importantly, RLC-phosphorylation independent forms of force potentiation have also been observed in disuse models of rat hindlimb muscle (e.g., MacIntosh et al, 2008; Rassier et al, 1999). Thus, the purpose of this research was to determine the shortening speed and stimulation frequency dependence of tetanic force potentiation in skMLCK$^{-/-}$ muscles without the ability to phosphorylate the myosin RLC.

### *Results and Discussion*

The main finding of this study was that of a speed-dependent (i.e. 0.50 > 0.30 > 0.10 $V_{max}$) increase in concentric force potentiation with an attendant effect of shortening speed on the stimulus frequency at which the most potentiation was observed. For example, the magnitude of force potentiation in the current study was positively associated with shortening speed when collapsed across frequencies (data shown in Figure 4.10, Panel A). Relative concentric forces following the PS (averaged for all stimulation frequencies) at 0.10, 0.30, and 0.50 $V_{max}$ were 0.85 ± 0.02, 1.17 ± 0.02, and 1.27 ± 0.02 of pre-PS values, respectively. Relative concentric forces at 0.30 and 0.50 $V_{max}$ were significantly greater than 0.10 $V_{max}$ ($P < .0001$). Additionally, relative concentric forces at 0.50 $V_{max}$ were significantly greater than 0.30 $V_{max}$ ($P = .016$), although when examined at each frequency, muscles shortening at 0.50 $V_{max}$ produced significantly higher relative concentric force than 0.30 $V_{max}$ at all but the lowest stimulation frequency (10 Hz).

The present results from skMLCK$^{-/-}$ muscles necessitates a reinterpretation of previous results from wildtype muscles from this laboratory. For example, Gittings et al, (2012) used identical procedures to show a shortening speed and stimulation frequency dependence of concentric force potentiation of wildtype muscles (Gittings et al, 2012). Assuming that there was no contribution from the small amount of RLC phosphorylation detected at rest in our skMLCK$^{-/-}$ muscles, we now conclude that a RLC phosphorylation-independent mechanism for concentric force potentiation exists alongside RLC phosphorylation (see also Gittings et al, 2015). Gittings et al. (2012) examined the shortening speed and stimulus frequency dependence of concentric force potentiation exclusively in wildtype muscles due to the unavailability of skMLCK$^{-/-}$ mice at that time. By comparing current results from skMLCK$^{-/-}$ muscles with past results from wildtype muscles, we are able to place both studies into better perspective. In this respect, although wildtype muscles potentiated more than skMLCK$^{-/-}$ muscles at the two fastest shortening speeds and at all stimulus frequencies, the shortening speed and frequency dependence for potentiation was similar in both genotypes. Moreover, the additional potentiation displayed by wildtype muscles appears to be due to the roughly equivalent, additive, influence of RLC phosphorylation dependent and independent mechanisms. Interestingly, the biggest differences between the wildtype and skMLCK$^{-/-}$ genotypes

appears to be at slow shortening speeds (i.e. 0.10 $V_{max}$) where the absence of skMLCK catalyzed phosphorylation of the RLC appears to decrease, as opposed to maintain, tetanic force at most stimulus frequencies.

Our results thus lead to the inevitable conclusion that, although RLC phosphorylation is required for maximal potentiation of concentric force at moderate shortening speeds, a complementary mechanism exists. Although the nature of this mechanism is unknown, stimulation-induced elevation in free cytosolic $Ca^{2+}$ levels ($[Ca^{2+}]_i$) have previously been implicated in PTP. For example, Smith et al. (2013) used the mouse lumbrical, a unique fast twitch muscle which does not display skMLCK catalyzed RLC phosphorylation (Ryder et al, 2007), to show that PTP of isometric twitches was associated with elevations in resting $[Ca^{2+}]_i$. These authors thus concluded that, although the intracellular transient triggering potentiated twitches was unaltered, stimulation-induced changes to resting $[Ca^{2+}]_I$ may have saturated intracellular $Ca^{2+}$ buffers, including perhaps TnC, to produce a relatively short lived PTP in the absence of RLC phosphorylation (Smith et al, 2013). Although the relevance of these findings to the current results are uncertain, they do perhaps provide a plausible explanation for a RLC-phosphorylation independent form of concentric force potentiation in EDL muscles from skMLCK$^{-/-}$ muscles.

In summary, the present results suggest that the shortening-speed and stimulus-frequency dependence of concentric force potentiation at tetanic frequencies is similar for RLC phosphorylation dependent and RLC phosphorylation independent mechanisms. Further work is clearly required to elucidate the relative contributions of RLC phosphorylation – dependent and - independent mechanism to potentiation in the murine muscle model.

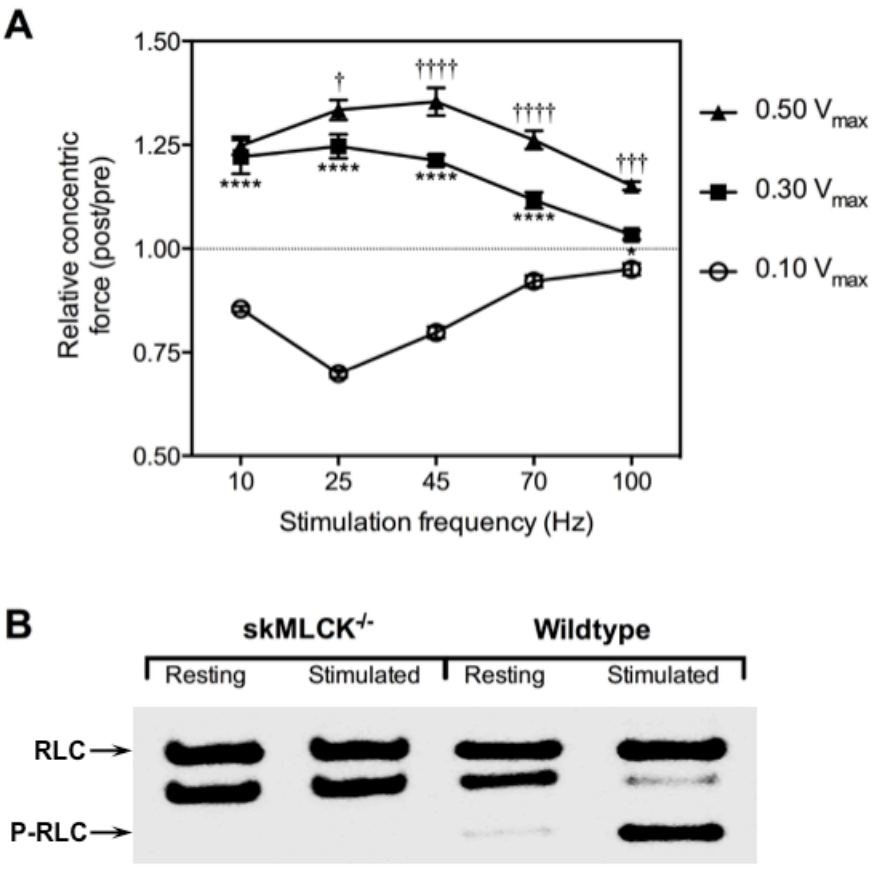


*Figure 4.10. Shortening speed and frequency dependence of concentric force potentiation in EDL muscles devoid of skMLCK.*

**(A)** Concentric forces were potentiated at 0.50 and 0.30 $V_{max}$ across all frequencies, while concentric forces were depressed at 0.10 $V_{max}$. * $P < .05$, **** $P < .0001$ between 0.10 and 0.30 $V_{max}$; † $P < .05$, ††† $P < .001$, †††† $P < .0001$ between 0.30 and 0.50 $V_{max}$. **(B)** Representative urea/glycerol-PAGE blot depicting the absence of stimulation-induced increases of RLC phosphate content in skMLCK$^{-/-}$. *RLC*, regulatory light chain of myosin; *RLC-P*, monophosphorylated regulatory light chain. Introduction of the negatively charged phosphate moiety to the RLC causes phosphorylated RLCs to migrate further in the gel than unphosphorylated RLCs, producing the lowermost band shown in stimulated wildtype muscle above.

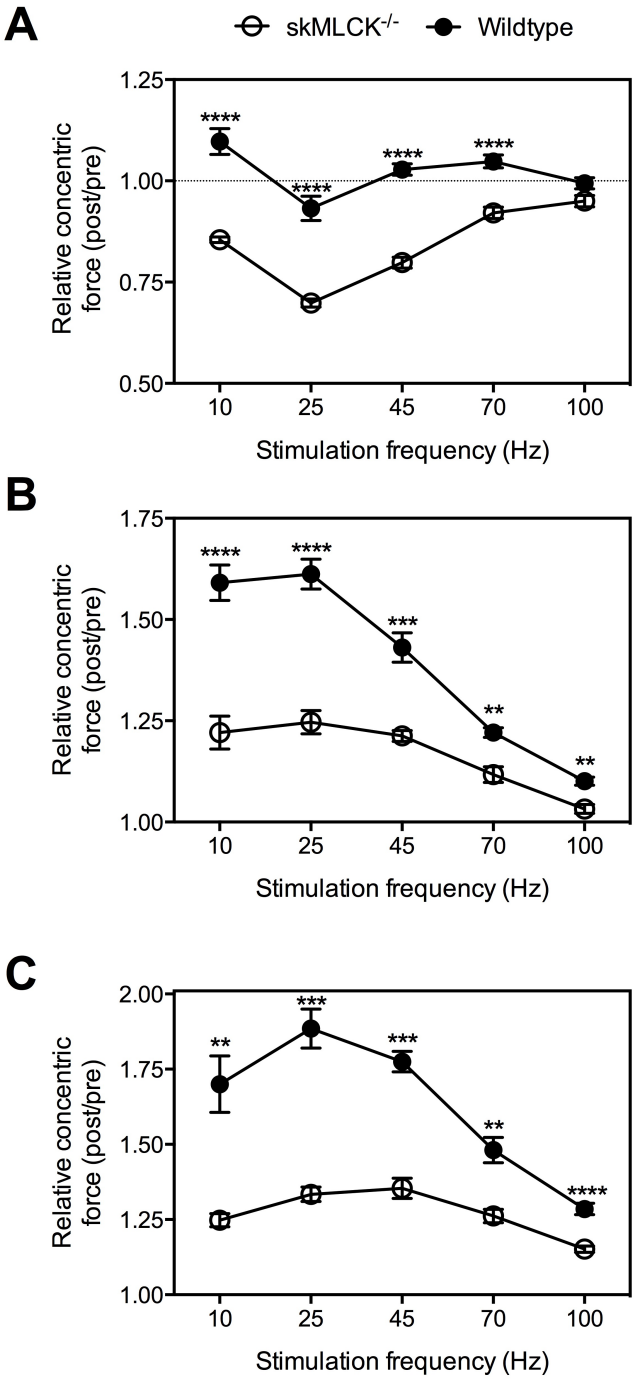


*Figure 4.11. Comparison of relative concentric force between wildtype and skMLCK$^{-/-}$ EDL muscles.*

Muscles were stimulated at 10, 25, 45, 70 and 100 Hz at 0.10 $V_{max}$ **(A)**, 0.30 $V_{max}$ **(B)**, and 0.50 $V_{max}$ **(C)**. *Closed circles*, wildtype; *Open circles*, skMLCK$^{-/-}$; ** $P < .01$, *** $P < .001$, **** $P < .0001$ between wildtype and skMLCK$^{-/-}$. Wildtype data was previously published by our lab using identical methods (Gittings et al, 2012) and is included to demonstrate give perspective to our present study.

## *Materials and Methods*

*Animals*

Adult skMLCK$^{-/-}$ C57BL/6 mice (20-25 g) were sampled randomly from our colony housed within the Brock University Comparative Bioscience Facility. Mice were housed on a 12:12h light-dark cycle, with standard mouse chow and water provided *ad libitum*. All procedures were carried out in accordance with the Canadian Council for Animal Care, and approved by the Brock University Animal Care Committee.

*Experimental protocol*

This experimental protocol is identical to one previously described by our lab in work studying wildtype muscle. For a more in depth discussion of methods see Gittings et al., (2012). In brief, animals were anesthetized with an intraperitoneal injection of sodium pentobarbital (60 mg/kg body weight), diluted from a stock concentration (Euthanyl, 240 mg/mL) with 0.9% saline. Once animals reached the appropriate depth of sedation, the extensor digitorum longus (EDL) was surgically isolated after tying non-absorbent silk 4-0 sutures to the proximal and distal tendons. Animals were then euthanized with an intracardiac injection of sodium pentobarbital (120 mg/kg). The muscles were suspended in an in vitro in muscle testing system (Aurora Scientific Inc.) within a vertical jacketed organ bath containing Tyrode's solution maintained at 25°C. One tendon's suture was fastened to the lever arm of a servomotor/force transducer, while the other was fastened to an immovable clamp submerged within the organ bath. Field electrical stimulation was applied by flanking platinum electrodes, while muscle length was controlled using custom software. Preliminary equilibration procedures were completed as previously described (Gittings et al, 2012).

Concentric force production was assessed in the unpotentiated (control) and potentiated states (experimental) in response to stimulation at 10, 25, 45, 70 and 100 Hz while the muscle was shortening at 0.10, 0.30 or 0.50 $V_{max}$. Pairs of passive and active shortening ramps were elicited 10 s before and 10 s after the potentiating stimulus to determine unpotentiated and potentiated concentric force. Potentiation was calculated as relative concentric force of each muscle before and after being subjected to a potentiating stimulus (i.e. post/pre). Each muscle was assigned to one of the three shortening speeds, and tested at all activation frequencies in a randomized order; thus, the testing procedure was repeated five times for each individual muscle. Between consecutive procedures, the

muscle remained quiescent for 20 min, allowing muscles to return to basal conditions. See Figure 4.12 for a schematic of the experimental protocol.

Parallel experiments were conducted to determine myosin RLC phosphate content in both unpotentiated and potentiated muscles that were quick frozen in tongs pre-cooled in liquid $N_2$. All muscles were stored at -80°C until analyzed by urea/glycerol-PAGE. Details regarding these methods have been previously described (Ryder et al, 2007).

### *Statistics*

After initial assessment of normality and homogeneity of variance, a two-way repeated measures analysis of variance (ANOVA) was conducted to examine the effect of shortening speed [0.10, 0.30, or 0.50 $V_{max}$] and stimulation frequency [10, 25, 45, 70, or 100 Hz] on relative concentric force (i.e. potentiation). The assumption of sphericity was met ($P$ = .024), and results revealed a statistically significant interaction between the effects of shortening speed and stimulation frequency on concentric force potentiation [$F(8,36)=53.37$, $P < .0001$, $\eta^2 = .144$]. Thus, the simple effects were examined; that is, the differences in potentiation among the different shortening speeds were considered at each frequency, separately. Post-hoc analyses were conducted using Tukey's multiple comparison tests. Statistical significance was at a $P < .05$, and results are summarized in Figure 4.10, Panel A. To better summarize the data, concentric force potentiation was collapsed across frequencies for each shortening speed, and a one-way ANOVA was conducted to examine the effect of shortening speed [0.10, 0.30 or 0.50 $V_{max}$] on potentiation. Results revealed a statistically significant difference between shortening speeds [$F(2,9) = 120.3$, $P < .0001$, $\eta^2 = .991$]. Post-hoc analyses were conducted using Tukey's HSD and statistical significance was at a $P < .05$. Additionally, multiple *t*-tests, using the Holm-Sidak correction for multiple comparisons, were performed to compare the previously published wildtype values (Gittings et al, 2012) to the current skMLCK$^{-/-}$ values at each frequency and speed. Tests were run without assuming an equal S.D. Results are summarized in Figure 4.11, Panels A-C. All data are presented as Means ± SEM.

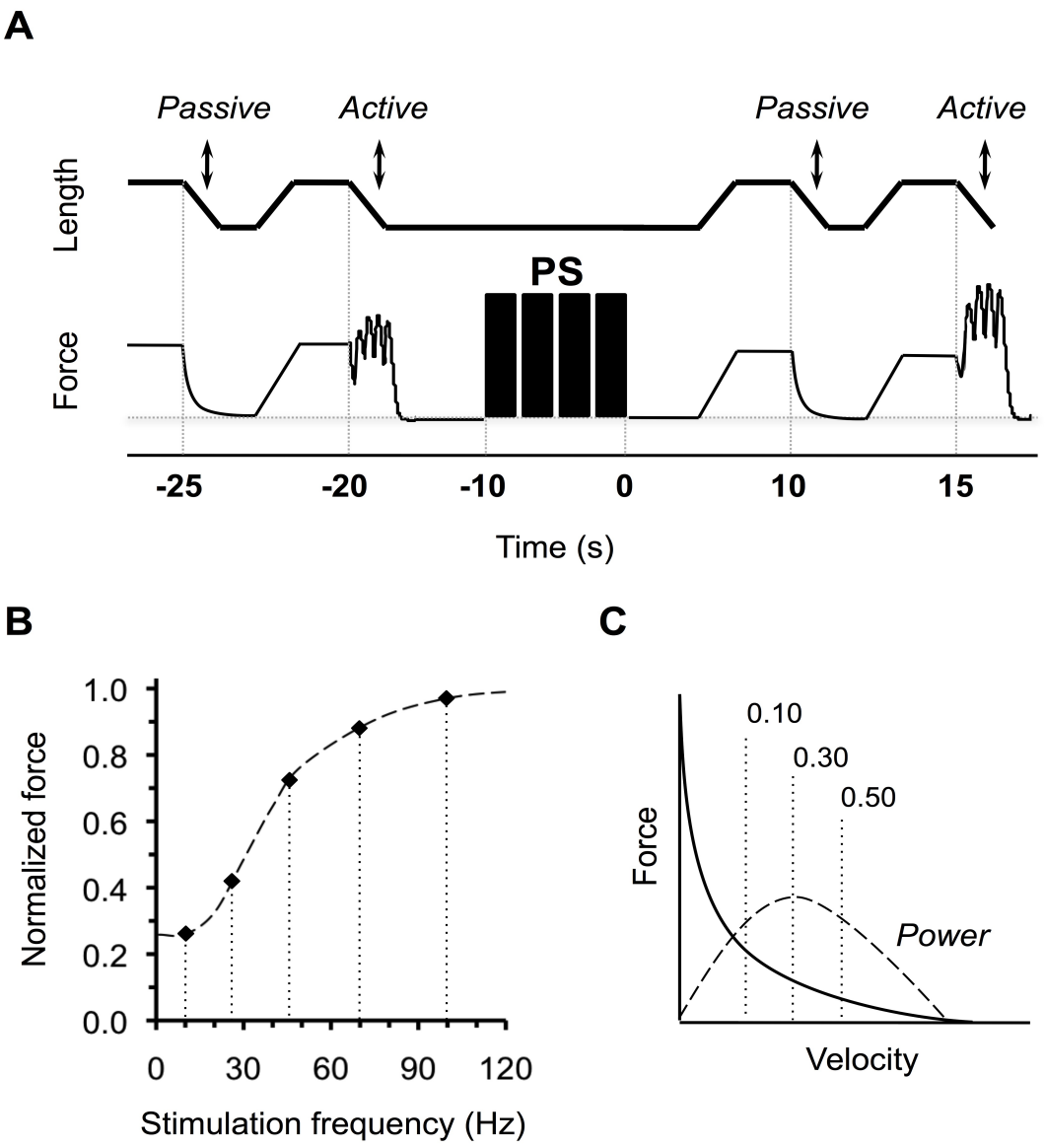


*Figure 4.12. Experimental protocol for determining the influence of shortening speed and activation frequency on relative concentric force of skMLCK$^{-/-}$ mouse EDL muscles in vitro (25°C).*

(**A**) The experimental protocol involved collecting unpotentiated and potentiated force data utilizing a pair of shortening ramps. Both a passive and an active shortening ramp (shortening from 1.10 to 0.90 of the optimal length for force production, $L_o$) were applied 10 s before, and 10 s after, a potentiating stimulus. The potentiating stimulus consisted of four brief high-frequency volleys (100 Hz, 400 ms) within a 10 s window. Muscles were activated at shortening velocities (0.10, 0.30 and 0.50 $V_{max}$) that span peak power (**C**), and activation frequencies (10, 25, 45, 70, and 100 Hz) spanning the Force-Frequency Curve (**B**).

***Acknowledgments***

We are grateful to Dr. James Stull for providing the skMLCK$^{-/-}$ breeder pairs used to establish our colony, as well as skRLC antibody used for analysis of RLC phosphate content.

### *Competing interests*

The authors declare no competing financial interests.

### *Funding*

This work was supported by a grant from the Natural Sciences and Engineering Research Council of Canada to R.V. [no. 2014-05122].

## *References*


Gittings, W., Huang, J., Smith, I. C., Quadrilatero, J., & Vandenboom, R. (2011). The effect of skeletal myosin light chain kinase gene ablation on the fatigability of mouse fast muscle. *J. Muscle. Res Cell Motil*. 31, 337-348.

Gittings, W., Huang, J., & Vandenboom, R. (2012). Tetanic force potentiation of mouse fast muscle is shortening speed dependent. *J. Muscle. Res Cell Motil*. 33, 359-368.

Grange, R.W., Vandenboom, R., Xeni, J., & Houston, M.E. (1998) Potentiation of in vitro concentric work in mouse fast muscle. *J Appl Physiol* 84: 236-

Klug, G.A., Botterman, B.R. & Stull, J.T. (1982)The effect of low frequency stimulation on myosin light chain phosphorylation in skeletal muscle. *J Biol Chem* 257: 4670–4688.

MacIntosh, B.R., Smith, M.J. & Rassier, D.E. (2008) Staircase but not posttetanic potentiation in rat muscle after spinal cord hemisection. *Muscle Nerve* 38(5): 1455–1465.

Manning, D.R. & Stull, J.T. (1982) Myosin light chain phosphorylation - dephosphorylation in mammalian skeletal muscle. *Am J Physiol* 242: C234–C241.

Moore, R.L. & Stull, J.T. (1984) Myosin light chain phosphorylation in fast and slow skeletal muscles in situ. *Am J Physiol Cell Physiol* 247(5): C462–C471.

Moore, R.L., Houston, M.E., Iwamoto, G.A. & Stull, J.T. (1985) Phosphorylation of rabbit skeletal muscle myosin in situ. *J Cell Physiol* 125: 301–305.

Moore, R.L., Palmer, B.L., Williams, S.L., Tanabe, H., Grange, R.W. & Houston, M.E. Effect of temperature on myosin phosphorylation in mouse skeletal muscle. *Am J Physiol* 259: C432–C438.

Palmer, B.M. & Moore, R.L. (1989) Myosin light chain phosphorylation and tension potentiation in mouse skeletal muscle. *Am J Physiol* 257: C1012–C1019.

Rassier, D.E., Tubman, L.A. & MacIntosh, B.R. Staircase in mammalian muscle without light chain phosphorylation. *Braz J Med Biol Res* 32(1): 121–129.

Ryder, J. W., Lau, K. S., Kamm, K. E., & Stull, J. T. (2007). Enhanced skeletal muscle contraction with myosin light chain phosphorylation by a calmodulin-sensing kinase. *J. Biol. Chem.* 282(28), 20447-20454.

Smith, I. C., Gittings, W., Huang, J., McMillan, E. M., Quadrilatero, J., Tupling, A., R., & Vandenboom, R. (2013). Potentiation in mouse lumbrical muscle without myosin light chain phosphorylation: Is resting calcium responsible? *J. Gen. Physiol*. 141, 297-308.

Smith, I. C., Vandenboom, R., & Tupling, A. R. (2014). Juxtaposition of the changes in intracellular calcium and force during staircase potentiation at 30 and 37°C. *J. Gen. Physiol.* 144(6), 561-570.

Stull, J. T., Kamm, K. E., & Vandenboom, R. (2011). Myosin light chain kinase and the role of myosin light chain phosphorylation in skeletal muscle. *Arch. Biochem. Biophys*. 510, 120-128.

Vandenboom, R., Gittings, W., Smith, I. C., Grange, R. W., & Stull, J. T. (2013). Myosin phosphorylation and force potentiation in skeletal muscle: Evidence from animal models. *J. Muscle Res. Cell Motil.* 34, 317-332.

Vandenboom, R., Xeni, J., Bestic, N. & Houston, M.E. (1997) Increased force development rates of fatigued skeletal muscle are graded to myosin light chain phosphate content. *Am J Physiol* 272: 1980–1984.

Vandenboom, R., Grange, R.W. & Houston, M.E. (1995) Myosin phosphorylation enhances rate of force development in fast-twitch skeletal muscle. *Am J Physiol* 268: 596–603.

Xeni J, Gittings W, Caterini D, Huang J, Houston ME, Grange RW, Vandenboom R. (2011) Myosin light chain phosphorylation and potentiation of dynamic function in mouse fast muscle. *Pflugers Archiv* 362: 349–358.

# Chapter 5

## Study #2

**The force dependence of isometric and concentric potentiation in mouse muscle with and without skeletal myosin light chain kinase**

William Gittings, Harish Aggarwal, James T. Stull, and Rene Vandenboom

As published in: Canadian Journal of Physiology and Pharmacology, 93(1), 23–32, 2015

**Author contributions:**

*William Gittings*: study design, data collection and experimentation, manuscript writing
*Harish Aggarwal*: assistance with skMLCK protein expression analysis
*Dr. James T. Stull*: skMLCK$^{-/-}$ mice breeding pairs, technical assistance
*Dr. Rene Vandenboom*: study design input, funding (NSERC), manuscript writing

Running head: Force dependence of potentiation


## *Abstract*

The isometric potentiation associated with myosin phosphorylation is force dependent. The purpose of this study was to assess the influence of a pre-existing period of isometric force on the concentric force potentiation displayed by mouse muscles with and without the ability to phosphorylate myosin. We tested isometric (ISO) and concentric (CON) potentiation, as well as concentric potentiation after isometric force (ISO-CON), in muscles from wildtype and skeletal myosin light chain kinase-deficient ($skMLCK^{-/-}$) mice. A potentiating stimulus increased (i.e., potentiated) mean concentric force in the ISO-CON and CON conditions to 1.31 ± 0.02 and 1.35 ± 0.02 (wildtype) and to 1.19 ± 0.02 and 1.21 ± 0.01 ($skMLCK^{-/-}$) of prestimulus levels, respectively (data n = 6-8, $p < 0.05$). No potentiation of mean isometric force was observed in either genotype. The potentiation of mean concentric force was inversely related to relative tetanic force level ($P/P_o$) in both genotypes. Moreover, concentric potentiation varied greatly within each contraction type and was negatively correlated with unpotentiated force in both genotypes. Thus, although no effect of pre-existing force was observed, strong and inverse relationships between concentric force potentiation and unpotentiated concentric force may suggest an influence of attached and force-generating crossbridges on potentiation magnitude in both wildtype and $skMLCK^{-/-}$ muscles.



Keywords: concentric, isometric, myosin, phosphorylation, regulatory light chains, shortening ramps, tetanus, cooperativity, skMLCK knockout

## *Introduction*

A notable characteristic of fast twitch skeletal muscle contraction is that of force potentiation, the transient increase in muscle force observed during or following contractile activity (reviewed by Vandenboom et al. 2013). Classic studies showed that the potentiation of isometric force displayed by rodent skeletal muscle varied inversely with force level. For example, in experiments in which force was varied via stimulation frequency, temperature, or drug administration (Close and Hoh, 1968a, 1968b; Krarup 1981a, 1981b), the relative magnitude of force potentiation tended to decrease as force level was increased and vice versa. In addition, the potentiation of concentric twitch force has recently been shown to be greater than that for isometric twitch force (Caterini et al. 2011; Xeni et al. 2011) and the potentiation of concentric force is proportional to shortening speed at tetanic stimulus frequencies (Gittings et al. 2012). Although it is unclear whether these latter differences are a function of force level or contraction type, force dependence appears to be one of the most robust features of the force potentiation displayed by animal fast twitch skeletal muscle.

Evidence from a variety of models suggests that phosphorylation of the myosin regulatory light chain (RLC), catalyzed by skeletal muscle myosin light chain kinase (skMLCK), is the primary, but perhaps not only, mechanism for potentiation. For example, strong temporal correlations between RLC phosphorylation and isometric twitch potentiation have been obtained from a number of rodent fast twitch skeletal muscle models (Klug et al. 1982; Manning and Stull, 1979, 1982; Palmer and Moore, 1989; Ryder et al. 2007; Vandenboom et al. 1993, 1995). Moreover, ablation of the skMLCK gene, and corresponding absence of RLC phosphorylation, has been shown to eliminate or attenuate isometric twitch potentiation in the mouse EDL muscle (Gittings et al. 2011; Zhi et al. 2005). Consistent with this, rat soleus muscle has been shown to express much lower levels of skMLCK with parallel reductions in stimulation-induced elevations in RLC phosphorylation and isometric twitch potentiation (Moore and Stull, 1984). Thus, although altered $Ca^{2+}$ homeostasis may contribute (Smith et al. 2013), RLC phosphorylation has been suggested to be a "molecular memory" that enhances muscle force during or following contraction (Stull et al. 2011).

Permeabilized rabbit skeletal muscle fibres have been used to study RLC phosphorylation-mediated potentiation. The studies show that phosphorylation of the

RLC increases the sensitivity of the contractile proteins to $Ca^{2+}$ without altering maximal $Ca^{2+}$ activated force (e.g., Persechini et al. 1985; Sweeney and Kushmerick, 1985; Sweeney and Stull, 1986). A model accounting for the ability of myosin RLC phosphorylation to enhance suboptimal, but not optimal, steady state force, based on crossbridge cycling kinetics, has been presented by Sweeney and Stull (1990). There is also evidence, however, that cooperative aspects of thin filament activation may influence the force dependence of potentiation. For example, Metzger et al. (1989) used permeabilized skeletal muscle fibres from rabbit gastrocnemius muscle to show that disruption of cooperative activation via extraction of troponin C eliminated phosphorylation-dependent increases in $Ca^{2+}$ sensitivity. Because this effect was reversed with reconstitution of troponin C, these results were interpreted to suggest that the potentiation of steady-state force in permeabilized skeletal muscle fibre models may be influenced by cooperative interactions between thick and thin filament proteins. This outcome may also account for the force dependence of potentiation displayed by various intact skeletal muscle models.

The purpose of this study was to examine the force dependence of concentric force potentiation in mouse skeletal muscles with and without the ability to phosphorylate the myosin RLC (wildtype and skMLCK$^{-/-}$, respectively). To this end, we compared concentric force potentiation with and without a pre-existing period of isometric force in both genotypes. We hypothesized that isometric force would decrease the relative magnitude (i.e., post/pre) of concentric potentiation compared with when it was not present. The rationale for these experiments was that a population of strongly bound and force-generating crossbridges would influence potentiation via a cooperative influence on thin filament activation (as tested in the ISO-CON condition).

## *Methods*

All procedures received full ethical approval from the Brock University Animal Care Committee (ACC). Adult wildtype and skMLCK$^{-/-}$ mice were used in these studies. Wildtype C57BL/6 mice (age 3 months; mass 20.2 ± 0.3 g) were ordered from Charles River (St. Constant, QC), and were housed for ~1 week before experiments began. The skMLCK$^{-/-}$ mice (C57Bl/6 background) were obtained from our own breeding colony (age, 4–5 months; mass 24.9 ± 1.7 g). Details regarding the generation and characterization of the skMLCK$^{-/-}$ animals have been presented previously (Zhi et al. 2005; Gittings et al. 2011). On the day of an experiment adult mice were anaesthetized with a peritoneal injection of sodium pentobarbital (60 mg/kg body mass). The EDL muscle was surgically excised and suspended in a jacketed vertical bath, containing continuously oxygenated Tyrode's solution maintained at 25° C (Lannergren et al., 2000). Muscle stimulation was applied using flanking platinum electrodes, provided by a Model 701B biphasic stimulator (ASI) with voltage set to 1.25 times the voltage required to fully activate the muscle and elicit a maximal twitch. Following muscle suspension a 30 min equilibration period took place during which optimal length for isometric twitch force ($L_o$) was determined. Muscle length was controlled via LINUX software and force data obtained from a dual-mode servomotor (Model 300C-LR, Aurora Scientific Inc., Aurora, Ont., Canada). All experiments were collected at 2000 Hz and saved to disk for further analysis (ASI 600a software).

### *General experimental protocol*

A major purpose of our experiments was to test the influence of a brief period of pre-existing isometric force on subsequent concentric force potentiation. Related to this, 2 different concentric force regimes were employed to determine if stimulus timing (i.e. started before or during shortening) influenced this response. A secondary purpose was to compare the responses noted above in wildtype and in skMLCK$^{-/-}$ muscles, muscles with and without the ability to phosphorylate the RLC. The general protocols and design of our experiments were based on previous work from our lab (e.g. Gittings et al., 2012). After preliminary procedures had been performed (i.e., equilibration and determination of optimal length, $L_o$), the muscles were subjected to each of 3 conditions in randomized order. Each of the 3 conditions was similar except for certain details regarding the stimulation timing. Identical procedures were used for both the wildtype and skMLCK$^{-/-}$

genotype; the latter, therefore, served as a negative control (n = 8 for all conditions) for the absence of RLC phosphorylation. For each genotype, potentiation was induced by a series of 4 brief but high frequency volleys (100 Hz for 400 ms) within a 10 s time window. This protocol has been demonstrated to produce near maximal potentiation and minimal fatigue of EDL muscles from wildtype mice (Vandenboom et al., 1997; Xeni et al., 2011). In each condition, this tetanic potentiating stimulus (PS) was bracketed by identical contractile conditions (Figure 5.1), timed to occur before (unpotentiated) and after (potentiated), with potentiation magnitude calculated as post-force/pre-force. Each of the 3 test conditions was separated by ≥ 20 min to allow potentiation to dissipate. This experimental design, including repeated application of a tetanic PS, has been shown to allow stable twitch and/or tetanic forces as well as repeatable potentiation of isometric twitch forces (Gittings et al., 2012). Moreover, the serial application of 3–5 tetanic PS has been shown to produce repeatable increases (up to ~55% total RLC phosphorylated) in mouse EDL muscle at 25° C (Caterini et al., 2011).

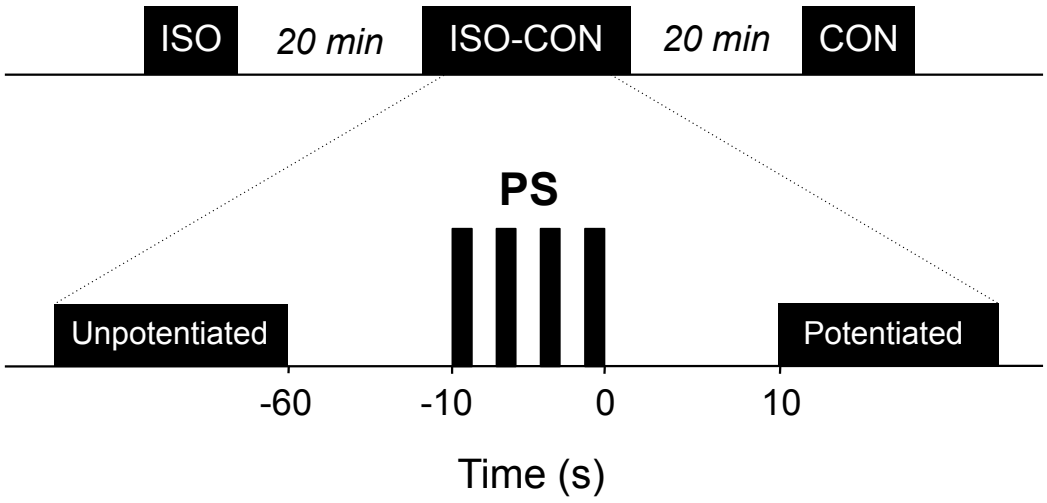


*Figure 5.1. Experimental timeline*

Posttetanic potentiation (PTP) was studied three times in each muscle, one for each condition (ISO, isometric; CON, concentric, and ISO-CON, isometric and concentric). The order of these conditions was alternated between experiments. Unpotentiated and potentiated data were collected via a pair of length ramps, one passive and one stimulated, applied just prior to and after the application of a tetanic potentiating stimulus (PS). The PS used to induce a potentiated response consisted of 4 brief (400 ms) but high frequency (100 Hz) volleys occurring within 10s.

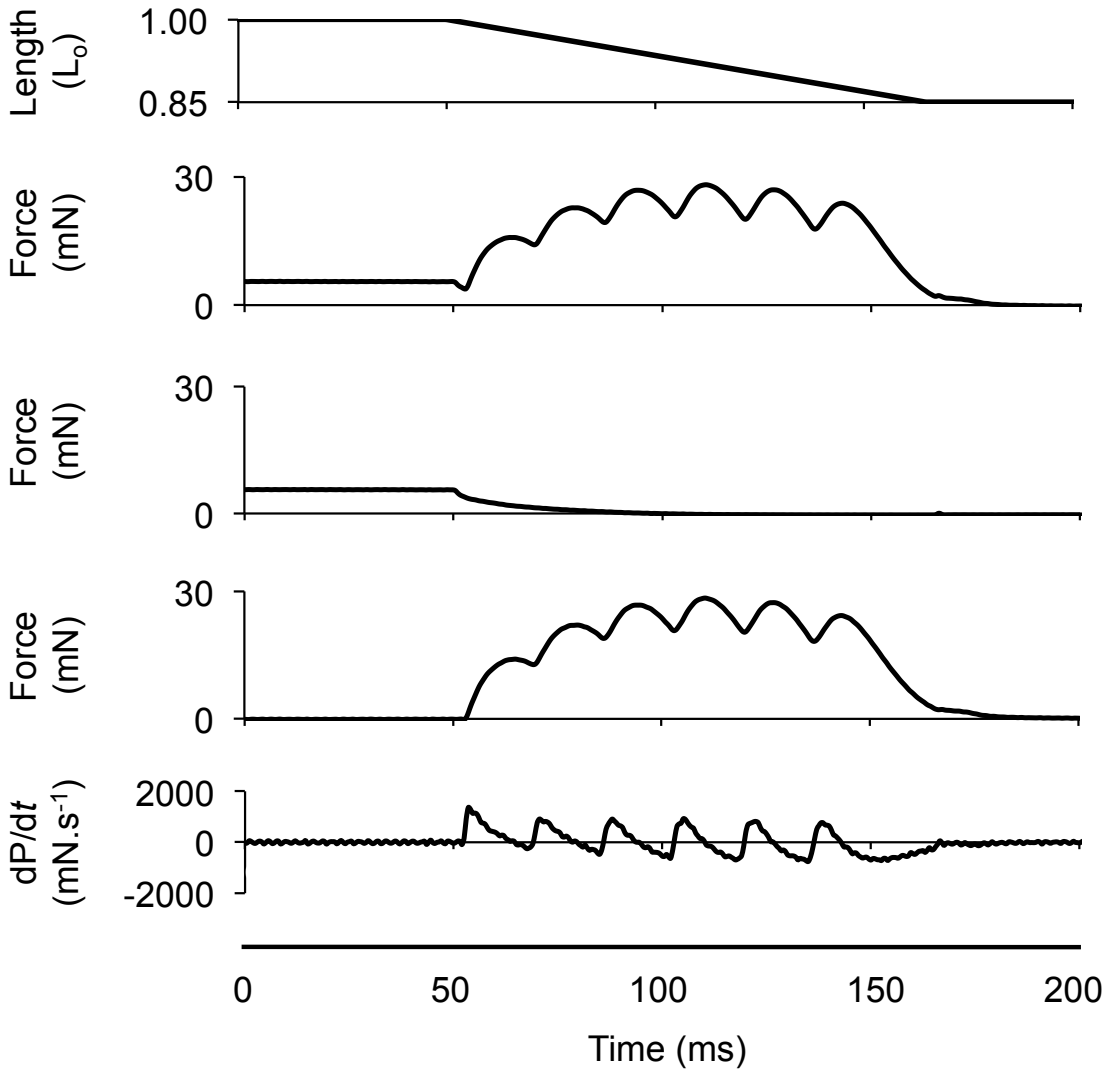


*Figure 5.2. Experimental protocol for determining influence of PTP on force responses of mouse EDL muscle in vitro (25 °C).*

Representative records illustrating method use for determination of mean active concentric force and force kinetics. At top is shown length record with corresponding force traces for one contraction shown below. During each length ramp the muscle was allowed to shorten from 1.00 to 0.85 of optimal length ($L_o$); length amplitude was thus fixed at 15% $L_o$. Muscles were not stimulated until 2 ms after the length ramp was initiated to avoid prior isometric force development. Total, passive, and active forces are shown with differentiated record of active force shown at bottom. Mean forces reported in Table 1 were the arithmetic average of the last 50 ms of stimulation in each condition, although forces over each 25 ms of stimulation were calculated for subsequent data analysis.

*Contractile conditions*

Three different contractile conditions were employed to assess the effect of pre-existing isometric force on concentric force potentiation in wildtype and skMLCK$^{-/-}$ muscles. In all experiments, the sequence of the 3 conditions was randomized to avoid any potential order-effect. The conditions were classed as being isometric (ISO), concentric (CON), or isometric and concentric (ISO-CON). The precise way in which parameters of muscle length and stimulation were manipulated to achieve these aims is described in Figure 5.3. In the ISO condition, the ability of the tetanic PS to potentiate isometric force was assessed by stimulating muscles at 60 Hz for 100 ms while muscle length was fixed at 1.0 $L_o$. The ability of the tetanic PS to potentiate concentric force in the CON condition was assessed by stimulating muscles at 60 Hz for 100 ms, with the stimulus volley beginning coincident with the shortening ramp. During the ramp, muscle length was continuously shortened from 1.00 to 0.85 $L_o$. With a duration of 115 ms, the length ramp was equivalent to ~25% of maximum shortening velocity ($V_{max}$) of mouse EDL muscle at 25° C (Gittings et al. 2011). In addition to the above, we also tested a second concentric condition in which stimulation of muscles (60 Hz for 100 ms) did not begin until midway through the shortening ramp (shortening from 1.05 to 0.85 $L_o$ in 155 ms, at 25% $V_{max}$, with a 30 ms delay). However, the absolute and relative force responses measured during this condition were virtually identical to the CON condition described above, and thus we have omitted details regarding this condition from our analysis. The influence of pre-existing isometric force on concentric force potentiation caused by the tetanic PS was assessed in the ISO-CON condition by the application of a single high-frequency volley (i.e., 60 Hz for 200 ms), during which muscle length was fixed at 1.00 $L_o$ during the initial 100 ms of the stimulus volley and then allowed to shorten from 1.00 to 0.85 $L_o$ during the latter 100 ms of the stimulus volley. An unavoidable consequence of this protocol was a transition phase in which shortening of the series elastic component occurred; however, the steady-state isometric and concentric forces measured during the fixed length and shortening phases of this protocol, respectively, were generally similar to those observed in the ISO and CON conditions.

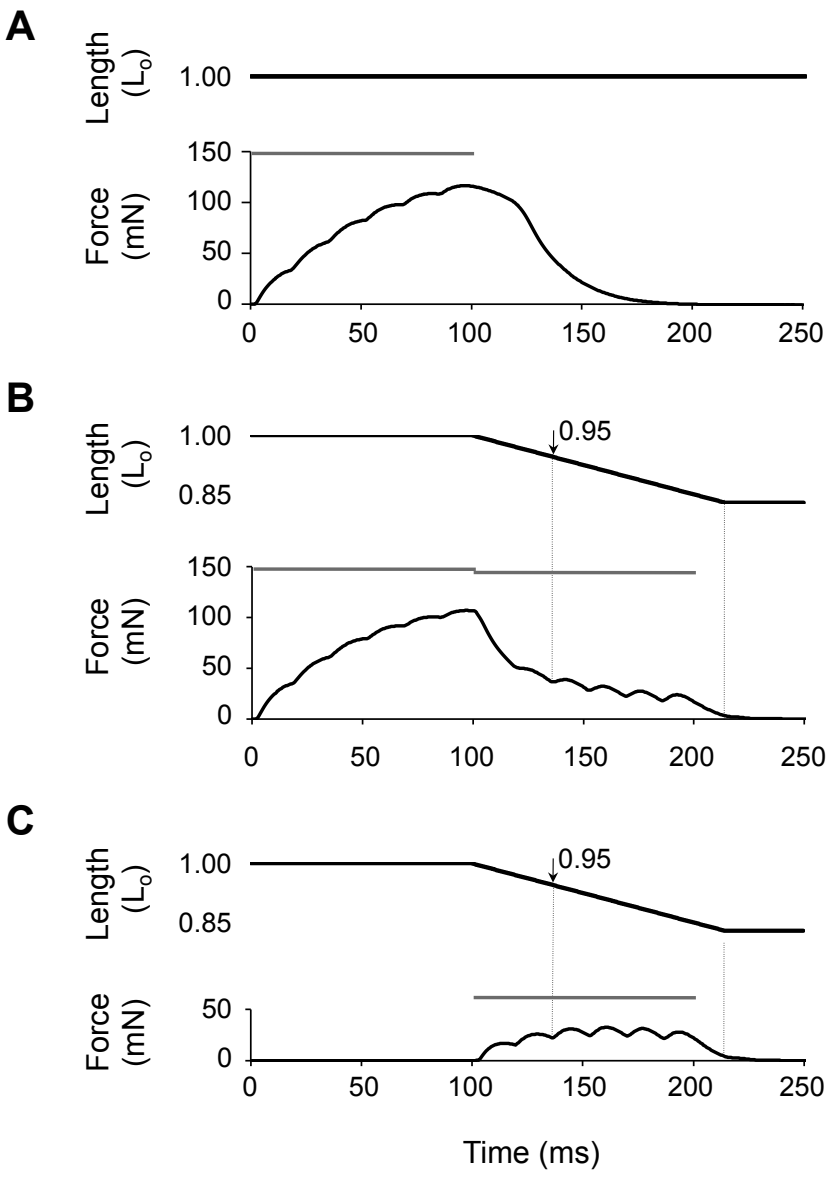


*Figure 5.3. Representative length, force, and stimulus records representing the different contractile conditions used in the experiments.*

Unpotentiated contractions from wildtype are shown; the exact same procedure was used for the skMLCK$^{-/-}$ genotype. Muscles were activated at 60 Hz in all conditions. Particulars for each condition are detailed as follows: (**A**) Isometric – Length was fixed at optimal length ($L_o$), muscles stimulated for 100 ms. (**B**) Isometric-Concentric – Muscle length initially was held at 1.00 Lo before being shortened to 0.85 $L_o$ (in 115 ms). Stimulation of muscle began while muscle length was fixed and continued during shortening (100 + 100 ms, respectively). Vertical dotted lines in each panel depict where mean isometric and (or) concentric force was calculated. (**C**) Concentric – Muscle length was changed from 1.00 to 0.85 $L_o$; the duration of this ramp was 115 ms. During these ramps muscles shortened at a rate equivalent to $0.25V_{max}$. Stimulation of muscles commenced with the onset of the ramp and lasted for 100 ms.

*Force analysis*

The quantification of mean force during each contraction was performed as shown in Figure 5.3 and represents the arithmetic mean value of the active force record from 50–100 ms of stimulation for the isometric and concentric conditions and for 150–200 ms of stimulation in the ISO-CON state. In each case this time period corresponded to the final 50 ms of force production during the tetanus. Briefly, for each condition that included a concentric portion (CON and ISO-CON), a passive force trace was subtracted from the total force trace to yield an active force record; during the ISO-CON condition, only the concentric phase of the contraction was analyzed. To accomplish this, the identical ramp sequence was performed twice for each condition, with only the second receiving stimulation. This method was intended to retain force information primarily related to active crossbridge versus passive function. The first derivative of the active force record was used to determine peak rate of force development (+dP/dt) and force relaxation (-dP/dt), expressed as mN per second.

*Cross-correlations*

A goal of this work was to better understand the relationship between relative potentiation magnitude and existing force level. To help do this we performed a cross-correlation analysis (Nelson-Wong et al., 2009) between "instantaneous" potentiation and unpotentiated force. Instantaneous potentiation refers to the force–time curve produced by dividing the potentiated force record by the respective unpotentiated force record for each condition and genotype. Because the tetanic PS used in these experiments cause little fatigue (e.g. Gittings et al. 2012), this approach may provide a useful "real time" view of the relative difference in force between a potentiated and an unpotentiated contraction. The cross-correlation analysis was performed using SPSS Statistics for Windows (version 19.0; IBM Corp., Armonk, N.Y., USA) according to the following formula:

$$R_{xy}(\tau) = \frac{\sum_{n-1}^{N}[(x_n - \bar{x})(y_{n-\tau} - \bar{y})]}{\sqrt{\sum_{i=1}^{N}(x_i - \bar{x})^2 \sum_{i=1}^{N}(y_i - \bar{y})^2}} \qquad (11)$$

The cross-correlation function $R_{xy}(\tau)$ was created from the unpotentiated force (x) and instantaneous potentiation (y) functions, where N is the number of data points in the sampling period and ($\tau$) is the lag time that coincided with the highest correlation

between the 2 signals. The force records used in this analysis were sampled over the same 50 ms interval as used to calculate mean forces for each condition (as described above).

*Western blotting for skMLCK protein expression*

The absence of skMLCK protein expression in mice from our breeding colony was established by Western blotting. We randomly harvested EDL and soleus muscles from different litters of putative skMLCK$^{-/-}$ mice (≥4 generations) and these muscles were homogenized in buffer solution containing 250 mmol/L sucrose, 100 mmol/L KCl, 5 mmol/L EDTA, pH 6.8, and protease/phosphatase inhibitors (Roche Diagnostics, Indianapolis, Ind., USA). 15g of protein was loaded per well and standard SDS–PAGE electrophoresis was performed using a 10% gel. Proteins were transferred to a polyvinylidene fluoride and were blocked for 1 h in 5% skim milk-TBST then incubated overnight at 4° C in 2.5% skim milk-TBST in primary monoclonal antibodies. Detailed methods can be found in Appendix I.

*Statistical analysis*

All data are presented as Means ± SEM. For all procedures, a P-value of $P < 0.05$ was considered significant. We tested the changes in force and force kinetics caused by the tetanic PS (after vs. before) and evaluated the main effect(s) of genotype, condition (ISO, ISO-CON, CON), and pulse number on the outcome variable.

To evaluate whether each absolute contractile measure changed significantly following the tetanic PS, a two-tailed paired t-test was used to determine differences between means (before vs. after). A two-way repeated measures ANOVA was used to test the main effect(s) of genotype and experimental condition on the relative change (i.e. Post/Pre) in mean force/force kinetics and pulse-by-pulse potentiation between the ISO-CON and CON conditions. Post hoc analysis (Šidák) was conducted to further evaluate the differences in means between conditions and genotypes.

## *Results*

Experiments examining the influence of a tetanic PS on potentiation of isometric and concentric force were performed on muscles with and without the ability to phosphorylate the RLC. Data comparing the potentiation of isometric and concentric forces in the ISO, ISO-CON, and CON conditions will be presented together with genotype differences (wildtype and skMLCK$^{-/-}$, respectively). Mean force responses from wildtype and skMLCK$^{-/-}$ experiments are compiled in Table 1. These values are similar to previous reports from our laboratory (Gittings et al. 2011, 2012). Experimental records depicting this influence are shown in Figure 5.4 for all conditions and both genotypes with a summary of all data shown in Panel C.

*Potentiation in the ISO condition*

Mean isometric force of wildtype muscles was increased to 1.06 ± 0.03 of unpotentiated levels by the tetanic PS. In contrast, the tetanic PS reduced mean isometric force of skMLCK$^{-/-}$ muscles to 0.94 ± 0.01 of pre-PS levels. These data reveal a large genotype-dependent difference in isometric potentiation in mouse EDL muscle.

*Potentiation in the ISO-CON condition*

Mean concentric force of wildtype muscles was increased to 1.31 ± 0.02 of unpotentiated levels by the tetanic PS. In skMLCK$^{-/-}$ muscles the tetanic PS increased concentric force to 1.19 ± 0.01 of unpotentiated levels. Thus, although both wildtype and skMLCK$^{-/-}$ muscles displayed increases there was a genotype-dependent difference in concentric potentiation observed following a period of pre-existing isometric force.

*Potentiation in the CON condition*

Mean concentric force of wildtype muscles was increased to 1.35 ± 0.02 of unpotentiated levels by the tetanic PS. In skMLCK$^{-/-}$ muscles the tetanic PS increased concentric force to 1.21 ± 0.01 of unpotentiated levels. Similar to the ISO-CON condition, there was a genotype-dependent difference in concentric potentiation observed, although both types were increased relative to control. Consequently, there was no observed interaction between genotype and contractile conditions. Because the increase in concentric forces observed in the ISO-CON and CON conditions were similar (Figure 5.4, Panel C), no apparent influence of pre-existing force on potentiation was observed.

*Table 5.1. Mean forces in EDL muscles from wildtype and skMLCK$^{-/-}$ mice*

| | **wildtype** | | |
|---|---|---|---|
| | Control | Potentiated | Δ(%) |
| ISO | 102.9 ± 11.1 | 108.2 ± 10.8 | 1.06 ± 0.03 |
| ISO-CON | 25.3 ± 2.3 | 33.1 ± 2.8 * | 1.31 ± 0.02 † |
| CON | 27.6 ± 2.6 | 37.1 ± 3.3 * | 1.35 ± 0.02 † |
| | **skMLCK$^{-/-}$** | | |
| | Control | Potentiated | Δ(%) |
| ISO | 108.9 ± 4.0 | 102.0 ± 3.6 | 0.94 ± 0.01 |
| ISO-CON | 27.4 ± 1.2 | 32.5 ± 1.0 * | 1.19 ± 0.02 † |
| CON | 28.7 ± 0.9 | 34.7 ± 1.1 * | 1.21 ± 0.01 † |

All data are presented as Mean ± SEM (n = 6-8). Mean forces expressed in mN. Isometric force was calculated for last 50 ms of stimulation for each contraction type (see Figure 1 for details). Relative force is calculated as the value after the tetanic conditioning stimulus divided by the corresponding value before the tetanic conditioning stimulus. Muscles were stimulated at 60 Hz in all conditions; the timing and duration of stimulation varied depending on the ramp length change protocol employed. Note that values for ISO-CON condition reflect only the concentric phase of the contraction.
*absolute value after tetanic PS significantly different than before ($P < 0.05$)
†relative ISO-CON and CON values different from corresponding ISO value ($P < 0.05$)

*Table 5.2. Rate of force development in wildtype and skMLCK$^{-/-}$ mice*

| | **wildtype** | | |
|---|---|---|---|
| | Control | Potentiated | Δ(%) |
| ISO | 1895 ± 185 | 2717 ± 270 * | 1.44 ± 0.05 † |
| CON | 955 ± 65 | 909 ± 52 | 0.96 ± 0.03 |
| | **skMLCK$^{-/-}$** | | |
| | Control | Potentiated | Δ(%) |
| ISO | 2232 ± 141 | 2808 ± 156 * | 1.27 ± 0.05 † |
| CON | 1090 ± 50 | 1070 ± 51 | 0.98 ± 0.02 |

All data are presented as Mean ± SEM (n=6-8). Rate of force development expressed as +mN.s$^{-1}$. Relative change is calculated as value after tetanic conditioning stimulus divided by value before. Muscles were stimulated at 60 Hz in all conditions; the timing and duration of stimulation varied depending on the ramp length change protocol employed. The concentric rate of force development was not assessed during ISO-CON condition.
*absolute value after the tetanic PS significantly different than before ($P < 0.05$)
†relative ISO value different from corresponding CON relative value ($P < 0.05$)

*Table 5.3. Rate of force relaxation in wildtype and skMLCK$^{-/-}$ mice*

| | **wildtype** | | |
|---|---|---|---|
| | Control | Potentiated | Δ(%) |
| ISO | 2143 ± 323 | 2367 ± 342 | 1.11 ± 0.03 |
| ISO-CON | 823 ± 65 | 859 ± 73 | 1.05 ± 0.07 |
| CON | 800 ± 56 | 905 ± 61 * | 1.13 ± 0.02 |
| | **skMLCK$^{-/-}$** | | |
| | Control | Potentiated | Δ(%) |
| ISO | 1991 ± 113 | 1834 ± 66 * | 0.93 ± 0.03 † |
| ISO-CON | 983 ± 48 | 969 ± 34 | 0.99 ± 0.02 |
| CON | 940 ± 46 | 1047 ± 37 * | 1.12 ± 0.03 |

All data are presented as Mean ± SEM (n=6-8). Rate of force relaxation expressed as -mN.s$^{-1}$. Relative change is calculated as value after tetanic conditioning stimulus divided by value before. Muscles were stimulated at 60 Hz in all conditions; the timing and duration of stimulation varied depending on the ramp length change protocol employed. Relaxation values for ISO-CON condition reflect the concentric phase of the contraction only.
*absolute value after the tetanic PS significantly different than before ($P < 0.05$)
†relative ISO value different from corresponding ISO-CON/CON values ($P < 0.05$)

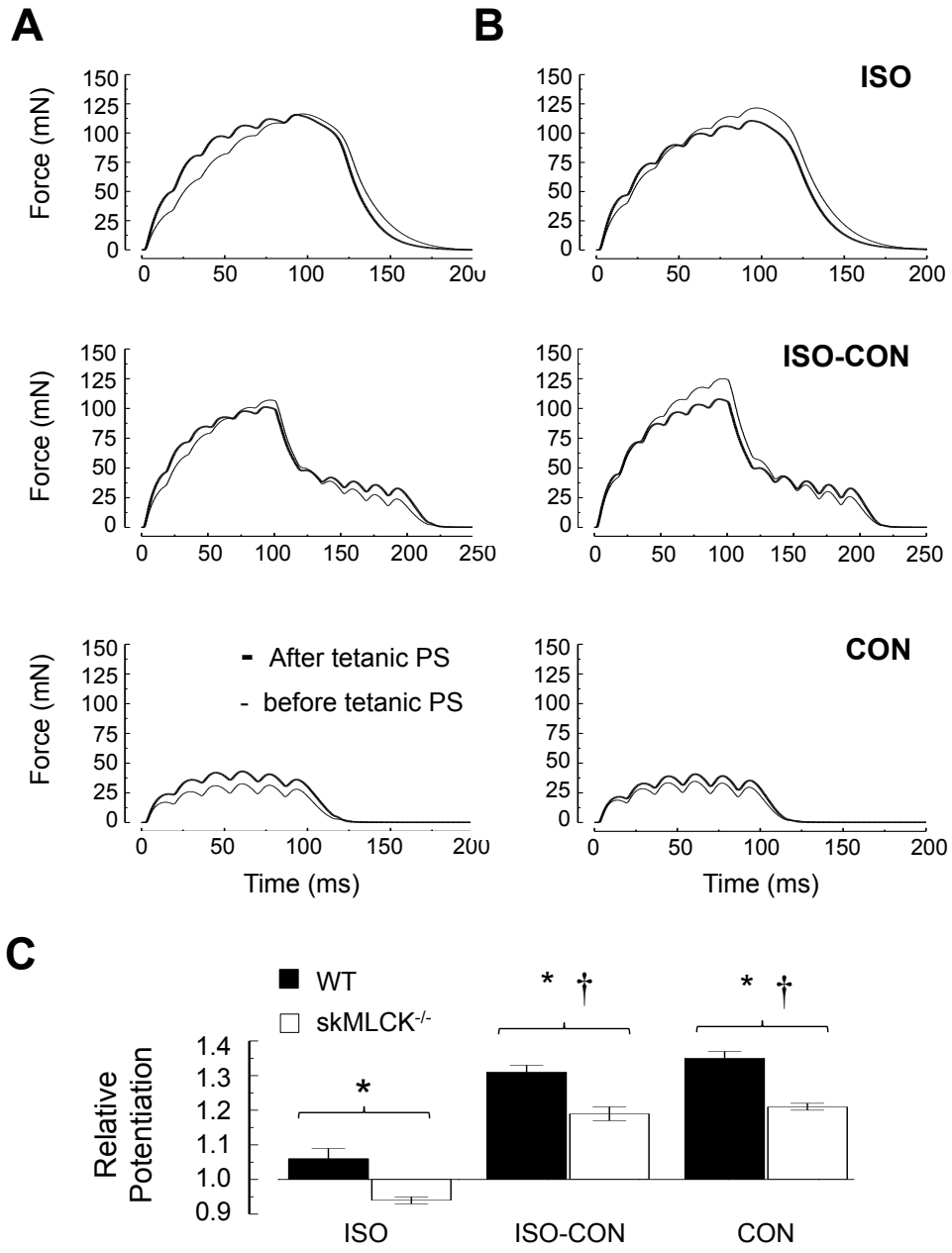


*Figure 5.4. Representative force traces and summary of potentiation in each condition*

(**A**) Mean force traces showing the influence of the tetanic potentiating stimulus (PS) on wildtype muscles. In each panel, force records are the mean of all muscles used in our experiments (n=6-8) with ISO, ISO-CON and CON conditions at top, middle, and bottom, respectively. (**B**) Representative force traces from skMLCK$^{-/-}$ muscles as shown for wildtype muscles. (**C**) Summary of relative force change of both genotypes in the isometric (ISO), isometric and concentric (ISO-CON), and concentric (CON) conditions (n = 6-8).
*wildtype value significantly greater than skMLCK$^{-/-}$ value ($P < 0.05$)
†ISO-CON values greater than ISO values for both genotypes ($P < 0.05$)

*Force dependence of potentiation*

A plot of relative potentiation versus relative force ($P/P_o$) for each condition and genotype is shown in Figure 5.5, Panel A. This plot demonstrates an inverse relationship between potentiation and force across different conditions (ISO, CON, and ISO-CON). In addition, although potentiation was greater in wildtype than skMLCK$^{-/-}$ muscles, the slope of the relationship between potentiation and force was similar between genotypes. A plot of potentiation versus force level, as determined from different time windows within the ISO condition, is shown in Figure 5.5, Panel B. These data also demonstrate an inverse relationship between potentiation and force when the ISO and CON conditions are plotted together, with a similar slope for both genotypes.

*Instantaneous potentiation*

The force–time curves corresponding to "instantaneous" potentiation for each condition and genotype are shown in Figure 5.6. In the ISO condition, instantaneous potentiation was greatest at the onset of contraction and then declined gradually, with minor oscillations, as force increased to its peak in both wildtype and skMLCK$^{-/-}$ muscles (Figure 5.6, top panels). In contrast, instantaneous potentiation in the CON condition was lowest at the onset of contraction and then increased rapidly to a relatively steady state featuring large oscillations (bottom panels). In the ISO-CON condition, instantaneous potentiation resembled aspects of both the ISO and CON conditions (middle panels). As an example, the gradual decline in isometric potentiation at the onset of contraction seemed to mimic that observed in the ISO condition while the oscillations in instantaneous potentiation observed during the latter phases of shortening resembled those observed in the CON condition.

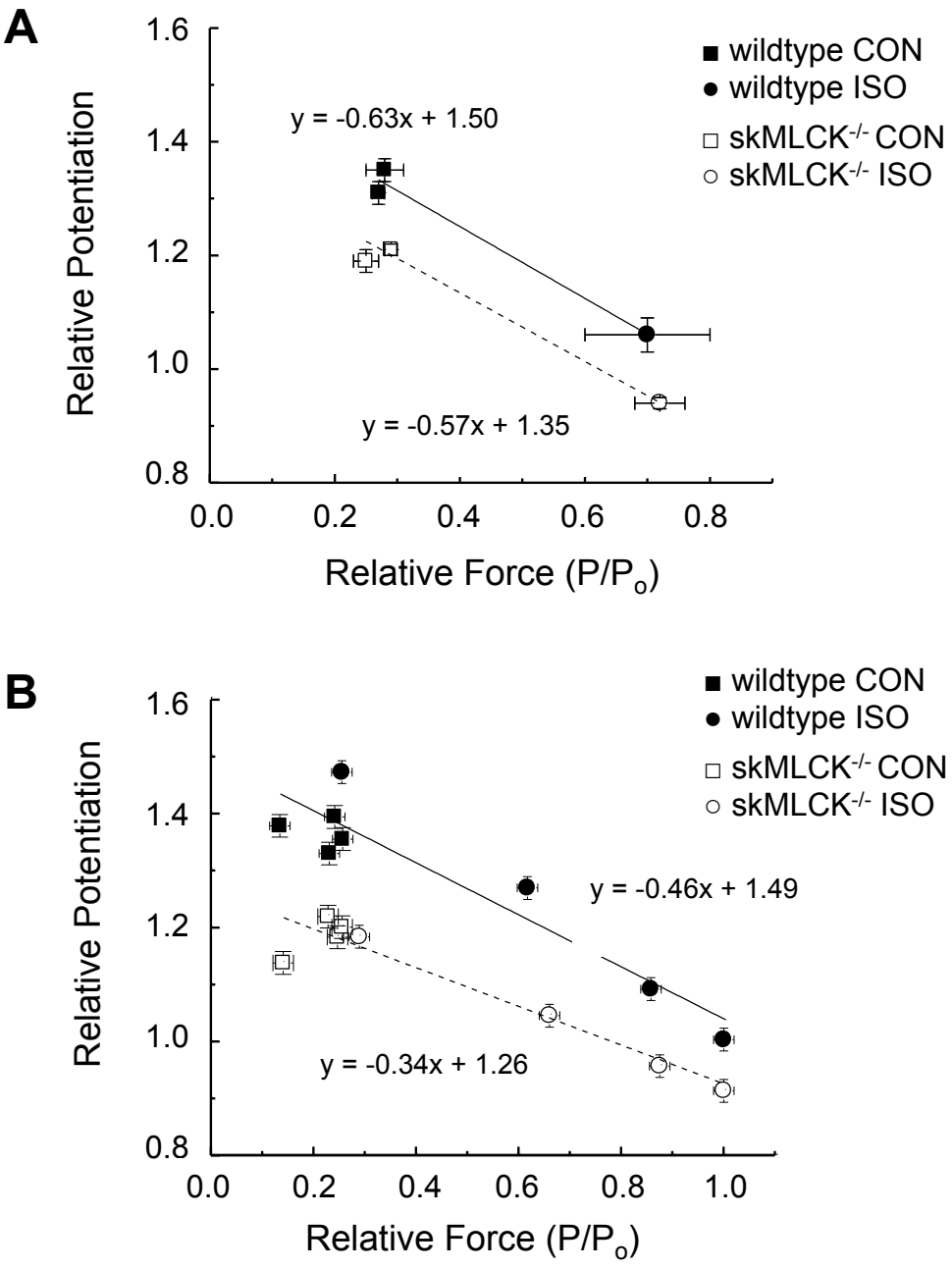


*Figure 5.5. Force dependence of the PTP response*

(**A**) Plot of mean concentric force potentiation (post/pre) versus peak force ($P/P_o$) in the ISO and CON conditions. The equation describing the relationship between potentiation and force for wildtype (r = 0.92) and skMLCK$^{-/-}$ (r = 0.96) muscles is shown. Relative force was calculated by dividing peak force observed during each condition by the peak tetanic force during the PS that preceded it. Although potentiation was greater for wildtype muscles in each condition ($P < 0.05$), the slope of the potentiation:force relationship was similar for both genotypes. (**B**) Plot of mean potentiation (post/pre) versus mean force (force/peak) when calculated for each 25 ms time window within the ISO and CON conditions. The equation describing the relationship between potentiation and force for wildtype (r = 0.87) and skMLCK$^{-/-}$ (r = 0.90) muscles is shown.

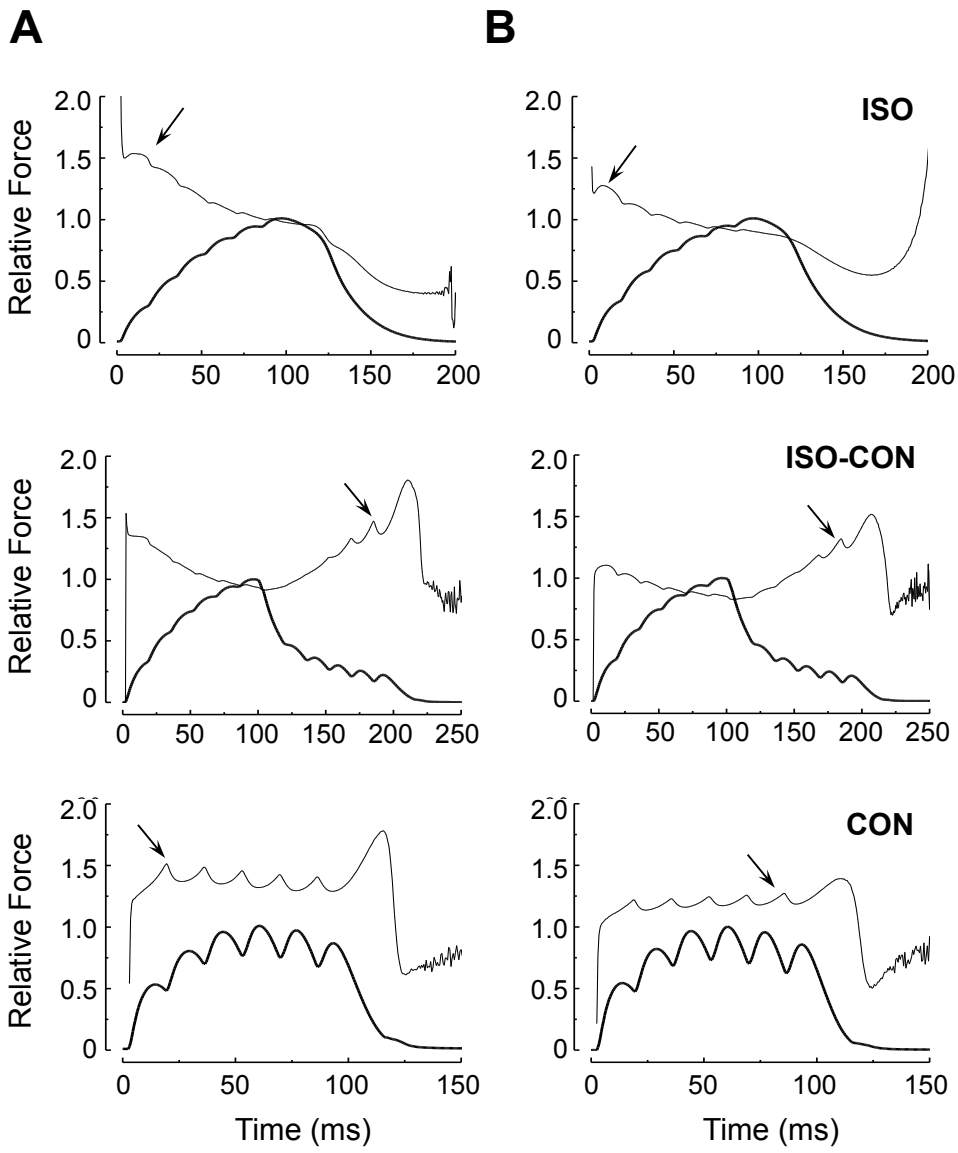


*Figure 5.6. Representative plots of instantaneous potentiation and unpotentiated force versus contraction time in each condition.*

(**A**) Wildtype and (**B**) skMLCK$^{-/-}$ responses. In each panel the unpotentiated force (thick line) is normalized to its peak and instantaneous potentiation (thin line) is normalized to unpotentiated force with arrows indicating peak potentiation during stimulation. Cross-correlation analysis was performed to compare the relationship between instantaneous potentiation and unpotentiated force as depicted in these figures. $R_{xy}(\tau)$ values for muscles in the ISO, ISO-CON, and CON conditions were -0.98, -0.95, and -0.87, respectively. $R_{xy}(\tau)$ values for skMLCK$^{-/-}$ muscles in the ISO, ISO-CON, and CON conditions were -0.93, -0.89, and -0.89, respectively.

*Cross-correlation analysis*

A strong inverse correlation was found between instantaneous potentiation (i.e., potentiated/unpotentiated) and unpotentiated force during the 50 ms sampling period we tested for each condition. In wildtype muscles the cross-correlations were -0.98, -0.95, and -0.87 for the ISO, ISO-CON, and CON conditions. Similarly, in skMLCK$^{-/-}$ muscles the cross-correlations were – 0.93, – 0.89, and – 0.89 for the ISO, ISO-CON, and CON conditions. Importantly, no time delays between unpotentiated force and potentiation were required to produce these strong correlations (i.e., time delay ≤1 ms for all conditions and genotypes). No contraction type or genotype differences were present in these cross correlations.

*Rate of force development and relaxation*

Unpotentiated and potentiated values for the rate of force increase (+dF/dt) and decrease (-dF/dt) for each condition and each genotype are shown in Table 2. Although the isometric +dF/dt was increased in both genotypes, this increase was greater for wildtype than for skMLCK$^{-/-}$ muscles. Conversely, the concentric +dF/dt was not increased in either genotype by the tetanic PS. With respect to force relaxation rate, isometric –dF/dt was increased in wildtype and decreased in skMLCK$^{-/-}$ muscles by the tetanic PS. On the other hand, concentric –dF/dt was unchanged and increased in the ISO-CON and CON conditions, respectively, in both wildtype and skMLCK$^{-/-}$ muscles.

*Pulse by pulse potentiation*

Data plotted in Figure 5.7 demonstrates the condition versus pulse number interaction for concentric potentiation in the ISO-CON and CON conditions (genotype differences were not studied in this analysis). A pulse-by-pulse increase in concentric potentiation was observed in the ISO-CON but was not present in the CON condition even though mean concentric potentiation did not differ between conditions.

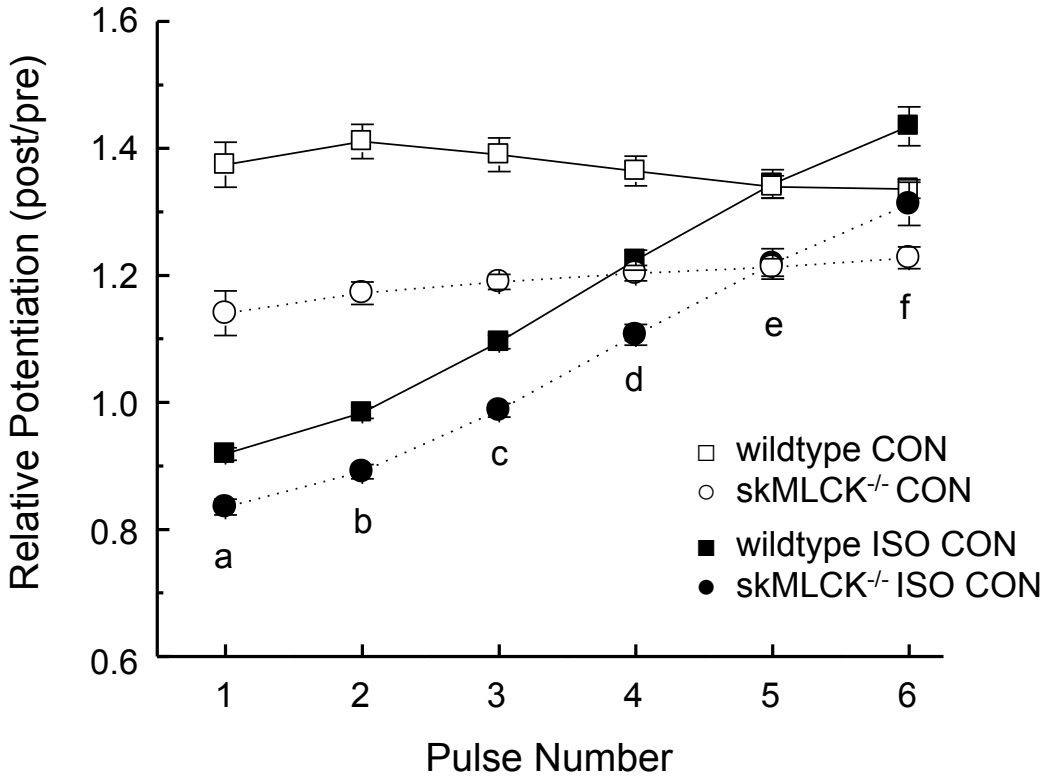


*Figure 5.7. Pulse by pulse potentiation in ISO-CON and CON conditions*

Plot of concentric force potentiation (post/pre) versus pulse number during the concentric (CON) and isometric and concentric (ISO-CON) conditions for wildtype and skMLCK$^{-/-}$ muscles. Wildtype values were greater than skMLCK$^{-/-}$ values independent of pulse number and condition but there was no interaction between genotype and pulse number or condition. However, there was a significant effect of pulse number in the ISO-CON condition for both genotypes.
$^{a,b,c,d,e,f}$ significant increase in potentiation with each succeeding pulse ($P < 0.05$)

*SkMLCK protein expression*

Protein blotting confirmed that skMLCK is not expressed in EDL muscles from our skMLCK$^{-/-}$ mice. The example blot shown in Figure 5.8 demonstrates a clear band of skMLCK protein at 70 kD in wildtype muscles that was absent in skMLCK$^{-/-}$ muscles.

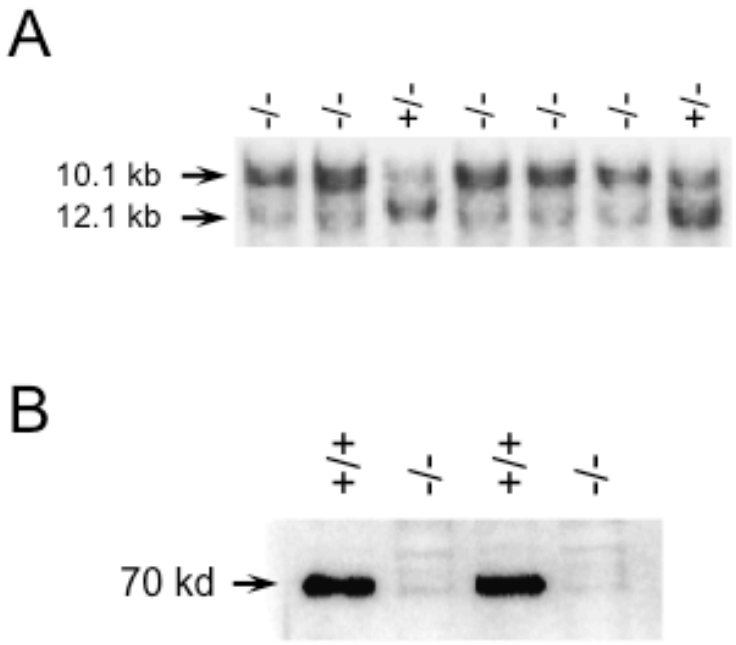


*Figure 5.8. Tail sample genotyping and protein expression*

(**A**) Southern blotting analysis of DNA extracted from tail samples to differentiate heterozygous ($^{+/-}$) from skMLCK$^{-/-}$ mice in our colony (see Zhi et al. 2005 for detailed methods). (**B**) Western blotting was conducted in whole muscle homogenates to demonstrate skMLCK expression in EDL muscle from wildtype ($^{+/+}$) and skMLCK$^{-/-}$ mice. Muscle tissue was sampled randomly from various litters to confirm the absence of skMLCK$^{-/-}$ in the colony. Arbitrary units of protein density are 9034.3 ± 430.0 and 23.8 ± 4.1 for wildtype and skMLCK$^{-/-}$ muscles, respectively ($n = 6$, $P < 0.05$). Consistent with previous work, these data indicate that skMLCK$^{-/-}$ muscles were mostly incapable of phosphorylating the regulatory light chain (Zhi et al. 2005).

## *Discussion*

The purpose of this study was to examine the force-dependence of potentiation in mouse skeletal muscles with and without the ability to phosphorylate the myosin RLC (wildtype and skMLCK$^{-/-}$, respectively). Although no effect of isometric force on mean concentric force was detected in either genotype, we did detect a novel form of force-dependence in that the relative magnitude of concentric potentiation covaried strongly with force in all conditions and in both genotypes. Consequently, although potentiation was always greater in wildtype than in skMLCK$^{-/-}$ muscles, the force-dependence of potentiation we observed was not dependent on RLC phosphorylation. The covariance of potentiation with force was consistent with a mediating influence of attached and force generating crossbridges on potentiation, one that may include a cooperative influence of attached crossbridges (Metzger et al. 1989).

### *Comparison of wildtype versus skMLCK$^{-/-}$ muscles*

By using muscles from wildtype and skMLCK$^{-/-}$ mice we were able to assess potentiation in muscles with and without skMLCK, respectively; an approach that allowed us to isolate the influence of RLC phosphorylation per se. Although we did not determine RLC phosphorylation, previous work has shown that tetanic stimulation similar to what we used increases RLC phosphorylation to 55% of maximal levels in wildtype muscles but does not increase this value in skMLCK$^{-/-}$ muscles (Gittings et al. 2011; Vandenboom et al. 2013). Previous work has uncoupled potentiation from RLC phosphorylation in rat skeletal muscle (MacIntosh et al. 2008; Rassier et al. 1997), thus the surprisingly large concentric force potentiation displayed by skMLCK$^{-/-}$ muscles in this study may have been due to a secondary mechanism, perhaps involving alterations in resting $Ca^{2+}$ (Smith et al. 2013). Further work is needed to establish the relative contribution of these respective mechanisms to potentiation, at least for concentric forces during unfused tetani. Finally, although skMLCK$^{-/-}$ muscles displayed significant concentric force potentiation, the magnitude of potentiation was always greater in wildtype muscles. In addition, although neither genotype displayed potentiation of peak isometric force, wildtype muscles displayed greater values than skMLCK$^{-/-}$ muscles (Figure 5.4, Panel C). Thus, skMLCK catalyzed phosphorylation of the RLC may be required for maximum levels of either force type in mouse EDL muscle.

*Force-dependence of potentiation*

A striking aspect of our results was the apparent dependence of potentiation magnitude on force both across different conditions and within potentiated contractions. For example, the data plotted in Figure 5.5 shows how relative potentiation (i.e., post/pre) varied with peak force ($P/P_o$) when the ISO, ISO–CON, and CON conditions are compared. The direct relationship between potentiation and force across these conditions seems to suggest that it was force level per se, and not force type (i.e., concentric vs. isometric), that mediates potentiation magnitude. This outcome is in fact consistent with previous studies showing that isometric twitch potentiation is inversely related to force levels under a variety of experimental conditions (Close and Hoh, 1968a; Krarup, 1981a, 1981b; Moore et al. 1990; Palmer and Moore, 1989; Vandenboom and Houston, 1996). Our results, however, extend these data by showing that the inverse relationship between potentiation and force also holds for concentric contractions studied using high-frequency stimulation rates. Moreover, our plots of instantaneous potentiation versus unpotentiated force reveal how concentric and (or) isometric potentiation level varies during tetanic stimulation independent of change to peak force levels. As an example of this, concentric force potentiation may be seen to vary approximately 180° out of phase with unpotentiated force in both the ISO-CON and CON conditions. This was generally true for both genotypes although the peak-to-peak variation in potentiation was greater for wildtype than for skMLCK$^{-/-}$ muscles. Importantly, these records also show that although peak isometric force was not potentiated, there was a significant potentiation of the isometric force rise in the ISO condition. This pattern is in fact consistent with the increased +dF/dt often reported for isometric contractions in response to high-frequency stimulation (Vandenboom et al. 1995). Interestingly, the reverse pattern was observed in the CON condition where the absence of increase in instantaneous potentiation at stimulation onset in both genotypes accords with the lack of increase in concentric +dF/dt that we observed (also Grange et al. 1995).

Perhaps the most compelling evidence for a crossbridge-mediated influence on potentiation magnitude, however, was the strong, negative correlation we found between instantaneous potentiation and unpotentiated force. In general terms, these correlations may suggest a rapid feedback mechanism between the population of attached, force-generating crossbridges and potentiation magnitude. Although the mechanistic link is not

known, cooperative influences between thick and thin filament proteins seem the probable route (Metzger et al. 1989). Further, because no distinctions were present between genotypes, this apparent force dependence for potentiation may occur independently of skMLCK-catalyzed phosphorylation of the RLC. Models for crossbridge action accounting for a crossbridge influence on isometric and/or concentric potentiation exist (Sweeney et al. 1993; Vandenboom et al. 2013), but the precise contribution of cooperative mechanisms to these models remains unknown.

*Cooperative influences*

An important assumption of the present work was that by comparing concentric forces in the ISO-CON and CON conditions, we were able to compare the magnitude of potentiation when force levels were similar. It is not possible to assay thin filament activation in an intact skeletal muscle preparation but an influence of attached crossbridges on thin filament activation has been detected in permeabilized (Morris et al. 2001; Swartz and Moss, 1992; Swartz et al. 1996) and intact vertebrate skeletal fibres (Vandenboom et al. 1998; Zot and Potter, 1989). Paramount in this scenario is that although $Ca^{2+}$ binding to TnC regulates force development, cooperative interactions between cycling crossbridges and regulatory proteins may be required to fully activate the contractile apparatus (McKillop and Geeves, 1993; Maytum et al. 1999; Lehrer, 2011). Recent modeling work suggests that this effect may be accomplished via a flexible link between troponin and tropomyosin (Mijailovich et al. 2012). As we did not detect any differences in mean force potentiation between the ISO-CON and CON conditions, we must reject the hypothesis that cooperative interactions within the contractile apparatus influences potentiation, at least in the context of our experimental model. On the other hand, we did observe a pulse-by-pulse increase in concentric force potentiation in the ISO-CON but not the CON condition, despite similar mean potentiation in both conditions. We believe that the increase in potentiation with pulse number in the ISO-CON condition is generally consistent with the force dependence of potentiation, where unpotentiated force was declining as opposed to steady in the ISO-CON versus CON conditions, respectively, and there is no reason to invoke any interactions with the cooperative activation of the thin filament.

*Force kinetics*

RLC phosphorylation has been associated with enhanced isometric force development rate of mouse skeletal muscle (Vandenboom et al. 1995). The isometric +dF/dt was increased more in wildtype than in skMLCK$^{-/-}$ muscles; however, this parameter was increased in both genotypes by the tetanic PS (Table 5.2). Moreover, Smith et al. (2013) showed increases in isometric twitch +dF/dt of mouse lumbrical muscle without RLC phosphorylation, suggesting additional mechanisms may contribute to this change. In contrast, the absence of change to concentric +dF/dt in both genotypes is consistent with the data of Grange et al. (1995) for after-loaded twitch contractions. In addition, although RLC phosphorylation is associated with a slowed relaxation rate from high force levels in both cat and mouse muscle *in vitro* (Brown and Loeb, 1999; Gittings et al. 2011) as well as permeabilized rabbit psoas skeletal fibres (Patel et al. 1998), we did not observe this effect (Table 5.2). An explanation for this outcome is that the force levels produced by 60 Hz of stimulation may have been too low to induce this particular response. Interestingly, however, a very large and dynamic increase in potentiation was observed coincident with relaxation in the ISO-CON and CON conditions in both genotypes (Figure 5.6). This effect was also observed during relaxation from the ISO condition in skMLCK$^{-/-}$ but not wildtype muscles. Although the reasons for these increases are unknown they are consistent with the idea that potentiation magnitude varies with existing force level.

*Functional implications*

Force dependence for potentiation may have important ramifications for muscle function *in vivo*. If our results may be extrapolated to locomotor function of fast twitch skeletal muscle *in vivo*, changes in contraction type and force level during the stretch-shortening cycle (e.g., Johnston and Altringham, 1988) will produce large variations in instantaneous potentiation magnitude as, in a potentiated muscle fibre, low force output will be enhanced to a much greater degree than high force.

### *Limitations*

We did not actively monitor sarcomere length and thus cannot account for the possible contribution of nonuniformities in sarcomere length, known to occur during loaded shortening (Julian and Morgan, 1979). Similarly, complications because of differences in series elastic component length between conditions on our results cannot completely be ruled out, particularly in the ISO-CON condition. It would, however, be surprising if these factors accounted for any differences in contractile performance between wildtype and skMLCK$^{-/-}$ muscles. Although this was a mechanical study and we did not assay muscle metabolites, we observed little or no fatigue across conditions, which suggests that neither metabolite accumulation nor depletion was likely to have greatly influenced our results.

### *Summary*

We found that peak concentric, but not peak isometric, forces can be potentiated in mouse EDL muscles without the skMLCK enzyme. However, because concentric force potentiation of skMLCK$^{-/-}$ muscles was approximately 50% of that observed in wildtype muscles, RLC phosphorylation was required for maximal potentiation. Moreover, because the concentric force potentiation observed in wildtype and skMLCK$^{-/-}$ muscles was force dependent, this dependence does not necessarily require RLC phosphorylation. Although previous models describing the influence of cycling crossbridges on potentiation do not include a cooperative component, cooperative interactions between thick and thin filaments may mediate, at least in part, the force-dependence of potentiation.

### *Acknowledgements*

This study was supported by funds provided by the Natural Sciences and Engineering Research Council of Canada (R.V.). We thank Dr. David Gabriel for help with data analysis.

### *Disclosures*

The authors do not have any conflicting interests regarding the findings or interpretations of this manuscript.

## *References*


Brown, I.E., and Loeb, G.E. 1999. Measured and modeled properties of mammalian skeletal muscle. I. The effects of post-activation potentiation on the time course and velocity dependencies of force production. J. Muscle Res. Cell Motil. 20: 443–456. PMID: 10555063.

Caterini, D., Gittings, W., Huang, J., and Vandenboom, R. 2011. The effect of work cycle frequency on the potentiation of dynamic force in fast twitch mouse muscle. J. Exp. Biol. 214: 3915–3923. doi:10.1242/jeb.061150. PMID:22071182.

Close, R., and Hoh, J.F. 1968*a*. Influence of temperature on isometric contractions of rat skeletal muscles. Nature, 217(5134): 1179–1180. doi:10.1038/ 2171179a0. PMID:5643098.

Close, R., and Hoh, J.F. 1968*b*. The after-effects of repetitive stimulation on the isometric twitch contraction of rat fast skeletal muscle. J. Physiol. 197: 461– 477. PMID:5716854.

Geeves, M.A., and Holmes, K.C. 2005. The molecular mechanism of muscle con- traction. Adv. Protein Chem. 71: 161–193. doi:10.1016/S0065-3233(04)71005-0. PMID:16230112.

Gittings, W., Huang, J., Smith, I.C., Quadrilatero, J., and Vandenboom, R. 2011. The effect of skeletal myosin light chain kinase gene ablation on the fatigability of mouse fast muscle. J. Muscle Res. Cell Motil. 31: 337–348. doi:10.1007/ s10974-011-9239-8. PMID:21298329.

Gittings, W., Huang, J., and Vandenboom, R. 2012. Tetanic force potentiation of mouse fast muscle is shortening speed dependent. J. Muscle Res. Cell Motil. 33(5): 359–368. doi:10.1007/s10974-012-9325-6. PMID:23054096.

Gordon, A.M., Homsher, E., and Regnier, M. 2000. Regulation of contraction in striated muscle. Physiol. Rev. 80: 853–924. PMID:10747208.

Grange, R.W., Cory, C.R., Vandenboom, R., and Houston, M.E. 1995. Myosin phosphorylation augments the force-displacement and force-velocity relationships of mouse fast muscle. Am. J. Physiol. 269: C713–C724. PMID: 7573402.

Johnston, I., and Altringham, J. 1988. Muscle function in locomotion. Nature, 335(6193): 767–768. doi:10.1038/335767a0. PMID:3185706.

Julian, F.J., and Morgan, D.L. 1979. The effect on tension of nonuniform distribution of length changes applied to frog muscle fibres. J. Physiol. 293: 379– 392. PMID:315465.

Klug, G.A., Botterman, B.R., and Stull, J.T. 1982. The effect of low frequency stimulation on myosin light chain phosphorylation in skeletal muscle. J. Biol. Chem. 257: 4688–4690. PMID:7068657.

Krarup, C. 1981*a* Temperature dependence of enhancement and diminution of tension evoked by staircase and by tetanus in rat muscle. J. Physiol. 311: 373–387. PMID:7264973.

Krarup, C. 1981*b*. The effect of dantrolene on the enhancement and diminution of tension evoked by staircase and by tetanus in rat muscle. J. Physiol. 311: 389–400. PMID:7264974.

Lännergren, J., Bruton, J.D., and Westerblad, H. 2000. Vacuole formation in fatigued skeletal muscle fibres from frog and mouse: effects of extracellular lactate. J. Physiol. 526(3): 597–611. doi:10.1111/j.1469-7793.2000.00597.x. PMID: 10922011.

Lehrer, S.S. 2011. The 3-state model of muscle regulation revisited: is a fourth state involved? J. Muscle Res. Cell Motil. 32: 203–208. doi:10.1007/s10974-011- 9263-8. PMID:21948173.

MacIntosh, B.R., and Willis, J.C. 2000. Force-frequency relationship and potentiation in mammalian skeletal muscle. J. Appl. Physiol. 88(6): 2088–2096. PMID:10846022.

MacIntosh, B.R., Smith, M.J., and Rassier, D.E. 2008*a*. Staircase but not posttetanic potentiation in rat muscle after spinal cord hemisection. Muscle Nerve, 38(5): 1455–1465. doi:10.1002/mus.21096. PMID:18932208.

MacIntosh, B.R., Taub, E.C., Dormer, G.N., and Tomaras, E.K. 2008*b*. Potentiation of isometric and isotonic contractions during high-frequency stimulation. Pflugers Arch. 456: 449–458. doi:10.1007/s00424-007-0374-4. PMID:18004591.

Manning, D.R., and Stull, J.T. 1979. Myosin light chain phosphorylation and phosphorylase A activity in rat extensor digitorum longus muscle. Biochem. Biophys. Res. Commun. 90(1): 164–170. doi:10.1016/0006-291X(79)91604-8. PMID: 496969.

Manning, D.R., and Stull, J.T. 1982. Myosin light chain phosphorylation- dephosphorylation in mammalian skeletal muscle. Am. J. Physiol. 242: C234–C241. PMID:7065172.

Maytum, R., Lehrer, S.S., and Geeves, M.A. 1999. Cooperativity and switching within the three-state model of muscle regulation. Biochemistry, 38(3): 1102– 1110. doi:10.1021/bi981603e. PMID:9894007.

McKillop, D.F., and Geeves, M.A. 1993. Regulation of the interaction between actin and myosin subfragment 1: evidence for three states of the thin filament. Biophys. J. 65(2): 693–701. doi:10.1016/S0006-3495(93)81110-X. PMID: 8218897.

Metzger, J.M., Greaser, M.L., and Moss, R.L. 1989. Variations in cross-bridge attachment rate and tension with phosphorylation of myosin in mammalian skinned skeletal muscle fibres. J. Gen. Physiol. 93: 855 – 883. doi:10.1085/jgp. 93.5.855. PMID:2661721.

Mijailovich, S.M., Kayser-Herold, O., Li, X., Griffiths, H., and Geeves, M.A. 2012. Cooperative regulation of myosin-S1 binding to actin filaments by a continuous flexible Tm-Tn chain. Eur. Biophys. J. 41(12): 1015–1032. doi:10.1007/ s00249-012-0859-8. PMID:23052974.

Moore, R.L., and Stull, J.T. 1984. Myosin light chain phosphorylation in fast and slow skeletal muscles in situ. Am. J. Physiol. Cell Physiol. 247(5): C462–C471.

Moore, R.L., Palmer, B.L., Williams, S.L., Tanabe, H., Grange, R.W., and Houston, M.E. 1990. Effect of temperature on myosin phosphorylation in mouse skeletal muscle. Am. J. Physiol. 259: C432–C438.

Morris, C.A., Tobacman, L.S., and Homsher, E. 2001. Modulation of contractile activation in skeletal muscle by a calcium-insensitive troponin C mutant. J.Biol. Chem. 276: 20245–20251. doi:10.1074/jbc.M007371200. PMID:11262388.

Nelson-Wong, E., Howarth, S., Winter, D.A., and Callaghan, J.P. 2009. Application of autocorrelation and cross-correlation analyses in human movement and rehabilitation research. J. Orthop. Sports Phys. Ther. 39(4): 287–295.doi:10.2519/jospt.2009.2969. PMID:19346626.

Palmer, B.M., and Moore, R.L. 1989. Myosin light chain phosphorylation and tension potentiation in mouse skeletal muscle. Am. J. Physiol. 257: C1012–C1019.

Patel, J.R., Diffee, G.M., Huang, X.P., and Moss, R.L. 1998. Phosphorylation of myosin regulatory light chain eliminates force-dependent changes in relaxation rates in skeletal muscle. Biophys. J. 74: 360–368. doi:10.1016/S0006- 3495(98)77793-8. PMID:9449336.

Persechini, A., Stull, J.T., and Cooke, R. 1985. The effect of myosin phosphorylation on the contractile properties of skinned rabbit skeletal muscle fibres. J. Biol. Chem. 260: 7951–7954. PMID:3839239.

Rassier, D.E., Tubman, L.A., and MacIntosh, B.R. 1997*a*. Length-dependent potentiation and myosin light chain phosphorylation in rat gastrocnemius muscle. Am. J. Physiol. 273(1): C198–C204.

Rassier, D.E., Tubman, L.A., and MacIntosh, B.R. 1997*b*. Staircase in mammalian muscle without light chain phosphorylation. Braz. J. Med Biol. Res 32(1): 121–129. PMID:10347779.

Ryder, J.W., Lau, K.S., Kamm, K.E., and Stull, J.T. 2007. Enhanced skeletal muscle contraction with myosin light chain phosphorylation by a calmodulin- sensing kinase. J. Biol. Chem. 282: 20447–20454. doi:10.1074/jbc.M702927200. PMID:17504755.

Smith, I.C., Gittings, W., Bloemberg, D., Huang, J., Quadrilatero, J., Tupling, A.R., and Vandenboom, R. 2013. Potentiation in mouse lumbrical muscle without myosin light chain phosphorylation: is resting calcium responsible? J. Gen. Physiol. 141(3): 297–308. doi:10.1085/jgp.201210918. PMID:23401574.

Stull, J.T., Kamm, K.E., and Vandenboom, R. 2011. Myosin light chain kinase and the role of myosin light chain phosphorylation in skeletal muscle. Arch. Biochem. Biophys. 510: 120–128. doi:10.1016/j.abb.2011.01.017. PMID: 21284933.

Swartz, D.R., and Moss, R.L. 1992. Influence of a strong-binding myosin analogue on calcium-sensitive mechanical properties of skinned skeletal muscle fibres. J. Biol. Chem. 267: 20497–20506. PMID:1400367.

Swartz, D.R., Moss, R.L., and Greaser, M. 1996. Calcium alone does not fully activate the thin filament for S1 binding to rigor myofibrils. Biophys. J. 71: 1891–1904. doi:10.1016/S0006-3495(96)79388-8. PMID:8889164.

Sweeney, H.L., and Kushmerick, M.J. 1985. Myosin phosphorylation in permeabilized rabbit psoas fibers. Am. J. Physiol. 249(3 Pt 1): C362–C365. PMID: 4037077.

Sweeney, H.L., and Stull, J.T. 1986. Phosphorylation of myosin in permeabilized mammalian cardiac and skeletal muscle cells. Am. J. Physiol. 250(4 Pt 1): C657–C660. PMID:3754389.

Sweeney, H.L., and Stull, J.T. 1990. Alteration of cross-bridge kinetics by myosin light chain phosphorylation in rabbit skeletal muscle: implications for regulation of actin-myosin interaction. Proc. Natl. Acad. Sci. U.S.A. 87: 414–418. doi:10.1073/pnas.87.1.414. PMID:2136951.

Sweeney, H.L., Bowman, B.F., and Stull, J.T. 1993. Myosin light chain phosphorylation in vertebrate striated muscle: regulation and function. Am. J. Physiol. 264: C1085–C1095. PMID: 8388631.

Vandenboom, R., and Houston, M.E. 1996. Phosphorylation of myosin and twitch potentiation in fatigued skeletal muscle. Can. J. Physiol. Pharmacol. 74(12): 1315–1321. doi:10.1139/y96-144. PMID:9047041.

Vandenboom, R., Grange, R.W., and Houston, M.E. 1993. Threshold for force potentiation associated with skeletal myosin phosphorylation. Am. J. Physiol. 265: C1456–C1462. PMID:8279509.

Vandenboom, R., Grange, R.W., and Houston, M.E. 1995. Myosin phosphorylation enhances rate of force development in fast-twitch skeletal muscle. Am. J. Physiol. 268: C596–C603. PMID:7900767.

Vandenboom, R., Xeni, J., Bestic, M., and Houston, M.E. 1997. Increased force development rates of fatigued skeletal muscle are graded to myosin light chain phosphate content. Am. J. Physiol. 272: R1980–R1984. PMID:9227617.

Vandenboom, R., Claflin, D.R., and Julian, F.J. 1998. Effects of rapid shortening on rate of force regeneration and myoplasmic [$Ca^{2+}$] in intact frog skeletal muscle fibres. J. Physiol. 511: 171–180. doi:10.1111/j.1469-7793.1998.171bi.x. PMID:9679172.

Vandenboom, R., Gittings, W., Smith, I.C., Grange, R.W., and Stull, J.T. 2013. Myosin phosphorylation and force potentiation in skeletal muscle: evidence from animal models. J. Musc. Res. Cell Motil. 34: 317–332. doi:10.1007/s10974- 013-9363-8.

Xeni, J., Gittings, W., Caterini, D., Huang, J., Houston, M.E., Grange, R.W., and Vandenboom, R. 2011. Myosin light chain phosphorylation and potentiation of dynamic function in mouse fast muscle. Pflugers Archiv. 362: 349–358. doi:10.1007/s00424-011-0965-y. PMID:21499697.

Zhi, G., Ryder, J.W., Huang, J., Ding, P., Chen, Y., Zhao, Y., Kamm, K.E., and Stull, J.T. 2005. Myosin light chain kinase and myosin phosphorylation effect frequency-dependent potentiation of skeletal muscle contraction. Proc. Natl. Acad. Sci. U.S.A. 102: 17519–17524. doi:10.1073/pnas.0506846102. PMID:16299103.

Zot, A.S., and Potter, J.D. 1989. Reciprocal coupling between troponin C and myosin crossbridge attachment. Biochemistry, 28(16): 6751–6756. doi:10.1021/ bi00442a031. PMID:2790028.

# Chapter 6

## Study #3

**Genotype specific interaction of posttetanic potentiation and the catchlike property in mouse skeletal muscle with and without RLC phosphorylation**

Author List: William Gittings, Jordan Bunda, James T. Stull, and Rene Vandenboom

As published in: Under review by *Muscle & Nerve* (Submitted June 2015)

**Author contributions:**

*William Gittings*: study design, data collection and experimentation, manuscript writing

*Jordan Bunda*: assistance with myosin RLC phosphorylation analysis

*Dr. James T. Stull*: skMLCK$^{-/-}$ mice breeding pairs, technical assistance

*Dr. Rene Vandenboom*: study design input, funding (NSERC), manuscript writing

## *Abstract*

Running head: Catchlike property and posttetanic potentiation

***Introduction*:** Posttetanic potentiation (PTP) and the catchlike property (CLP) enhance contractile function in skeletal muscle. We investigated the CLP during dynamic performance in mouse hindlimb muscles with (wildtype) and without (skMLCK$^{-/-}$) the primary mechanism for PTP (myosin phosphorylation) (in vitro, 25ºC).
***Methods***: EDL muscles of both genotypes were stimulated with constant-frequency and catchlike trains (CFT and CLT), before and after a potentiating stimulus (PS).
***Results***: Before the PS, the CLT increased concentric force/work relative to the CFT but this effect was greater for skMLCK$^{-/-}$ than wildtype muscles. After the PS, the catchlike effect was reduced in wildtype muscles but unchanged in skMLCK$^{-/-}$ muscles that did not display PTP. ***Discussion***: These data suggest that PTP interferes with the CLP during concentric force development at moderate speeds of shortening. We conclude that the physiological utility of each mechanism and their interactions provide important modulations to fast skeletal muscle function.

Keywords: myosin phosphorylation, regulatory light chain, myosin light chain kinase knockout, catchlike property, potentiation

## *Introduction*

Burke and colleagues were the first to report on the effect that closely spaced stimulus pulses (i.e. < 10 ms) known as *doublets* had on increasing force relative to constant frequency stimulation in cat triceps surae muscle (Burke et al, 1970). This example of the so-called 'catchlike property' (CLP) has since been demonstrated in a variety of human (Desmedt and Godaux, 1977) and animal (e.g., rat, cat and mouse) skeletal muscles, where it augments either isometric or dynamic (i.e. isotonic or concentric) force responses (Abbate et al, 2000; Binder-Macleod and Barrish, 1992; Burke et al, 1976; Sandercock and Heckman, 1997). Although the influence of the CLP is reported to be greater for slow than for fast twitch skeletal muscles it may represent a ubiquitous property of the intact mammalian neuromuscular system; doublets and triplets have been observed during movement in both humans and in rats (Griffin et al, 1998; Hennig and Lomo, 1985). It is unclear, however, whether these represent functional motor patterns or spontaneous "errors" in neuromuscular transmission (Garland and Griffin, 1999).

Although well documented for fast and slow skeletal muscle of animals as well as the more mixed muscle types of humans, the mechanism for the CLP is still not understood. Work by Burke et al (1976) demonstrated that the CLP is an inherent property of the skeletal muscle cell and not due to changes in motoneuron excitability or transmission at the neuromuscular junction. One mechanism that has been proposed for the CLP is that the arrival of closely spaced pulses at the onset of stimulation may rapidly stretch the series elastic component to increase muscle stiffness compared to constant frequency stimulation, a change that might increase the transmission of mechanical force along or between sarcomeres Binder-Mcleod and Barrish, 1992; Burke et al, 1976; Nielson, 2009; Parmiggiani and Stein, 1981). An alternate hypothesis is that closely spaced pulses at the onset of stimulation augments intracellular $Ca^{2+}$ levels above that experienced during constant frequency stimulation (Duchateau and Hainaut, 1986), a change which would be expected to increase force by promoting thin filament activation and thus cross-bridge recruitment (Abbate et al, 2002). In principal, both of these hypotheses could be expected to increase both the rate and extent of force development as well as perhaps the maintenance of force associated with the CLP. Interestingly, although the SEC hypothesis is largely untested, attempts to verify the altered [$Ca^{2+}$] hypothesis

have failed to detect prolonged changes in intracellular $Ca^{2+}$ in single intact frog skeletal muscle fibres (Abbate et al, 2002). As a result, although the influence of the CLP is not in question, the precise intracellular mechanism remains unresolved.

An interesting aspect of the CLP is that it may interact with other modulations of contractile function displayed by skeletal muscles of different animals. For example, the CLP has been shown to be greater in fatigued than unfatigued turtle muscle (Callister et al, 2003). In addition, the CLP has been shown to interact with posttetanic potentiation (PTP), the increase in twitch or low frequency force output observed following high frequency stimulation (Connolly et al, 1971). For example, the effects of the potentiation influence may sometimes mimic that of the CLP (Abbate et al, 2000). Thus, although often studied separately, the CLP and PTP may occur simultaneously and thus may interact to modulate muscle contractility *in vivo*. An interaction between CLP and PTP was first demonstrated by Burke and colleagues, who showed that PTP blunted the influence of the CLP in cat gastrocnemius muscle *in situ* (Burke et al, 1976). Similarly, Ding et al. (2003) showed a negative linear relationship between the magnitude of the CLP and potentiation in human quadriceps muscle. These authors speculated that the decreased effectiveness of the CLP in the potentiated versus unpotentiated state was due to some interaction between increases in the $Ca^{2+}$ activation of the contractile apparatus and the increased $Ca^{2+}$ sensitivity mediated by myosin RLC phosphorylation.

A major limitation of previous studies examining the interaction of PTP with the CLP is the inherent difficulty in parsing out the concurrent influence of these respective phenomena. Thus, the purpose of the present study was to investigate the interaction between PTP and the CLP on concentric force/work enhancement in mouse hindlimb muscles from wildtype and myosin light chain kinase deficient mice ($skMLCK^{-/-}$); muscles phenotypes with and without the ability to phosphorylate the RLC and display PTP (Gittings et al, 2011; Zhi et al, 2005). Because these mechanisms operate concurrently in fast twitch skeletal muscle we hypothesized that interactions between the two outcomes would mitigate or attenuate the CLP in wildtype but not in $skMLCK^{-/-}$ muscle. Our results may have implications for understanding the functional roles of these intrinsic muscle properties.

## *Methods*

*In vitro muscle preparation and experimental setup*

Protocols and techniques utilized during the animal phase of the experiments received ethical approval from the Brock University Animal Care Committee. Adult wildtype C57BL/6 mice (20-30g) were purchased from Charles River (St. Constant, QC) and were housed at the Brock University Comparative Bioscience Facility for at least one week before entering the study. Similarly aged skMLCK$^{-/-}$ mice were obtained as needed from our own breeding colony at Brock University: details of the breeding and characterization of these knockout animals has been presented previously (Gittings et al, 2015; Zhi et al, 2005). Muscles from wildtype and skMLCK$^{-/-}$ animals were subjected to identical experiments, with the later serving as an experimental control, allowing us to study the interaction between the concentric force increase caused by the catchlike property with the concentric force enhancement caused by myosin RLC phosphorylation.

Animals were initially anaesthetized with a peritoneal injection of sodium pentobarbitol (60 mg/kg body weight). The extensor digitorum longus (EDL) muscles were surgically removed from both hindlimbs; the first was immediately mounted for experimentation while the second was incubated at resting length in an oxygenated bath containing cooled Tyrode's solution (~5-10°C) until needed. For contractile experiments, muscles were suspended in a vertical organ bath using non-compliant 4-0 silk suture- the distal suture was clamped directly to the electrode assembly and the proximal suture was secured to the servomotor arm via a short stainless steel wire. Contractile experiments were conducted at 25° C with the muscle immersed in continuously gassed (95% $O_2$, 5% $CO_2$) Tyrode's solution (Lännergren et al, 2000).

All experimental procedures were conducted under software control (600A Aurora Scientific Inc., Aurora, ON). Muscle stimulation was applied using flanking platinum electrodes at a voltage set to ~1.25 times the threshold required to elicit maximal twitch force. Muscle length control and force data measurement were conducted using a dual-mode servomotor (Model 305B, Aurora Scientific Inc., Aurora, ON). Initial muscle length (mm) at optimal length for maximal twitch force ($L_o$) was measured using a horizontal stereo zoom microscope and all subsequent length ramp parameters were normalized to $L_o$. Contractile data was collected at 2000 Hz and saved to the hard drive for later analysis.

*Experimental timeline and contractile experiments*

EDL muscles were incubated for 30 minutes prior to contractile experiments- during this equilibration period a single twitch was elicited every 3 minutes to track viability by confirming a stable force response. Optimal length ($L_o$) for maximal isometric twitch force was determined prior to the initiation of the main contractile experiment.

PTP was induced using a high frequency potentiating stimulus (PS) known to increase myosin RLC phosphorylation while inducing less than 10% fatigue (four 100 Hz, 400ms tetani in 10 s)(Zhi et al, 2005, Gittings et al, 2012). Importantly, muscles from skMLCK$^{-/-}$ animals do not demonstrate an increase in myosin RLC phosphate content following this regime of activation (Gittings et al, 2011). To quantify the effect of PTP on contractile function, identical stimulation protocols were always elicited before and after the PS to calculate the relative change (i.e. post/pre).

The catchlike property (CLP) was measured by comparing the contractile response of two stimulation protocols: the constant frequency train (CFT) and the catchlike train (CLT). The CFT consisted of a 200 ms stimulus at 32 Hz. The CLT stimulus was identical to the CFT except for a single additional pulse that was elicited at the onset of the train (the inter-pulse interval of the initial doublet was 10 ms). To quantify the catchlike effect, the relative difference in contractile parameters between the CFT and the CLT was calculated (i.e. CLT/CFT).

All stimulation protocols were elicited during fixed-amplitude ramps where length was shortened from 1.10 to 0.85 $L_o$ at a constant velocity equivalent to 0.25 of maximal shortening velocity ($V_{max}$) for mouse EDL muscles (Brooks and Faulkner, 1988; Gittings et al, 2011). Stimulation was applied during muscle shortening (10 ms after the initiation of the length ramp) and force relaxation occurred prior to the completion of the length ramp. Consequently, force development occurred at ~1.08 $L_o$ and peak force was generally reached coincident with the muscle crossing its optimal length. Immediately prior to each stimulus event, an identical shortening ramp was conducted without stimulation to determine the passive (non-contractile) force response of the muscle for data analysis purposes (see Contractile data analysis for details).

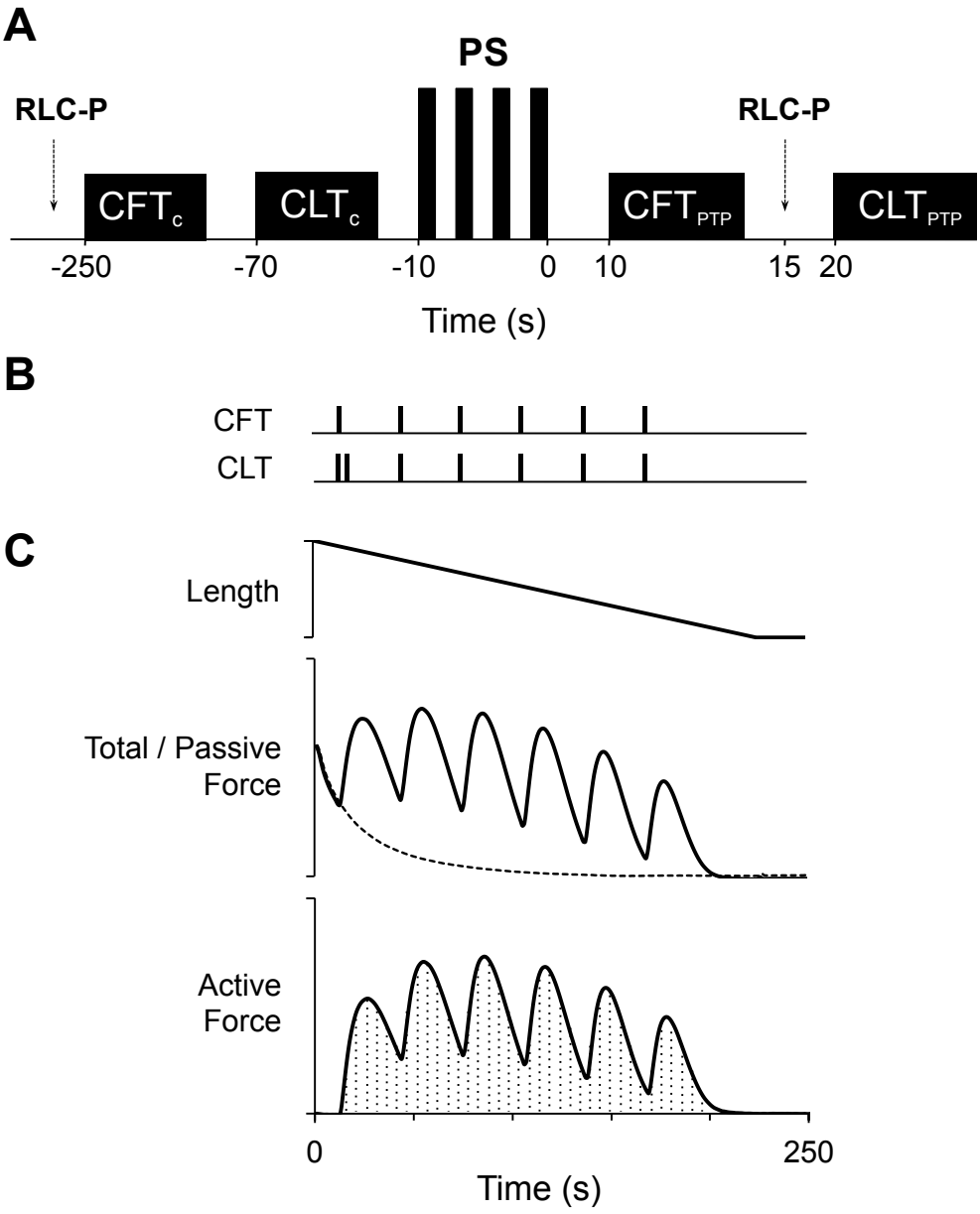


*Figure 6.1. Experimental timeline and representative length/force traces*

(**A**) Experimental timeline for quantifying posttetanic potentiation (PTP) and the catchlike property (CLP) in mouse EDL muscles. A constant frequency train (*CFT*) and catchlike train (*CLT*) were elicited before and after a potentiating stimulus (PS). In parallel experiments, muscles were frozen prior to stimulation and 15 s after the cessation of the PS for determination of myosin RLC phosphorylation. PTP and the CLP were determined as the relative change in force/work between paired responses (i.e. *PTP/C* and *CLT/CFT*, respectively). (**B**) Stimulus patterns (200ms): *CFT* – 32Hz, *CLT* – 32Hz + additional pulse (10 ms inter-pulse interval). (**C**) Length and force traces during ramp shortening at 25% of maximal shortening velocity. A*ctive force* traces were calculated by subtracting *passive force* traces from *total force* traces. Contractile parameters were sampled from the active force-time trace (shaded area represents work performed).

The experimental timeline and details are shown in Figure 6.1. In each experiment, the CFT and CLT were both elicited prior to and following the PS. Importantly, the sequence of these protocols was alternated between experiments to avoid any possible order effect (note: the order was held constant within each experiment). The unpotentiated (*control*) CFT and CLT responses were separated by 3 minutes to avoid the possible effect(s) of potentiation/fatigue; however, both stimulation protocols occurred in short succession after the PS to coincide with the time at which PTP is maximal (10-20s)(Gittings et al, 2011). As we alternated the order of the control conditions (Pre-PS) and the potentiated responses that followed the PS between experiments, and conducted identical experiments in both genotypes, we assume that any observed differences in PTP are attributable to the PS and not the experimental design itself.

*Contractile data analysis*

The raw (total) and passive force traces for each stimulus protocol were used to calculate the active force response of the muscle. Active forces were obtained by subtracting the passive force response from the matching total force response as previously described (Gittings et al, 2012; Gittings et al, 2015). Peak force (mN) was calculated as the highest active force value reached during the stimulus period regardless of timing. Mechanical work ($J \bullet kg^{-1}$) was determined by calculating the integral of the force-displacement plot for each stimulus period and was normalized to muscle wet mass. Values representing the kinetics of force development and relaxation were sampled from the first derivative function ($dP/dt$) of the active force trace, expressed in $mN \bullet s^{-1}$. The greatest positive and negative values during the stimulus period were used to describe the maximal rate of force development ($+dP/dt$) and maximal rate of force relaxation ($-dP/dt$), respectively.

*Fusion Index (FuI)*

The first and last pulses during each unfused tetanic force record were analyzed to determine the Fusion Index (FuI), a measure that quantifies the level of summation during the onset and cessation of the stimulus (Celichowski and Grottel, 1995; Krutki et al, 2008). The method for calculation of FuI is explained in Figure 6.2, and represents the ratio of the lowest inter-pulse force reached to the maximum force attained during the first and last pulse of each stimulus train ($FuI_i$ and $FuI_f$, respectively). FuI was used as an objective measure to explore the relationship between changes in force kinetics via

PTP/CLP and the modulation of muscle work via summation, as well as to compare how the observed effects may have differed over the course of the stimulus.

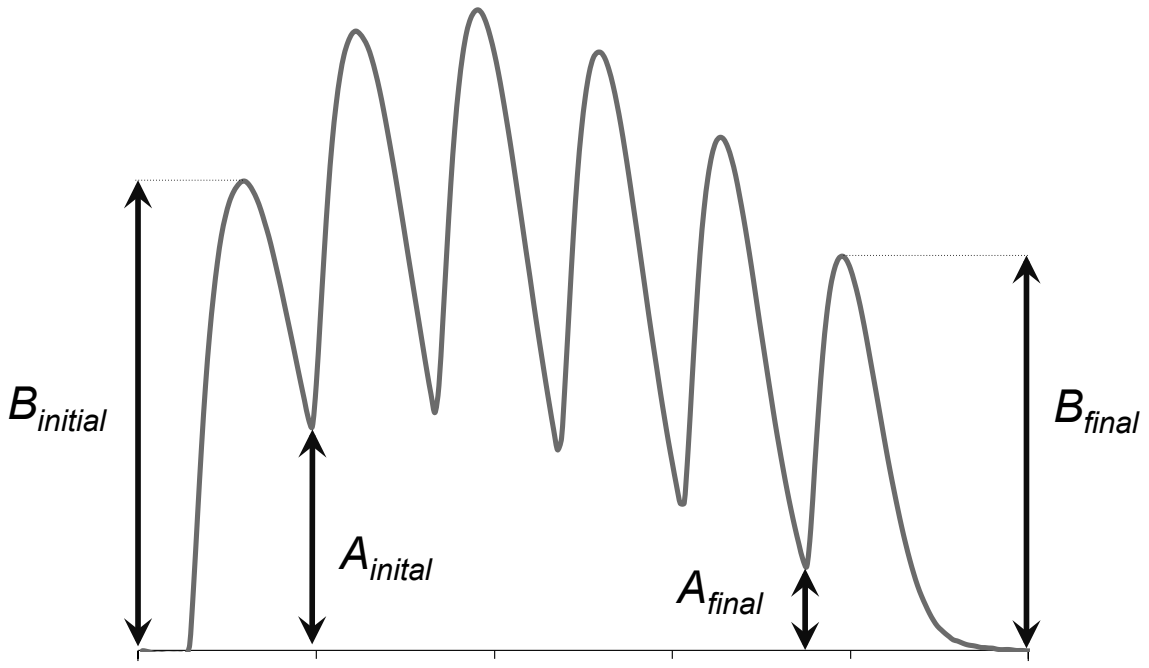


*Figure 6.2. Method for calculation of initial and final Fusion Index (FuI) during unfused tetanic force traces.*

FuI is the ratio of the lowest force reached during interpulse relaxation to the maximal force attained during the first (initial) and last (final) pulse of the stimulus train (Celichowski and Grottel, 1995; Krutki et al, 2008), and is intended to describe the general manifestation of changes in force kinetics and summation caused by CLP and PTP. Initial Fusion Index ($FuI_i = A_{inital} / B_{initial}$), Final Fusion Index ($FuI_f = A_{final} / B_{final}$).

*Myosin RLC phosphorylation analysis*

Parallel experiments were conducted to determine the myosin RLC phosphate content of wildtype and skMLCK$^{-/-}$ EDL muscles sampled prior to and 15s following the PS to coincide with control and potentiated contractile responses. Muscles were frozen in liquid nitrogen-cooled tongs and stored at -80°C until needed. Myosin RLC phosphorylation analysis was conducted using urea-glycerol PAGE as previously described (Zhi et al, 2005).

*Statistical analysis*

Significant differences between the various responses were evaluated with a repeated measures ANOVA, using absolute and relative contractile parameters (peak force, work, force kinetics, and Fusion Index) as dependent variables, genotype as a between factor (i.e. wildtype vs. skMLCK$^{-/-}$), and CLP and PTP as within factors (i.e. CFT vs. CLT, and control vs. potentiated, respectively). A two-way ANOVA was used to test for differences in myosin RLC phosphorylation levels between wildtype and skMLCK$^{-/-}$ groups of unstimulated and stimulated muscles. Post hoc analysis using the Šidák correction was used to identify significant differences between genotypes and within each genotype for repeated contractile measures ($P < 0.05$). All results are reported as Mean ± SEM.

## *Results*

In this study we examined the interaction of PTP and the CLP in muscles with and without the ability to phosphorylate the myosin RLC (wildtype and skMLCK$^{-/-}$ muscles, respectively). We compared the influence of stimulus paradigms that included a doublet versus one that did not (CLT and CFT, respectively), both before and after a tetanic potentiating stimulus (control and PTP, respectively). Because these four conditions were repeated in both wildtype and skMLCK$^{-/-}$ muscles we were able to determine the influence of RLC phosphorylation mediated force potentiation on the CLP. Raw data from all conditions and both genotypes are presented in Table 6.1.

*Influence of the CLP in wildtype and skMLCK$^{-/-}$ muscles*

A representative example of the influence of an initial doublet at the onset of stimulation on control (unpotentiated) concentric responses for wildtype and skMLCK$^{-/-}$ muscles is shown in Figure 6.3 (left panels). In both genotypes, the CLT increased peak concentric force and work during the initial, but not latter, pulses of the volley compared to the CFT, an effect that increased the total work performed. The changes in work were, however, much greater for skMLCK$^{-/-}$ than for wildtype muscles ($P < 0.05$). The relative responses for wildtype and skMLCK$^{-/-}$ muscles are summarized in Figure 6.4.

*Effect of potentiating stimulation on contractile responses in wildtype and skMLCK$^{-/-}$ muscles*

Representative examples displaying the influence of the PS on concentric responses is shown for both genotypes in Figure 6.3 (right vs. left panels). In wildtype muscles, the PS greatly increased peak concentric force and work of each pulse, an effect that greatly increased the overall work performed during the potentiated (control) vs. unpotentiated (PTP) contractions ($P < 0.05$). In contrast, the PS did not alter peak concentric force of skMLCK$^{-/-}$ muscles and there was a substantial decrease (~15%) in the total work performed after compared to before stimulation. Summary data showing relative changes in work for wildtype and skMLCK$^{-/-}$ muscles due to the PS are shown in Figure 6.4B.

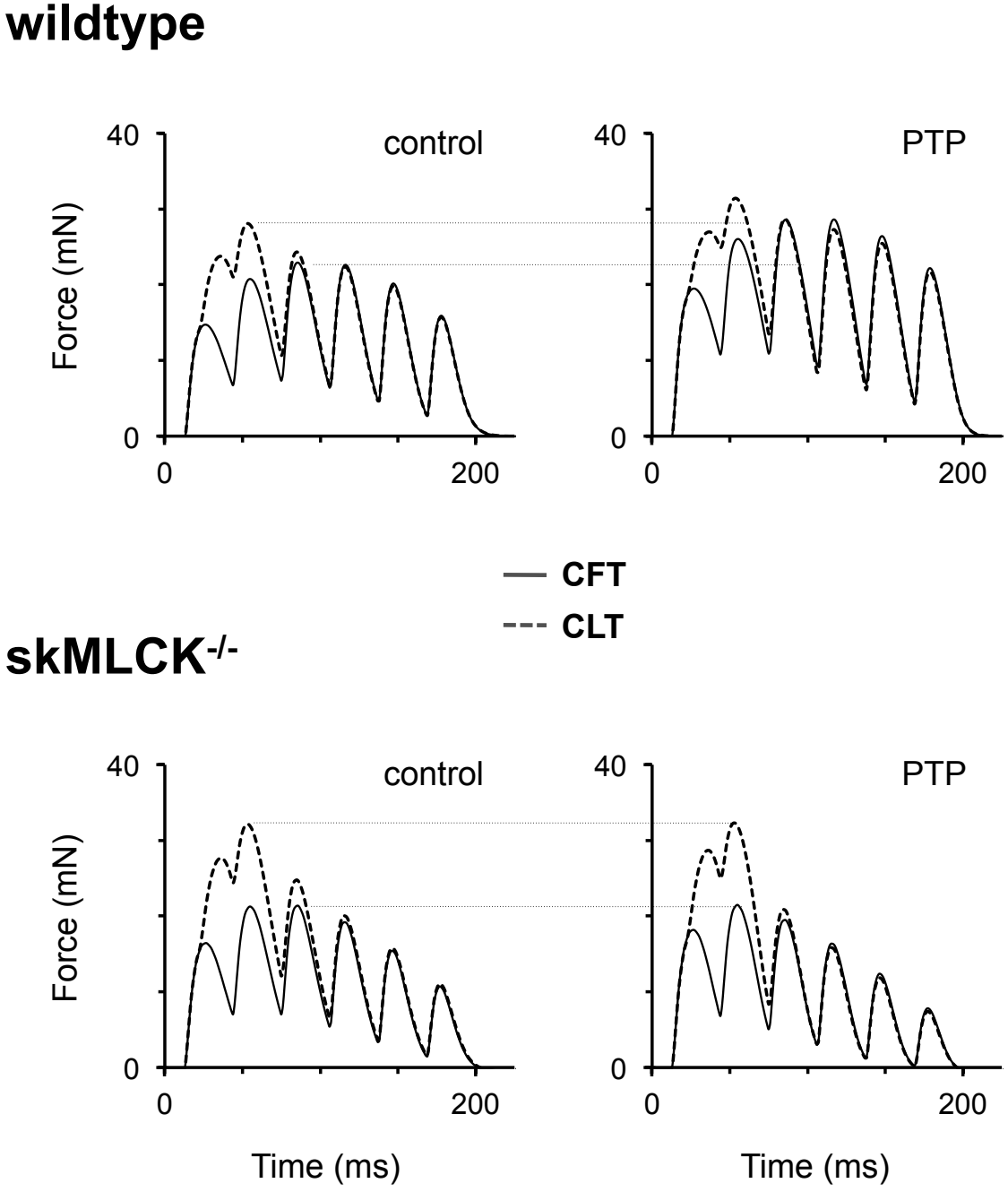


*Figure 6.3. Representative active force traces in wildtype and skMLCK$^{-/-}$ muscles for responses before (control) and after (PTP) the potentiating stimulus.*

In each panel, *CFT* traces (solid line) are contrasted against CLT traces (dotted line). Dotted horizontal lines demonstrate the effect of PTP by comparing peak force reached in each stimulus train between *control* and *PTP* traces.

*Table 6.1. Contractile parameters in wildtype and skMLCK$^{-/-}$ muscles*

| | Control | | Potentiated | |
|---|---|---|---|---|
| | $CFT_c$ | $CLT_c$ | $CFT_{PTP}$ | $CLT_{PTP}$ |
| *Peak Force (mN)* | | | | |
| wildtype | $23.97 \pm 1.57^{a}$ | $29.50 \pm 2.16^{b}$ | $30.43 \pm 1.88^{b}$ | $33.52 \pm 2.55^{c}$ |
| skMLCK$^{-/-}$ | $22.53 \pm 0.98^{a}$ | $33.70 \pm 0.90^{b}$ | $22.08 \pm 1.15^{a}*$ | $32.89 \pm 1.74^{b}$ |
| *Work (J•kg$^{-1}$)* | | | | |
| wildtype | $2.54 \pm 0.18^{a}$ | $3.01 \pm 0.20^{b}$ | $3.51 \pm 0.23^{c}$ | $3.79 \pm 0.24^{d}$ |
| skMLCK$^{-/-}$ | $2.20 \pm 0.13^{b}$ | $2.93 \pm 0.13^{c}$ | $1.91 \pm 0.16^{a}*$ | $2.43 \pm 0.17^{b}*$ |
| *Work/pulse (J•kg$^{-1}$)* | | | | |
| wildtype | $0.42 \pm 0.03^{a}$ | $0.43 \pm 0.03^{a}$ | $0.59 \pm 0.04^{c}$ | $0.54 \pm 0.03^{b}$ |
| skMLCK$^{-/-}$ | $0.37 \pm 0.02^{a}$ | $0.42 \pm 0.02^{b}$ | $0.32 \pm 0.03^{a}*$ | $0.35 \pm 0.02^{a}*$ |
| *+dP/dt (mN•s$^{-1}$)* | | | | |
| wildtype | $3119 \pm 174^{a}$ | $3059 \pm 169^{a}$ | $3731 \pm 208^{b}$ | $3688 \pm 207^{b}$ |
| skMLCK$^{-/-}$ | $2773 \pm 110^{a}$ | $2718 \pm 126^{a}$ | $2854 \pm 106^{a}*$ | $2779 \pm 127^{a}*$ |
| *-dP/dt (-mN•s$^{-1}$)* | | | | |
| wildtype | $1181 \pm 63^{a}$ | $1192 \pm 67^{a}$ | $1471 \pm 87^{b}$ | $1452 \pm 95^{b}$ |
| skMLCK$^{-/-}$ | $1033 \pm 58^{a}$ | $1222 \pm 69^{b}$ | $1141 \pm 67^{a}*$ | $1510 \pm 132^{c}$ |

Data are Mean ± SEM (n=9). Constant frequency (CFT) and catchlike (CLT) trains.
*skMLCK$^{-/-}$ value is lower than corresponding wildtype value ($P < 0.05$)
$^{a,b,c,d}$ within group comparisons ($P < 0.05$)

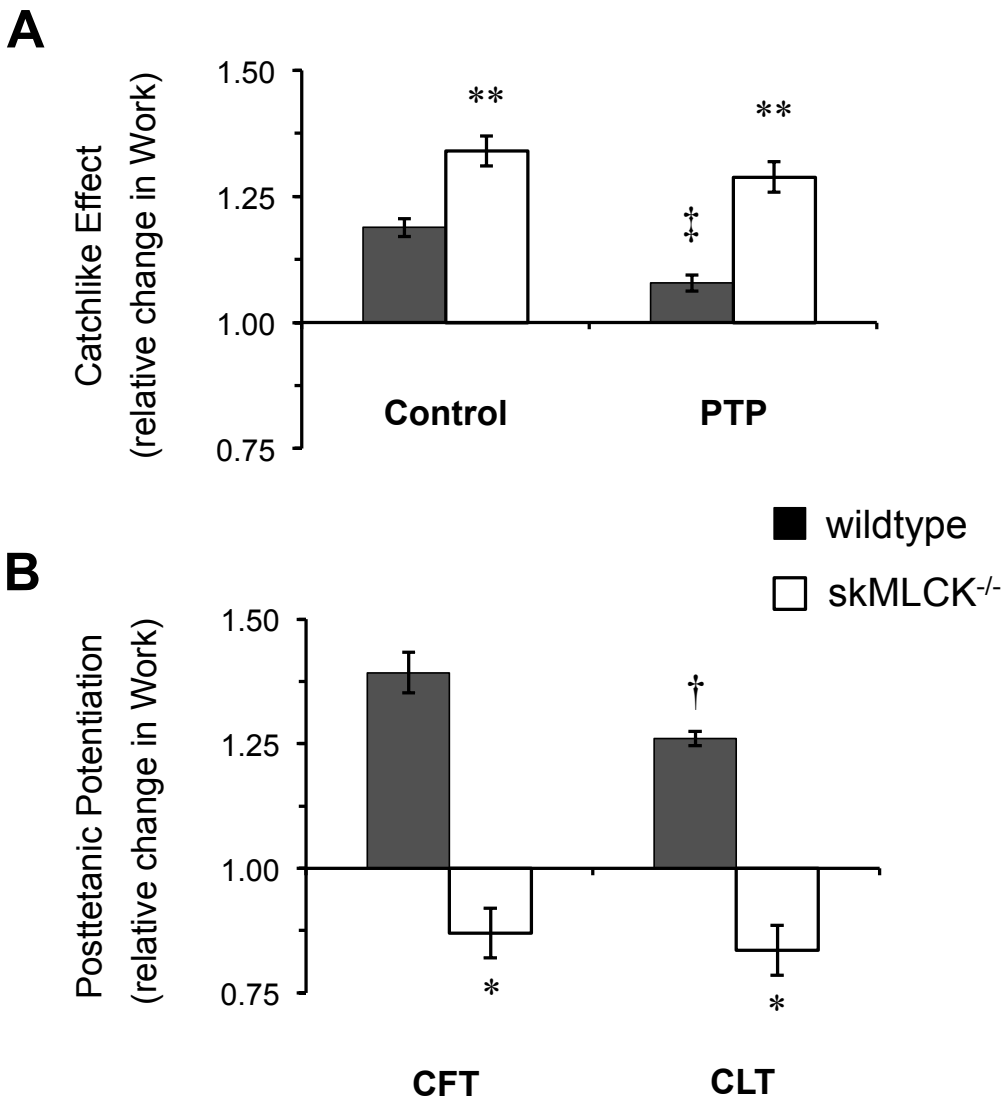


*Figure 6.4. Summary data of concentric PTP and the CLP*

(**A**) Catchlike property in wildtype and skMLCK$^{-/-}$ muscles, shown separately for both the *control* and *potentiated* conditions (in each case the *CLT* response is compared to the *CFT* response, *CLT/CFT*).
**skMLCK$^{-/-}$ value is greater than corresponding wildtype value ($P < 0.05$)
‡wildtype *PTP* value is less than *control* value ($P < 0.05$)

(**B**) Posttetanic potentiation in wildtype and skMLCK$^{-/-}$ muscles, shown separately for both the *CFT* and *CLT* stimulus trains (in each case the *potentiated* response is compared to the *control* response, PTP/C).
*skMLCK$^{-/-}$ value is less than corresponding wildtype value ($P < 0.05$)
†wildtype *CLT* value is less than corresponding *CFT* value ($P < 0.05$)

*Interaction of CLP and PTP in wildtype muscles*

A consistent outcome in wildtype muscles was that PTP had a greater 'potentiating' effect than the CLP on concentric force and work (i.e. PTP/CON > CLT/CFT). In terms of the influence of PTP on the CLP, inspection of wildtype force traces in Figure 6.3 reveals that the relative influence of the CLT was greatly diminished after compared to before the PS. This effect was mediated largely by the greater increase in the CFT vs. the CLT after the PS. This interaction between the CLP and PTP is summarized in Figure 6.4 and 6.5 for all muscles.

*Interaction of CLP and PTP in skMLCK$^{-/-}$ muscles*

In direct contrast to wildtype muscles, and consistent with the absence of RLC phosphorylation (and PTP), the influence of the CLP was greater than PTP in skMLCK$^{-/-}$ muscles. Because of this, and in contrast to wildtype muscles, inspection of the force records in Figure 6.3 and the data in Table 6.1 reveals that the relative influence of the CLT vs. CFT conditions on concentric force and work was similar both before and after the PS. Thus, there was no interaction between the CLP and PTP in these muscles, as summarized in Figure 6.4A and 6.4B for skMLCK$^{-/-}$ muscles.

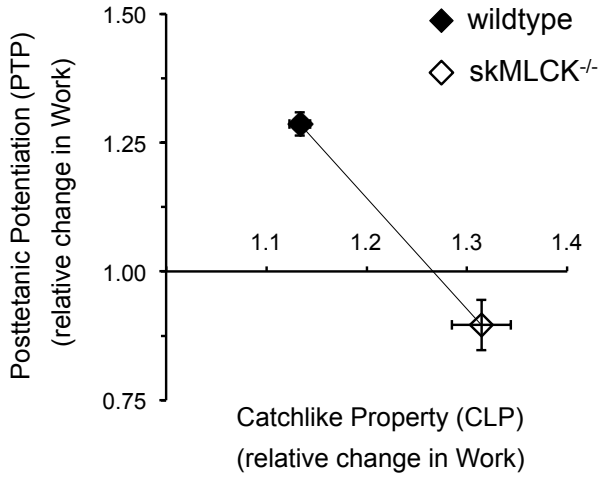


*Figure 6.5. Plot of posttetanic potentiation (PTP) versus the catchlike property (CLP)*

There was an inverse relationship between the mechanisms of force enhancement. For PTP, values for each muscle are calculated as the average degree of potentiation of muscular work for the *CFT* and *CLT* conditions. For the CLP measure, values for each muscle were calculated as the mean enhancement of work in both the unpotentiated (*control*) and potentiated (*PTP*) state.

*Kinetics of force development in wildtype and skMLCK$^{-/-}$ muscles*

As shown in Table 6.1, the CLT did not increase the concentric rate of force development (+dP/d*t*) of wildtype muscles relative to the CFT in either the CON or PTP conditions ($P < 0.05$). In contrast, the PS greatly enhanced the concentric +dP/d*t* of wildtype muscles in both the CFT and CLT conditions by 20 and 21%, respectively ($P < 0.05$). Similar to wildtype muscles, the concentric +dP/d*t* was not altered by the CLT relative to the CFT in skMLCK$^{-/-}$ muscles (see Table 6.1). Similarly, and in contrast to wildtype muscles, the concentric +dP/d*t* in skMLCK$^{-/-}$ muscles was not altered by the PS for either the CFT or CLT conditions.

*Kinetics of force relaxation in wildtype and skMLCK$^{-/-}$ muscles*

As shown in Table 6.1 with respect to the CLP, the concentric rate of force relaxation (-dP/d*t*) in wildtype muscles was not different in the CLT relative to the CFT condition in either the CON or PTP condition. In contrast, the concentric -dP/d*t* was increased in the CLT vs. CFT condition in skMLCK$^{-/-}$ muscles, an effect that was greater in the PTP than CON state (32 and 18%, respectively) ($P < 0.05$). With respect to PTP, the PS enhanced the concentric -dP/d*t* of wildtype muscles in both the CFT and CLT conditions by 24 and 22%, respectively ($P < 0.05$). The PS had a similar effect on concentric -dP/d*t* of skMLCK$^{-/-}$, as values were increased by 12 and 27% relative to the CON state for both CFT and CLT, respectively.

*Fusion Index in wildtype and skMLCK$^{-/-}$ muscles*

The Fusion Index (FuI) was measured in each muscle during the first and last pulse of each stimulation period (see Table 6.2). The effect of the double pulse on force summation was readily apparent in both genotypes and conditions as $FuI_i$ was augmented approximately two-fold in the CLT condition when compared to the CFT condition (i.e. 2.07±0.06 and 1.94±0.06 in skMLCK$^{-/-}$ and wildtype muscles, respectively). The $FuI_f$ was not different between these conditions in either wildtype or skMLCK$^{-/-}$ muscles, however. This is consistent with an influence of the CLP early, but not late, during a submaximal unfused tetanus for both genotypes. With respect to PTP, the PS moderately increased both $FuI_i$ and $FuI_f$ by 10 - 20% in wildtype muscles ($P < 0.05$), a change that was observed in both the CFT and CLT conditions. In contrast, $FuI_f$ was decreased in skMLCK$^{-/-}$ muscles to 0.04±0.01 and 0.03±0.01 after the PS in CFT and CLT conditions,

respectively ($P < 0.05$). As a result of these changes, skMLCK$^{-/-}$ muscles showed reduced tetanic fusion compared to wildtype muscles after (but not before) the PS in both the CFT and CLT conditions.

*Table 6.2. Fusion Index (FuI) in wildtype and skMLCK$^{-/-}$ muscles*

| | **Control** | | | |
|---|---|---|---|---|
| | $CFT_c$ | | $CLT_c$ | |
| | *Initial* | *Final* | *Initial* | *Final* |
| wildtype | $0.45 \pm 0.02^{b}$ | $0.17 \pm 0.02^{a}$ | $0.87 \pm 0.01^{c}$ | $0.17 \pm 0.02^{a}$ |
| skMLCK$^{-/-}$ | $0.43 \pm 0.01^{b}$ | $0.13 \pm 0.02^{a}$ | $0.88 \pm 0.01^{c}$ | $0.15 \pm 0.02^{a}$ |
| | **Potentiated** | | | |
| | $CFT_{PTP}$ | | $CLT_{PTP}$ | |
| | *Initial* | *Final* | *Initial* | *Final* |
| wildtype | $0.55 \pm 0.02^{b}$ † | $0.20 \pm 0.02^{a}$ † | $0.92 \pm 0.01^{c}$ † | $0.20 \pm 0.02^{a}$ † |
| skMLCK$^{-/-}$ | $0.37 \pm 0.02^{b}$ *‡ | $0.04 \pm 0.01^{a}$ *‡ | $0.87 \pm 0.01^{c}$ * | $0.03 \pm 0.01^{a}$ *‡ |

Data are Mean ± SEM (n=9). Constant frequency train (CFT) and catchlike train (CLT). Fusion Index is unitless; see Figure 6.2 for description of calculation.
*skMLCK$^{-/-}$ value is lower than corresponding wildtype *potentiated* value ($P < 0.05$),
†*potentiated* value is greater than corresponding wildtype *control* value ($P < 0.05$),
‡*potentiated* value is less than corresponding skMLCK$^{-/-}$ *control* value ($P < 0.05$).
$^{a,b,c,d}$ within group comparisons ($P < 0.05$)

*Myosin RLC phosphorylation response to the potentiating stimulus*

Representative blots of myosin RLC phosphate content from wildtype and skMLCK$^{-/-}$ muscles are shown in Figure 6.6. Muscles were frozen prior to stimulation (control) and 15 s after the PS (PTP), a time point which corresponded to the timing of stimulation for potentiated responses in the main experiments. In these blots it is clear that while wildtype muscles exhibited a ~3 fold increase, skMLCK$^{-/-}$ muscles did not demonstrate an increase in myosin RLC phosphate content following stimulation.

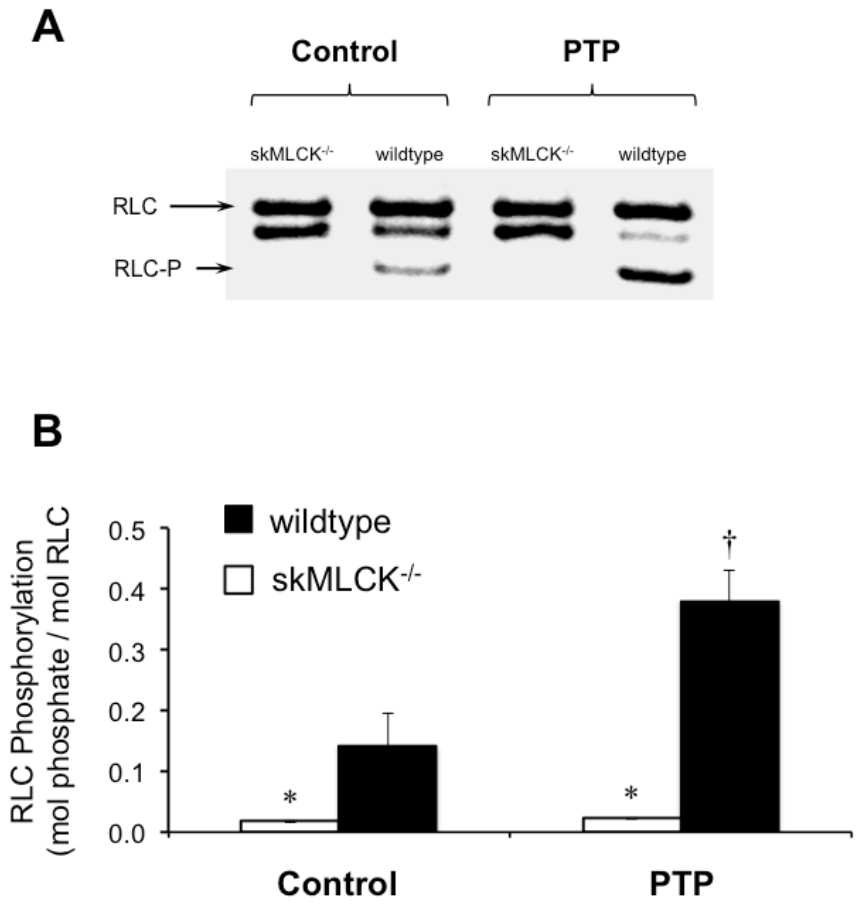


*Figure 6.6. Quantification of myosin RLC phosphate content before and after the potentiating stimulus in wildtype and skMLCK$^{-/-}$ muscles.*

Details of the methods have been presented previously.[17,18] (**A**) Representative blot from Urea-glycerol PAGE in whole extensor digitorum longus EDL muscle homogenates. (**B**) Quantification of fractional myosin RLC phosphate content was conducted using Image Studio Lite, LI-COR Biosciences, Lincoln, Nebraska, USA. RLC phosphorylation was calculated as the ratio of the phosphorylated band to total light chain content (RLC phosphorylation = [RLC-P] / [RLC] + [RLC-P]). We found no evidence of any increase in phosphorylation with stimulation in skMLCK$^{-/-}$ blots from muscles samples frozen after the potentiating stimulus.

*skMLCK$^{-/-}$ value is less than corresponding wildtype value ($P < 0.05$)

†RLC phosphorylation in wildtype muscles is significantly greater in muscles frozen 15 s after the PS ($P < 0.05$)

## *Discussion*

The purpose of this study was to test for the robustness of the CLP in muscles with and without myosin RLC phosphorylation, the primary mechanism for PTP (Gittings et al, 2011; Zhi et al, 2005). Our main finding was that the magnitude of the CLP was enhanced in skMLCK$^{-/-}$ muscles relative to wildtype muscles, indicating an interaction with PTP. These results support the concept of an interference effect between the PTP and the CLP (Burke et al, 1976; Ding et al, 2003), and suggest that they may be redundant mechanisms of force enhancement in mouse fast muscle.

### *The catchlike effect*

Our examination of the CLP in mouse EDL during ramp shortening demonstrated a large but relatively brief augmentation of peak force and work. Further, this effect was similar in both genotypes and thus largely independent of PTP *per se*. For example, the force traces shown in Figure 6.3 demonstrate that the catchlike effect was all but dissipated within ~100 ms of the onset of stimulation. Furthermore, analysis of the Fusion Index (FuI) data revealed no differences in the final summation of the unfused tetani between CFT and CLT stimulus trains in any condition or genotype. These results are consistent with the previous observation that imposing a length perturbation can reduce or negate the catchlike augmentation in force that might otherwise last ≥ 1s (Sandercock and Heckman, 1997), and with the general trend that the CLP is reduced during nonisometric conditions vs. isometric activation (Binder-Mcleod and Barrish, 1992). Hence, it is possible that the increase in compliance produced by the shortening ramps may have obscured or abbreviated the effect of the CLP on force development or maintenance via changes in series elastic compliance or stiffness (Parmiggiani and Stein, 1981; Sandercock and Heckman, 1997). The absence of any change to maximal rate of force development (+d$P$/d$t$) with the CLP in both genotypes and conditions provides further evidence that a decrease in SEC imposed by the initial doublet, if present, was not of sufficient magnitude to influence the kinetics of force development in the progressively shortening muscle. This finding is in contrast to other reports of the CLP during concentric stimulation in human muscle that demonstrate an increase in rate of force development with doublet stimulation (Binder-Mcleod and Lee, 1996). The reason for this discord is unclear but may be due to differences in the experimental models and parameters used in the respective studies.

*Muscular work normalized to pulse number*

The work performed during each stimulus period was normalized to pulse number to account for the 'extra' pulse added during the CLT and to evaluate the utility of the CLP via the unitary effect of doublet stimulation on contractile function. In both wildtype and skMLCK$^{-/-}$ muscles, this correction reduced the magnitude of the catchlike effect significantly. For example, the increase in work per pulse with the CLP (CLT/CFT) in the control (non-potentiated) condition was 1.02 ±0.02 and 1.15 ±0.03 in wildtype and skMLCK$^{-/-}$ muscles, respectively. Considered in this context, the effect of the CLP on muscular work performed during shortening is small compared to the magnitude and timing of its effect on peak force. Moreover, the correction of work to pulse number reveals an important point of comparison between the mechanisms of enhancement: the CLP may operate primarily via a 'non-linear' increase in force summation[1] and is limited by the duration of the effect, while PTP augments contractile function through a less-acute increase in the force response per pulse via $Ca^{2+}$ sensitivity (Persechini et al, 1985). Evidence for this interpretation can be found in the analysis of the force traces themselves. For example, the CLP exerts its greatest effect by doubling the initial Fusion Index ($FuI_i$); while in wildtype muscles, PTP produces a moderate increase (~20%) in $FuI_i$ that persists throughout the stimulation period (Table 6.2).

*Posttetanic potentiation (PTP)*

The activation history-dependent increase in isometric or dynamic force that defines potentiation is an important characteristic of the mammalian fast twitch skeletal muscle phenotype. Although highly species, paradigm, and temperature dependent, the potentiated state may be the normal operating state of fast skeletal muscles (Brown and Loeb, 1998). If so, understanding the interaction between potentiation phenomena and the CLP seems imperative to understanding muscle function during locomotion. A novel aspect of our data was the absence of concentric force potentiation during either the CFT or the CLT in skMLCK$^{-/-}$ muscles following the PS; stimulation which increased concentric force and work of wildtype muscles in these respective conditions by up to 40%. Moreover, the ~20% increase in rate of force development observed in wildtype muscles after the PS is evidence of an increased rate of myosin crossbridge binding and force production via myosin RLC phosphorylation (Vandenboom et al, 2013). Collectively, these studies suggest that, although other mechanisms may contribute in a

stimulation-paradigm and contraction type dependent manner, myosin RLC phosphorylation was the primary mechanism for PTP in the current work.

Interestingly, the absence of concentric PTP in skMLCK$^{-/-}$ muscles in the current study is dissimilar to recent work from our lab that reported a 20-30% potentiation of mean concentric force during 100 ms tetanic stimulation at 60Hz in the same genotype (shortening at 0.25$V_{max}$)(Gittings et al, 2015). These apparently inconsistent results may be explained, however, by changes in force kinetics that may alter the summation of unfused tetani and are stimulation frequency dependent. For example, it has been reported that during slow shortening ramps in the potentiated state, rate of force relaxation was significantly faster at low stimulation frequencies (≤ 45Hz) but slowed at high stimulation frequencies (≥ 70Hz)(Gittings et al, 2012). In the current experiments, unfused tetanic stimulation at 32 Hz in the potentiated state showed an increase in force relaxation rates (~20%), which may had led to a decrease in initial and final Fusion Index (FuI) in skMLCK$^{-/-}$ muscles. These effects on force kinetics and summation may therefore have led to a decrease in work performed in the potentiated state during the CFT and CLT stimulus trains (to 0.87 ±0.06 and 0.84 ±0.05 of control values, respectively). This observation is significant as it demonstrates that the PTP present in wildtype muscles not only caused an increase in contractile function compared to the control condition, but also may have opposed the effects that resulted in the reduced force summation demonstrated by skMLCK$^{-/-}$ muscles.

*Interactions of the CLP and PTP*

Although our study is not the first to examine the interaction between PTP and the CLP, it is the first to do so using skMLCK$^{-/-}$ muscles and quantification of myosin RLC phosphorylation and thus provides important new information regarding the interaction of these phenomena. For example, in that the control (non-potentiated) state the catchlike effect of doublet stimulation in skMLCK$^{-/-}$ muscles was nearly twofold greater than in wildtype muscles. Changes in force kinetics did not account for these differences, as initial and final Fusion Index (FuI) values were not different between genotypes in the CFT or CLT conditions (see Table 6.2). Furthermore, the small but non-significant difference in rate of force development between genotypes does not provide a mechanistic explanation for this observation. We therefore propose that the baseline difference in myosin RLC phosphorylation between the genotypes may have been

sufficient to affect the magnitude of the CLP even in the control (non-potentiated) state. Critically, because the skMLCK$^{-/-}$ muscles were enzymatically incapable of phosphorylating the RLC (Figure 6.6), we were able to unambiguously test for the influence of RLC phosphorylation-mediated force potentiation on the CLP. Thus, although we cannot discount potentiation due to other mechanisms, such as stimulation-induced elevations in resting calcium (Smith et al, 2013), our results suggest that RLC phosphorylation mediated enhancements to concentric force and work may have mitigated the influence of the CLP. From a mechanistic point of view, the increase in myosin RLC phosphorylation in wildtype muscles following the PS may have interfered with the magnitude of the catchlike effect through an increase in $Ca^{2+}$ sensitivity or the associated increase in rate of force development via enhanced crossbridge binding. For example, it has be suggested that the catchlike effect of doublet stimulation may be the result of an initial augmentation of $Ca^{2+}$ release (Duchateau and Hainaut, 1986), which in turn may cooperatively produce a state of increased $Ca^{2+}$ sensitivity, further enhancing myosin crossbridge binding and force maintenance (Abbate et al, 2002). Therefore, in light of the present results, the force response to doublet stimulation in an already $Ca^{2+}$-sensitized state (i.e. elevated myosin RLC phosphorylation) would theoretically be neutralized or at least diminished in the 'potentiated' state.

The alternative hypothesis to the above is associated with the idea that the augmentation of force by the CLP is due to an increased stiffness of the series-elastic component (Parmiggiani and Stein, 1981). If so, this effect may be greater at shorter muscle lengths (Lee et al, 1999) where compliance is presumably increased. Similarly, myosin RLC phosphorylation is directly associated with an increase in the rate of crossbridge attachment that results in greater fibre stiffness and enhanced rate of force development (Sweeney and Stull, 1990; Vandenboom et al, 1995). Consequently, in the present study, it is plausible that an increase in myosin RLC phosphate content following the PS may have limited the effectiveness of doublet stimulation on force development. Specifically, the rapid force development, enhanced FuI, and enhanced peak force observed during the CFT in the potentiated state ($CFT_{PTP}/CFT_C$) would render it less amenable to the catchlike effect.

A secondary interaction produced in the current study was the stimulus train-specific PTP response in wildtype muscles, where the potentiation of force and work were greater in the CFT vs. CLT (data shown in Table 6.1 and Figure 6.4, Panel B).

Without discounting the interacting mechanisms summarized above, it is also likely that force level itself contributed to this effect. For example, we have recently shown that isometric and concentric PTP are negatively associated with force level in mouse EDL muscles (Gittings et al, 2015). Thus, the so-called force-dependency of PTP may be apparent when comparing the CFT and CLT responses that followed the PS, as the ~23% greater force observed in the $CLT_c$ (vs. the $CFT_c$) would limit the efficacy of the PTP effect.

*Physiological significance*

The precise physiological roles of the CLP and PTP, singly or together, remain uncertain; however, it is clear that modulation of contractile function is an important hallmark of fast skeletal muscles. Understanding the interaction of these mechanisms and with regulatory control schemes for skeletal muscle will help provide a better indication of how muscles accomplish critical tasks such as locomotion and movement. For example, the addition of an initial doublet was capable of augmenting force summation and muscular work even in potentiated wildtype muscles. This catchlike effect would be particularly useful during brief physiological activation of skeletal muscles where minimizing the time to peak tension and/or overcoming movement inertia are of prime importance. Indeed, Hennig and Lomo (1987) noted that doublet pulses were characteristic of fast motor units in the EDL muscles of freely moving rats, and that ~60% of stimulus trains were comprised of 6 pulses or less. With respect to PTP, the increased myosin RLC phosphate content in potentiated wildtype muscles was associated with the highest quantity of work performed per pulse and ≥50% more work performed per contraction than in $skMLCK^{-/-}$ muscles. Thus, PTP is evidently a less-acute mechanism of force enhancement that promotes the development and maintenance of force summation during unfused tetani.

*Limitations and assumptions*

Due to technical limitations, we did not measure intracellular $[Ca^{2+}]$ or actively monitor sarcomere lengths in the intact EDL muscles used during the experiments. Therefore, we cannot rule out the possible contributions of these factors to the results and conclusions presented. The CLP and PTP are dependent on a variety of experimental factors such as muscle length, stimulation frequency, contraction type, muscle/motor unit type, and fatigue. Thus, further work is required to provide a more

comprehensive account of the interaction between these mechanisms and the current findings should be considered with these factors in mind when applied or cited.

*Summary*

The present study provides a novel description of the interaction between the CLP and PTP in skeletal muscle by investigating the coexistence of these mechanisms in fast skeletal muscles with and without skMLCK. The data supports previous observations that the CLP is diminished in the presence of force potentiation (Burke et al, 1976; Ding et al, 2003), and importantly, highlights the role of stimulation-induced elevations in myosin RLC phosphorylation in this interaction. Despite the apparent redundancy and interference of these mechanisms, however, there is strong evidence that each have functional utility in the fast muscle phenotype.

## *Financial Disclosure*

The authors have no conflicting financial or nonfinancial relationships with respect to the current work. This study was supported by funds provided by the Natural Sciences and Engineering Research Council of Canada (RV).

## *Conflict of Interest*

The authors do not have any conflicting interests regarding the findings or interpretations of this manuscript.

## *References*


Abbate F, Sargeant AJ, Verdijk PWL, and de Haan A (2000). Effects of high-frequency initial pulses and posttetanic potentiation on power output of skeletal muscles. J Appl Physiol 88:35-40.

Abbate F, Bruton JD, De Haan A and Westerblad H (2002). Prolonged force increase following a high frequency burst is not due to a sustained elevation of $[Ca^{2+}]_i$. American Journal of Physiology & Cell Physiology, 283, C42–C47.

Binder-Macleod SA and Barrish WJ (1992). Force response of rat soleus muscle to variable-frequency train stimulation. Journal of Neurophysiology, 68, 1068–1078.

Binder-Macleod, S.A., & Kesar, T. (2005). Catchlike property of skeletal muscle: Recent findings and clinical implications. Muscle & Nerve, 31(6), 681-693.

Binder-Macleod SA, Lee SC. (1996) Catchlike property of human muscle during isovelocity movements. J Appl Physiol. 80(6): 2051-9.

Brooks SV, Faulkner JA. (1988) Contractile properties of skeletal muscles from young, adult and aged mice. J Physiol. 404:71-82.

Brown IA, Loeb GE. (1998). Post-activation potentiation: a clue for simplifying models of muscle dynamics. Am Zool 38: 743-754.

Burke RE, Rudomin P and Zajac FE (1976). The effect of activation history on tension production by individual muscle units. Brain Research, 109(3), 515-529.

Burke RE, Rudomin P, Zajac FE 3rd. (1970) Catch property in single mammalian motor units. Science. 168(3927): 122-124.

Callister RJ, Reinking RM, Stuart DG. (2003). Effects of fatigue on the catchlike property in a turtle hindlimb muscle. J Comp Physiol. 189(12): 857-66.

Celichowski J, Grottel K (1995) The relationship between fusion index and stimulation frequency in tetani of motor units in rat medial gastrocnemius. Arch Ital Biol 133:81–87.

Connolly R, Gough W, Winegrad S. (1971) Characteristics of the isometric twitch of skeletal muscle immediately after a tetanus. A study of the influence of the distribution of calcium within the sarcoplasmic reticulum on the twitch. J Gen Physiol. 57(6): 697-709.

Desmedt JE and Godaux E. (1977) Ballistic contractions in man: characteristic recruitment pattern of single motor units of the tibialis anterior muscle. J Physiol. 264(3): 673-693.

Ding J, Storaska J and Binder-MacLeod S (2003). Effect of potentiation on the catchlike property of human skeletal muscles. Muscle & Nerve, 27(3), 312-319.

Duchateau J and Hainaut K (1986). Nonlinear summation of contractions in striated muscle. II. Potentiation of Intracellular $Ca^{2+}$ movements in single barnacle muscle fibres. Journal of Muscle Research & Cell Motility, 7,18–24.

Garland SJ, Griffin L. (1999) Motor unit double discharges: statistical anomaly or functional entity? Can J Appl Physiol. 24(2): 113-130.

Gittings W, Huang J, Smith I, Quadrilatero J, Vandenboom R (2011) The effect of skeletal myosin light chain kinase gene ablation on the fatigability of mouse fast muscle. J Muscle Res Cell Motil 31: 337-348.

Gittings W, Aggarwal H, Stull JT, Vandenboom R. (2015) The force dependence of isometric and concentric potentiation in mouse muscle with and without skeletal myosin light chain kinase. Can J Physiol Pharmacol. 93(1): 23-32.

Gittings W, Huang J. and Vandenboom, R (2012). Tetanic Force Potentiation of Mouse Fast Muscle is Shortening Speed Dependent. Journal of Muscle Research and Cell Motility 33(5): 359-368, 2012.

Griffin L, Garland SJ, Ivanova T. (1998) Discharge patterns in human motor units during fatiguing arm movements. J Appl Physiol. 85(5): 1684-1692.

Hennig R, Lømo T. (1985). Firing patterns of motor units in normal rats. Nature. 314(6007): 164-166.

Hennig R, Lømo T. (1987) Gradation of force output in normal fast and slow muscles of the rat. Acta Physiol Scand. 130(1): 133-142.

Krutki P, Pogrzebna M, Drzymała H, Raikova R, Celichowski J. (2008) Force generated by fast motor units of the rat medial gastrocnemius muscle during stimulation with pulses at variable intervals. J Physiol Pharmacol. 59(1): 85-100.

Lännergren J, Bruton JD, Westerblad H. Vacuole formation in fatigued skeletal muscle fibres from frog and mouse: effects of extracellular lactate. J Physiol. 526 Pt 3:597-611.

Lee SCK, Gerdom ML, and Binder-Macleod SA. (1999) Effects of length on the catchlike property of human quadriceps femoris muscle. Physical Therapy. (79): 738-748.

Nielsen BG. (2009) Calcium and the role of motoneuronal doublets in skeletal muscle control. Eur Biophys J. 38(2): 159-73.

Parmiggiani F, Stein RB. (1981) Nonlinear summation of contractions in cat muscles. II. Later facilitation and stiffness changes. J Gen Physiol. 78(3): 295-311.

Persechini A, Stull JT, Cooke R. (1985) The effect of myosin phosphorylation on the contractile properties of skinned rabbit skeletal muscle fibers. J Biol Chem 260: 7951–7954.

Sandercock TG, Heckman CJ. (1997) Doublet potentiation during eccentric and concentric contractions of cat soleus muscle. J Appl Physiol. 82(4): 1219-28.

Smith I, Gittings W, Bloemberg D, Huang J, Quadrialtero J, Tupling AR and Vandenboom R (2013). Potentiation in Mouse Lumbrical Muscle Without Myosin Light Chain Phosphorylation: Is Resting Calcium Responsible? Journal of General Physiology, 141(3): 297-308.

Sweeney, H.L., and Stull, J.T. (1990). Alteration of cross-bridge kinetics by myosin light chain phosphorylation in rabbit skeletal muscle: implications for regulation of actin-myosin interaction. Proc. Natl. Acad. Sci. U.S.A. 87: 414–418.

Vandenboom, R., Grange, R.W., and Houston, M.E. (1995). Myosin phosphorylation enhances rate of force development in fast-twitch skeletal muscle. Am. J. Physiol. 268: C596–C603.

Vandenboom R, Gittings W, Smith IC, Grange RW and JT Stull. (2013) Myosin Phosphorylation and Force Potentiation in Skeletal Muscle: Evidence from Animal Models. Journal of Muscle Research and Cell Motility 34(5-6): 317-332.

Zhi, G, Ryder, J, Huang, J, Ding, P, Chen, Y, Zhao, Y, Kamm, K, & Stull, J. (2005). Myosin light chain kinase and myosin phosphorylation effect frequency-dependent potentiation of skeletal muscle contraction. Proceedings of the National Academy of Sciences USA, 102(48), 17519-17524.

# Chapter 7

## Study #4

**The economy of working fast skeletal muscles in the presence and absence of myosin phosphorylation**

Author List: William Gittings, Jordan Bunda, and Rene Vandenboom

As published in: Not yet submitted for publication

**Author contributions:**

*William Gittings*: study design, data collection and experimentation, manuscript writing

*Jordan Bunda*: assistance with myosin RLC phosphorylation and metabolite analysis

*Dr. James T. Stull*: skMLCK$^{-/-}$ mice breeding pairs, technical assistance

*Dr. Rene Vandenboom*: study design input, funding (NSERC), manuscript writing

## *Abstract*

Running head: Posttetanic potentiation and contractile economy

The physiological role of myosin regulatory light chain (RLC) phosphorylation in fast skeletal muscle is unclear, as the resultant potentiation of contractile function comes with an undetermined energetic cost. We conducted *in vitro* experiments (25°C) to quantify contractile economy (i.e. energy cost/work performed) in potentiated extensor digitorum longus (EDL) muscles from wildtype and myosin light chain kinase knockout ($skMLCK^{-/-}$) mice. Economy values were calculated as the ratio of total work performed to high-energy phosphate consumption (HEPC) during a period of repeated isovelocity contractions that followed a potentiating stimulus (PS). The PS enhanced contractile parameters (concentric force and work) in both genotypes, although the effect was significantly greater in wildtype (1.38±0.03 and 1.51±0.03) vs. $skMLCK^{-/-}$ (1.10±0.04 and 1.10±0.05) muscles ($P < 0.05$, n=8 for all data). During the experimental period of repetitive stimulation in the potentiated state, wildtype muscles performed ~58% more total work than $skMLCK^{-/-}$ muscles (94.05±3.80 vs. 59.55±4.10 $J \bullet kg^{-1}$; $P < 0.001$) without a concomitant increase in HEPC (19.03±3.37 vs. 16.02±3.41 μmol~P; P = 0.27) or genotype difference in economy (5.74±0.67 vs. 4.61±0.71 $J \bullet kg^{-1} \mu mol \sim P^{-1}$; P = 0.27). Importantly, when relative genotype differences were analyzed, the quantity of total work performed was ~3 fold greater than the increase in HEPC for wildtype muscles. Our results support the physiological importance of myosin RLC phosphorylation-mediated potentiation as a mechanism that is capable of augmenting contractile function without a significant energetic cost.

Keywords: potentiation, myosin phosphorylation, regulatory light chain, myosin light chain kinase knockout, economy

## *Introduction*

Repetitive or sustained activation of fast skeletal muscles invariably leads to the progressive depression in contractile function known as fatigue (Allen et al, 2008). Various peripheral mechanisms can modulate excitation-contraction coupling in order to ensure ATP homeostasis during high rates of energy turnover (Myburgh, 2004; MacIntosh et al, 2012). It is also apparent that central motor drive may be down regulated to serve a similar purpose (i.e. the 'muscle wisdom hypothesis')(Enoka and Stuart, 1992; Gandevia, 2001). The net effect of these mechanisms is often a decrease in force capacity, shortening velocity, and slowed relaxation (Westerblad et al, 2010); outcomes that occur concurrently with a decrease in $Ca^{2+}$ sensitivity of the myosin filaments during sustained use (MacIntosh, 2003). Consequently, there has long been interest in factors that might preserve contractile function during prolonged activation. An example of such a mechanism is the modification of the myosin motor by phosphorylation of the regulatory light chain (RLC), which potentiates contractile function (Sweeney and Stull, 1986) and increases the $Ca^{2+}$ sensitivity of the contractile proteins (Persechini et al, 1985). Importantly, it was also been suggested that myosin RLC phosphorylation could represent a potentiation mechanism that might oppose the effects of fatigue (Grange et al, 1993; Rassier et al, 2000). Sweeney et al (1993) stated that RLC phosphorylation was an ideal modulatory mechanism as it consumes little energy and may be important for fine-tuning and achieving optimal muscle performance. In studies that have attempted to elucidate the relative contribution of the major ATP using processes in skeletal muscle (i.e. $Na^+/K^+$-ATPase, SERCA, myosin-ATPase), myosin RLC phosphorylation is generally not accounted for (Barclay et al, 2008; Zhang et al, 2006). Yet, Homsher (1987) estimated that up to 5% of energy consumed during a 5s tetanus might be attributable to skMLCK-mediated RLC phosphorylation. Thus, although the regulation and functional effects of myosin RLC phosphorylation are well understood (as reviewed by Stull et al, 2011), its physiological role and effect on muscle energetics remains unclear.

It has been proposed that the potentiated state is the normal operating condition of fast skeletal muscles (Brown and Loeb, 1998); however, the potentiation of contractile function has been associated with an increased energetic cost for contraction (Abbate et al, 2001). Importantly, although myosin RLC phosphorylation is widely accepted as the primary mechanism for activity-dependent potentiation (Macintosh et al, 2010), there are

alternative mechanisms that may contribute (Smith et al, 2013). Thus, the effect of myosin RLC phosphorylation on contractile economy (i.e. work performed/energy cost)(Goldspink, 1978) is unclear, and to our knowledge there is no study that has quantified the energetic requirement of RLC phosphorylation during muscle activation in the potentiated state. Early attempts to answer this research question suggested that myosin RLC phosphorylation was associated with a decreased energy cost for prolonged isometric tetani (Crow and Kushmerick, 1982a) and a reduced actomyosin turnover rate (Crow and Kushmerick, 1982b) in mouse extensor digitorum longus muscles. Subsequently, in the same experimental model, it was reported that there was no consistent relationship between phosphorylation of the light chains and rate of chemical usage (Barsotti and Butler, 1984), and that myosin RLC phosphorylation does not modulate crossbridge cycling rate (Butler et al, 1983). In the two decades that have passed since these findings were reported, an explanation to reconcile these studies or produce a truly comprehensive answer has been absent. This research problem is especially difficult to resolve because skMLCK and myosin-ATPase are simultaneously activated by the same $Ca^{2+}$ release signal (Blumenthal and Stull, 1980), and a host of other factors may alter the energetic cost for contraction during repetitive use (i.e. stimulation frequency/duration, contraction type, muscle length, fibre type, temperature, fatigue)(Rall et al, 1984).

The purpose of this work was to study the contractile economy of fast skeletal muscles during an intermittent period of concentric work in the presence and absence of the intact myosin RLC phosphorylation mechanism. To accomplish this we conducted identical experiments with extensor digitorum longus (EDL) muscles from wildtype and myosin light chain kinase knockout ($skMLCK^{-/-}$) mice, quantifying economy as the ratio of total work performed to high-energy phosphate consumption (HEPC) during a period of repeated isovelocity concentric contractions. Our genotype comparison allowed us to extend previous work (Abbate et al, 2001) by attempting to quantify the specific effect of myosin RLC phosphorylation on contractile economy in the potentiated state. We hypothesized that in response to the same stimulus regime, wildtype muscles would perform significantly more work but would demonstrate a proportionally greater energy turnover (HEPC) than $skMLCK^{-/-}$ muscles due to the cost of RLC phosphorylation.

## *Methods*

### *Study design*

All animal handling procedures and techniques received prior approval from the Brock University Animal Care Committee. Adult wildtype (C57BL/6) mice (≥10weeks) were sourced from Charles River Laboratories (St. Constant, QC) and housed at the Brock University Comparative Bioscience Facility until use. Age-matched (±2months), sexually mature skMLCK$^{-/-}$ mice from our breeding colony at Brock entered the study as needed. Body masses of mice used in this study were similar between genotypes (21.34±0.70g and 22.78±0.22g for skMLCK$^{-/-}$ and wildtype mice, respectively). The characterization and development of the skMLCK$^{-/-}$ animals has been explained previously (Zhi et al., 2005, Gittings et al., 2011, 2015). Identical experiments were conducted on both genotypes to investigate the contractile economy of skeletal muscles with and without the ability to phosphorylation the myosin RLC when stimulated. Economy was calculated as the ratio of the total work done during a series of concentric contractions to the High Energy Phosphate Consumption (HEPC) measured using fluorometric assays (Abbate et al., 2001a; Zhang et al., 2006).

### *In vitro EDL muscle preparation*

On the day of an experiment, animals were anaesthetized with an IP injection of sodium pentobarbitol (60 mg/kg body weight). The extensor digitorum longus (EDL) muscles were surgically removed from both hindlimbs and immediately incubated at resting length in an oxygenated bath containing cooled Tyrode's solution (~5-10° C) until needed. Muscles were suspended vertically using non-compliant 4-0 silk suture in the 1200A intact muscle apparatus (Aurora Scientific Inc., Aurora, ON). The distal suture was clamped directly to the electrode assembly and the proximal suture was secured to the servomotor arm via a short stainless steel wire. Contractile experiments were conducted at 25° C with the muscle immersed in continuously gassed (95% $O_2$, 5% $CO_2$) Tyrode's solution (Lannergren et al., 2000).

### *Contractile Experiments*

Each experiment commenced with an incubation period of 30 minutes to allow the muscle to equilibrate: during this stage the stability of muscle twitch force was tracked using a single stimulation every three minutes. Stimulation intensity was set to

~1.25 times the voltage required for maximal twitch force to ensure that all fibres were in the preparation were activated. Optimal length ($L_o$) was determined using the micrometer attached to the bath assembly and stimulating the muscle at small length increments (1-2% $L_o$) to find maximal twitch force.

The experimental timeline and details of the isovelocity shortening ramps used are shown in Figure 7.1. To measure concentric force and power, muscles were stimulated at 75 Hz for 50 ms during constant velocity shortening from 1.05 to 0.9 $L_o$. The rate of ramp shortening was equivalent to 40% of maximal shortening velocity as determined previously in our lab using the Slack Test technique (Gittings et al 2011). Stimulation was timed such that force was developed 2 ms after the start of shortening and force relaxation occurred just prior to the completion of the ramp. Identical passive ramps were conducted without stimulation to estimate the non-contractile force component and subtract it from the total force trace as previously described (Gittings et al 2012, 2015).

The Potentiating Stimulus (PS) used in these experiments has been shown to elevate myosin RLC phosphorylation levels in wildtype muscles with only mild fatigue (Gittings et al., 2011, 2012). Baseline measures of concentric force and power were collected using a single control stimulus that was applied prior to the PS. Following the PS, the same stimulation protocol was repeated 20 times at the rate of 1 stimulus per second. Immediately following the final stimulus, the muscle was rapidly frozen in liquid nitrogen-cooled tongs and stored at -80° C for subsequent biochemical analysis.

*Analysis of contractile parameters*

The raw (total) and passive force traces for each stimulus were used to calculate the active force response of the muscle. Active forces were obtained by subtracting the passive force response from the matching total force response as previously described (Gittings et al., 2012). Peak force (mN) was calculated as the highest active force value reached during the stimulus period regardless of timing. Mechanical work ($J \bullet kg^{-1}$) was determined by calculating the integral of the force-displacement plot for each stimulus period and normalizing it to muscle wet mass. The kinetics of force development ($+dP/dt$) and relaxation ($-dP/dt$) were sampled at the start and end of each stimulation period from the first derivative function of the active force trace, expressed in $mN \bullet s^{-1}$.

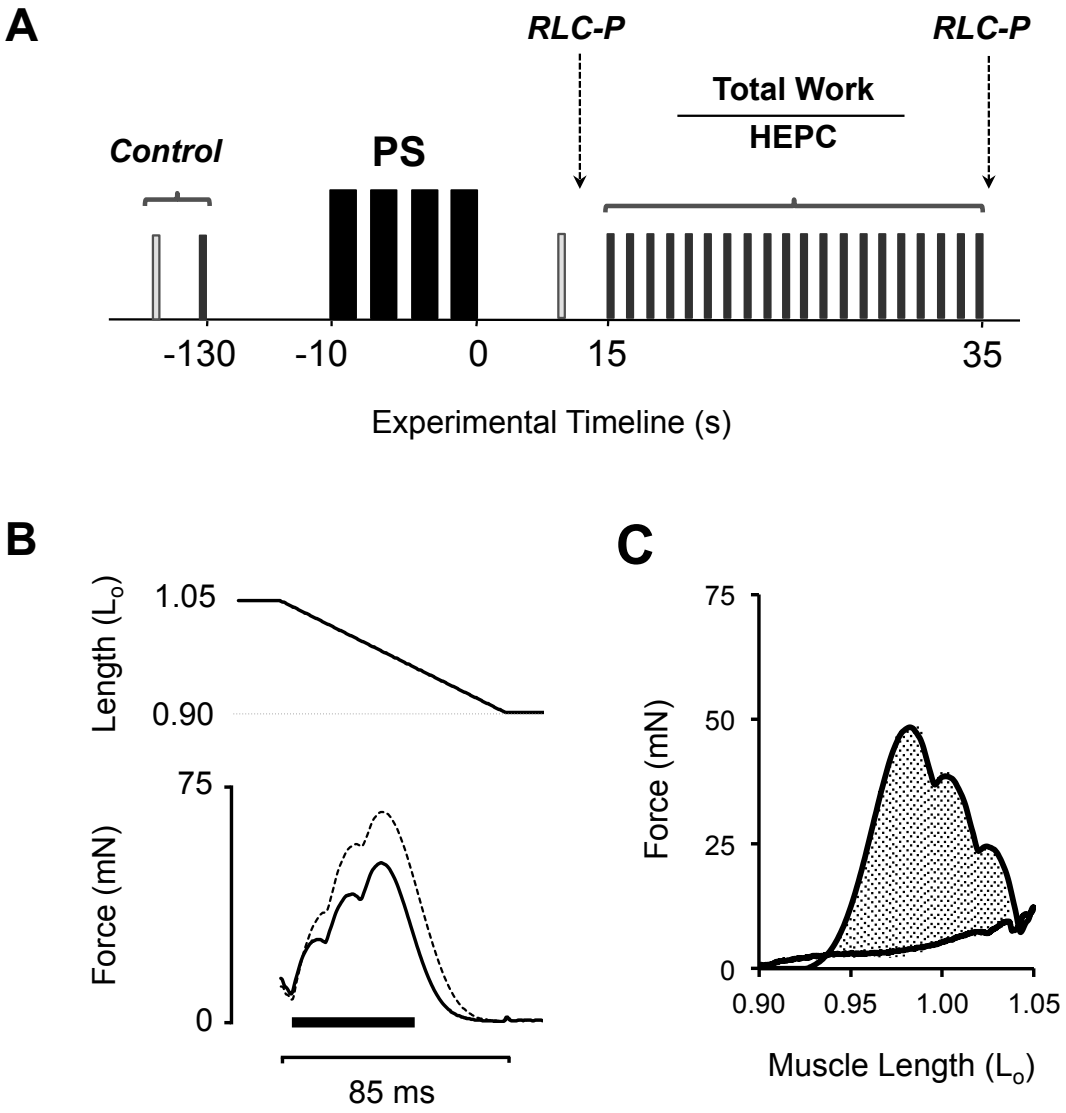


*Figure 7.1. Experimental timeline and shortening ramp parameters*

(**A**) Experimental timeline utilized for all contractile experiments. Initially, a baseline force response (*control*) was elicited in the unpotentiated state; then, following the Potentiating Stimulus (PS), the identical parameters were repeated once per second for twenty seconds. For control and potentiated responses, a passive length ramp (open bars) without accompanying stimulation preceded active length ramps with stimulation (shaded bars). Prior to and following the series of potentiated stimuli, muscles were frozen for biochemical analysis of myosin RLC phosphorylation (RLC-P) and High Energy Phosphate Consumption (HEPC). (**B**) Example length and force traces during ramp shortening from 1.05 to 0.90 $L_o$ at 0.25 $V_{max}$ for control (solid line) and potentiated (dashed line) responses. The thick black line represents the evoked stimulation period (50ms, 75Hz). (**C**) Example force-displacement plot ('work loop') that was used to quantify the work performed during each stimulus period.

*High energy phosphate consumption (HEPC)*

Muscles from both genotypes were rapidly frozen with liquid nitrogen-cooled tongs before and after the period of repeated concentric stimuli to assess the energetic cost associated with the work performed. Fluorometric assays were conducted on lyophilized (FreeZone 4.5, LABCONCO, Kansas City, MO, USA) and powdered whole muscle homogenate samples following the removal of sutures and connective tissue. Powdered muscle samples were mixed thoroughly and aliquoted to 0.5 mL microcentrifuge tubes. Metabolites were extracted from aliquots of lyophilized tissue using 0.5 M perchloric acid ($HClO_4$), and neutralized with 2.3 M potassium carbonate ($KHCO_3$). The concentrations of metabolites were analyzed in triplicate using fluorometric techniques as previously described (Bergmeyer et al., 1983; Harris et al., 1974). Three assays were used to identify the relative concentration of the metabolites of interest, including ATP, phosphocreatine (PCr), creatine (Cr), and lactate ($La^-$)(see Appendix III for detailed methods). Concentrations of ADP and inorganic phosphate ($P_i$) were calculated from known $K_{eq}$ values and ΔPCr, respectively. To adjust for variability in solid non-muscle constituents, all raw metabolite values were normalized to total Cr content (i.e. divided by the sum of PCr + Cr, then multiplied by mean total Cr content for the whole material) (Zhang et al., 2006). High-Energy Phosphate Consumption (HEPC), a measure of ATP turnover determined through anaerobic ATP production, was determined from changes in PCr, $La^-$, and ATP using the HEPC equation (HEPC = 1.5ΔLactate - ΔPCr - 2Δ[ATP]). As the study design did not allow metabolite concentrations to be sampled from the same muscle at more than one time point, the delta term (Δ) signifies the differences in metabolite concentrations between different muscles frozen before and after repetitive stimulation (i.e. *Post-PS* vs. *Final*). Multiple methods were tested to pair muscles for this comparison, however all methods resulted in the same statistical outcome (i.e. no genotype difference in HEPC). *Method 1* involved pairing the muscles in their original experimental order: full contractile experiments were conducted initially and muscles were frozen immediately after stimulation (*Final*), then parallel incubations were conducted with muscles frozen before repetitive stimulation (Post-PS). *Method 2* used the genotype difference terms presented in Table 7.5 to calculate a single, global HEPC value for each genotype (note: for this method, propagation of errors led to a vastly inflated standard deviation). *Method 3* involved the ordering of metabolite values

in each group by PCr content, as this metabolite represented the largest change between time points and thus was responsible for the greatest data variability. As mentioned previously, each method resulted in the same statistical outcome, but *Method 3* produced the least variable data and therefore offered the best opportunity for a powerful comparison of means between genotypes.

*Myosin RLC phosphate content*

Parallel experiments were conducted to determine the myosin RLC phosphate content of wildtype and skMLCK$^{-/-}$ muscles sampled prior to and following the period of concentric work to coincide with the time points for HEPC analysis. Muscles were frozen with liquid nitrogen-cooled tongs and stored at -80° C until needed. Myosin RLC phosphorylation analysis was conducted using Urea-Glycerol PAGE as previously described (Zhi et al 2005; see Appendix III for detailed methods).

*Statistical Analysis*

Two-tailed Student's t-tests were used to examine the effect of genotype (wildtype or skMLCK$^{-/-}$) on Total Work performed, High Energy Phosphate Consumption (HEPC), and Economy. A two-way repeated measures ANOVA was conducted to test the effect of genotype (wildtype or skMLCK$^{-/-}$) on work per contraction during the period of repetitive stimulation (*control* vs. *stimulation #1* vs. *stimulation #20*). To further evaluate significant interactions and planned comparisons (i.e. between genotypes), post-hoc testing was performed using the Šidák correction. A two-way factorial ANOVA was used to examine the effect of genotype (wildtype or skMLCK$^{-/-}$) and time point (*Post-PS* vs. *Final*) on the concentrations of the following metabolites: ATP, PCr, Cr and Lactate. To evaluate genotype differences and significant differences between time points, post-hoc testing was performed using Tukey's HSD test. The critical p-value for significance was $P < 0.05$. All data are reported as mean ± SEM.

## *Results*

### *Contractile Data*

*EDL muscle characteristics and isometric forces*

Summary mass, length, and physiological cross-sectional area (PCSA) of EDL muscles utilized for contractile experiments are presented in Table 7.1. No genotype differences were evident for these measurements.

*Table 7.1. Muscle characteristics from wildtype and skMLCK$^{-/-}$ mice*

| | Mass (mg) | Length (mm) | PCSA (mm$^2$) |
|---|---|---|---|
| **wildtype** | 12.50 ± 0.14 | 12.47 ± 0.14 | 2.15 ± 0.04 |
| **skMLCK$^{-/-}$** | 12.44 ± 0.19 | 12.48 ± 0.12 | 2.14 ± 0.05 |

All data are presented as Mean ± SEM (n=8). PCSA, physiological cross-sectional area

Table 7.2 contains isometric data for maximal twitch ($P_t$) and tetanic forces ($P_o$), as well as twitch: tetanus ratio, for wildtype and skMLCK$^{-/-}$ muscles. Maximal isometric twitch force was measured before all stimulation (i.e. unpotentiated), and peak tetanic force for each muscle was sampled from the first tetanus during the high-frequency (100Hz) potentiating stimulus (PS). Note: the forces produced in response to 100Hz stimulation during the PS may not represent the peak tetanic force possible in these muscles; however, previous force-frequency experiments in our lab have demonstrated that 100Hz stimulation produces ≥95% of true maximal tetanic force. Therefore, to avoid additional supramaximal stimulation, the existing data from the PS was used as a surrogate for $P_o$. No genotype differences in these measurements were found; moreover, the comparison of specific tension (force/PCSA) in wildtype and skMLCK$^{-/-}$ muscles did not reveal differences for twitches (31.7±2.3 and 31.0±2.5 mN/mm$^2$, respectively) or tetani (107.1±8.6 and 107.7±9.0 mN/mm$^2$, respectively).

*Table 7.2. Baseline isometric contractile parameters in wildtype and skMLCK$^{-/-}$ muscles*

| | $P_t$ (mN) | $P_o$ (mN) | $P_t$:$P_o$ |
|---|---|---|---|
| **wildtype** | 67.63 ± 3.63 | 229.04 ± 15.67 | 0.30 ± 0.01 |
| **skMLCK$^{-/-}$** | 65.55 ± 3.98 | 227.80 ± 14.81 | 0.29 ± 0.01 |

All data are presented as Mean ± SEM (n=8). $P_t$, peak twitch force; $P_o$, peak tetanic force (100Hz); $P_t$:$P_o$, twitch to tetanus ratio

*Potentiation of concentric force and work during repetitive stimulation*

An identical stimulation and ramp-shortening paradigm was elicited once before (*control*) and twenty times following the PS: absolute force and work responses are presented in Table 7.3 and relative changes in work performed per stimulation (i.e. PTP) are summarized in Figure 7.2, Panel A. Representative active force traces are displayed in Figure 7.2, Panel B for the *control* stimulation as well as the first and last stimuli in the potentiated train. Genotype differences in concentric force and work were evident in every comparison, including both control and potentiated responses ($P < 0.05$).

Following the PS, concentric forces were potentiated in both genotypes, although the effect was greater in wildtype than skMLCK$^{-/-}$ muscles (to 1.38±0.03 and 1.10±0.04, respectively)($P < 0.05$). During the 20s of repetitive stimulation following the PS, skMLCK$^{-/-}$ forces were consistently potentiated between 9 and 15% above the *control* value. The magnitude of force potentiation in wildtype muscles during this period remained between 30 and 35%; however, the force response at stimulation #20 was slightly lower than stimulation #1 (from 38% to 30%, respectively).

Analysis of the concentric portion of the force-displacement function for each stimulus (i.e. concentric work) showed that work increased significantly following the PS in both genotypes (to 1.10±0.05 and 1.51±0.03 in skMLCK$^{-/-}$ and wildtype muscles, respectively)($P < 0.05$). As with peak force, the magnitude of the effect was significantly greater in wildtype than skMLCK$^{-/-}$ muscles ($P < 0.05$). Interestingly, although the PTP effect in skMLCK$^{-/-}$ muscles for peak force and work were similar (10%), the enhancement of work in wildtype muscles was greater than the enhancement of peak force (51% vs. 38%).

The work performed during each of the twenty potentiated stimuli was summed for each muscle to quantify the total work performed in the potentiated state (see Figure

7.4, Panel A). The moderate genotype difference in work per stimulation produced a substantial cumulative effect when pooled, as wildtype muscles performed ~58% more total work than skMLCK$^{-/-}$ muscles in response to the same stimulus regime ($P < 0.05$).

*Kinetics of force development and relaxation*

Summary data for rate of force development (+dP/d*t*) and rate of relaxation (-dP/d*t*) during the *control* condition, as well as during the first (*stimulation #1*) and last (*stimulation #20*) of the potentiated stimuli are presented in Table 7.3. Although there were no genotype differences in +dP/d*t* during the *control* condition, the wildtype value was greater than the skMLCK$^{-/-}$ following the PS ($P < 0.05$). This represents a relative increase of ~30% in wildtype muscles vs. ~12% in skMLCK$^{-/-}$ muscles as a result of the PS. This genotype difference was not maintained until stimulation #20, although wildtype and skMLCK$^{-/-}$ values were both still elevated above the control value (1.18±0.03 and 1.15±0.02, respectively)($P < 0.05$).

Interestingly, rate of force relaxation (-dP/d*t*) was faster in wildtype muscles than skMLCK$^{-/-}$ muscles before and following the PS ($P < 0.05$). Following the PS, -dP/d*t* increased similarly in both genotypes (~15%)($P < 0.05$). The faster kinetics of relaxation persisted throughout the potentiated stimulation period in skMLCK$^{-/-}$ muscles but wildtype values returned to near-control values by stimulation #20.

*Table 7.3. Concentric contractile parameters before and after the PS*

| | Control | Post-PS | Final |
|---|---|---|---|
| *Peak Force, mN* | | | |
| **wildtype** | $53.57 \pm 2.05^{a}$ | $73.61 \pm 2.23^{c}$ | $69.09 \pm 1.9^{b}$ |
| **skMLCK$^{-/-}$** | $43.17 \pm 1.85^{a}*$ | $47.54 \pm 2.98^{b}*$ | $48.07 \pm 3.00^{b}*$ |
| *Work per stim, J.kg$^{-1}$* | | | |
| **wildtype** | $3.21 \pm 0.17^{a}$ | $4.81 \pm 0.19^{c}$ | $4.59 \pm 0.18^{b}$ |
| **skMLCK$^{-/-}$** | $2.55 \pm 0.15^{a}*$ | $2.82 \pm 0.18^{b}*$ | $2.97 \pm 0.23^{b}*$ |
| *+dP/dt, mN.s$^{-1}$* | | | |
| **wildtype** | $2303 \pm 89^{a}$ | $2992 \pm 132^{c}$ | $2718 \pm 134^{b}$ |
| **skMLCK$^{-/-}$** | $2143 \pm 81^{a}$ | $2407 \pm 129^{b}*$ | $2467 \pm 138^{b}$ |
| *-dP/dt, mN.s$^{-1}$* | | | |
| **wildtype** | $1659 \pm 51^{a}$ | $1901 \pm 75^{b}$ | $1727 \pm 90^{a}$ |
| **skMLCK$^{-/-}$** | $1411 \pm 67^{a}*$ | $1601 \pm 86^{b}*$ | $1538 \pm 64^{b}*$ |

All data are presented as Mean ± SEM (n=8). +dP/d*t*, rate of force development; -dP/d*t*, rate of force relaxation.
*skMLCK$^{-/-}$ value is less than wildtype value ($P < 0.05$)
$^{a,b,c}$ within group comparisons ($P < 0.05$)

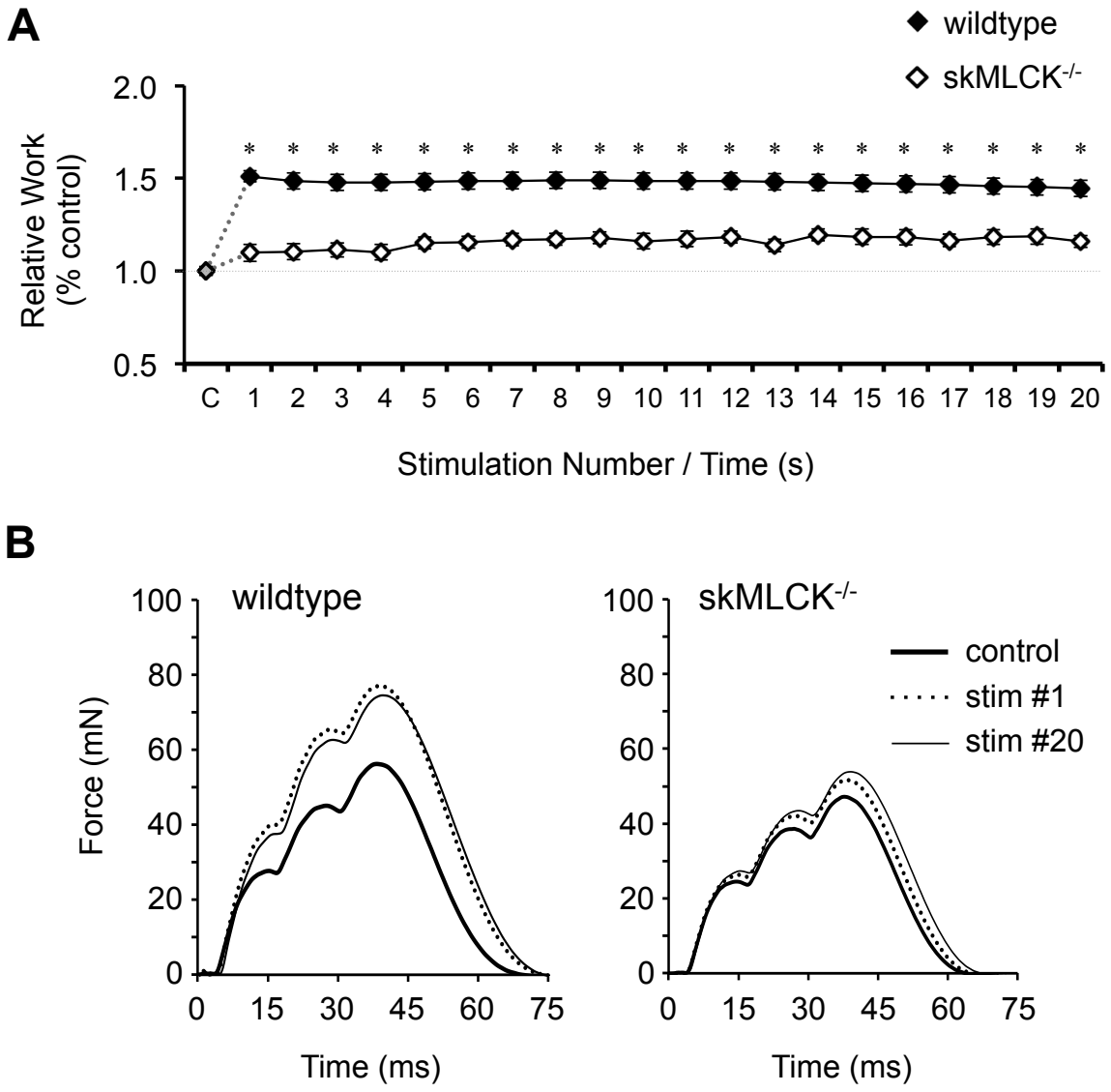


*Figure 7.2. Potentiation of work and representative force traces*

(**A**) Relative change in work performed per stimulation (i.e. potentiation) when compared to the control response for each genotype. *wildtype value is greater than the corresponding skMLCK$^{-/-}$ value at each time point ($P < 0.05$, n=8). (**B**) Shown are representative active force traces for muscles of both genotypes; individual traces show *control* responses (solid, thick line) overlaid with the first (dotted line) and last (solid, thin line) of the series of potentiated stimuli.

***Biochemical Data***

*Muscle metabolites*

Fluorometric assays were used to determine the concentration of ATP, PCr, Cr, and Lactate in samples extracted from muscles frozen before and after the period of repetitive concentric stimulation (n=8). In both genotypes, this activation resulted in a depletion of [PCr] and an accumulation of [Cr] and [Lactate] ($P < 0.05$). In contrast, [ATP] levels were sustained in both genotypes when samples frozen before and after stimulation were compared. Genotype differences were evident for [ATP], as skMLCK$^{-/-}$ levels were lower than wildtype values ($P < 0.05$). Otherwise, lactate levels following stimulation were lower in skMLCK$^{-/-}$ muscles than wildtype muscles ($P < 0.05$).

*Table 7.4. Metabolite concentrations normalized to total creatine content*

| | [ATP] | [PCr] | [Cr] | [Lactate] |
|---|---|---|---|---|
| *Post-PS values* | | | | |
| **wildtype** | 26.7 ± 0.5 | 49.2 ± 1.5 | 52.0 ± 1.5 | 3.5 ± 0.1 |
| **skMLCK$^{-/-}$** | 21.7 ± 0.4* | 46.9 ± 2.1 | 55.5 ± 2.1 | 2.8 ± 0.2 |
| *Final values* | | | | |
| **wildtype** | 26.9 ± 0.4 | 38.4 ± 0.6† | 60.5 ± 0.6† | 8.5 ± 0.1† |
| **skMLCK$^{-/-}$** | 21.2 ± 0.4* | 36.8 ± 1.0† | 63.8 ± 1.2† | 6.0 ± 0.2†* |

All data are presented as Mean ± SEM (n=8).
*skMLCK$^{-/-}$ value is less than wildtype value ($P < 0.05$);
† within group comparisons, *Final* value different from *Post-PS* value ($P < 0.05$).

*High energy phosphate consumption (HEPC)*

Within each genotype, the differences in muscle metabolite concentrations between time points (i.e. *Post-PS* vs. *Final*) were used to estimate the energetic cost of the muscular work performed (i.e. anaerobic ATP turnover). Table 7.5 includes the mean difference terms for each genotype (i.e. -2Δ[ATP], Δ[PCr], 1.5Δ[Lactate]). Of these values, only Lactate values were different between genotypes, as the increase in [Lactate] following the stimulation period was smaller in skMLCK$^{-/-}$ vs. wildtype muscles ($P < 0.05$). In both genotypes, the degradation of PCr was similar, and as mentioned above,

ATP levels were not significantly different between time points (i.e. ATP levels were buffered).

The results of HEPC calculations are shown in Figure 7.4, Panel B for all wildtype and skMLCK$^{-/-}$ muscles. Although wildtype values for HEPC were ~18% greater than skMLCK$^{-/-}$ counterparts, this difference was not statistically significant ($P$ = 0.27).

*Table 7.5. High Energy Phosphate Consumption: Calculation Terms*

| | -2Δ[ATP] | Δ[PCr] | 1.5Δ[Lactate] |
|---|---|---|---|
| **wildtype** | -0.47 ± 1.41 | 10.80 ± 2.79 | 7.45 ± 0.22 |
| **skMLCK$^{-/-}$** | 0.89 ± 0.91 | 10.11 ± 3.43 | 4.88 ± 0.42* |

All data are presented as Mean ± SEM (n=8).
*skMLCK$^{-/-}$ value is significantly lower than wildtype value ($P < 0.05$).

*Myosin RLC phosphorylation*

EDL muscles were quick-frozen with liquid nitrogen-cooled tongs during incubations conducted in parallel with the contractile experiments; representative blots and summary data are shown in Figure 7.3, Panel A and B, respectively. As expected, wildtype samples frozen ~15s after the PS and following the 20s period of repetitive stimulation displayed a prominent phosphorylated band. The fractional RLC phosphate content was similar between these time points (~41-42%), which spanned the interval over which total muscular work and HEPC were measured. In stark contrast, and consistent with the removal of the dedicated enzyme (skMLCK) for this mechanism, skMLCK$^{-/-}$ samples frozen following the PS or the 20s period of intermittent stimulation (75Hz) did not display an obvious or consistent phosphorylated band. Fractional RLC phosphate content for these muscles was ~2-3% (range 1-4%). This finding is consistent with previous reports that a small degree of baseline phosphorylation (≤9%) may exist in skMLCK$^{-/-}$ muscles, which may result from the phosphorylation of an adjacent serine residue by an undetermined kinase that is not activated by stimulation (Zhi et al, 2005).

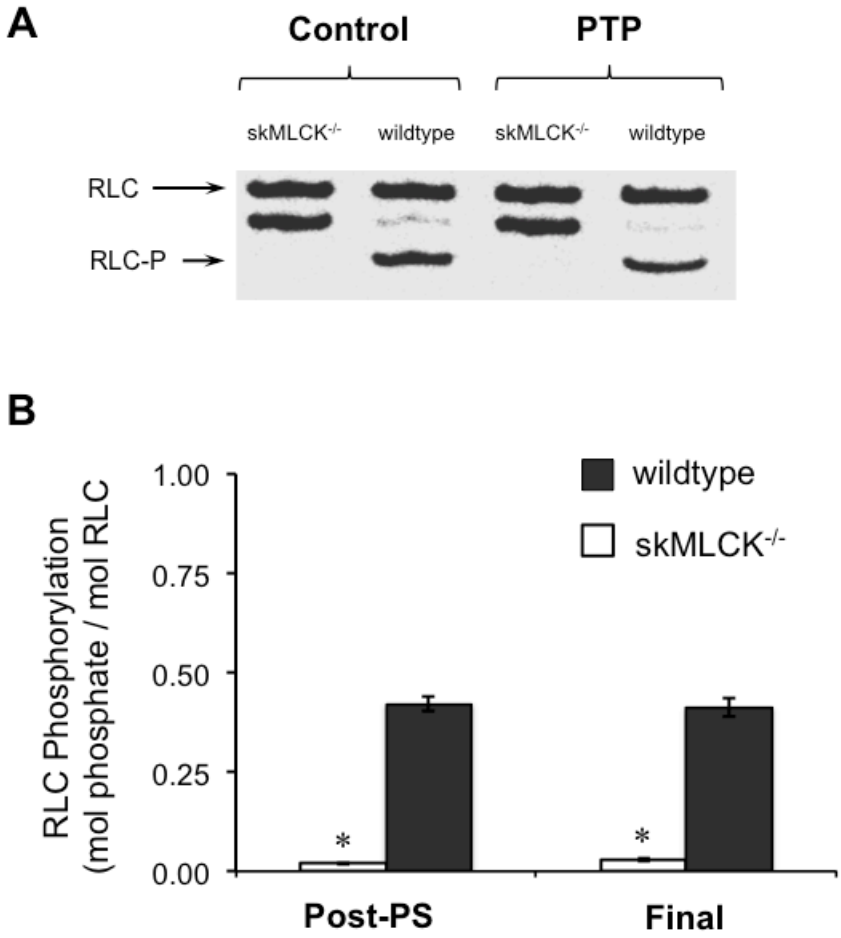


*Figure 7.3. Myosin RLC phosphorylation analysis*

(**A**) Representative blots from Urea-glycerol PAGE analysis of wildtype and skMLCK$^{-/-}$ whole muscle homogenates quick-frozen before and immediately after the period of repeated stimuli. Protein density was measured using Image Studio Lite, LI-COR Biosciences, Lincoln, Nebraska, USA, and fractional RLC phosphate content was calculated as the ratio of the phosphorylated band to total light chain content (RLC phosphorylation = [RLC-P] / [RLC] + [RLC-P]). (**B**) Myosin RLC phosphate content in wildtype and skMLCK$^{-/-}$ muscles.
*skMLCK$^{-/-}$ value is less than corresponding wildtype value ($P < 0.05$)

***Economy***

The contractile Economy for each genotype was calculated from the work performed by each muscle and the HEPC calculated between paired muscles frozen before and after the period of stimulation (as explained above). Figure 7.4, Panel C presents the results of this analysis for wildtype and skMLCK$^{-/-}$ muscles. Importantly, there was no statistical difference in Economy between the genotypes ($P$ = 0.27). This result was produced by opposite findings in contractile vs. biochemical analyses; specifically, the robust enhancement of work performed in wildtype muscles was associated with a small (~18%) but non-significant increase in HEPC.

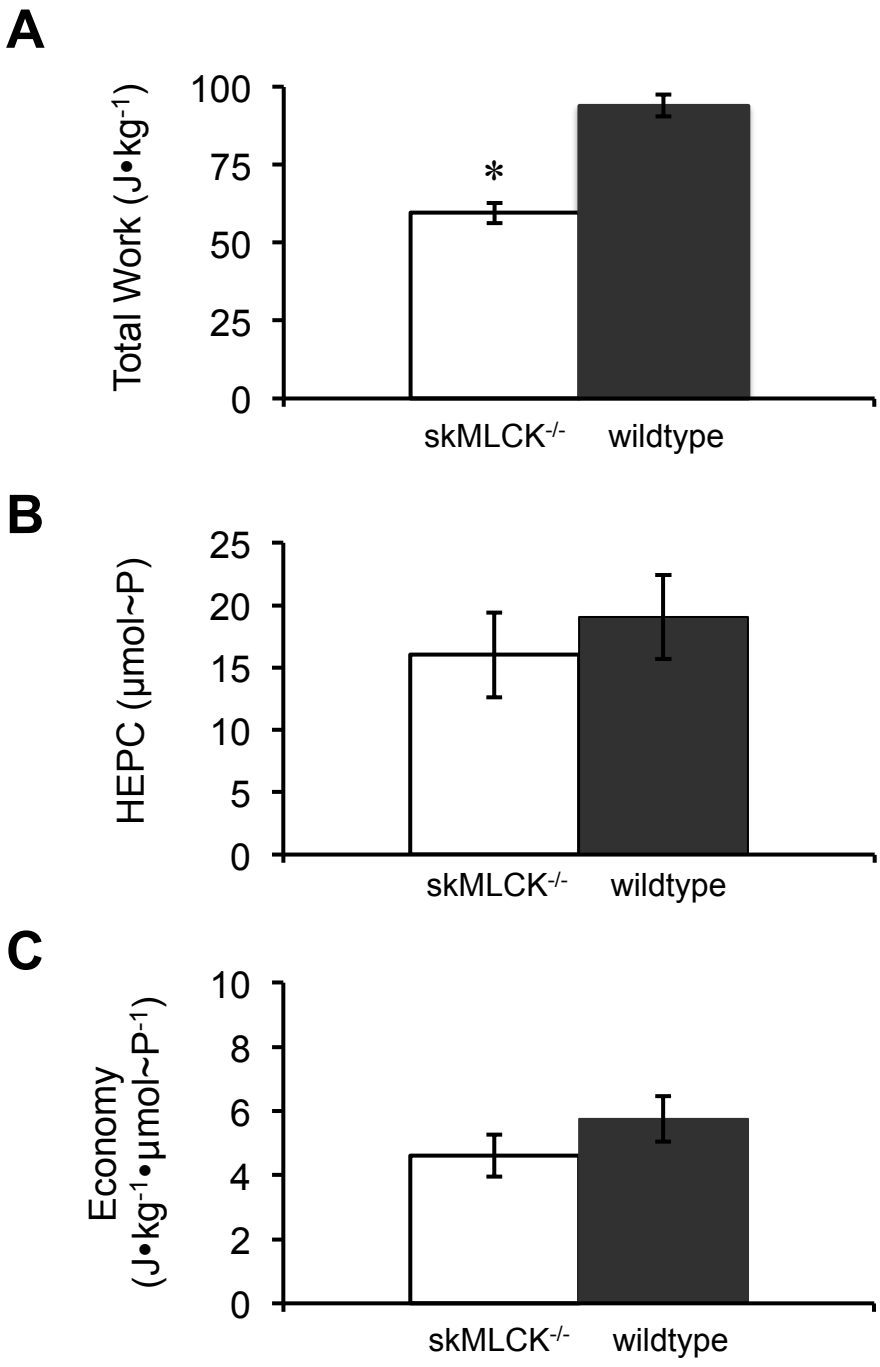


*Figure 7.4. Work Performed, HEPC, and Economy in wildtype and skMLCK$^{-/-}$ muscles*

(**A**) Total work performed during the series of repeated stimuli that followed the potentiating stimulus. *skMLCK$^{-/-}$ muscles performed significantly less total work than wildtype muscles ($P < 0.05$, n=8). (**B**) High energy phosphate consumption (HEPC) calculated from muscle metabolite values measured in frozen muscle homogenates ($P = 0.27$, n=8). (**C**) Economy (i.e. Total Work / HEPC) during repeated stimuli in wildtype and skMLCK$^{-/-}$ muscles ($P = 0.27$).

## *Discussion*

The purpose of this study was to determine (by directly comparing to wildtype counterparts) whether the ablation of RLC phosphorylation in skMLCK$^{-/-}$ mice would influence contractile economy during a period of intermittent concentric work in the potentiated state. The main finding was that wildtype muscles with an intact RLC phosphorylation mechanism produced ~58% more work than skMLCK$^{-/-}$ muscles during the brief period of repetitive stimulation without significantly increasing HEPC or altering economy. Myosin RLC phosphorylation is understood to augment the rate of crossbridge binding (Sweeney and Stull, 1990), and PTP is positively associated with shortening speed (Gittings et al. 2012); therefore, the relatively fast shortening ramps used in this study (0.40 $V_{max}$), along with brief stimulation duration (50 ms), were effective in exploiting this force potentiation mechanism. The greater potentiation of work than the augmentation of peak force in wildtype muscles is additional evidence that physiologically relevant parameters of muscle function are especially sensitive to modulation by myosin RLC phosphorylation (as discussed by Vandenboom et al. 2013). The complete results will be further discussed with respect to the role of RLC phosphorylation-dependent potentiation as a modulator of contractile function and energetics during physiological patterns of activation, such as those present during locomotion (Leblond et al, 2003) or in freely-moving animals *in vivo* (Hennig and Lomo, 1985; 1987).

*Energetic considerations of PTP and myosin RLC phosphorylation*

Our direct comparison of HEPC in wildtype and skMLCK$^{-/-}$ muscles demonstrated a small but non-significant difference in anaerobic energy turnover between genotypes. However, the study design/model does not allow us to separate the individual contributions of increased work (i.e. myosin-ATPase activity) and the energetic cost of maintaining RLC phosphorylation (i.e. skMLCK activity) to total HEPC. The greater final [Lactate] and larger change in lactate following stimulation (1.5*Δ[Lactate]) in wildtype muscles is the only statistical evidence of greater energetic turnover in the presence of myosin RLC phosphorylation. However, as these muscles performed much more work than skMLCK$^{-/-}$ counterparts during the same period of time this finding does not permit us to make conclusions about the interaction of myosin RLC phosphorylation with total ATP turnover. The observation that [ATP] was greater in wildtype vs.

skMLCK$^{-/-}$ muscles both before and after the period of repetitive stimulation is surprising and not readily explainable: there is no apparent reason that muscles in the presence of myosin RLC phosphorylation would contain a larger reservoir of ATP. However, this disparity should not have influenced the present results or conclusions as ATP levels in both groups were equally maintained during the short period of concentric work (i.e. -2Δ[ATP]), thus contributing little to the calculation of HEPC.

*Potentiation in skMLCK$^{-/-}$ muscles*

The potentiation of concentric force and work in skMLCK$^{-/-}$ muscles is part of the mounting evidence of alternate mechanism(s) that may modulate contractile function independent of myosin RLC phosphorylation (as reviewed by Vandenboom et al, 2013). In the current work, the potentiation of force and work in skMLCK$^{-/-}$ muscles was ~20-25% of the total wildtype response (~10 vs. 40-50%, respectively). However, if we make the assumption that this myosin RLC phosphorylation-independent mechanism of force enhancement was also present in wildtype muscles, then it may represent ~25-35% of the potentiation effect under the current experimental conditions. Recent evidence from our lab has shown that PTP in skMLCK$^{-/-}$ muscles was contraction-type dependent for 60Hz stimulation, as isometric responses showed posttetanic depression but concentric forces were augmented ~20% at 0.25 $V_{max}$ (Gittings et al. 2015). Thus, it is evident that alternate mechanisms of potentiation may be more sensitive to dynamic conditions, like wildtype muscles (as reviewed by Vandenboom et al. 2013). Finally, the present study has shown that the level of potentiation in skMLCK$^{-/-}$ was surprisingly stable throughout the period of repetitive stimulation (Figure 7.2, Panel A). Recent evidence has suggested that elevated resting $Ca^{2+}$ levels may potentiate twitch force in the absence of myosin RLC phosphorylation; however, this effect dissipated quickly and demonstrated a very brief time course (≤20s)(Smith et al. 2013). In the current experimental design, the repetitive concentric stimulation protocol did not commence until ~15s after the PS, therefore the skMLCK$^{-/-}$ muscles demonstrated a stable amount of potentiation between 15 and 35s. Therefore, we conclude that the operative myosin RLC phosphorylation-independent mechanism(s) may be stimulation-dependent. To this end, if elevated resting $Ca^{2+}$ contributed to PTP after the PS, the small duty cycle (0.05) used presently may have been sufficient to maintain the effect for the time period investigated.

*Economy of concentric work in the potentiated state*

The present study can be used to directly evaluate the findings of Abbate et al. (2001), who measured HEPC in potentiated rat hindlimb muscles *in situ* (to our knowledge the only study to specifically investigate the present research question under similar conditions). In that study, muscle work was measured in two groups during 10 repetitive concentric contractions at 60 Hz; in one group the series of contractions were preceded by an isometric potentiating stimulus (PRC) and the other was not (RC). The authors concluded that, when preceded by an isometric stimulus to potentiate the muscle, the increase in energy turnover (HEPC) in the potentiated state was greater than the increase in total work performed. Thus, it was concluded that PTP increases the energy cost of contractions (i.e. lower economy) in rat fast muscle, and this result was likely due to the increased performance of the muscle and not necessarily due to the potentiation mechanism itself (Abbate et al, 2001). Importantly, this study was limited by the following factors: *i)* in the non-potentiated group (RC), work per contraction increased during the 10 stimuli (i.e. staircase potentiation), *ii)* in the non-potentiated group (RC), RLC phosphate content was elevated to ~40% after the 10 contractions, *iii)* there was no control condition for stimulation without RLC phosphorylation, and *iv)* the PRC group received significantly more total stimulation than the RC group (+ 160Hz, 1s isometric tetanus). Consequently, the present work aimed to specifically address these limitations and experimental design challenges with the use of skMLCK$^{-/-}$ muscles. Importantly, the current work can account for each of the factors listed above: *i)* work per contraction was maintained at a stable level during the stimulus period, *ii)* the skMLCK$^{-/-}$ group is a true control condition for RLC phosphorylation, *iii)* both groups received the same stimulation paradigm, and *iv)* RLC phosphate content was stable in both groups when compared before and after the stimuli. In the present study, the larger amount of absolute work performed by wildtype muscles versus skMLCK$^{-/-}$ muscles (~58%) in the presence of RLC phosphorylation was of greater magnitude than the associated increase in HEPC (~18%). Thus, in addition to the finding that economy was not significantly different between genotypes, this result implies that an increase in performance by potentiation is not directly related or proportional to an increase in energy cost for work.

*Genotype differences in normalized force traces: effects of potentiation*

In our experiments, muscles in both groups were stimulated over the same length excursion and for the same duration (i.e. isovelocity). Thus, when evaluating differences

in work performed between groups, it is most prudent to focus on factors that influence the average force produced during the stimulus. Furthermore, if the relative difference in total work and total energy turnover are not directly correlated or proportional between groups, factors that might uncouple these elements should be considered in order to better understand how myosin RLC phosphorylation-mediated potentiation might influence economy. At the functional level of the crossbridge, the well-studied primary outcome of myosin RLC phosphorylation (i.e. the increased rate of crossbridge attachment)(Metzger et al, 1989) may be an important modulatory factor that influences: *i)* the number of crossbridges bound, or *ii)* the force produced per crossbridge. To evaluate this argument, Figure 7.5 displays force traces in both genotypes that have been normalized to peak force to allow direct comparison of contraction form/shape. During the control condition, there is little disparity between genotypes; however, clear differences arise in the muscles following the PS. For example, during force development wildtype muscles displayed greater summation between individual pulses, a factor that led to peak forces ~50% greater than in skMLCK$^{-/-}$ muscles. However, if the increased force production in wildtype muscles were due solely to a greater number of force-producing crossbridges, then the increase in ATP turnover should be similar in magnitude to the potentiation in force/work. To this end, it is plausible that myosin RLC phosphorylation may permit a greater fraction of energy liberated by each crossbridge cycle to be transferred longitudinally (i.e. increased force per ATP hydrolyzed). This effect may be the result of an increase in stiffness of the contractile apparatus via enhanced crossbridge binding and stiffening of the myosin lever arm (Sweeney and Stull, 1990; Greenberg et al, 2009), or a reduction in muscle-tendon compliance produced by rapid initial force development (as predicted by Hill, 1951). Interactions of potentiation via myosin RLC phosphorylation and mechanical factors such stiffness and compliance are not well understood, but may represent an essential relationship that gives this mechanism physiological/adaptive importance.

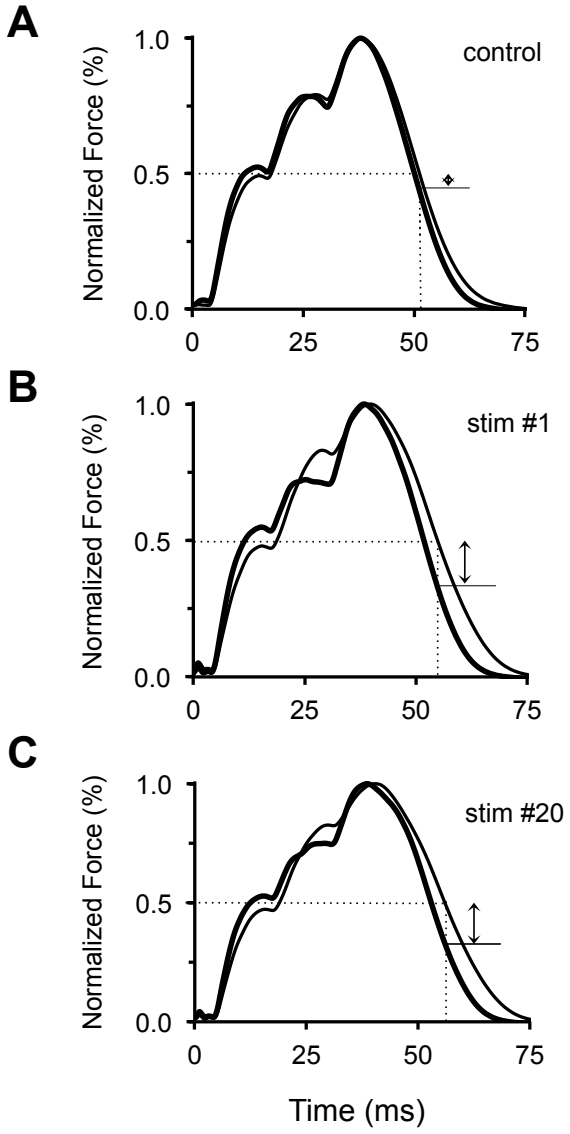


*Figure 7.5. Normalized active force traces*

Normalized active force traces for the *control* activation prior to the PS, as well as for the first (*stim #1*) and last (*stim #20*) of the repeated concentric activations in the potentiated state. In each panel, the thick line represents the average skMLCK$^{-/-}$ response and the thin line represents the average wildtype response for all muscles used in the contractile experiments (n=8). Traces were normalized to their own peak force to illustrate the genotype differences and in unfused tetanic shape when potentiated. At the point of half-relaxation in wildtype muscles (dotted line), the corresponding relative force level in skMLCK$^{-/-}$ muscles was 0.45 (*control*), 0.32 (*stim #1*), and 0.32 (*stim #20*).

An alternative contributor to the greater work performed in wildtype muscles is the prolonged force relaxation phase as compared to skMLCK$^{-/-}$ muscles (see Figure 7.5). To indicate these differences, the relative force level of skMLCK$^{-/-}$ muscles was noted at the half relaxation point (i.e. 0.50) of wildtype traces in each condition: force in skMLCK$^{-/-}$ muscles had decreased to ~0.45, 0.32, and 0.32 for the *control*, *stimulation #1*, and *stimulation #20*, respectively. The more rapid relaxation of force in the absence of myosin RLC phosphorylation has also been observed during high frequency isometric tetani (Gittings et al, 2011) and during relaxation from steady state force in skinned rabbit psoas fibres (Patel et al, 1998). However, despite the prolonged force response apparent in wildtype muscles, the maximal rate of force relaxation was lower in skMLCK$^{-/-}$ muscles at all three time points (data in Table 7.3). It has been observed that relaxation rates are positively associated with force/activation level (Patel et al, 1998); therefore, it is unclear whether myosin RLC phosphorylation itself reduced relaxation rates in the current study, as force levels between the groups were very different. Otherwise, the prolonged period of force relaxation in wildtype muscles observed currently may be attributed to a genotype difference in: *i)* the rate of $Ca^{2+}$ dissociation from troponin and/or sequestration into the SR, *ii)* a slowing of the myosin crossbridge cycle or detachment process, or *iii)* an increase in crossbridge attachment/re-binding during relaxation due directly to myosin RLC phosphorylation. However, in the intact muscle model it is not possible to individually parse out these potential factors. There is ongoing debate with respect to the effect of myosin RLC phosphorylation on the crossbridge cycle, and whether it increases the duty cycle of the crossbridge by slowing ADP release and/or limits the rate of crossbridge detachment and shortening velocity (Franks-Skiba et al, 2006; Greenberg et al, 2009; Greenburg et al, 2010; Karatzaferi et al, 2008). Conversely, there is opposing mechanistic evidence that myosin does not influence the rate of crossbridge detachment in skinned fibres (Metzger et al, 1989; Persechini et al, 1985; Sweeney and Stull, 1990), or as evidenced by measurement of unloaded shortening velocity in intact muscles (Butler et al, 1983; Gittings et al, 2011). These contradictory reports are difficult to reconcile due to the inherent differences between experimental models and methods used. The current findings are consistent with the theory that elevated myosin RLC phosphate content may decrease the energy cost for force production via an increase in the duty cycle of the crossbridge powerstroke, an effect

which would allow wildtype muscles to perform more work without a proportional increase in energetic cost.

*Force potentiation: Implications for the economy of muscular work in vivo*

In light of the present findings we cannot definitively quantify the effect that potentiation might have on the economy of *in vivo* muscle function. However, our observation that muscular work was meaningfully enhanced in wildtype muscles vs. skMLCK$^{-/-}$ muscles, without a significant additional energetic cost or adjustment to economy, has important physiological implications. A proximate consequence of this finding is that, to perform a given absolute amount of work, potentiated muscles in the presence of myosin RLC phosphorylation may have a reduced activation requirement (i.e. reduced MU firing rate or fewer active MUs). Interestingly, this concept is consistent with reports from human studies that motor unit firing rates required to maintain submaximal force levels may decrease when muscles are potentiated (Adam and De Luca, 2005; Inglis et al, 2011; Smith et al, 2011); an outcome which may reflect an afferent feedback loop that modulates central motor drive (Inglis et al, 2011). If this down-regulation in muscular activation was significant, it could also reduce the energetic requirement for ion trafficking in the muscle (i.e. $Na^+/K^+$-ATPase and SERCA) and thus may render muscles more economical.

Finally, it is unlikely that muscles operate under conditions of constant load or shortening velocity *in vivo*, as physiological activation of muscles such as the EDL may be initiated near-isometric and proceed to shorten once the required force level is met (James et al., 1995; Marsh, 1999). In potentiated muscles, a greater rate and extent of force production via myosin RLC phosphorylation allows a given amount of work to be performed in a shorter time period (i.e. greater power)(Grange et al, 1995; MacIntosh and Bryan, 2002; MacIntosh et al, 2008). Moreover, the augmented rate of force development via enhanced crossbridge binding in the potentiated state might permit intact muscle-tendon complexes to perform more negative work during movements that support body mass (i.e. locomotion) and thus transfer a greater fraction of series-elastic energy into positive work.

*Assumptions and limitations*

i. We did not partition total ATP turnover to separately account for the fraction of energy used for ion pumping (i.e. activation energy turnover, $Na^+/K^+$-ATPase, SERCA) vs. energy used to power myosin force development (i.e. crossbridge energy turnover, Myosin-ATPase); thus, we cannot account for genotype-dependent differences in energy consumed for each component, if present.

ii. Our measurement of energetic cost for work (i.e. HEPC) does not quantify the aerobic contribution to total ATP usage; therefore, the measurement of HEPC represents the energy used for substrate level/anaerobic metabolic processes. Westra et al (1988) have reported that for sustained isometric tetani at 60Hz up to 30s, aerobic contribution to total energy turnover is ≤9% (rat quadriceps, 35° C). Moreover, the muscle type used in that study has a more oxidative fibre type profile than mouse EDL muscles (see Ariano et al, 1973; Delp and Duan, 1996 for fiber typing info); thus this estimate of aerobic contribution may be an overestimation with respect to the current study. Importantly, the current study assumes that there is no genotype-dependent aerobic contribution to total energy usage that might influence the conclusions and interpretation of the results.

iii. Sodium cyanide (NaCN) has previously been used to inhibit mitochondrial oxidative phosphorylation (Albaum, 1946; Barsotti & Butler, 1984), and the use of this technique would in theory have eliminated aerobic contribution to metabolism. However, it has been shown that NaCN can induce a brief potentiation of twitch force that is followed by a progressive depression of force (Adler et al. 1999). These authors also suggested that the depression in force was most likely caused by progressive acidosis due to increased lactate production and a possible reduction in the sensitivity of the contractile proteins to $Ca^{2+}$ by NaCN exposure. Consequently, due to these potential confounding factors and the assumption that aerobic contributions would be minor during such a brief period of work, the choice was made not to use NaCN in our experiments.

iv. We did not actively monitor or measure sarcomere lengths during concentric stimulation. Therefore, it is unclear how nonuniformities during shortening (Julian and Morgan, 1979) or relaxation (Edman and Flitney, 1982) may have contributed to the differences in force development and relaxation observed between genotypes.

v. The study design allowed the measurement of economy over a period of steady work output and myosin RLC phosphorylation. However, this period was kept relatively brief (20s) to avoid any complicating effects of fatigue on the results, which may have become genotype dependent (given the large discrepancy in work output between wildtype and skMLCK$^{-/-}$ muscles). Importantly, unlike total work performed, differences between genotypes in energy turnover during this period may have been too small to quantify statistically without a prolonged assessment period OR by using an improved method for assessment of ATP turnover (higher measurement precision/resolution).

vi. The current results and interpretations are specific to the experimental model/conditions studied, and caution should be used when extrapolating these findings to other settings or to describe *in vivo* function. For example, PTP associated with myosin RLC phosphorylation is stimulation frequency, shortening speed, fibre type, and temperature-dependent. Consequently, the relationship between work/power and energy cost for contraction (i.e. Economy) may be quite variable depending on the study parameters.

vii. For all metabolite calculations, it is assumed that the muscle preparation relies solely on anaerobic substrate-level phosphorylation during the brief contractile bout. In addition, HEPC is calculated using an equation with the following inherent assumptions: (i) glycogen is the sole source for lactate production during contraction, and (ii) any decrease in ATP within the muscle is associated with a stoichiometric increase in IMP (Zhang et al., 2006).

## *References*


Abbate, F., Van Der Velden, J., Stienen, G. J., & de Haan, A. (2001). Post-tetanic potentiation increases energy cost to a higher extent than work in rat fast skeletal muscle. Journal of Muscle Research and Cell Motility, 22(8), 703–710.

Adam, A., & De Luca, C. J. (2005). Firing rates of motor units in human vastus lateralis muscle during fatiguing isometric contractions. Journal of Applied Physiology, 99(1), 268–280.

Albaum, H. G., Tepperman, J., & Bodansky O. (1946). The in vivo inactivation by cyanide of brain cytochrome oxidase and its effect on glycolysis and on the high energy phosphorus compounds in brain. Journal of Biological Chemistry, 164, 45–51.

Allen, D. G., Lamb, G. D., & Westerblad, H. (2008). Skeletal Muscle Fatigue: Cellular Mechanisms. Physiological Reviews, 88(1), 287–332.

Ariano, M. A., Edgerton, V. R., & Armstrong, R. B. (1973). Hindlimb Muscle Fiber Populations of Five Mammals. Journal of Histochemistry & Cytochemistry, 21(1), 51–55.

Barclay, C. J., Lichtwark, G. A., & Curtin, N. A. (2008). The energetic cost of activation in mouse fast-twitch muscle is the same whether measured using reduced filament overlap or N-benzyl-p-toluenesulphonamide. Acta Physiologica (Oxford, England), 193(4), 381–391.

Barsotti, R. J., & Butler, T. M. (1984). Chemical energy usage and myosin light chain phosphorylation in mammalian skeletal muscle. Journal of Muscle Research and Cell Motility, 5(1), 45–64.

Bergmeyer, H. U., Grabl, M., & Walter, H. E. (1983). Methods in enzymatic analysis.

Blumenthal, D. K., & Stull, J. T. (1980). Activation of skeletal muscle myosin light chain kinase by calcium(2+) and calmodulin. Biochemistry (Washington), 19(24), 5608–5614.

Brown, I. E., & Loeb, G. E. (1998). Post-Activation Potentiation—A Clue for Simplifying Models of Muscle Dynamics. American Zoologist, 38(4), 743–754.

Butler, T. M., Siegman, M. J., Mooers, S. U., & Barsotti, R. J. (1983). Myosin light chain phosphorylation does not modulate cross-bridge cycling rate in mouse skeletal muscle. Science, 220(4602), 1167–1169.

Crow, M. T., & Kushmerick, M. J. (1982a). Myosin light chain phosphorylation is associated with a decrease in the energy cost for contraction in fast twitch mouse muscle. Journal of Biological Chemistry, 257(5), 2121–2124.

Crow, M. T., & Kushmerick, M. J. (1982b). Phosphorylation of myosin light chains in mouse fast-twitch muscle associated with reduced actomyosin turnover rate. Science, 217(4562), 835–837.

Delp, M. D., & Duan, C. (1996). Composition and size of type I, IIA, IID/X, and IIB fibers and citrate synthase activity of rat muscle. Journal of Applied Physiology, 80(1), 261–270.

Edman, K. A. P., & Flitney, F. W. (1982). Laser diffraction studies of sarcomere dynamics during "isometric" relaxation in isolated muscle fibres of the frog. The Journal of Physiology, 329(1), 1–20.

Enoka, R. M., & Stuart, D. G. (1992). Neurobiology of muscle fatigue. Journal of Applied Physiology, 72(5), 1631–1648.

Franks-Skiba, K., Lardelli, R., Goh, G., & Cooke, R. (2007). Myosin light chain phosphorylation inhibits muscle fiber shortening velocity in the presence of vanadate. American Journal of Physiology. Regulatory, Integrative and Comparative Physiology, 292(4), R1603–R1612.

Gandevia, S. C. (2001). Spinal and supraspinal factors in human muscle fatigue. Physiological Reviews.

Gittings, W., Aggarwal, H., Stull, J. T., & Vandenboom, R. (2015). The force dependence of isometric and concentric potentiation in mouse muscle with and without skeletal myosin light chain kinase. Canadian Journal of Physiology and Pharmacology, 93(1), 23–32.

Gittings, W., Huang, J., & Vandenboom, R. (2012). Tetanic force potentiation of mouse fast muscle is shortening speed dependent. Journal of Muscle Research and Cell Motility, 33(5), 359–368.

Gittings, W., Huang, J., Smith, I. C., Quadrilatero, J., & Vandenboom, R. (2011). The effect of skeletal myosin light chain kinase gene ablation on the fatigability of mouse fast muscle. Journal of Muscle Research and Cell Motility, 31(5-6), 337–348.

Goldspink, G. (1978). Energy turnover during contraction of different types of muscle. Biomechanics VI-A.

Grange, R. W., Cory, C. R., Vandenboom, R., & Houston, M. E. (1995). Myosin phosphorylation augments force-displacement and force-velocity relationships of mouse fast muscle. Am J Physiol, 269(3 Pt 1), C713–24.

Grange, R. W., Vandenboom, R., & Houston, M. E. (1993). Physiological significance of myosin phosphorylation in skeletal muscle. Canadian Journal of Applied Physiology, 18(3), 229–242.

Greenberg, M. J., Mealy, T. R., Watt, J. D., Jones, M., Szczesna-Cordary, D., & Moore, J. R. (2009). The molecular effects of skeletal muscle myosin regulatory light chain phosphorylation. American Journal of Physiology. Regulatory, Integrative and Comparative Physiology, 297(2), R265–74.

Harris, R. C., Hultman, E., & Nordesjö, L. O. (1974). Glycogen, glycolytic intermediates and high-energy phosphates determined in biopsy samples of musculus quadriceps femoris of man at rest. Methods and variance of values. Scandinavian Journal of Clinical and Laboratory Investigation, 33(2), 109–120.

Hennig R, Lømo T. (1985) Firing patterns of motor units in normal rats. Nature. 314(6007): 164-166.

Hennig, R., & Lømo, T. (1987). Gradation of force output in normal fast and slow muscles of the rat. Acta Physiologica Scandinavica, 130(1), 133–142.

Hill, A. V. (1951). The Effect of Series Compliance on the Tension Developed in a Muscle Twitch. Proceedings of the Royal Society of London B: Biological Sciences, 138(892), 325–329.

Homsher, E. (1987). Muscle enthalpy production and its relationship to actomyosin ATPase. Physiology, 49(1), 673–690.

Inglis, J. G., Howard, J., McIntosh, K., Gabriel, D. A., & Vandenboom, R. (2011). Decreased motor unit discharge rate in the potentiated human tibialis anterior muscle. Acta Physiologica (Oxford, England), 201(4), 483–492.

James, R. S., Altringham, J. D., & Goldspink, D. F. (1995). The mechanical properties of fast and slow skeletal muscles of the mouse in relation to their locomotory function. The Journal of Experimental Biology, 198(Pt 2), 491–502.

Julian, F. J., & Morgan, D. L. (1979). The effect on tension of non-uniform distribution of length changes applied to frog muscle fibres. The Journal of Physiology, 293(1), 379–392.

Karatzaferi, C., Franks-Skiba, K., & Cooke, R. (2008). Inhibition of shortening velocity of skinned skeletal muscle fibers in conditions that mimic fatigue. American Journal of Physiology. Regulatory, Integrative and Comparative Physiology, 294(3), R948–R955.

Myburgh, K.M. (2004). Protecting muscle ATP: positive roles for peripheral defense mechanisms-introduction. Medicine and Science in Sports and Exercise, 36(1), 16–19.

Lännergren, J., Bruton, J. D., & Westerblad, H. (2000). Vacuole formation in fatigued skeletal muscle fibres from frog and mouse: effects of extracellular lactate. The Journal of Physiology, 526(3), 597–611.

Leblond, H., L'Espérance, M., Orsal, D., & Rossignol, S. (2003). Treadmill locomotion in the intact and spinal mouse. The Journal of Neuroscience, 23(36), 11411–11419.

Macintosh, B. R. (2003). Role of Calcium Sensitivity Modulation in Skeletal Muscle Performance. Physiology, 18(6), 222–225.

Macintosh, B. R. (2010). Cellular and Whole Muscle Studies of Activity Dependent Potentiation. In D. E. Rassier, Muscle Biophysics (Vol. 682, pp. 315–342). New York, NY: Springer New York.

Macintosh, B. R., & Bryan, S. N. (2002). Potentiation of shortening and velocity of shortening during repeated isotonic tetanic contractions in mammalian skeletal muscle. Pflügers Archiv: European Journal of Physiology, 443(5-6), 804–812.

Macintosh, B. R., Holash, R. J., & Renaud, J.-M. (2012). Skeletal muscle fatigue--regulation of excitation-contraction coupling to avoid metabolic catastrophe. Journal of Cell Science, 125(Pt 9), 2105–2114.

Macintosh, B. R., Taub, E. C., Dormer, G. N., & Tomaras, E. K. (2008). Potentiation of isometric and isotonic contractions during high-frequency stimulation. Pflügers Archiv : European Journal of Physiology, 456(2), 449–458.

Marsh, R. L. (1999). How muscles deal with real-world loads: the influence of length trajectory on muscle performance. The Journal of Experimental Biology, 202(Pt 23), 3377–3385.

Metzger, J. M., Greaser, M. L., & Moss, R. L. (1989). Variations in cross-bridge attachment rate and tension with phosphorylation of myosin in mammalian skinned skeletal muscle fibers. Implications for twitch potentiation in intact muscle. The Journal of General Physiology, 93(5), 855–883

Patel, J. R., Diffee, G. M., Huang, X. P., & Moss, R. L. (1998). Phosphorylation of myosin regulatory light chain eliminates force-dependent changes in relaxation rates in skeletal muscle. Biophysical Journal, 74(1), 360–368.

Persechini, A., Stull, J. T., & Cooke, R. (1985). The effect of myosin phosphorylation on the contractile properties of skinned rabbit skeletal muscle fibers. Journal of Biological Chemistry, 260(13), 7951–7954.

Rall, J. A. (1984). Energetic aspects of skeletal muscle contraction: implications of fiber types. Exercise and Sport Sciences Reviews, 13, 33–74.

Rassier, D. E., & MacIntosh, B. R. (2000). Coexistence of potentiation and fatigue in skeletal muscle. Brazilian Journal of Medical and Biological Research, 33(5), 499–508.

Smith, C. B., Cheng, A. J., & Rice, C. L. (2011). Potentiation of the triceps brachii during voluntary submaximal contractions. Muscle & Nerve, 43(6), 859–865.

Smith, I. C., Gittings, W., Huang, J., McMillan, E. M., Quadrilatero, J., Tupling, A. R., & Vandenboom, R. (2013). Potentiation in mouse lumbrical muscle without myosin light chain phosphorylation: is resting calcium responsible? The Journal of General Physiology, 141(3), 297–308.

Stull, J. T., Kamm, K. E., & Vandenboom, R. (2011). Myosin light chain kinase and the role of myosin light chain phosphorylation in skeletal muscle. Archives of Biochemistry and Biophysics, 510(2), 120–128.

Sweeney, H. L., & Stull, J. T. (1986). Phosphorylation of myosin in permeabilized mammalian cardiac and skeletal muscle cells. American Journal of Physiology -- Legacy Content, 250(4 Pt 1), C657–C660.

Sweeney, H. L., & Stull, J. T. (1990). Alteration of cross-bridge kinetics by myosin light chain phosphorylation in rabbit skeletal muscle: implications for regulation of actin-myosin interaction. Proc Natl Acad Sci, 87(1), 414–418.

Sweeney, H. L., Bowman, B. F., & Stull, J. T. (1993). Myosin light chain phosphorylation in vertebrate striated muscle: regulation and function. American Journal of Physiology -- Legacy Content, 264(5 Pt 1), C1085–C1095.

Vandenboom, R., Gittings, W., Smith, I. C., Grange, R. W., & Stull, J. T. (2013). Myosin phosphorylation and force potentiation in skeletal muscle: evidence from animal models. Journal of Muscle Research and Cell Motility, 34(5-6), 317–332.

Westerblad, H., Bruton, J. D., & Katz, A. (2010). Skeletal muscle: Energy metabolism, fiber types, fatigue and adaptability. Experimental Cell Research, 316(18), 3093–3099.

Westra, H. G., de Haan, A., van Doorn, J. E., & de Haan, E. J. (1988). Anaerobic chemical changes and mechanical output during isometric tetani of rat skeletal muscle in situ. Pflügers Archiv : European Journal of Physiology, 412(1-2), 121–127.

Zhang, S.-J., Andersson, D. C., Sandström, M. E., Westerblad, H., & Katz, A. (2006). Cross bridges account for only 20% of total ATP consumption during submaximal isometric contraction in mouse fast-twitch skeletal muscle. American Journal of Physiology. Cell Physiology, 291(1), C147–C154.

Zhi, G., Ryder, J. W., Huang, J., Ding, P., Chen, Y., Zhao, Y., et al. (2005). Myosin light chain kinase and myosin phosphorylation effect frequency-dependent potentiation of skeletal muscle contraction. Proceedings of the National Academy of Sciences of the United States of America, 102(48), 17519–17524.

# Chapter 8: General Discussion

### *Summary of results*

*Study #1: Shortening speed dependence of tetanic force potentiation*

In these experiments, we determined that the magnitude and extent of concentric force potentiation in wildtype EDL muscles is highly sensitive to muscle shortening speed. Increasing the rate of ramp shortening from near isometric to moderate speeds greatly increased the activation frequency domain over which concentric force was potentiated. Moreover, at moderate and fast shortening speeds, there was an apparent interaction between potentiation and force summation as the magnitude of potentiation was greater at moderate vs. low frequencies of stimulation.

Identical experiments in skMLCK$^{-/-}$ muscles were conducted subsequently once our breeding colony was established. Unexpectedly, this work showed that in the absence of myosin RLC phosphorylation, significant concentric PTP was present. Consistent with the main study and with the wildtype response, the magnitude of potentiation in skMLCK$^{-/-}$ muscles was shortening speed dependent. PTP in skMLCK$^{-/-}$ muscles was approximately half of the wildtype response, a fraction that was relatively stable across conditions.

*Study #2: Force dependence of isometric and concentric force potentiation*

We investigated and compared the magnitude of PTP during isometric conditions and during moderate speed ramp shortening in wildtype and skMLCK$^{-/-}$ muscles. In the presence of elevated RLC phosphate content, wildtype muscles showed greater potentiation in all conditions. In both genotypes, when preceded by a brief period of isometric stimulation, concentric potentiation was not significantly reduced when compared to concentric activation only.

We were surprised to observe a moderate amount of concentric PTP in skMLCK$^{-/-}$ muscles as well, and like Study #1 the magnitude was approximately half of the wildtype response. For isometric conditions, forces were depressed in skMLCK$^{-/-}$ muscles following the potentiating stimulus (PS), which was likely the result of increases in force relaxation kinetics and a small amount of fatigue from the PS itself.

In both genotypes, the size of the potentiation response was dependent on the force level achieved during the stimulation; and interestingly, the instantaneous potentiation trace was highly correlated to force oscillations during the incompletely

fused tetani. Thus, the factors that underlie to the force dependence of PTP may be independent of RLC phosphorylation.

*Study #3: Posttetanic potentiation (PTP) and the Catchlike Property (CLP)*

This study provided a novel description of the interaction between the CLP and PTP in skeletal muscle by investigating the coexistence of these mechanisms in fast skeletal muscles with and without skMLCK expression. The magnitude of the catchlike effect was diminished in the presence of force potentiation, and stimulation-induced elevation in myosin RLC phosphorylation was implicated in this interaction. For example, in wildtype muscles, the high degree of PTP was associated with a lower amount of enhancement by the CLP as compared to skMLCK$^{-/-}$ muscles (i.e. inverse genotype relationship). In contrast to Study #1 and 2, we did not observe any PTP in skMLCK$^{-/-}$ muscles, which may have been related to the low/moderate stimulation frequency used (32Hz). Finally, we observed that despite the apparent redundancy and interference of the CLP and PTP mechanisms, there is evidence that each have functional utility in the fast muscle phenotype. For example, the CLP is most effective as an acute mechanism to augment peak force production over a brief interval, and PTP represents an activation history-dependent memory that is capable of augmenting peak force and work performed throughout a period of stimulation and beyond.

*Study #4: Contractile economy in potentiated muscles*

These experiments studied the energetic cost of performing concentric work during a period of physiologically relevant activity in wildtype and skMLCK$^{-/-}$ muscles to investigate the effect of myosin RLC phosphorylation on contractile economy in the potentiated state. Without the intact RLC phosphorylation mechanism, skMLCK$^{-/-}$ muscles performed significantly less work than wildtype counterparts in response to the same stimulus.

We compared muscle metabolite concentrations in muscles frozen before and after the period of stimulation to calculate High Energy Phosphate Consumption (HEPC), a measure of anaerobic energy turnover. HEPC values were higher in wildtype muscles but the genotype difference was not statistically significant. When economy was calculated (Total Work/HEPC), there was no difference between genotypes despite the large disparity in work performed. A noteworthy difference between genotypes was observed when studying the normalized force traces from the beginning and end of the

stimulation period, as wildtype muscles demonstrated a prolongation of the relaxation phase of the contraction when compared to skMLCK$^{-/-}$ muscles.

### *Potentiation in skMLCK$^{-/-}$ muscles: Novel mechanistic information*

The development of skMLCK$^{-/-}$ animals by the lab of Dr. James Stull at the University of Texas was a breakthrough in our research area, and the finding that isometric twitch potentiation was abolished in these animals was robust mechanistic support for the role of RLC phosphorylation (Zhi et al. 2005). However, in that study, skMLCK$^{-/-}$ muscles demonstrated staircase potentiation that was approximately half of the wildtype response in magnitude. Consequently, it was suggested that PTP and Staircase, the two 'types' of Activity Dependent Potentiation (MacIntosh, 2010), were associated with different primary mechanisms. Gittings et al. (2011) were the first to replicate the findings of Zhi et al. (2005), and demonstrated that although the PTP response was attenuated in skMLCK$^{-/-}$ animals, progressive twitch amplification was evident when elicited during intermittent high frequency tetani (i.e. evidence of a staircase-like effect). The investigation of PTP in mouse lumbrical muscles by Smith et al. (2013) further developed our understanding of the alternate mechanism for potentiation by showing that following a brief potentiating stimulus, twitch forces were potentiated in the absence of elevated RLC phosphate content. These authors demonstrated that the short-lived twitch PTP (≤20s) was associated with an increase in resting [$Ca^{2+}$] following a brief potentiating stimulus, and is perhaps the best characterization to date of an operative myosin RLC phosphorylation-independent mechanism for potentiation.

The experiments presented in this thesis provide various novel insights into the manifestation of the so-called myosin RLC phosphorylation-independent mechanism for PTP; an effect that we attribute to the transient elevation in resting [$Ca^{2+}$] that follows evoked stimulation (Smith et al. 2013). The most important of these findings is that myosin RLC phosphorylation-independent factors may contribute up to half of the PTP response for concentric activations that span moderate shortening speeds (25-50% $V_{max}$) and encompass the physiological range of stimulation frequencies (10-100 Hz). We assume that the mechanism that produces the potentiation response in skMLCK$^{-/-}$ muscles also contributes equally to the potentiation of wildtype muscles; thus, by subtracting the

skMLCK$^{-/-}$ potentiation response from the wildtype response we have inferred the fraction of potentiation attributable to myosin RLC phosphorylation specifically.

The current experiments showed that forces in skMLCK$^{-/-}$ muscles can be readily potentiated up to ~30-35%, however this observation begs the question: Why was such a robust effect not identified previously in this genotype? (Gittings et al. 2011; Zhi et al. 2005). Based on the current work, we conclude that the speed and contraction-type dependence for PTP in skMLCK$^{-/-}$ muscles (Study #1 and 2, respectively) clarifies this question. Importantly, we did not observe potentiation in skMLCK$^{-/-}$ muscles during isometric activation at any frequency or shortening speed. In fact, skMLCK$^{-/-}$ muscles in Study #2 and Study #3 demonstrated a depression in force at 60Hz and a significant depression in work per contraction at 32Hz following the potentiating stimulus, respectively. Thus, the factors that sensitize muscles to the effects of myosin RLC phosphorylation in wildtype muscles also operate similarly with respect to alternative mechanisms for PTP, which may include alterations in $Ca^{2+}$ homeostasis that follow high frequency stimulation.

In conclusion, during physiological movements that involve moderate to fast shortening speeds, the present findings suggest that a significant fraction of the potentiation present in wildtype muscles may be attributed to mechanism(s) other than myosin RLC phosphorylation. However, the time course and details of these effects have not been well established. For example, the potentiation observed by Smith et al. 2013 independent of myosin RLC phosphorylation was not long lasting (≤20s). We therefore qualify our general conclusion with the hypothesis that if such an alternate mechanism for PTP resulted directly from the potentiating stimulus itself, it would have the greatest effect on contractile function immediately after activation and would dissipate quickly. By extension, intermittent activation at a regular frequency (i.e. staircase) would be more affected than irregular bursts of activity with significant periods of quiescence. In summary, the relative contribution of myosin RLC phosphorylation-dependent and independent mechanisms to potentiation is likely variable and influenced by many factors, such as the nature of the potentiating stimulus itself, contraction type, shortening speed, stimulation frequency, and other time-dependent factors.

### *Implications of potentiation and myosin phosphorylation on muscle force control*

The modulation of contractile function by force potentiation has been well studied; however, the current work makes some important novel contributions to our understanding of this phenomenon. In particular, the preceding experiments have shed light on the importance of myosin RLC phosphorylation as a modulator of force and work during dynamic conditions across the force-frequency and force-velocity relationships. The implications of these findings with respect to muscle force control are summarized below.

It has long been understood that the effect of myosin RLC phosphorylation is dependent on $Ca^{2+}$ activation level (Sweeney and Stull, 1990) and stimulation frequency (Vandenboom et al. 1993), with the greatest magnitude of potentiation at low levels of each. The significance of these initial findings to muscle function *in vivo* was unclear, as the fast-fatigable muscle fibre types that are most readily potentiated (Moore and Stull, 1984; Ryder et al. 2007) are used for the most forceful and highest intensity conditions that require high levels of activation and stimulation frequencies. The speed dependence of potentiation demonstrated in Study #1 provides important insight with regard to this relationship. At moderate to fast speeds of shortening, the range of stimulation frequencies that can be modulated by potentiation span the physiological range of motor unit firing rates for murine EDL muscles *in vivo* (Hennig and Lomo, 1985: Schiaffino and Reggiani. 2011). In addition, the robust effect of potentiation on rate of force development was present at all stimulation frequencies (also shown by Vandenboom et al. 1995), supporting the theory that brief stimulation at any level of activation can be potentiated (see also MacIntosh et al 2008 for related findings for rat muscles *in situ*). The implications of these findings with respect to *in vivo* function is a flattening of the force-frequency and force-velocity relationships, where maximal force and shortening velocity remain unaffected (Gittings et al. 2011), and contractile function is augmented the most in conditions where force levels are the lowest (i.e. at low frequency and high velocity). This theory is directly supported by the force-dependence of potentiation observed in Study #2; and importantly, underlies the contraction-type dependence of potentiation in isometric vs. concentric contractions. Thus, a logical extension of the previous discussion is the conclusion that force potentiation can modulate contractile

function by: *i)* augmenting force production in response to a given activation signal, *ii)* preserving a given submaximal force level at a lower activation level, and/or *iii)* enabling a muscle to augment shortening speed or displacement at the same relative load.

We cannot directly assess the molecular basis for the observed effects of potentiation on contractile function in the current experiments; however, our results are generally consistent with the theory that RLC phosphorylation modifies myosin motor function by increasing the rate constant for binding of force-producing crossbridges (Brenner, 1988). For example, the force-dependence of potentiation shown in Study #2 suggests that as force levels increase, the fraction of force-producing crossbridges bound to actin is proportionally higher, and thus the enhancement of crossbridge binding by myosin RLC phosphorylation is less effective. Furthermore, the instantaneous correlation between potentiation and force during unfused tetani in Study #2 was further evidence that the mechanistic basis for potentiation is tightly associated with the dynamic conditions present in shortening muscles.

In summary, we suggest that the magnitude of potentiation demonstrated in a given circumstance is a function of the myosin RLC phosphate content, but also the specific parameters that reflect the fraction of force-producing crossbridges bound to actin (i.e. contraction type, shortening velocity, stimulation frequency). This theory is supported by various observations from the current work, including: *i)* the increase in PTP with faster shortening speeds (Study #1), *ii)* the increase in PTP for concentric vs. isometric contractions (Study #2), *iii)* the increase in pulse-by-pulse potentiation during the isometric-concentric transition (Study #2), and *iv)* the decrease in PTP that occurred coincident with the CLP in wildtype muscles (Study #3). Interestingly, the potentiation observed in wildtype and skMLCK$^{-/-}$ muscles displayed the same force, contraction-type, stimulation frequency, and shortening speed dependence. Thus, we must conclude that the myosin RLC phosphorylation-independent mechanism which caused potentiation in skMLCK$^{-/-}$ muscles may be manifest in a similar manner as myosin RLC phosphorylation. Smith et al. 2013 suggested that the twitch potentiation associated with an increase in resting [$Ca^{2+}$] may have been caused by saturation of intracellular $Ca^{2+}$ buffers leading to greater free [$Ca^{2+}$] and troponin occupancy upon activation, or via a direct modification of crossbridge distribution/structure by elevated resting [$Ca^{2+}$]. However, as we did not measure or characterize the $Ca^{2+}$ signaling in these experiments,

we cannot speculate on the nature or effect of this alternative mechanism on crossbridge kinetics in the current work.

*Posttetanic Potentiation (PTP) and the Catchlike Property (CLP)*

The *in vitro* model used presently does not approximate the control of muscle force that occurs *in vivo* by the nervous system via motor unit recruitment and rate coding. However, by examining the contractile response to identical stimulation patterns in wildtype and skMLCK$^{-/-}$ muscles, both before and after a potentiating stimulus, we were able to unambiguously evaluate the individual effects of the CLP and PTP on the enhancement of force and work. Initial doublets are characteristic of fast skeletal muscle motor units *in vivo* (Hennig and Lomo, 1987); therefore, gaining a better understanding of the interaction between this pattern of activation and PTP is relevant and useful.

The experiments in Study #3 demonstrated that both mechanisms were effective in enhancing peak force and work but these responses were genotype specific. In particular, the finding that the magnitude of the catchlike effect was decreased after the PS in wildtype muscles, but not in skMLCK$^{-/-}$ muscles, demonstrated an interference effect between the mechanisms of contractile enhancement directly attributable to myosin RLC phosphorylation (consistent with the findings of Burke et al. 1976; Ding et al. 2003). The apparent redundancy and interference of these mechanisms in skeletal muscle might be best described as biological degeneracy, i.e. the ability of elements that are structurally or functionally different to produce the same outcome or yield the same output (Edelman and Gally, 2001). Tononi et al. (1999) suggest that degeneracy is high in systems that have many elements which may affect the output in a similar but independent manner, a description that may apply well to the plethora of factors that are known to either potentiate or depress contractile function in skeletal muscle. With respect to PTP and the CLP, the common outcome of these mechanisms was an increase in the rate and/or extent of force development, which were shown to effectively augment the summation of pulses and work performed relative to the control stimulus (unfused constant frequency train, 32Hz).

Our examination of the CLP in mouse EDL during ramp shortening demonstrated a large but relatively brief augmentation of peak force and work that was all but dissipated within ~100 ms of the onset of stimulation. This finding was consistent with the previous observation that imposing a length perturbation can reduce or negate the

catchlike augmentation in force that might otherwise last ≥ 1s (Sandercock and Heckman, 1997), and with the general trend that the CLP is reduced during nonisometric conditions vs. isometric activation (Binder-Macleod and Barrish, 1992). Without a direct measure of stiffness and in the absence of any change to maximal rate of force development with the CLP, we cannot directly assess the mechanism by which the doublet stimulation augmented peak force. Otherwise, the increase in work performed during the catchlike train (CLT) versus the constant frequency train (CFT) was all but negated when work performed during each stimulus was normalized to the number of pulses (i.e. CLT = CFT + 1 pulse). Thus, the net effect of the CLP on muscular work was small compared to its effect on the magnitude and timing of its effect on peak force. Moreover, the correction of work to pulse number revealed an important point of comparison between the mechanisms of enhancement: the CLP may operate primarily via a 'non-linear' increase in force summation (Burke et al. 1970) and is limited by the duration of the effect, while PTP augments contractile function through a less-acute increase in the force response per pulse via $Ca^{2+}$ sensitivity (Persechini et al. 1985).

Also in Study #3, we observed that the rate of force relaxation was increased following the potentiating stimulus in both genotypes, but this effect translated into reduced force summation and a significant reduction in work performed in skMLCK$^{-/-}$ muscles only. The intact myosin RLC phosphorylation mechanism and resulting potentiation in wildtype muscles therefore directly opposed this effect and augmented the summation of pulses in the unfused tetani after the PS. Thus, although we did not identify the exact mechanism for faster relaxation rates following the PS, this characteristic of potentiated twitches (Krarup, 1981) seems to be the result of previous activation and not due myosin RLC phosphorylation. Consequently, a potential benefit to elevated myosin RLC phosphate content might be the preservation of force summation at low to moderate frequencies in the potentiated state where increases in force relaxation rates might induce a right-ward shift in the force-frequency relationship. More work is needed to evaluate this hypothesis, however, given that changes in relaxation rates following a potentiating stimulus are highly dependent on stimulation frequency (Study #1, Figure 4.7, Panel B).

In summary, the precise physiological roles of the CLP and PTP, singly or together, remain uncertain; however, it is clear that modulation of contractile function is an important hallmark of fast skeletal muscles. Understanding the interaction of these mechanisms and with regulatory control schemes for skeletal muscle will help provide a

better indication of how muscles accomplish critical tasks such as locomotion and movement. For example, the addition of an initial doublet was capable of augmenting force summation and muscular work even in potentiated wildtype muscles. This catchlike effect would be particularly useful during brief physiological activation of skeletal muscles where minimizing the time to peak tension and/or overcoming movement inertia are of prime importance. With respect to PTP, the increased myosin RLC phosphate content in potentiated wildtype muscles was associated with the highest quantity of work performed per pulse and ≥50% more work performed per contraction than in skMLCK$^{-/-}$ muscles. Thus, PTP is evidently a less-acute mechanism of force enhancement that promotes the development and maintenance of force summation during unfused tetani.

*Myosin RLC phosphorylation, Posttetanic Potentiation, and Rate Coding*

The present work *in vitro* has other implications for physiological functioning *in vivo*, where an intact afferent feedback system may relay information from active muscles to integrate with and modify descending motor drive. Garland and Gossen (2002) have suggested that potentiation may be a fundamental mechanism through which forces can be maintained during sustained use despite characteristic reductions in the motor unit discharge rate, known as the muscle wisdom hypothesis (Marsden et al 1983). In fact, it has been shown that submaximal forces can be maintained in the presence of twitch potentiation and decreases in motor unit firing rates (De Luca et al. 1996). This association between force potentiation and decreasing motor unit firing rates has also been shown during submaximal voluntary force maintenance (Person and Kudina, 1972; Adam & De Luca, 2005; Erim et al., 1996; and Dorfman et al. 1990) and transiently following maximal voluntary potentiating activity (Klein et al., 2001; Inglis et al., 2011). However, the fast skeletal muscles in animals that most readily and significantly demonstrate potentiation are not associated with sustained maintenance of submaximal forces (i.e. phasic rather than tonic). For example, Hennig and Lomo (1985) observed that fast-fatigable motor units might regulate force by number of pulses rather than varying interpulse intervals. Consequently, more work is required to better understand the relationship between the potentiation-state of skeletal muscles and motor unit firing rates; this work can only be conducted *in vivo* with an intact feedback system of afferent information to the motor cortex. Additionally, the fibre-type specificity of potentiation in human skeletal muscles is poorly understood compared to animals.

### *Implications of potentiation and myosin phosphorylation on energetics and economy*

The effect of myosin RLC phosphorylation and force potentiation on muscle energetics is perhaps the least understood aspect of these mechanisms; however, gaining a better understanding of this topic might be instrumental in assigning a physiological role for them. In theory, myosin RLC phosphorylation might increase energy turnover directly through skMLCK activity, or indirectly via enhanced crossbridge binding and higher myosin ATPase activity or by performing more total work. Conversely, energy turnover might decrease in the potentiated state if myosin RLC phosphorylation modifies the crossbridge cycle to reduce the rate of ATP hydrolysis, or alternatively, if muscles were to perform a given amount of work at a lower level of activation when potentiated vs. unpotentiated (i.e. reducing the ATP cost for activation). These possibilities are discussed below with respect to the current findings as they relate to the economy of contractile function in the potentiated state.

To date the direct energetic requirement of myosin RLC phosphorylation by skMLCK has not been quantified, although Homsher (1987) estimated that it might consume up to 5% of the total ATP consumed during a 5s isometric tetanus. The technical challenge in accomplishing this task in the intact cell is that skMLCK would have to be activated while simultaneously controlling for $Na^+/K^+$, myosin and sarco/endoplasmic reticulum $Ca^{2+}$-ATPases: a tall order! Presently, wildtype and skMLCK$^{-/-}$ muscles in Study #4 received the same stimulation (and thus theoretically had the same activation energy requirement); however, there was a genotype difference in total work performed and thus we cannot differentiate the genotype difference in ATP cost for myosin RLC phosphorylation from that used for performing work. Although the fraction of total energy used for myosin RLC phosphorylation in working muscles is undoubtedly small, this may not be the case for resting muscles. It has been suggested that myosin RLC phosphorylation may be a mechanism that regulates the so-called Super Relaxed State (SRX) of myosin crossbridges *in vivo*, and the low level of phosphorylation present in resting muscles (~20-30%) may contribute to muscle thermogenesis (Cooke, 2011). As such, the transfer of only ~20% of the myosin heads from the SRX to the 'resting' state could double resting muscle thermogenesis (Cooke, 2011). However, it is clear that more work is necessary to investigate how the energy

associated with myosin RLC phosphorylation might influence energy turnover during rest or in working muscles.

Abbate et al. (2001) reported that PTP increased the energy cost for work in medial gastrocnemius muscles of the rat *in situ*; however, the effectiveness of the study was limited by the experimental design (as discussed in detail in Study #4). Conversely, Barsotti and Butler (1984) have reported that there was no consistent relationship between myosin RLC phosphorylation and rate of energy usage during isometric tetani in mouse EDL muscles. Importantly, both studies were limited by the absence of a true control condition for muscle work in the absence of myosin RLC phosphorylation, and the present work using skMLCK$^{-/-}$ muscles was directly able to address this methodological challenge. In Study #4, we reported that wildtype muscles perform considerably more work than skMLCK$^{-/-}$ muscles without a statistically significant increase in energy cost (i.e. High Energy Phosphate Consumption). Thus, as the increased contractile performance associated with myosin RLC phosphorylation was not accompanied by an equal or proportional increase in energy cost, we challenge the conclusions of Abbate et al. (2001). Furthermore, during the relatively brief period of work investigated presently, there was no genotype difference in Economy (i.e. total work/HEPC). However, it is unknown whether genotype differences in energy cost for contraction might exist during prolonged use or in other experimental conditions, and this warrants further investigation to comprehensively understand the effects of myosin RLC phosphorylation and potentiation on contractile economy.

The finding that wildtype muscles performed more total work than skMLCK$^{-/-}$ counterparts, without a proportional increase in energy turnover and in spite of any additional energetic cost of myosin RLC phosphorylation per se, suggests that the relationship between ATP hydrolysis and force production at the level of the crossbridge may have been different. Research using skinned fibres and *in vitro* motility assays have reported that myosin RLC phosphorylation may be associated with an increase in the duty cycle of the myosin crossbridge following ATP hydrolysis (Greenberg et al, 2009; Greenburg et al, 2010; Karatzaferi et al, 2008). Specifically, it has been suggested that RLC phosphorylation may stiffen or increase the stability of the myosin head, and might slow the rate of strain-dependent ADP release (Greenberg et al, 2009). In theory, these effects might decrease the energy cost for contraction if the efficiency of the myosin crossbridge were increased through modulation by RLC phosphorylation. However, in

the absence of an intact cell and contractile apparatus, it is unclear how these findings are relevant to *in vivo* function. For example, studies in intact muscles of the mouse have reported that unloaded shortening velocity, an indicator of maximal crossbridge turnover rate, is either not affected (Butler et al. 1983; Gittings et al. 2011) or decreased (Crow and Kushmerick, 1982) with myosin RLC phosphorylation. A related observation in the current work, and consistent with previous work (Brown and Loeb, 1999; Gittings et al. 2011), is the prolongation of the force trace during relaxation in wildtype compared to skMLCK$^{-/-}$ muscles. In fact, the genotype difference in relative force level at the same time point shown in Figure 7.5 may underlie the significant difference in work performed per contraction between wildtype and skMLCK$^{-/-}$ muscles. Patel et al. (1998) have suggested that the decrease in relaxation with RLC phosphorylation may be caused by a slowing of the rate constant for transition of crossbridges from strongly bound to weakly bound states, or a disruption of $Ca^{2+}$ and crossbridge activation-dependent changes in relaxation rates. Importantly, the results from Study #4 showed no genotype differences in force relaxation rates despite the apparent difference in the shape of the force traces. Therefore, the effect of myosin RLC phosphorylation on force relaxation remains unclear and may depend on a variety of other factors; for example, in Study #1 we demonstrated that the change in relaxation rates following the potentiating stimulus were dependent on stimulation frequency.

Finally, the current findings might have secondary implications for the economy of *in vivo* contractile function. As discussed previously, the potentiation associated with myosin RLC phosphorylation may permit the maintenance of submaximal forces, or the same amount of work to be performed, at a lower activation level (i.e. duration or frequency of stimulation). Although the energetic cost of the contractile activity would remain the same, the activation energy required might be considerably different due to a reduced energy cost for ion transport (i.e. $Na^+/K^+$-ATPase and SERCA activity); an effect which would reflect the increase in $Ca^{2+}$ sensitivity of the contractile proteins by myosin RLC phosphorylation.

In summary, the potentiation of contractile function by myosin RLC phosphorylation was not accompanied by a significant energy cost or alteration to the economy of muscular work. To our knowledge, this is the first study to investigate the economy and energy cost for work in the absence of myosin RLC phosphorylation. However, the precision of our metabolic measurements may not have been sufficient to

identify a genotype difference in energy turnover, and thus may have limited the effectiveness of the work (see Study #4 and limitations section below).

## *Conclusions & Significance*

*Summary*

The objective of this thesis was to investigate the effects of myosin RLC phosphorylation on mechanical and biochemical parameters in fast muscles from wildtype and skMLCK$^{-/-}$ mice to better understand the modulation of dynamic contractile function by posttetanic potentiation. From these experiments it is evident that concentric force and work can be meaningfully augmented across a broad range of stimulation frequencies and shortening protocols following potentiating activity. The relative effect of myosin RLC phosphorylation appears to be the greatest during conditions where force levels are the lowest or compromised (i.e. fast shortening, low stimulation frequency, and maintaining summation during unfused tetani). Unlike the acute but brief augmentation of force development by neural mechanisms such as the catchlike property, potentiation by myosin RLC phosphorylation is characterized by a longer-lasting enhancement of contractile function due to the slow deactivation of the mechanism. The slow de-phosphorylation of the RLC by MLCP may be important to minimize the energetic requirement of the mechanism; and importantly, the current results support the position that the potentiation of contractile function by myosin RLC phosphorylation does not significantly influence the contractile economy of working fast skeletal muscles.

The meaningful potentiation of concentric forces in the absence of myosin RLC phosphorylation, as observed presently in skMLCK$^{-/-}$ muscles, is a novel and important finding. Although this modulation of dynamic contractile function may be a transient by-product of evoked stimulation related to altered $Ca^{2+}$ homeostasis, it is likely an important contributor to the initial potentiation response following activation or during repetitive use.

> There probably are many properties of muscle that appear of minor significance when viewed from the narrow frame of reference of the biochemist or physiologist. Yet once the function is fully understood in the context of how an animal actually uses its muscles and the energetic consequences of the use, minor factors may be integral in the fine-tuning necessary for optimal muscle performance. RLC phosphorylation clearly has effects on the myosin cross-bridge properties in vertebrate striated muscle. Furthermore, the biochemical properties of this phosphorylation system are ideal for a modulatory mechanism that will itself consume little energy. The importance of its role undoubtedly will increase in proportion to our understanding of muscle function. (Sweeney, Bowman, and Stull, 1993)

Although the potentiation of twitch force following activity or during repetitive low frequency stimulation is a remarkable phenomenon in skeletal muscle, labeling this as the primary outcome of RLC phosphorylation may underrepresent the role of this fine-tuning of the myosin molecular motor. In fact, as the details of this modulatory mechanism are elucidated, the importance and utility of myosin RLC phosphorylation seems to increase. However, in contrast to slow and cardiac muscles types where myosin RLC phosphorylation is an necessary component for function (Kamm and Stull, 2001), its expression and utility is largely restricted to fast isoforms of skeletal muscle (Stull et al. 2011). Thus, the variations in RLC phosphorylation capacity that exist between muscles, as well as the function of the different light chain isoform expression in skeletal muscle, are not completely understood. Whether myosin RLC phosphorylation exists to augment the maximal capacity of skeletal muscles to develop force and power, or alternatively to preserve $Ca^{2+}$ sensitivity and contractile function during muscle fatigue, is an important research problem to investigate. Alternatively, this mechanism might contribute to the regulation resting muscle thermogenesis (Cooke, 2011), or else it is an evolutionary remnant that has persisted since the differentiation of skeletal muscles (Duggal et al 2014). However, and perhaps most appropriately, the most important objective might be to better understand how it modulates human motor function and movement.

*Assumptions*

The current experiments and analysis were conducted with assumptions relating to the experimental model, study design and methods, and statistical procedures used.

Intact mouse EDL muscle *in vitro*

- To keep muscles viable *ex vivo* they are incubated in a physiological solution. We assume that the Tyrode solution used currently provides the EDL muscle preparation with similar ions concentrations found *in vivo*.
- We assume that muscles used in the current experiments were viable throughout the procedures conducted. According to modeling of diffusive oxygen supply to intact skeletal muscles *in vitro*, the conditions in the current experiments (i.e. muscle diameter, temperature, and duty cycle) did not exceed the theoretical parameters that would limit tissue viability (Barclay, 2005). The stability of twitch and tetanic force records were used to monitor viability during each experiment, and the randomization of repeated trials was used to wash out any potential concerns in this regard over the course of the experiments.

Study design and methods

- A central assumption is that any apparent differences between genotypes in the current experiments are attributable to the ablation of skMLCK, and that no significant phenotypic adaptations have occurred which would disproportionately influence the findings. We have no direct evidence that the genotypes differ meaningfully in any parameter; however, a comprehensive characterization of the skMLCK$^{-/-}$ muscles over their normal lifespan has not been conducted. We have taken every effort to subject muscles from both genotypes to identical experimental procedures; therefore, we assume that any experimental factors or sources of variability affected the genotypes equally.
- Our comparison of wildtype and skMLCK$^{-/-}$ responses to infer the relative contribution of myosin RLC phosphorylation-dependent and independent mechanisms is accompanied by an important assumption: that the mechanism which produced the potentiation response in skMLCK$^{-/-}$ muscles also contributed equally to the potentiation of wildtype muscles.
- For biochemical procedures on frozen muscle samples, we assume that the procedures involved in the storage, homogenization and analysis of muscle tissue will accurately reflect the true conditions sampled at the time of freezing. We have reduced the freezing time of muscles to ~1-2s, and with liquid nitrogen-cooled tongs we are able to freeze the muscle in its experimental apparatus without movement or handling.
- For calculations of High Energy Phosphate Consumption (HEPC) in Study #4, HEPC is calculated with the following assumptions; that glycogen is the sole source for lactate production during contraction, and that any decrease in ATP within the muscle is associated with a stoichiometric increase in IMP (Zhang et al., 2006).
- Our method used to calculate active forces involved the applications of passive length ramps ~5-10s before stimulation. We assume that this passive length perturbation does not induce phosphorylation (wildtype) or alter contractile function, factors which might influence the subsequent force responses. To this end, Grange et al. (1998) have previously shown that SINE wave length excursions at 7Hz are not sufficient to influence myosin RLC phosphorylation or subsequent contractile function.
- It was assumed that the magnitude of passive muscle lengthening (10-20% $L_o$) used currently did not cause significant damage to the contractile apparatus (muscles were

never stretched to lengths longer than 1.1 $L_o$). These parameters are below those suggested by Brooks et al. (1995) as necessary to produce significant damage.

Other mechanisms for PTP

- As discussed in the literature review, mechanisms that other than myosin RLC phosphorylation and altered $Ca^{2+}$ handling might potentiate muscle force following previous activation. As we did not measure or control for such a wide variety of confounding factors, we must assume that tertiary mechanisms for PTP did not contribute to the current results or genotype differences observed.

Statistical procedures

- The statistical tests used to evaluate significant differences were conducted under various assumptions, including; *i)* independence of sampling and observation between muscles, *ii)* homogeneity of variance between and within subjects (sphericity), *iii)* normality of the dependent variable within the population, and *iv)* independence of observational error from confounding effects. Where necessary and appropriate, these assumptions were tested using procedures and corrections built into the statistical software (SPSS).

*Limitations*

The present results and interpretations are subject to a variety of limitations that should be considered when transferring or applying the findings.

- The observations and conclusions of the current study are limited primarily to fast twitch skeletal muscle function *in vitro*. Mouse EDL muscles are relatively homogeneous with respect to fibre type composition, and extrapolating the physiological role of myosin RLC phosphorylation to larger, heterogeneous muscles may be problematic.
- The present in vitro experiments were conducted at sub-physiological temperatures (25°C). Thus, the present findings may not precisely approximate the true effect of myosin RLC phosphorylation on muscle function *in vivo*. For example, there is evidence that contractile parameters in intact muscles *in vitro* may be significantly difference when responses are compared at 25 and 35°C (Faulkner et al. 1990). It has been shown that the magnitude of potentiation is positively associated with temperature (Moore et al. 1990); therefore, the current work may actually under-estimate the true magnitude of the effect *in vivo*.
- Electrical field stimulation of EDL muscles *in vitro* is very different from muscle activation *in vivo* (i.e. lacking innervation by an intact motor nerve and cortical control of motor unit recruitment and firing rates).
- The *in vitro* muscle environment, although an approximation of physiological conditions, is also limited with respect to oxygen and substrate delivery (i.e. diffusion vs. circulation).
- During the current experiments, we did not measure or control sarcomere lengths; as a surrogate for whole muscles, we used optimal muscle length for peak twitch force ($P_t$) as the reference length for ramp procedures and relative length excursion magnitudes. We cannot account for the possible effects of non-uniformities in sarcomere lengths that may have influenced the observed results.
- Following surgical removal and suturing near the muscle-tendon junction, the *in vitro* muscle preparation does not retain the same series compliance found *in vivo*. Thus, although the experimental model may be effective in studying the function of the isolated contractile element(s), the amount of compliance within a muscle-tendon unit can significantly affect contractile function (Lichtwark and Barclay, 2010). For example, when considered *in vivo*, muscles may operate near isometric to produce high forces and harness the elastic energy (stretch/compliance) stored in the proximal and distal tendons (March et al, 1999). The mouse EDL muscle preparation cannot directly explain the importance of myosin RLC phosphorylation and force potentiation to contractile function within the intact hindlimb anatomy *in vivo*.
- When possible, a repeated-measures design was utilized when appropriate to minimize variability between levels of the independent variables. However, within each project, a contractile or biochemical observation from each subject (i.e. muscle) was not always collected for all levels of the independent variable(s). For example, in Study #1 each muscle was only tested for one of the three shortening speeds, as muscle viability would not persist long enough for stable measurements at each level of all conditions. Additionally, muscles could not be frozen at more than one time point for

quantification of myosin RLC phosphate content or muscle metabolites. This comparison of independent samples was not problematic for comparisons with a large effect size (i.e. myosin RLC phosphorylation following stimulation), but may have influenced the less-powered comparisons (i.e. HEPC).

- The calculation of HEPC in Study #4 was conducted between independent muscles frozen at different time points. Consequently, as a measure HEPC showed much higher variability than Total work performed, for example. This error was propagated when calculating Economy and may have partially obscured possible genotype differences, if present.

*Future Studies & Unresolved Questions*

Investigation of the following research questions would directly extend and complement the present work, as well as contribute to the elucidation of the physiological role and utility of myosin RLC phosphorylation and potentiation in skeletal muscle.

Mechanistic / In Vitro

- Are there compensatory adaptations in skMLCK$^{-/-}$ mice that appear due to the absence of myosin RLC phosphorylation?
- Does myosin RLC phosphorylation prolong or slow the relaxation phase of contraction by altering the crossbridge cycle? Is this effect load dependent?
- Is there a cooperative effect of myosin RLC phosphorylation on force development by influencing activation level?
- Does myosin RLC phosphorylation alter biophysical properties of skeletal muscle fibres, such as sarcomere stiffness or compliance, to alter force development or longitudinal force transmission?
- What is the precise energetic cost of phosphorylating the RLC and maintaining elevated phosphate content during sustained use?
- What is the energetic cost of producing equal amounts of work with or without RLC phosphorylation? (i.e. normalizing output but differing levels of activation)
- Does phosphorylation of the various regulatory light chain isoforms expressed in skeletal muscle result in different structural responses? Does a light chain isoform-dependence for myosin RLC phosphorylation underlie or contribute to the characteristic fibre type-dependence for potentiation?

Functional / In Vivo

- Does the absence of myosin RLC phosphorylation in skMLCK$^{-/-}$ mice affect daily activity levels or $VO_2$ requirements for activities such as locomotion when compared to wildtype animals?
- Following 'conditioning' activity, does the human body reduce motor unit firing rates or de-recruit motor units as a response to 'sensing' potentiation and integrating this information into its motor control pattern?
- Does potentiation contribute to the muscle wisdom hypothesis? (i.e. the decrease in motor unit firing rate during sustained activation).
- Is potentiation an operative mechanism in all motor units or in just a small segment that activate the fastest fibers in a muscle?
- Is there a physiological interaction between the catchlike property and potentiation or do the mechanisms simply represent complementary neural and muscular strategies to fine tune contractile function?

## *References*


Abbate, F., Van Der Velden, J., Stienen, G. J., & de Haan, A. (2001). Post-tetanic potentiation increases energy cost to a higher extent than work in rat fast skeletal muscle. Journal of Muscle Research and Cell Motility, 22(8), 703–710.

Adam, A., & De Luca, C. J. (2005). Firing rates of motor units in human vastus lateralis muscle during fatiguing isometric contractions. Journal of Applied Physiology, 99(1), 268–280.

Barsotti, R. J., & Butler, T. M. (1984). Chemical energy usage and myosin light chain phosphorylation in mammalian skeletal muscle. Journal of Muscle Research and Cell Motility, 5(1), 45–64.

Binder-Macleod, S. A., & Barrish, W. J. (1992). Force response of rat soleus muscle to variable-frequency train stimulation. Journal of neurophysiology,68(4), 1068-1078.

Brenner, B. (1988). Effect of Ca2+ on cross-bridge turnover kinetics in skinned single rabbit psoas fibers: implications for regulation of muscle contraction. Proceedings of the National Academy of Sciences, 85(9), 3265–3269.

Brown, I. E., & Loeb, G. E. (1999). Measured and modeled properties of mammalian skeletal muscle. I. The effects of post-activation potentiation on the time course and velocity dependencies of force production. Journal of Muscle Research and Cell Motility, 20(5-6), 443–456.

Burke, R. E., Rudomin, P., & Zajac, F. E. (1970). Catch property in single mammalian motor units. Science, 168(3927), 122-124.

Burke, R. E., Rudomin, P., & Zajac, F. E., III. (1976). The effect of activation history on tension production by individual muscle units. Brain Research, 109(3), 515–529.

Butler, T. M., Siegman, M. J., Mooers, S. U., & Barsotti, R. J. (1983). Myosin light chain phosphorylation does not modulate cross-bridge cycling rate in mouse skeletal muscle. Science, 220(4602), 1167–1169.

Cooke, R. (2011). The role of the myosin ATPase activity in adaptive thermogenesis by skeletal muscle. Biophysical reviews, 3(1), 33-45.

Crow, M. T., & Kushmerick, M. J. (1982). Phosphorylation of myosin light chains in mouse fast-twitch muscle associated with reduced actomyosin turnover rate. Science, 217(4562), 835–837.

De Luca, C. J., Foley, P. J., & Erim, Z. (1996). Motor unit control properties in constant-force isometric contractions. Journal of Neurophysiology, 76(3), 1503–1516.

Ding, J., Storaska, J. A., & Binder-Macleod, S. A. (2003). Effect of potentiation on the catchlike property of human skeletal muscles. Muscle & Nerve, 27(3), 312–319.

Dorfman, L. J., Howard, J. E., & McGill, K. C. (1990). Triphasic behavioral response of motor units to submaximal fatiguing exercise. Muscle & Nerve, 13(7), 621–628.

Duggal, D., Nagwekar, J., Rich, R., Midde, K., Fudala, R., Gryczynski, I., & Borejdo, J. (2014). Phosphorylation of myosin regulatory light chain has minimal effect on kinetics and distribution of orientations of cross bridges of rabbit skeletal muscle. American Journal of Physiology. Regulatory, Integrative and Comparative Physiology, 306(4), R222–33.

Edelman, G. M., & Gally, J. A. (2001). Degeneracy and complexity in biological systems. Proceedings of the National Academy of Sciences, 98(24), 13763–13768.

Erim, Z., De Luca, C. J., Mineo, K., & Aoki, T. (1996). Rank-ordered regulation of motor units. Muscle & Nerve, 19(5), 563–573.

Garland, S. J., & Gossen, E. R. (2002). The Muscular Wisdom Hypothesis in Human Muscle Fatigue. Exercise and Sport Sciences Reviews, 30(1), 45.

Gittings, W., Huang, J., Smith, I. C., Quadrilatero, J., & Vandenboom, R. (2011). The effect of skeletal myosin light chain kinase gene ablation on the fatigability of mouse fast muscle. Journal of Muscle Research and Cell Motility, 31(5-6), 337–348.

Gittings, W., Huang, J., & Vandenboom, R. (2012). Tetanic force potentiation of mouse fast muscle is shortening speed dependent. Journal of Muscle Research and Cell Motility, 33(5), 359–368.

Gittings, W., Aggarwal, H., Stull, J. T., & Vandenboom, R. (2015). The force dependence of isometric and concentric potentiation in mouse muscle with and without skeletal myosin light chain kinase. Canadian Journal of Physiology and Pharmacology, 93(1), 23–32.

Greenberg, M. J., Mealy, T. R., Jones, M., Szczesna-Cordary, D., & Moore, J. R. (2010). The direct molecular effects of fatigue and myosin regulatory light chain phosphorylation on the actomyosin contractile apparatus. American Journal of Physiology. Regulatory, Integrative and Comparative Physiology, 298(4), R989–96.

Greenberg, M. J., Mealy, T. R., Watt, J. D., Jones, M., Szczesna-Cordary, D., & Moore, J. R. (2009). The molecular effects of skeletal muscle myosin regulatory light chain phosphorylation. American Journal of Physiology. Regulatory, Integrative and Comparative Physiology, 297(2), R265–74.

Hennig, R., & Lømo, T. (1985). Firing patterns of motor units in normal rats. 314(6007), 164–166.

Hennig, R., & Lømo, T. (1987). Gradation of force output in normal fast and slow muscles of the rat. Acta Physiologica Scandinavica, 130(1), 133–142.

Homsher, E. (1987). Muscle enthalpy production and its relationship to actomyosin ATPase. Physiology, 49(1), 673–690.

Inglis, J. G., Howard, J., McIntosh, K., Gabriel, D. A., & Vandenboom, R. (2011). Decreased motor unit discharge rate in the potentiated human tibialis anterior muscle. Acta Physiologica (Oxford, England), 201(4), 483–492.

Kamm, K. E., & Stull, J. T. (2001). Dedicated myosin light chain kinases with diverse cellular functions. Journal of Biological Chemistry, 276(7), 4527-4530.

Karatzaferi, C., Franks-Skiba, K., & Cooke, R. (2008). Inhibition of shortening velocity of skinned skeletal muscle fibers in conditions that mimic fatigue. American Journal of Physiology. Regulatory, Integrative and Comparative Physiology, 294(3), R948–R955.

Klein, C. S., Ivanova, T. D., Rice, C. L., & Garland, S. J. (2001). Motor unit discharge rate following twitch potentiation in human triceps brachii muscle. Neuroscience Letters, 316(3), 153–156.

Krarup, C. (1981). Enhancement and diminution of mechanical tension evoked by staircase and by tetanus in rat muscle. Journal of Physiology, 311, 355–372.

Macintosh, B. R. (2010). Cellular and Whole Muscle Studies of Activity Dependent Potentiation. In D. E. Rassier, Muscle Biophysics (Vol. 682, pp. 315–342). New York, NY: Springer New York.

Macintosh, B. R., Taub, E. C., Dormer, G. N., & Tomaras, E. K. (2008). Potentiation of isometric and isotonic contractions during high-frequency stimulation. Pflügers Archiv : European Journal of Physiology, 456(2), 449–458.

Marsden, C. D., Meadows, J. C., & Merton, P. A. (1983). "Muscular wisdom" that minimizes fatigue during prolonged effort in man: peak rates of motoneuron discharge and slowing of discharge during fatigue. Advances in Neurology, 39, 169–211.

Moore, R. L., & Stull, J. T. (1984). Myosin light chain phosphorylation in fast and slow skeletal muscles in situ. American Journal of Physiology-Cell Physiology,247(5), C462-C471.

Patel, J. R., Diffee, G. M., Huang, X. P., & Moss, R. L. (1998). Phosphorylation of myosin regulatory light chain eliminates force-dependent changes in relaxation rates in skeletal muscle. Biophysical Journal, 74(1), 360–368.

Persechini, A., Stull, J. T., & Cooke, R. (1985). The effect of myosin phosphorylation on the contractile properties of skinned rabbit skeletal muscle fibers. Journal of Biological Chemistry, 260(13), 7951–7954.

Person, R. S., & Kudina, L. P. (1972). Discharge frequency and discharge pattern of human motor units during voluntary contraction of muscle. Electroencephalography and Clinical Neurophysiology, 32(5), 471–483.

Ryder, J. W., Lau, K. S., Kamm, K. E., & Stull, J. T. (2007). Enhanced skeletal muscle contraction with myosin light chain phosphorylation by a calmodulin-sensing kinase. Journal of Biological Chemistry.

Sandercock, T. G., & Heckman, C. J. (1997). Doublet potentiation during eccentric and concentric contractions of cat soleus muscle. Journal of Applied Physiology, 82(4), 1219–1228.

Schiaffino, S., & Reggiani, C. (2011). Fiber types in mammalian skeletal muscles. Physiological Reviews.

Smith, I. C., Gittings, W., Huang, J., McMillan, E. M., Quadrilatero, J., Tupling, A. R., & Vandenboom, R. (2013). Potentiation in mouse lumbrical muscle without myosin light chain phosphorylation: is resting calcium responsible? The Journal of General Physiology, 141(3), 297–308.

Stull, J. T., Kamm, K. E., & Vandenboom, R. (2011). Myosin light chain kinase and the role of myosin light chain phosphorylation in skeletal muscle. Archives of Biochemistry and Biophysics, 510(2), 120–128.

Sweeney, H. L., & Stull, J. T. (1990). Alteration of cross-bridge kinetics by myosin light chain phosphorylation in rabbit skeletal muscle: implications for regulation of actin-myosin interaction. Proceedings of the National Academy of Sciences of the United States of America, 87(1), 414–418

Sweeney, H. L., Bowman, B. F., & Stull, J. T. (1993). Myosin light chain phosphorylation in vertebrate striated muscle: regulation and function. American Journal of Physiology -- Legacy Content, 264(5 Pt 1), C1085–C1095.

Tononi, G., Sporns, O., & Edelman, G. M. (1999). Measures of degeneracy and redundancy in biological networks. Proceedings of the National Academy of Sciences, 96(6), 3257–3262.

Vandenboom, R., Gittings, W., Smith, I. C., Grange, R. W., & Stull, J. T. (2013). Myosin phosphorylation and force potentiation in skeletal muscle: evidence from animal models. Journal of Muscle Research and Cell Motility, 34(5-6), 317–332.

Vandenboom, R., Grange, R. W., & Houston, M. E. (1993). Threshold for force potentiation associated with skeletal myosin phosphorylation. American Journal of Physiology -- Legacy Content, 265(6 Pt 1), C1456–62.

Vandenboom, R., Grange, R. W., & Houston, M. E. (1995). Myosin phosphorylation enhances rate of force development in fast-twitch skeletal muscle. American Journal of Physiology -- Legacy Content, 268(3 Pt 1), C596–603.

Zhi, G., Ryder, J. W., Huang, J., Ding, P., Chen, Y., Zhao, Y., et al. (2005). Myosin light chain kinase and myosin phosphorylation effect frequency-dependent potentiation of skeletal muscle contraction. Proceedings of the National Academy of Sciences of the United States of America, 102(48), 17519–17524.

# Appendix I: skMLCK protein expression by SDS-PAGE

*Original methods from Eric Herbst: details/modifications are listed below.*

## *Background*

Western blotting is a technique that identifies specific proteins in a given sample or extract after their separation using polyacrylamide gel electrophoresis. The polyacrylamide gel is placed to a membrane, which is typically nitrocellulose or PVDF (polyvinylidene fluoride), and the application of an electrical current induces the proteins to migrate from the gell to the membrane on which they become immobilized. The membrane is then a replica of the gel protein and can be stained with an antibody.

## *Sample Preparation*

Homogenization

1. Make up homogenization buffer:
    - 250mM sucrose = 21.4g
    - 100mM KCl = 1.865g
    - 5mM EDTA = 0.4695
    - add 225mL $dH_2O$, fix pH 6.8, top up to 250mL $dH_2O$ and mix well, store in fridge
2. Remove wanted buffer and add protease inhibitor tablet (from antibody drawer) (Roche, 1 tablet /10mL) and add phosphatase inhibitor (Roche, 1 tablet /10mL)
3. Prepare glass homogenizers with ~ 200µL of buffer, tear in scale, remove ~ 10mg chunk of muscle from sample for analysis, add muscle and weigh
    - keep on ice when possible
4. Correct buffer volume in homogenizer so that 10µL of buffer is present for every 1mg of sample
5. Homogenize well on ice

Protein Determination

1. Make up or remove BSA standard (1mg/ml) from -20
2. Make up standard:

| Final Conc. (mM) | Volume of BSA (µL) | Volume of $dH_2O$ (µL) |
|---|---|---|
| 1 | leave as is | 0 |
| 0.5 | 500 from '1' | 500 |
| 0.25 | 500 from '0.5' | 500 |
| 0.125 | 500 from '0.25' | 500 |
| 0.05 | 100 from '0.5' | 900 |
| 0 | 0 | Leave as is |

3. Pipette everything in triplicate in a clear microtitre plate. Pipette the samples as 9µL of $dH_2O$ and 1µL of sample for whole homogenate (10x dilution), 9.5µL of $dH_2O$ and 0.5µL of sample for mitochondrial suspension (20x dilution).

4. Add 200μL of diluted buffer (1:4 with Bio-Rad Protein Assay Dye Reagent : $dH_2O$)
5. Let incubate for 5min and read absorbance as wavelength 595nm
6. In excel run polynomial curve with blanks subtracted, multiply determined y-intercept by 10 to determine protein concentration for whole homogenates, by 20 for mitochondrial isolations.
7. To prep samples for blotting[1] (best done on same day as SDS PAGE):

| | |
|---|---|
| **Total Volume** (TV) | Optional 25 - 100 μL |
| **Sample Volume** (SV) | $SV = TV \bullet \frac{[\text{Desired Final Protein}]}{[\text{Protein}]}$ |
| **Sample (Laemelli) Buffer** (SB) | $SB_f = \frac{TV}{[SB_i]}$ (i.e. $\frac{\text{TV}}{5}$ for 5x $SB_i$) |
| **Water** ($dH_20$) | $dH_2O = TV - SV - SB$ |
| **1M DTT**[2]** | = 10% of total volume |

## *SDS PAGE Procedure*

Electrophoresis Preparation

1. Before using glass plates, wipe with methanol and a kim wipe
2. Assemble the glass-holding apparatus with the short plate facing to the front. Ensure plates are flush and level before locking and inserting onto the gel casting stand.
3. Prepare gels (makes 2):

| Percent Gel | $dH_2O$ (ml) | Protogel (ml) (30% acrylamide) | Gel Buffer (ml) |
|---|---|---|---|
| **4 (Stacking)** | **6.1** | **1.3** | **2.5 Stacking** |
| 6 | 5.3 | 2.0 | 2.5 Resolving |
| 8 | 4.62 | 2.67 | 2.5 Resolving |
| **10 (Running)** | **3.96** | **3.33** | **2.5 Resolving** |
| 12 | 3.29 | 4.0 | 2.5 Resolving |
| 15 | 2.29 | 5.0 | 2.5 Resolving |

4. Before pouring the **running gel**, add 100μL APS (60mg/600μL) and 10μL of TEMED. Swirl and pour until reaching the depth of the comb. Use methanol to remove any bubbles and dump once hardened
5. Before pouring the **stacking gel**, add 100μL APS and 20μL TEMED. Swirl and pour until the top of the short plate is reached. Insert combs of desired size. Once hardened, remove combs and rinse with $dH_2O$
6. Place gel cassettes into electrode assembly with the short plates facing inwards, clamp down firmly and place into mini-tank
7. Boil samples for 5-minutes and place subsequently on ice for 5-minutes while preparing *running buffer* (50mL 10x running buffer + 450mL $dH_2O$)

[1] If [protein] is <1, cannot reliably perform blotting

[2] DTT is optional. Effects redundant with β-mercaptoethanol (in Laemelli buffer)

8. Fill the inner chamber of the apparatus with diluted running buffer add ~200mL to the outside chamber
9. Load the standard[3] and the appropriate amount of sample into each well. (Note: to determine the appropriate amount of sample to load, perform a separate optimization with varying amounts of protein. 5-10μL may be used successfully if just practicing).
10. Run electrophoresis at 120-volts for 90-minutes or until the blue dye travels to the bottom edge of the plate. If tiny bubbles rise then electrophoresis is working[4]. Prepare transfer buffer.

### *Transfer*

1. Remove gels carefully, discard the stacking gel, and transfer to a plastic try to equilibrate in transfer buffer
2. Create the "transfer sandwich":
    - white/clear side of the holder
    - sponge/ fibre pad (presoaked in transfer buffer)
    - filter paper (presoaked in transfer buffer)
    - membrane (PVDF presoaked in methanol)
    - Gel
    - filter paper (presoaked in transfer buffer)
    - sponge/ fibre pad (presoaked in transfer buffer)
    - black side of the holder

    *Be sure to roll out any air bubbles, close firmly, and place the black side of the holder to the black (/back) side of the electrophoresis apparatus.
3. Fill the tank with transfer buffer and the surrounding environment with plenty of ice to prevent from cooking the gel and add a stir-bar to help with heat loss.
4. Run the transfer at 100-volts for 60-minutes

### *Antibodies*

1. Discard the gel and filter papers and transfer the membranes to small dishes
2. Block with 20mL TBST-5% skim milk[5] or TBST-3% BSA solution (4.5g skim milk powder in 90mL) for 1-hour
3. Discard blocking solution and add $1^{o}$ AB in TBST-5% skim milk, incubating for 1-hour or overnight[6] with the appropriate dilution

| Antibody | Size (kDa) | Dilution | Amount (μL in 10mL) |
|---|---|---|---|

[3] Lui says: "5μL works nicely"
[4] Thing's aren't going well if:

- the amount of buffer inside the tank is going down (you have a leak!)
- the bands form a "sad face" (you may be running the gel at too high a voltage or have a leak)

[5] Can substitute with a TBST-3% BSA solution (3.0g BSA in 100mL TBST)
[6] McMeekin says: "overnight works better"

| | | | |
|---|---|---|---|
| PDK 1-4 | 46-48 | 1:200 | 50[7] |
| PDP1c | 53 | 1:3000 | 3.3 |
| PDP2 | 60 | 1:3000 | 3.3 |
| PDH E1α | 41 | 1:5000 | 2 |
| PDH E2 | 52 | 1:5000 | 2 |
| PDH E2/E3bp | 50 | 1:1000 | 10 |
| CS | 50 | 1:500 | 20 |
| COX (subunits 2-4) | 20-26 | 1:000 | 10 |
| ANT | 30 | 1:200 | 50[8] |

4. Wash 3-5x 5-minutes with TBST (10mL)
5. Add 2$^{o}$ Ab (dependent on 1$^{o}$ Ab) in TBST-5% skim milk solution for 1-hour with the appropriate dilution

| **Secondary** | **Dilution** | **Amount** (μL in 10 mL) |
|---|---|---|
| Anti-mouse | 1:5000 | 2 |
| Anti-goat | 1:20000 | 0.5 |
| Anti-rabbit | 1:10000 | 1 |

### *Enhanced Chemiluminesence*

1. Wash 3x 5-minutes with TBST [9]
2. Combine 1mL of each chemiluminescent HPR substrate (peroxide solution + luminal reagent) over membrane and continue to pipette over membrane or let rock for 5-minutes
3. Place membrane protein-side down on glass and cover back with parafilm
4. Take an initial photo with a pin beside the standard that represents the weight of your protein for overlapping later if need be. Take a subsequent photo with the appropriate exposure time and analyze later with "Imagej".

[7] Dunford used 5μL in 10mL successfully
[8] Herbst used 10μL in 10mL successfully
[9] Herbst says: In some instances, longer incubations in TBST produce cleaner blots (PDKs especially)

***Reagents:***

Homogenizing Buffer

- 250mM sucrose (21.4g)
- 100mM KCL (1.865g)
- 5mM EDTA (0.4695g)
- add 225mL $dH_2O$, fix pH 6.8, top up to 250mL $dH_2O$
- mix and store in fridge

Laemelli Buffer (2x Sample Buffer)

- 2.5ml 0.5M Tris-HCl pH 6.8
- 2ml glycerol
- 2ml 10% SDS
- 0.2mL 1% bromophenol blue
- 1ml β-mercaptoethanol
- 0.3mL $dH_2O$

Running Gel Buffer

- 1.5M Tris-HCl, pH 8.8

Stacking Gel Buffer

- 0.5M Tris-HCl, pH 6.8

10x Running Buffer, pH 8.3

- 250mM Tris base
- 1.92M glycine
- 1% SDS
- Store at $4^oC$. If precipitation occurs, warm to room temp before use.

10x Transfer Buffer (semi-dry)

- 312.5mM Tris base (3.786g)
- 2.4M glycine (18g)
- fill to 100mL with $dH_2O$
- *before use, dilute 80mL in 720 mL $dH_2O$ and add 200mL of methanol

10x TBS

- 200mM Tris base
- 1.37M NaCl
- 38mL of 1M HCl/L of TBS made
- adjust to pH 7.5

TBST

- dilute 100mL of 10x TBS in 900mL $dH_2O$
- add 4mL of 25% Tween 20 while stirring (polyoxyethylenesorbitan monolaurate)

*Specific procedure and details used by H. Aggarwal/W.Gittings*

- In liquid nitrogen, the frozen muscle samples were chipped off to an approximate weight of 10 mg. Homogenizations of the individual muscle samples were done in glass homogenizers on ice, with a homogenization buffer (250 mM sucrose, 100 mM KCl, 5 mM EDTA, pH 6.8; and 1 / 10mL each of protease and phosphatase inhibitor cocktail tablets [Roche Diagnostics, Indianapolis, IN, USA]) volume corrected to 25 µL/1 mg of sample.
- The whole homogenate protein concentration was determined using a Bradford Assay, using a BSA protein standard and 1:4 diluted Protein Assay Dye Reagent (Bio-Rad Laboratories, CA, USA) detected in the Synergy HT Microplate Reader (Bio-Tek Instruments, Winooski, VT, USA) read at 595nm in a 5 minute incubation.
- Samples were prepared by diluting the protein concentration to 2.0 µg / µL in dH2O with 1:3 total protein volume of 3x Laemelli sample buffer (1 M Tris-HCl pH 6.8, glycerol, 10% SDS, 1% bromophenol blue, β-mercaptoethanol).
- Standard SDS-PAGE electrophoresis was performed using a 10% running gel (4x Protogel Resolving Buffer [1.5 M Tris-HCl, pH 8.8], Protogel [30% w/v Acrylamide, 0.8% w/v Bis-Acrylamide]) and 4% stacking gel (Protogel Stacking Buffer [0.5 M Tris-HCl, 0.4% SDS, pH 6.8], Protogel), (National Diagnostics, Atlanta, GA, USA) mixed with 1:10 diluted Ammonium Persulfate electrophoresis reagent (Sigma Chemical Co, St. Louis, MO, USA) and TEMED electrophoresis reagent N,N,N',N'-Tetramethylethylenediamine (Bio-Rad Laboratories, CA, USA) to create the gels.
- Samples were both boiled and put on ice for 5 minutes, then 15 µg (7.5 µL) of protein was loaded per lane beside 7.5 µL (1.5 mg / ml) of the Protein Standards Kaleidoscope (Bio-Rad Laboratories, CA, USA) loaded as a ladder.
- The electrophoresis was done with the inner chamber of the electrode assembly apparatus filled with 10x running buffer (250mM Tris base, 1.92M glycine, 1% SDS), and was run at 120 volts for 90 minutes.
- The tank method of electrophoretic transfer was used (Bio-Rad Laboratories, CA, USA) with sponges, filter paper, and the gels equilibrated in 10x transfer buffer (312.5mM Tris base, 2.4M glycine, 200mL methanol, 10mL 10% SDS [for 1L]), to transfer the proteins onto a 0.45 polyvinylidene fluoride (PVDF) Immobilon-P Transfer Membrane (Millipore Corporation, Billerica, MA, USA) presoaked in methanol and run in the transfer buffer at 100 volts for 60 minutes.
- The membranes were blocked for 1 hour in 5% skim milk-TBST buffer (10x diluted 200mM Tris Base, 1.37M NaCl, pH 7.5, 0.4% w/v 25% Tween 20), then incubated overnight at 4°C in 2.5% skim milk-TBST containing a 1:3500 dilution of primary monoclonal antibodies against skMLCK.
- The membranes were washed in approximately 10 mL of TBST in 3 cycles of 5 minutes, then incubated for 1 hour in 2.5% skim milk-TBST containing a 1:2000 dilution of bovine anti-goat IgG-HRP (Santa Cruz Biotechnology, Santa Cruz, CA, USA) secondary antibody.
- The membranes were washed in approximately 10 mL of TBST in 3 cycles of 5 minutes, then visualized by pipetting 2mL of chemiluminescent HRP substrate Luminata Forte Western (Millipore Corporation, Billerica, MA, USA) over the membrane for 5 minutes, and detected with the FluorChem 5500 (Alpha Innotech, San Leandro, CA, USA) after a 2-minute exposure.
- The relative densities of the bands were quantified with ImageJ (National Institute of Health, Bethesda, MD, USA) with results expressed in arbitrary units. The homogenization and blotting procedure was done 4-5 times to ensure similar results.

# Appendix II: Quantification of myosin RLC phosphate content

*Urea/Glycerol-PAGE with Immunoblotting: Original methods from Dr. James Stull (Texas) modified and organized by Jordan Bunda, BSc.*

Myosin regulatory light chains (RLCs) are small ($18 - 20\ kDa$) acidic (pI about 4.8 with net charge of -18) proteins that migrate easily in polyacrylamide gels containing glycerol for density. RLCs are denatured with trichloroacetic acid (TCA) and solubilized in urea to dissociate RLC from myosin heavy chain. The addition of a single phosphate introduces two additional negative charges at pH 8.6 (the pH of the running buffer) so the phosphorylated protein migrates faster than the non-phosphorylated RLC. Thus, the phosphorylation measurements are quantitative (mol per mol), not relative (degree of change) after measurements of the protein band density by immunoblotting.

### *Sample Preparation*

*Prepare Stock Solutions*

*Acetone-Based Protein Precipitation Solution (5 mL)*

10% Trichloroacetic acid (TCA), 10 mM DTT in ice-cold acetone (-20 C)

| | |
|---|---|
| TCA *(T8657)* | 0.5 g |
| DTT *(D0632)* | 7.71 mg |
| Acetone | 2.5 mL |
| Dissolve | |
| Acetone | Q.S. to 5 mL |

*N.B. Make fresh on day of sample preparation, and store in -20 C until use.*

*Water-Based Protein Precipitation Solution (5 mL)*

10% Trichloroacetic acid (TCA), 10 mM DTT in

| | |
|---|---|
| TCA *(T8657)* | 0.5 g |
| DTT *(D0632)* | 7.71 mg |
| $dH_2O$ | 2.5 mL |
| Dissolve | |
| $dH_2O$ | Q.S. to 5 mL |

*N.B. Make fresh on day of sample preparation, and store in -20 C until use.*

*Prepare Buffers*

*Gel Buffer (500 mL)*

| | |
|---|---|
| Trizma base | 13.7 g |
| Glycine | 10.0 g |
| $dH_2O$ | 250 mL |
| Dissolve | |
| $dH_2O$ | Q.S. to 500 mL |

*N.B. Store at 2-8 C.*

*Sample Buffer*

| | |
|---|---|
| 8 M Urea | 1.83 mL |
| Urea Gel Buffer | 167.0 uL |
| 0.5 M DTT | 40.0 uL |
| Saturated Sucrose | 100 uL |
| 0.2% Bromophenol Blue | 40.00 uL |
| 0.4 M EDTA | 1.00 uL |

*N.B. Make fresh on day of sample prep.*

*Sample Denaturation*

1. Pipet 0.5 mL Acetone-Based Protein Precipitation Solution into as many microcentrifuge tubes as you have muscle samples (pre-labeled), and freeze in liquid $N_2$
2. Measure frozen weight of muscle sample (~10 mg for EDLs) and record
3. Remove microcentrifuge tube from $N_2$, open lid and place on ice
4. Introduce muscle preparation (sutures removed) to the microcentrifuge tube of frozen Acetone-Based Protein Precipitation Solution slurry, as it forms a slurry when warming up to about -35°C on ice
5. Remove the tubes from ice and allow them to come to room temperature

*Sample Homogenization*

1. Transfer each denatured muscle sample (tissue only, no liquid) to a ground glass homogenizing tube, and pipet in 0.5 mL Water-Based Protein Precipitation Solution
2. Homogenize muscle sample thoroughly
3. Transfer the homogenate to a microcentrifuge tube by pouring – samples may sit on ice for 10 mins or more
4. Centrifuge at 2000 RPM for 3 minutes at room temperature – do not over pack the protein pellet or resuspension will be difficult
5. Discard the supernatant by pouring off into a waste beaker
6. Wash pellet with 0.5 mL of ether, 3 times for 5 minutes each to remove TCA
7. Let residual ether evaporate from the tube for 5 minutes in the hood or blow gently into the tube if you are impatient
8. DO NOT let the pellet go totally dry or resuspension will be difficult

*Resuspension*

1. Add 30 µL of urea sample buffer per mg frozen tissue weight
2. Vortex and manually disperse the pellet if necessary
3. pH should be around 9, check by confirming blue colour of the sample – if yellow/green at 2 M Tris base (pH 11) 1 µL at a time until colour becomes uniform between samples
4. Add ~__mg of urea to microcentrifuge tube that contains 300 µL of sample buffer
5. Shake samples for 15 minutes at RT, adding more urea if the others have dissolved

6. Repeat until same is saturated by urea – do NOT oversaturate or the sample will become solid and unusable
7. Store at -80°C if you do not use immediately.
8. Thaw samples on day of use in an ice bath, and mix after 1 hr of thawing
9. Do not heat urea samples on thawing – this can lead to breakdown of urea at high pH to cyanide with carbamylation of protein, which changes charge.

### *Hand Casting of Polyacrylamide Gels*

*10% (w/v) APS*

| | |
|---|---|
| Ammonium persulfate *(A3574)* | 0.10 g |
| $dH_2O$ | 1.0 mL |

*N.B. Make fresh when casting gels.*

*Urea/Glycerol Polyacrylamide Gels (2)*

| | |
|---|---|
| $dH_2O$ | 4.2 mL |
| Glycerol *(G5516)* | 9.0 mL |
| 30% Acrylamide/Bis 29:1 | 7.5 mL |
| Urea Gel Buffer | 1.9 mL |
| Stir 10 mins under vacuum to degas | |
| 10% APS | 100 uL |
| TEMED | 10 uL |
| Mix By Swirling | |
| Quickly pour into minigel apparatus & insert combs | |

*N.B. Make just prior to pouring. Gel starts polymerizing immediately after APS and TEMED are introduced to the solution – have everything ready to cast before adding these and move quickly.*

1. Place magnetic stir bar in small vacuum flask
2. Mix $dH_2O$, glycerol, acrylamide, and urea gel buffer in flask
3. Close flask and turn on vacuum
4. Stir for 10-15 minutes under vacuum to degas the solution
5. Prepare plates/combs for casting
6. Pour degassed solution into 50 mL falcon tube
7. Draw 100 uL of 10% APS and 10 µL TEMED in pipettes
8. Quickly add the APS and TEMED, mix by swirling – do NOT shake or you will regass the solution you just spent 15 minutes degassing
9. Cast gels using a disposable transfer pipet, pouring only into the centre of the plates – the solution will naturally spread and you do not need to move the pipet, as you may risk formation of bubbles
10. Insert newly cleaned combs, and wipe up any spillage before polymerization - this protocol does not use a stacking gel
11. Mix upper and lower buffers while gels polymerize (~45 mins)

*Lower Buffer (1 L)*

| | |
|---|---|
| Urea Gel Buffer | 83.0 mL |
| $dH_2O$ | Q.S. to 1000 mL |

*N.B. this buffer is poured into the electrophoresis tank.*

*Upper Buffer (200 mL)*

| | |
|---|---|
| DTT | 73.3 mg |
| Thioglycolate | 53.3 mg |
| Lower Buffer | 200 mL |

*N.B. this buffer is poured into the electrode assembly.*

## *Electrophoretic Separation of Proteins*

*Pre-Electrophoresis*

1. Carefully remove combs from polymerized gel – it must be removed while remaining parallel to the gel to prevent damage to any wells
2. Rinse wells with $dH_2O$ to remove any debris
3. Rinse wells with Upper Buffer immediately before pre-electrophoresis
4. Place gels into electrode assembly after wetting the gasket, ensuring that the plates are fully inserted into the brackets
5. Check seal for leak using $dH_2O$
6. Pre-electrophorese at 400 V for 1 hour to force thioglycolate into the gel – this reduces any residual APS that was used to initiate polymerization, preventing protein oxidation which will effect protein migration

*Electrophoretic Separation of Proteins*

1. Load 5-20 µL of each sample – this gel system does not have a stacking gel so the tip of the pipet should be close to the gel in the well with slow addition of the sample. Urea and sucrose were added for increased density so the sample should layer in the well as a sharp band
2. Amount to load depends on tissue source so optimal amount needs to be determined - Load at lease 5 µL to get good bands – if protein is too concentrated, sample can be diluted with urea sample buffer
3. Do NOT use the end wells, as samples in the end wells tend to distort
4. Electrophorese at 400 V for 85 minutes - Dye will run off gel but you can look at it during electrophoresis to make sure migration is normal
5. Prepare 1X Transfer Buffer from 10X Transfer Buffer stock during electrophoresis – 1 L is enough for 1-2 gels

*10X Transfer Buffer (1 L)*
1.9 M Glycine, 250 mM Tris, 0.5% (w/v) SDS

| | |
|---|---|
| Glycine | 144.12 g |
| Tris | 30.29 g |
| SDS | 5.0 g |
| $dH_2O$ | 500 mL |
| Dissolve | |
| $dH_2O$ | Q.S. to 1 L |

*N.B. Store at 2-8 C.*

*Transfer Buffer (1 L)*
192 mM Glycine, 25 mM Tris, 0.05% (w/v) SDS

| | |
|---|---|
| 10X Transfer Buffer | 100 mL |
| 100% Methanol | 200 mL |
| $dH_2O$ | 700 mL |

*N.B. Make from concentrated stock on the day of transfer.*

## *Protein Transfer From Polyacrylamide Gel to Nitrocellulose Membrane*

1. Cut ~8.5 x 7.0 cm pieces of nitrocellulose paper (0.45 mm pore size)
2. Pour 1x Transfer Buffer into trays in preparation for blotting sandwich
3. Disassemble electrode assembly, and remove gel cassettes
4. Separate plates using green plastic wedge
5. Cut off approximately one quarter of the upper part of gel
6. Notch the upper left corner of the gel to aid in discerning orientation later
7. Rinse gels gently in transfer buffer for 5 minutes to equilibrate
8. Place a magnetic stirbar into the transfer tank, half fill with cooled 1X Transfer Buffer and position on stirrer
9. Immerse nitrocellulose membrane in transfer buffer for 1 minute to wet it – it should be pre-notched in the upper left corner of the membrane to match the orientation of the gel
10. With the black (cathode) side of the gel holder cassette submerged in Transfer Buffer, assemble the blotting sandwich in the following order, wetting each layer before its addition: sponge, blotting paper, gel, nitrocellulose membrane, blotting paper and sponge
11. Roll after adding each layer to remove air bubbles – having enough Transfer Buffer in the tray to cover all layers will help when removing bubbles
12. Close the cassette, slide white latch to lock, and place into blotting module with the latch side up, and the black side of the cassette facing the black side of the blotting module
13. Repeat for any additional blots, then place the blotting module with the gel holder cassettes into the tank
14. Insert icepack into tank, add transfer buffer to the tank until the fill line is reach, and begin stirring
15. Place lid on top of the cell, connect cables to power supply, turn on power supply and transfer membrane at 25 V for 1 hour by selecting the pre-set method entitled "Transfer"

## *Immunobloting*

*Blocking of Non-Specific Sites*

1. Remove the nitrocellulose membrane from the blotting sandwich, and transfer to a square petri dish, ensuring that only the corner of the membrane is touched by tweezers and that the membrane remains protein-side up
2. Wash the membrane in TBST three times for 10 minutes each
3. Incubate with Blocking Buffer for 1 hour at room temperature to prevent non-specific binding in a clean tray

*Primary Anti-Body Incubation*

1. Wash membrane in TBST twice, 5-10 min per wash
2. Add 1:7,500 skMLCK polyclonal primary antibodies to fresh blocking buffer (i.e. 1.5 μL in 10 mL) in a clean tray and incubate with rocking overnight at 4°C

*Secondary Anti-Body Incubation*

1. Remove primary antibody and wash the membrane with TBST, six times for 10 minutes in a clean tray
2. Incubate with secondary antibody, 1:10,000 dilution of Goat Anti-Rabbit IgG-HRP in TBST (i.e 1 μL in 10 mL) for 1 hour in a clean tray

*Detection of Target Proteins*

1. Wash the membrane in TBST six times for 10 minutes
2. Transfer membrane to a clean tray after rinsing with $dH_2O$, and drip drying onto Kim Wipe
3. Make detection buffer using equal volumes of ECL Prime luminol and oxidizing reagents
4. Incubate the membrane in detection buffer for 2 minutes, constantly pipetting to cover entire membrane
5. Decant the ECL Prime, lift membrane with tweezers and blot all excess reagent from the corner of the membrane using a Kim Wipe
6. Cover membrane with sheet protector, and roll to remove air bubbles and/or excess liquid
7. Turn on the CCD imaging machine – flip the power switches at the back of the unit (bottom right) and on the shelf
8. Open the FluorChem application
9. Place blot on imager platform and center on the screen, zoom if necessary
10. Imager should be on setting 1 for chemiluminescence
11. Select “Chemidisplay”, “Normal Sensitivity/Resolution”, and check “UV” for “Transluminator” and “Reflective” settings
12. Select exposure time of 30-60 seconds, and select ‘Acquire Image’
13. Save image to appropriate folder

# Appendix III: Muscle lyophilization and fluorometric assays

*Urea/Glycerol-PAGE with Immunoblotting: Original methods from the lab of Dr. Sandra Peters modified and organized by Jordan Bunda, BSc.*

## *Lyophilization of Muscle Tissue*

1. Turn lyophilizer on by switch on both the condenser and vacuum unit
2. Press 'Refridgeration – Auto' and 'Vacuum' buttons
3. Close all valves on the tree
4. Ensure digital temperature and pressure gauges begin to drop
5. Pour liquid $N_2$ into thermoflask from storage dewar
6. Remove samples from -80°C freezer and place in $N_2$
7. Transfer samples into ventilated microcentrifuge tubes (if not in one already) ensuring they stay frozen
8. Precool LABCONCO 600 mL evacuation vessel with liquid $N_2$ in a metal bowl
9. Place samples in vessel, submerging the bottom of the flask in $N_2$
10. Close vessel with rubber top
11. With the vessel still sitting in liquid $N_2$, attach the metal tube to the vacuum tree
12. When a good seal has been made, open valve and the vessel should evacuate (very obvious to both see and hear)
13. Let machine run for minimum of 6 hours or over night (if you trust leaving it alone)
14. Check occasionally to ensure it is running properly
15. Shut machine down when finished
16. Store the lyophilized samples in -80°C in a box with desiccant if not extracting immediately
17. Open the circular lid of the condenser and allow it to return to room temperature
18. Wipe up condensation from the inside of the condenser after room temperature has been reached
19. Sign the log including name, date, usage etc.

## *Metabolite Extraction*

Often the preparation of the tissue is the most critical. In the case of metabolite assays, the most hazardous period is usually the period between the experimental stimulus and the moment the enzyme activity is finally stopped. Rapid freezing is essential; therefore, most metabolite analysis is performed on extracts prepared from frozen tissue. Most metabolites are assayed in protein-free extracts prepared with perchloric acid ($HClO_4$). $HClO_4$ is preferred because most of it can be easily removed by precipitation as a potassium salt. All of the following analyses are performed on freeze-dried tissue. Not only does it circumvent the problem of changing water contents in tissue, but also because the tissue is much easier to work with. Enzymes are rendered inactive in a water-free environment, and will remain so until water is re-added. Therefore, the weighing of the samples can be performed at room temperature and the tissue can be dissected free of connective tissues and blood.

**Required Solutions**

0.5 M PCA (500 m)

| | |
|---|---|
| 70% w/v Perchloric acid | 21.55 mL |
| $dH_2O$ | 125 mL |
| Mix | |
| $dH_2O$ | Q.S. to 500 mL |

*N.B. Store at 0-4 ℃ for up to 1 month; 70% PCA stored under fume hood.*

$d = 1.664\ g/mL$
$\%\ w/w = 70$
$MW = 100.46\ g/mol$
$C_{desired} = 0.5\ M$
$V_{desired} = 500\ mL$

$$Molarity = \left[\frac{(\%\times d)}{MW}\right]\times 10 = \left[\frac{(70\times 1.664\ g/mL)}{100.46\ g/mol}\right]\times 10 = 11.59466 \approx 11.60\ M$$

$C_1V_1 = C_2V_2$

$(11.60\ M)(V_1) = (0.5\ M)(0.5\ L)$

$$V = \frac{(0.5\ M)(0.5\ L)}{11.60\ M} = 21.55\ mL$$

1. In fume hood, pour PCA into small (>50 mL) beaker
2. Measure 21.6 mL of PCA in 25 mL graduated cylinder
3. Add 21.6 mL PCA to 125 mL $dH_2O$ in 500 mL graduated cylinder
4. Rinse 25 mL graduated cylinder with dH2O into 500 mL graduated cylinder
5. Bring to 500 mL with $dH_20$
6. Store in fridge (0-4ºC) for up to 1 month

2.3 M $KHCO_3$

| | |
|---|---|
| Potassium bicarbonate (237205) | 2.3 g |

| | |
|---|---|
| dH2O | 5 mL |
| Dissolve | |
| dH2O | Q.S. to 10 mL |

*N.B. Make fresh on day of extraction.*

MW = 100.12 g/mol
$C_{desired} = 2.3\ M$
$V_{desired} = 0.01\ L$

$$C = \frac{m}{V} \times \frac{1}{MW}$$

$$2.3\ M\ = \frac{mass\ KHCO_3}{(0.01\ L)}\left(\frac{1}{100.12\ g/mol}\right)$$

$$mass\ KHCO3 = (2.3\ mol/L)(0.01\ \cancel{L})(100.12\ g/mol) = 2.30276\ g$$

1. Weigh out 2.3 g $KHCO_3$
2. Measure ~5mL dH2O in small graduated cylinder
3. Add to small amount of distilled $H_2O$
4. Bring to 10.0 mL
5. Make fresh on day of extraction

**Confirm Neutral pH**

1. Calibrate the pH meter
2. Combine 4 mL PCA and 1 mL $KHCO_3$
3. Measure and record pH - values between 6.5 and 7.5 are acceptable

**Perchloric Acid Metabolite Extraction Procedure**

1. Freeze dry tissue (overnight to ensure all water is removed)
2. Store with dry rite in freezer until powdering
3. Tease out connective tissue and powder
4. Place in pre-weighed 12x75 glass centrifuge tube and weigh ($\sim 2.5\ mg$)
5. Place tubes in an ice bucket (make sure tubes remain cold)
6. Add 300 µL of pre-cooled 0.5 M PCA
7. Extract for 10 minutes, vortexing several times and ensure all tissue is in contact with PCA
8. Centrifuge for 10 minutes at 1000 G and 4°C– the glass tubes are compatible with the S4180 rotor (spinning helps remove some of the enzymes that can influence concentration)
9. Remove 270 µL, aliquot to micocentrifuge tube and place in freezer (-20ºC) for 10 min
10. To the frozen supernatant add 67.5 µL of 2.3 M $KHCO_3$ and vortex until liquid (addition of $KHCO_3$ to a frozen supernatant prevents foaming over)
11. Centrifuge for 10 min 0ºC at 15 000 G – the microcentrifuge tubes are compatible with the F2402H rotor - Potassium salt will precipitate.
12. Remove supernatant, aliquot to new pre-labeled microcentrifuge tubes – this is the extraction that will be assayed for metabolites.

**Using the Centrifuge**

1. Power on the unit by flicking the black switch on the back of the unit
2. When centrifuging, ensure that it is completely balanced and samples of the same volume are placed "across the street" from one another
3. Different rotors are used for different sized tubes and are stored in the drawer directly underneath the unit
4. To change rotor, remove central bolt and remove the current rotor, replace with the required rotor and replace and tighten the central bolt – this bolt does not need to be tightened with a ton of force, snug is fine. Program the correct rotor.
5. Press "Enter" after making any changes to the settings
6. Always turn unit off when you are finished and leave lid open
7. Record use of the unit on the tracking sheet attached to the side

### *Fluorometric Assays*

Pyridine nucleotides are natural oxidizing and reducing agents in a wide variety of enzyme systems. In the reduced form the nucleotide NADH/NADPH is fluorescent while in its oxidized form (NAD/NADP) it is not. The reduced form is also capable of fluorescent emission at 460nm when excited at 340nm. Due to these two physical properties, reactions can be quantified based directly on the change in the oxidative state of these coenzymes. Therefore the limiting factor, in the conversion of any of the metabolites, and production of the fluorescent material, NADH/NADPH, will be the amount of metabolite in the muscle because all other substrates/cofactors/enzymes in the assay are in excess. The presence of certain compounds in the assay, removes certain substrates, essentially forcing all reactions to occur one direction. Therefore the amount of fluorescence determined using the Fluorometer is directly proportional to the amount of the metabolite in the muscle.

*Muscle Adenosine Triphosphate (ATP) and Phosphocreatine (PCr) Assay*

$$\text{P-Creatine + ADP} \xrightarrow{\textit{Creatine Kinase}} \text{Creatine + ATP}$$

$$\text{ATP + Glucose} \xrightarrow{\textit{Hexokinase}} \text{ADP + Glucose-6-P}$$

$$\text{Glucose-6-P + NADP}^{+} \xrightarrow{\textit{Glucose-6- Dehydrogenase}} \text{6-P-Glucanolactone + NADPH}$$

| Reagent | Storage | Stock Conc. | Final Conc. | Volume in 25 mL | Volume in 50mL | Volume in 100mL |
|---|---|---|---|---|---|---|
| **1. Tris Buffer** *Trizma Base* (T1503) | Room Temp (Shelf) | 1.00 M | 50.0 mM | 1.25 mL | 2.50 mL | 5.00 mL |
| **2. $MgCl_2$** *Magnesium Chloride* (M8266) | Room Temp (Shelf) | 1.00 M | 1.00 mM | 25.00 µL | 50.00 µL | 100.00 µL |
| **3. DTT** *Dithiothreitol* (D0632) | 2 − 8 ℃ (Fridge) | 0.50 M | 0.5 mM | 25.00 µL | 50.00 µL | 100.00 µL |
| **4. Glucose** (G8270) | Room Temp (Shelf) | 100.00 mM | 100.00 µM | 25.00 µL | 50.00 µL | 100.00 µL |
| **5. NADP** (N5755) | −20 ℃ (Freezer) | 50.0 mM | 50.0 µM | 25.00 µL | 50.00 µL | 100.00 µL |
| **6. G-6-P-DH** (G5760) | 2 − 8 ℃ (Fridge) | 4920 U /ml | 0.03 U /mL | 1.00 µL | 2.00 µL | 4.00 µL |
| **7. ADP** (A2754) | −20 ℃ (Freezer) | Solid | – | – | – | – |
| **8. Creatine Kinase** (C3755) | −20 ℃ (Freezer) | 324 U/mg | – | – | – | – |
| **9. Hexokinase** (H4502) | −20 ℃ (Freezer) | 130 U/mg | – | – | – | – |
| ***Note:*** Mix reagents 1-5 together. Bring to volume with $dH_2O$ and adjust to pH 8.1. Then add reagent 6. Mix by inversion with enzymes. | | | | | | |

**Preparation of Dilute Enzyme**

For *PART 2*: Mix 2.5 µL of Hexokinase with 1ml of buffer. Mix by inversion. CAREFUL NOT TO FOAM

For *PART 3*. Mix ~1.5 mg of phosphocreatine kinase and 5 mg of ADP into 5 ml of buffer. Mix by inversion.

**Procedure for Assay (Note:** Run everything in triplicate)

Ensure you vortex each sample before pipetting

Part 1.

1. Fill first three wells – A1, A2 and A3 - with 10.00 $\mu L$ of $dH_2O$ per well
2. **F**ill the next five rows of wells with 10.00$\mu L$ of varying concentrations of ATP Standard
   B1, B2 and B3 0.05 mM
   C1, C2 and C3 0.1 mM
   D1, D2 and D3 0.2 mM
   E1, E2 and E3 0.3 mM
   F1, F2 and F3 0.4 mM
3. Fill the next five rows of wells with 10.00 $\mu L$ of varying concentrations of the PCr standard.
   (0.08 mM, 0.16 mM, 0.32 mM, 0.64 mM, 0.96 mM)
4. Add 10.00 $\mu L$ of sample to the appropriate wells
5. Add 185 $\mu L$ of buffer to each well
7. Incubate the plate for 25 minutes (if time permits - probably not necessary)
6. Read the plate at sensitivity of 80 (excitation setting 340, emission setting 460) (base line reading = R1)

Part 2.

1. Add 6 $\mu L$ of dilute Hexokinase to all of the wells
2. Incubate in the dark drawer for ~80 minutes (can also track by multiple measures)
3. Read the plate (excitation setting 340, emission setting 460)
   ($R2 - R1 = \ reflects\ ATP\ in\ extract$)

Part 3.

1. Add 6 $\mu L$ of dilute Creatine Kinase to all of the wells
2. Incubate in the dark drawer for ~120 minutes
3. Read the plate (excitation setting 340, emission setting 460)
   ($R3 - R2 = \ reflects\ PCr\ in\ extract$)

**ATP (A7699) Standard Curve**

To make fresh 2.0 mM solution: 5.69 mg ATP into 5 mL $dH_2O$

| Concentration (mM) | Stock Volume (µL) | $dH_2O$ Volume (µL) | Dilution Factor |
|---|---|---|---|
| 0.05 | 25 | 975 | 40.0 |
| 0.1 | 50 | 950 | 20.0 |
| 0.2 | 100 | 900 | 10.0 |
| 0.3 | 150 | 850 | 6.67 |
| 0.4 | 200 | 800 | 5.00 |

**Phosphocreatine (P7936) Standard Curve**

Stored in 8.0 mM aliquots in the -80ºC
To make 8.0 mM stock: 21.85 mg phosphocreatine into 10 mL $dH_2O$

| Concentration (mM) | Stock Volume (µL) | $dH_2O$ Volume (µL) | Dilution |
|---|---|---|---|
| 0.08 | 10 | 990 | 100.0 |
| 0.16 | 20 | 980 | 50.0 |
| 0.32 | 40 | 960 | 25.0 |
| 0.64 | 80 | 920 | 12.5 |
| 0.96 | 120 | 880 | 8.3 |

*Muscle Creatine (Cr) Assay*

$$\text{Creatine} + \text{ATP} \xrightarrow{\textit{Creatine Kinase}} \text{P-Creatine} + \text{ADP}$$

$$\text{ADP} + \text{Phophopyruvate} \xrightarrow{\textit{Pyruvate Kinase}} \text{ATP} + \text{Pyruvate}$$

$$\text{Pyruvate} + \text{NADH} \xrightarrow{\textit{Lactate Dehydrogenase (LDH)}} \text{Lactate} + \text{NAD}$$

| Reagent | Storage | Stock Conc. | Final Conc. | Volume 250 mL | Volume 50mL | Volume 100mL |
|---|---|---|---|---|---|---|
| **1. Imidazole** (I0250) | Room Temp | 1.00 M | 50 mM | 1.25 mL | 2.50 mL | 5.00 mL |
| **2. $MgCl_2$** *Magnesium Chloride* (M8266) | Room Temp | 1.00 M | 5.0 mM | 125.00 µL | 250.00 µL | 500.00 µL |
| **3. KCl** *Potassium Chloride* (P9541) | Room Temp | 1.00 M | 30.00 mM | 0.75 mL | 1.5 mL | 3.00 mL |
| **4. PEP** *Phosphoenol pyruvate* (P7002) | −20 ℃ (Freezer) | 10.0 mM | 25.0 µM | 60.0 µL | 120.00 µL | 240.00 µL |
| **5. ATP** (A2383) | −20 ℃ (Freezer) | SOLID | 200.0 µM | 3.00 mg | 6 mg | 12 mg |
| **6. NADH** (N8129) | −20 ℃ (Freezer) | 15.0 mM | 45 µM | 75.00 µL | 150.00 µL | 300.00 µL |
| **7. LDH** (L2500) | 2 − 8 ℃ (Fridge) | 5264 U /mL | 0.24 U /mL | 1.10 µL | 2.3 µL | 4.6 µL |
| **8. Pyruvate Kinase** (P1506) | 2 − 8 ℃ (Fridge) | 1252 U /mL | 0.75 U /mL | 15.00 µL | 30.00 µL | 60.00 µL |
| **9. Creatine Kinase** (C3755) | −20 ℃ (Freezer) | 324 U /mg | 3.6 U/mL | – | – | – |
| ***Note:*** Mix reagents 1-6 together. Bring to volume with distilled water and adjust to pH 7.5. Then add reagents 7 & 8. Mix by inversion when enzymes added. | | | | | | |

**Preparation of Dilute Enzyme**

For step 2. Mix 1.0 mg of Creatine Kinase with 2.6 ml of buffer. Mix by inversion.

**Before beginning to pipette the samples you must test the fluorescence of the buffer (might have to change gain)**

**Procedure for Assay**

Part 1.

1. Fill three wells with a blank (10.00 µL $dH_2O$ per well)

2. a. Vortex each concentration mixture before pipetting
   b. Fill the next five wells with 10.00µL of varying concentrations of Cr standard (0.1mM, 0.2 mM, 0.4 mM, 0.8 mM, 1.2 mM)

3. a. Vortex each sample before pipetting
   b. Add 10.00 µL of sample to the appropriate wells

4. Add 185 µL of buffer to each well
5. Incubate for 30 minutes
6. Read the plate at a sensitivity of 100 (excitation setting 340, emission setting 460) (base line reading)

Part 2.

1. Add 6 µL of dilute Creatine Kinase to all of the wells
2. Place in the dark for 55 minutes
3. Read the plate (excitation setting 340, emission setting 460)

**Note:** Everything analyzed in triplicate

Creatine (Sigma C0780-50g) Standard Curve
Stored in 10 mM aliquots in the -80ºC
To make 10 mM stock: 131.1 mg into 100 ml $dH_2O$

| Concentration (mM) | Stock Volume (µL) | $dH_2O$ Volume (µL) | Dilution Factor |
|---|---|---|---|
| 0.1 | 10 | 990 | 100 |
| 0.2 | 20 | 980 | 50 |
| 0.4 | 40 | 960 | 25 |
| 0.8 | 80 | 920 | 12.5 |
| 1.2 | 120 | 880 | 8.33 |

*Muscle Lactate Assay*

$$\text{Lactate} + \text{NAD}^+ \xrightarrow{Lactate\ Dehydrogenase} \text{pyruvate} + \text{NADH} + \text{H}^+$$

$$\text{Pyruvate} + \text{Hydrazine} \longrightarrow \text{Pyruvate Hydrazone}$$

| Reagent | Stock Conc. | Final Conc. | Volume 250 mL | Volume 50mL | Volume 100mL |
|---|---|---|---|---|---|
| **1. Hydrazine** | $1.00\ M$ | $100.0\ mM$ | $2.50\ mL$ | $5.00\ mL$ | $10.00\ mL$ |
| **2. Glycine** | $1.00\ M$ | $100.0\ mM$ | $2.50\ mL$ | $5.00\ mL$ | $10.00\ \mu L$ |
| **3. $NAD^+$** | $100.0\ mM$ | $0.5\ mM$ | $125\ \mu L$ | $250\ \mu L$ | $500.00\ \mu L$ |
| **4. LDH** | $5264\ U/mL$ | $8.00\ U/mL$ | – | – | – |
| ***Note:*** Mix reagents 1-3 together. Bring to volume with dH2O and adjust to pH 10. | | | | | |

**Preparation of Dilute Enzyme**

Add 60 µL of LDH to 1.0 ml of reagent. Mix by inversion. (For 50 ml do 120 µL of reagent). (17.25 µL if using L-2500, LDH)

**Procedure for Assay**

Part 1**.**

1. Fill three wells with a blank (10.00 µL $dH_2O$ per well)

2. a. Vortex each concentration mixture before pipetting
   b. Fill the next five wells with 10.00µL of varying concentrations of lactate standard (0.025 mM, 0.05 mM, 0.1 mM, 0.2 mM, 0.8 mM)

3. a. Vortex each sample before pipetting
   b. Add 10.00 µL of sample to the appropriately wells

4. Add 185 µL of buffer to each well
5. Incubate for 15 minutes
6. Read the plate at a sensitivity of 100 (excitation setting 340, emission setting 460) (base line reading)

Part 2**.**

1. Add 10 µL of dilute LDH to all of the wells

2. Place in the dark for 120 minutes

3. Read the plate (excitation setting 340, emission setting 460)

**Note:** Run everything in triplicate

Lactate Standard Curve

Pre-made lactate standard (4.44 mM)

| Conc (mM) | Stock (µL) | $dH_2O$ (µL) |
|---|---|---|
| 0.1 | 23 | 977 |
| 0.2 | 45 | 955 |
| 0.4 | 90 | 910 |
| 0.8 | 180 | 820 |
| 1.2 | 270 | 730 |

| Conc (mM) | Stock (µL) | $dH_2O$ (µL) |
|---|---|---|
| 0.025 | 5.6 | 994 |
| 0.05 | 11.25 | 988 |
| 0.1 | 22.5 | 978 |
| 0.2 | 45 | 955 |
| 0.8 | 180 | 820 |

$$Dilution\ Factor\ (DF) = \frac{total\ volume}{sample\ volume}$$

$$DF_{total} = DF_a \cdot DF_b$$

$$DF_a = \frac{Total\ Volume}{Sample\ Volume} = \frac{volume\ of\ PCA\ (\mu L) + muscle\ mass\ (\mu L)}{muscle\ mass\ (\mu L)}$$

$$DF_b = = \frac{volume\ of\ Supernatant\ (\mu L) + volume\ of\ KHCO_3 (\mu L)}{volume\ of\ Supernatant\ (\mu L)}$$